THE ROLE OF FORMIN DIAPHANOUS IN MYOBLAST FUSION AND SARCOMEROGENESIS IN *DROSOPHILA MELANOGASTER*

A Dissertation
Presented to the Faculty of Weill Cornell Graduate School
of Medical Sciences
in Partial Fulfillment of the Requirements for the Degree of
Doctor of Philosophy

by
Su Deng
May 2016

THE ROLE OF THE FORMIN DIAPHANOUS IN MYOBLAST FUSION AND SARCOMEROGENESIS IN DROSOPHILA MELANOGASTER

Su Deng, Ph.D.

Cornell University 2016

From fruit fly to human, muscle cells form through a number of highly conserved steps. During the development of muscle, the actin cytoskeleton plays critical roles in muscle cell fusion, muscle cell attachment, and the assembly of muscle contractile apparatus, known as the sarcomere. Disruption of the arrangement of actin severely impairs muscle function and results in muscle disease. To better understand the key steps in muscle development and how actin forms different structures to regulate muscle formation, maturation and homeostasis, we used *Drosophila melanogaster* as a model system to study two steps in muscle development: myoblast fusion and sarcomere assembly. The multinucleated muscles form through myoblast fusion. During fusion, actin filaments accumulate at the fusion site to form a focus structure that mediates fusion. The formation of the actin focus is regulated by Arp2/3—an actin regulator that polymerizes branched actin networks. In my thesis, I have identified two additional factors, the phospholipid PI(4,5)P2 and the formin Diaphanous (Dia), as required for myoblast fusion. During fusion, both PI(4,5)P2 and Dia accumulate at the fusion site. PI(4,5)P2 control the localization and activation of SCAR and WASp, which activate Arp2/3 and trigger the formation of branched actin. Dia, which builds linear actin filaments, plays two roles during actin focus formation: it dictates the level of linear F-actin polymerization, and it is required for appropriate

branched actin polymerization via localization of SCAR and WASp. The actin cytoskeleton is also a major component of sarcomere. I found that Dia plays a critical role for sarcomere growth in the indirect flight muscles of adult fruit fly. The localization of Dia in the sarcomere is mediated by PI(4,5)P2. Dia genetically interacts with the Gelsolin superfamily member Flightless I (FliI) to regulate thin filament length and sarcomere size, possibly through maintaining the G-actin pool and regulating actin dynamics of the thin filaments. Together, my thesis work identified new factors that regulate muscle formation, and significantly enhanced our understanding of how the actin dynamics are regulated during different stages of muscle development.

BIOGRAPHICAL SKETCH

Su Deng was born in Sichuan, China on October 19th, 1984. She grew up in Chongqing, China, with her parents, Li Deng and Ya Dong, who were both professors at the Southwest Normal University. She graduated in 2003 from the affiliated middle school of Southwest Normal University and entered the College of Life Sciences at Peking University. During her second year in College, Su joined the Ecology Laboratory. Under the supervision of Dr. Chongren Xu, Su investigated the mechanism through which the transgenic Bt cotton changed the feeding behaviors of the non-target insects. Su later conducted her undergraduate thesis research in the Developmental Biology Laboratory under the supervision of Dr. Bo Zhang, where she used zebrafish as animal model to study brain development. After graduating with a Bachelor degree of Biotechnology from Peking University in 2007, Su entered the graduate school of Peking Union Medical College to study human genetics in Dr. Xue Zhang's Laboratory. Due to family reasons, Su quit graduate school after the first year. In 2008, Su came to United States and volunteered in Dr. Palmer's lab in Weill Cornell Medical School, where she studied how high sodium concentration inhibits Epithelial Na Channel (ENaC) through a feedback mechanism. The work from her and her colleagues was published on *Channels (Austin)*, 2015. In 2009, Su was admitted to the Physiology, Biophysics and System Biology Program in Weill Cornell Medical School. Starting from 2010, Su conducted her thesis research in Dr. Baylies' lab at Sloan Kettering Institute to investigate muscle development. We used both *Drosophila* muscle and mouse C2C12 cell culture as model system to study muscle formation. The research work from Su and her colleagues led to publications in *PloS Genetics* and *Development*.

ACKNOWLEDGEMENTS

First, I would like to thank my PhD advisor Dr. Mary Baylies, who offered me a position in her laboratory and mentored me through my PhD study. Without her mentorship, my thesis work could never be done. Mary allowed me to choose projects that I want to follow when I just joined her lab. She always provided support and detailed suggestions whenever I encountered difficulties in my work. While doing research in Mary's lab, I learned a lot from Mary: how she handles pressure, how she plans ahead of time, the way she gives presentations, and most importantly, her consideration and caring for others. I am very grateful for the opportunity she offered me that not only allowed me to do good science, but also to become a better person.

I would also like to thank Dr. Ingo Bothe, a postdoctoral research fellow in Mary's laboratory. He taught me the basic knowledge and technology to work in a *Drosophila* lab. With his help, I was able to make progression on my project shortly after I joined the lab. He also taught me to think logically and discussed with me the details of my experimental design. He also gave me guidance of how to build data into figures and how to write papers while I was trying to submit my work.

I would also like to thank members and former members of the Baylies lab, especially Mridula Balakrishnan and David Soffar, who worked together with me on the sarcomere project; Dr. Jonathan Rosen, Dr, Krista Dobi, Meg Distini and Dr. Victoria Schulman, who proof read my thesis and other written documents. I would also like to thank everyone in the Baylies lab for their critiques and advice on my work, as well as their technical and mental support that helped me during the past few years.

I appreciate my thesis committee members, Dr. Jeremy Dittman, Dr. Jennifer Zallen and Dr. Michael Overholtzer, as well as my former thesis committee member Dr. Alan Hall (1952-2015), for all the critiques and feedback on my thesis work and thesis writing. They helped me to get through the landmarks of my PhD study: the ACE, committee meetings, and, finally, the thesis defense.

I am also grateful to my friends and classmates in Weill Cornell Medical College, especially Peipei Guo and Dan Jin, who discussed my experiments with me and provided technical support for my work.

I also want to thank my family. I thank my parents for the love and education that they gave me. I also thank my parents-in- law who took care of my life during the last two years of my PhD study. And finally, I wish to thank my husband, Ping, and my son, Han-Guang, who made New York not only the place for study and work, but also a place with affectionate memories.

Table of Contents

LIST OF FIGURES

CHAPTER ONE:

CHAPTER TWO:

CHAPTER THREE (PAPER OPTION):

CHAPTER ONE:

INTRODUCTION

I. Overview

Actin is one of the most conserved and abundant proteins found in all eukaryotic cells. Globular actin (G-actin) functions like the Lego unit of the cell: it can polymerize into filaments (F-actin), which serve as one of the major components of a cell's cytoskeleton. Just like Legos can be used to build different architectural forms, actin can also form different structures to coordinate a variety of cell behaviors and functions.

The formation of actin structures is coordinated in a series of stages: intracellular and extracellular signals trigger actin filament assembly or disassembly, filament organization is then controlled by molecules that incorporate with actin, then finally, the pattern of the specific actin structure is regulated temporally by the dynamics of actin. The study of actin has attracted much interest because of the prevalence of actin and actin based structures and the behaviors that it controls in eukaryotic cells. Moreover, the complexity of actin regulation allows for precise spatial and temporal control of actin structures in specific cell types, which in turn provides possible therapeutic targets for diseases in which actin activity is misregulated, such as muscular dystrophy and tumor metastasis.

My thesis research investigates actin structures in muscles based on two rationales: 1) Muscle cells contains abundant actin, and the organization and dynamics of actin are critical for muscle shape and function. In fact, mutations that disrupt actin levels or organization are the major causes of muscular dystrophy such as nemaline myopathy, actin myopathy and intranuclear rod myopathy, and 2)

Myogenesis involves a series of actin-based cellular events, such as cytokinesis, migration, myoblast fusion, cell-cell adhesion, endocytosis, and contraction. These cellular events are also seen in other types of cells. Studying actin structures in muscles gives us insights to how these cellular events are regulated.

Drosophila provides an ideal system for studying muscles. As in humans, *Drosophila* muscle forms through a number of conserved steps, from specification, to fusion, to attachment to tendon cells and finally to sarcomere and myofibril formation. Unlike human skeletal muscles, which contain bundles of muscle fibers, *Drosophila* muscle has a simple structure, yet the signaling pathways and machineries required for muscle formation, and the basic contractile unit share similarities to what is found in humans. These similarities and highly tractable fly genetics allow us to study muscle in *Drosophila* and apply what we learn to humans.

At the time I started my thesis, it was known that actin plays important roles in both *Drosophila* myoblast fusion and sarcomere function. For myoblast fusion, Arp2/3, which polymerizes branched actin filaments, was identified as essential for remodeling actin networks at the site of fusion. However, questions remained as to how signals are transduced from membrane to actin cytoskeleton and trigger fusion. It was also unknown whether there are additional actin regulators other than Arp2/3 that play roles during myoblast fusion. In my thesis research, I identified two additional factors, the phospholipid PI(4,5)P2 and the formin Diaphanous (Dia), as required for myoblast fusion. I also elucidated that the actin regulator Dia, which builds linear actin filaments, is also required for sarcomere elongation. My study of the role of Dia in myogenesis answered the long-standing question of what elongates actin filaments at the fusion site and in the sarcomere. I also demonstrated how Dia interacts with other actin regulators to build different structures at different stages of muscle development.

To place my work into context, the first section of this chapter will introduce the basic concepts in myogenesis, with a focus on myoblast fusion and sarcomerogenesis. I will also summarize the similarities and differences in muscle development between vertebrates and *Drosophila*. To familiarize the reader with actin remodeling, the second section of Chapter One will present the current knowledge of actin regulation. Chapter Two presents our findings on the role of phospholipids during myoblast fusion. Chapter Three presents the role of the formin, *diaphanous,* during myoblast fusion in *Drosophila* embryos. Chapter Four investigates the interplay between the actin regulator Diaphanous and Scar. Chapter Five focuses on sarcomere formation and homeostasis in *Drosophila* adult flight muscles and demonstrates the role of Diaphanous during sarcomere assembly. Chapter Six presents the conclusion. Chapter Seven covers materials and methods, and Chapter Eight lists the references.

II. Muscle development in *Drosophila*

A. Muscle cell differentiation in *Drosophila* embryos

The *Drosophila* muscles develop from the mesoderm. The mesoderm is the middle germ layer of an early embryo. The formation and specification of the mesoderm in the *Drosophila* embryo occur in three sequential steps: the first is to establish the dorsal-ventral axis of the embryo through a Transforming Growth Factor-α (TGF-α)-like signaling pathway. The second step is to activate the Toll pathway in a group of cells localized at the ventral side of embryo, which constitute the presumptive mesoderm. The third step is the activation of zygotic genes that trigger mesoderm formation (Figure 1.1).

The establishment of dorsal-ventral polarity starts at oogenesis. The localization of the oocyte's nucleus restricts the distribution of *gurken* mRNA to the

Figure 1.1. An overview of mesoderm formation. A. Establishment of dorsal-ventral polarity in the oocyte through the Gurken-Torpedo pathway. The oocyte's nucleus localizes to the dorsal-anterior side of the oocyte and provides positional information to restrict active Gurken to this region. Gurken interacts with its receptor Torpedo on the dorsal follicle cells and establishes dorsal fate. On the ventral side, without inhibition by the Gurken-Torpedo pathway, Pipe is expressed and activates the Toll pathway in the ventral oocyte through a serine protease-dependent cascade. **B.** Spatial restriction of active Toll pathway. The serine protease cascade triggered by ventrally localized Pipe results in proteolytic cleavage and activation of Spätzle. Spätzle binds and activates the Toll receptor pathway in the ventral region of the embryo. **C.** Activated Toll receptor promotes nuclei-entry of Dorsal. When the Toll signaling pathway is inactive, Cactus and Dorsal form a complex within a cell's cytoplasm. Activation of the Toll pathway results in the degradation of Cactus, and allows Dorsal to enter the nucleus. **D.** The transcription factor Dorsal and its downstream targets Twist and Snail work together to establish mesodermal cell fates and initiate mesoderm invagination. **E-F.** Schematic diagrams show the formation of the mesoderm (green) through invagination of ventral cells during gastrulation. (Adapted with permission from (Hartenstein, 1993; Wakabayashi-Ito and Ip, 2013)).

Figure 1.1. An overview of mesoderm formation

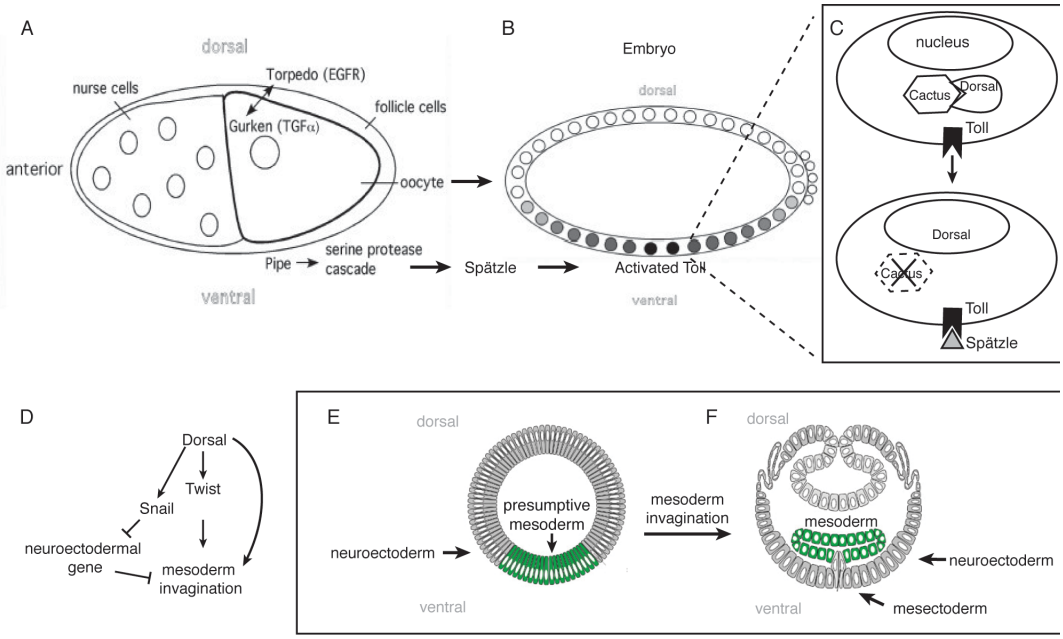

dorsal side of the oocyte (Neuman-Silberberg and Schüpbach, 1993). Gurken is a TGF-α-like ligand that can bind and activate its receptor Torpedo on the dorsal follicle cells (Roth et al., 1995). The interaction between Gurken and Torpedo triggers the establishment of dorsal-ventral polarity in the oocyte by activating the mitogen-activated protein kinase (MAPK) pathway (Nilson and Schüpbach, 1999). The Gurken-Topedo pathway also inhibits the expression of *pipe*, restricting Pipe expression to the ventral follicle cells (Sen et al., 1998). Pipe triggers a protease-dependent cascade reaction, which ultimately leads to cleavage of Spätzle at the ventral follicle cells (Chasan et al., 1992). Cleaved Spätzle binds its receptor Toll on the oocyte's membrane, and activates the Toll pathway on the ventral side of the embryo (Anderson et al., 1985; Hashimoto et al., 1991). Activation of the Toll pathway induces the degradation of Cactus (Belvin et al., 1995). Cactus is a member of the NF-**κ**-B inhibitor family that retains Dorsal in the cytoplasm. Upon Cactus degradation, Dorsal is allowed to enter the nuclei and induce specification of the mesoderm (Bergmann et al., 1996). Dorsal is an NF-**κ**-B transcription factor that regulates the expression of many zygotic genes. Among these genes, *snail* (Kosman et al., 1991) and *twist* are the most crucial ones, as the proteins that these genes encode are required for mesoderm specification and ventral invagination—a process that forms the mesoderm layer. Snail is a zinc-finger transcription factor that represses the expression of mesectodermal genes, and restricts neuroectoderm fate in the mesoderm (Ip et al., 1992; Kosman et al., 1991). Twist is a basic helix-loop-helix (bHLH) transcription factor that further activates the expression of downstream mesoderm proteins, such as *tinman (tin)* and *Drosophila myocyte enhancer factor 2* (*Dmef2)*. Twist is also a co-activator of Dorsal, which maintains the expression level of Snail (Leptin, 1991). Among the genes activated by Twist, *folded gastrulation (fog)*, which encodes a putatively secreted protein, is crucial for mesoderm invagination (Parks and Wieschaus, 1991). The secrete protein Fog

activates Rho GTPase through RhoGEF2 and triggers actin network remodeling (Barrett et al., 1997). The change of actin organization subsequently results in cell morphological changes, which are required for mesoderm invagination (Costa et al., 1994).

After invagination, the mesoderm cells undergo two rounds of cell division and migrate dorsally to coat the inner surface of the ectoderm (Leptin and Grunewald, 1990). The subsequent differentiation of the mesoderm depends on ectoderm-expressed proteins such as Decapentaplegic (Dpp) (Frasch, 1995; Staehling-Hampton et al., 1994), Hedgehog (Hh), Wingless (Wg) and Engrailed (En) (Azpiazu et al., 1996), as well as the pair-rule gene *even-skipped (eve)* (Azpiazu et al., 1996) and *sloppy paired (slp)* (Riechmann et al., 1997). Dpp is a TGFβ family member protein: high Dpp levels define the dorsal domain of the mesoderm and restrict the expression of *tin* to this region (Frasch, 1995). The NK homeodomain transcription factor Tin induces specification of the dorsal mesoderm into the visceral mesoderm, heart and dorsal muscles (Bodmer, 1993). The ventral domain of the mesoderm, influenced by Hh and Wg, will form the fat body and somatic muscles (Baylies et al., 1998). Eve and Slp are transcription factors that control segment patterning (Cadigan et al., 1994; Grossniklaus et al., 1992; Jaynes and Fujioka, 2004). Eve and Slp, in coordination with the ectodermally secreted Hh and Wg, establish the anterior-posterior section of each segment (reviewed in (Dobi et al., 2015)). In the Eve expressing compartment, Eve represses Twi expression in the mesoderm through the Notch signaling pathway (Tapanes-Castillo and Baylies, 2004). The combination of high Dpp and low Twi at the dorsal-anterior domain induces this region of the mesoderm to form the visceral mesoderm. In the ventral-anterior domain of the mesoderm, extrinsic Hh signaling and low Twi expression

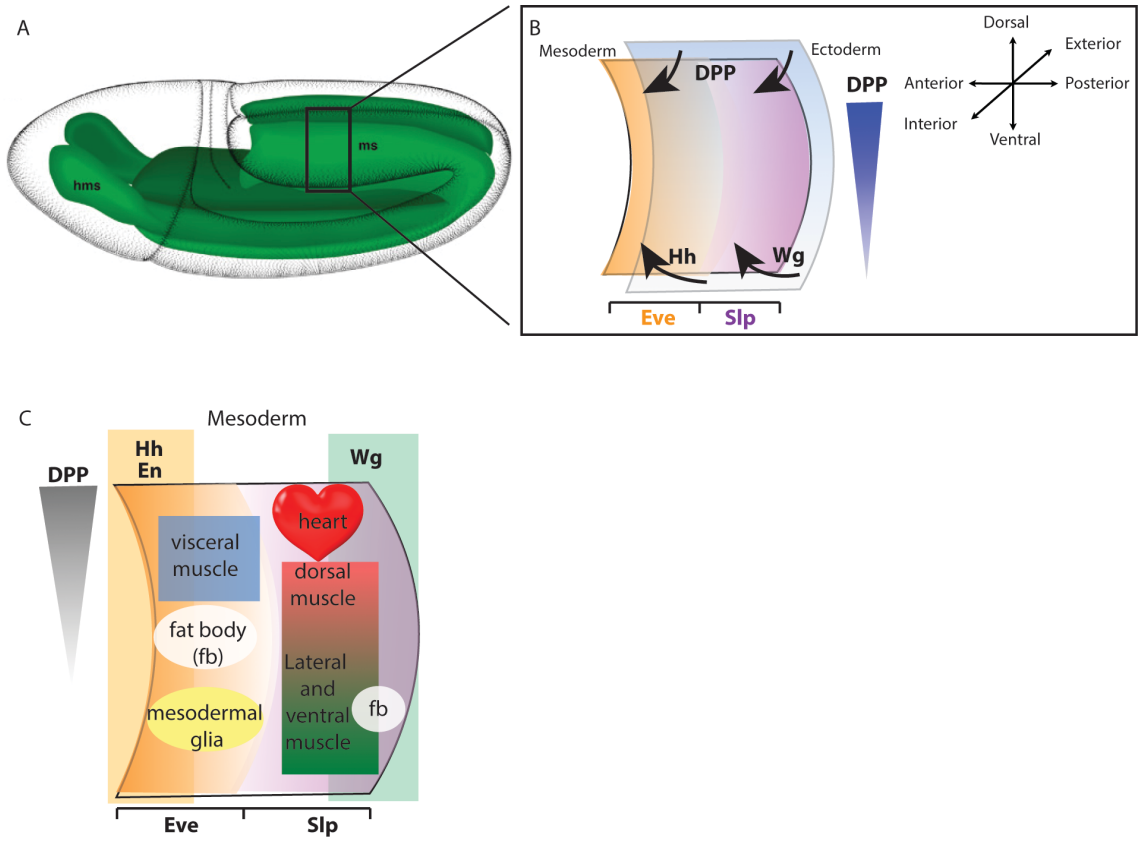

Figure 1.2. Signaling pathways that determine mesoderm partitioning. A. Diagram showing a stage 9 *Drosophila* embryo. The mesoderm is labeled in green. One presumptive hemisegment is shown in the boxed area. **B.** Ectodermally secreted proteins such as Decapentaplegic (DPP), Hedgehog (Hh) and Wingless (Wg) signal to the mesoderm, leading to subsequent partitioning of the mesoderm into different subtypes. **C.** Controlled by combinations of signaling pathways, cells in different regions of the mesoderm adopt a variety of cell fates, including cardiac muscles, visceral muscles, fat body, mesodermal glia and somatic muscles. Specification into somatic muscles depends on high Wg, Sloppy-Paired and Twist signaling at the ventral-posterior side of each mesodermal segment. (Adapted with permission from (Baylies et al., 1998; Hartenstein, 1993; Riechmann et al., 1998))

lead to the formation of the fat body and other mesoderm tissues. In the Slp expressing domain, Slp maintains the expression of Twi in this area of mesoderm (Riechmann et al., 1997). Dpp, Slp and Twi activities dorsally determine the formation of the heart, while Wg, Slp and Twi activities control the pattern of somatic muscle tissues (reviewed in (Baylies et al., 1998; Dobi et al., 2015)) (Figure 1.2).

After the allocation of the mesoderm to different tissues, the bHLH protein Lethal of Scute (L'sc) is expressed in clusters of promuscle cell groups, under the control of the RTK pathway (Carmena et al., 1995). In each cluster, a combination of the Notch and RTK-Ras signaling pathway activities restrict the expression L'sc to one cell—the muscle progenitor cell (Carmena et al., 1995; 1998b; Fuerstenberg and Giniger, 1998). Each progenitor cell then undergoes one round of asymmetric division to form either two founder cells (FC) or a FC and an adult muscle progenitor (AMP) (Carmena et al., 1998a; Ruiz Gomez and Bate, 1997). The cytoplasmic membrane-associated protein Numb plays a critical role in determining muscle fate. Numb antagonizes Notch-mediated lateral inhibition and allows the expression of muscle identity proteins in the muscle progenitor cells (Ruiz Gomez and Bate, 1997). Different combinations of identity transcription factor genes expressed in each muscle progenitor, such as *slouch, eve, Krüppel, apterous,* and *Nautilus,* determine the different cell identities of each FC, and hence, final muscle pattern (review in (Dobi et al., 2015)). Thirty FCs are specified, leading to the formation of 30 muscles in each hemisegment. Each muscle has its own unique size, shape and orientation (Figure 1.3).

After L'sc is restricted to one progenitor cell in each promuscle cell cluster, the remaining cells in the cluster adopt a fusion competent myoblast (FCM) fate

Figure 1.3. Overview of myoblast specification. A. Diagram of somatic muscle cell specification. The promuscle cell groups (blue) are determined by the expression of L'scute (L'sc). A combination of Notch and RTK-Ras signaling determines muscle progenitor cell fate (orange); the remainder of the promuscle cells become fusion competent myoblasts (FCMs, pink). Progenitor cells divide once to give rise to either two founder cells (FCs, grey) or a FC and an adult muscle progenitors (AMPs, yellow). **B.** The arrangement of the founder cells in one hemisegment of a stage 12 *Drosophila* embryo. Names of the final muscles are labeled with text. **C.** Color-coded muscles in one hemisegment of a stage 16 *Drosophila* embryo. Different colors show the expression patterns of muscle identity transcription factors. (Adapted with permission from (Artero et al., 2003; Dobi et al., 2015)).

Figure 1.3. Overview of myoblast specification.

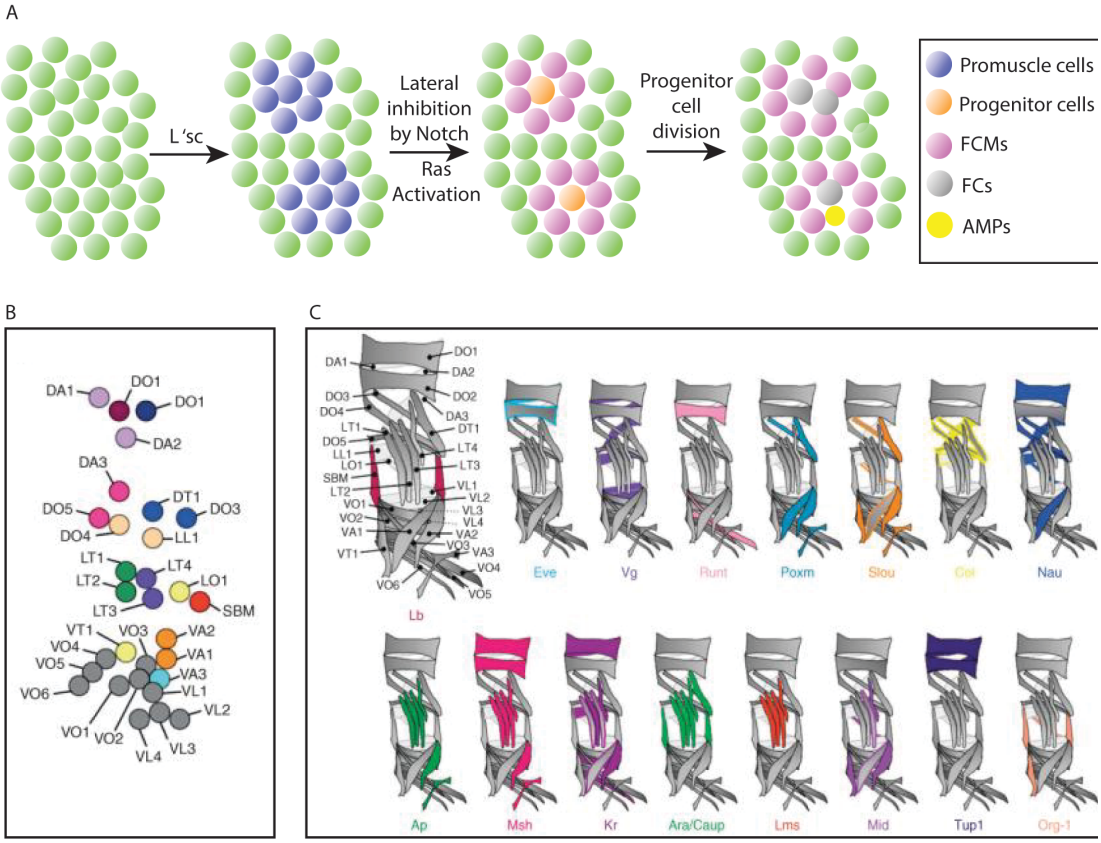

though Notch mediated lateral inhibition. Two key transcription factors, Lame duck (Lmd) and Tramtrack69 (Trk), are required for FCM specification. Lmd, a Gli superfamily protein, functions through activating and maintaining the expression of *Dmef2* and the FCM-specific fusion gene *sticks-and-stones (sns)* (Duan et al., 2001). Ttk, a zinc finger protein, functions through repressing the expression of FC genes, such as *dumbfounded (duf)*, in the FCMs (Ciglar et al., 2014). The specification of FCs and FCMs allows for fusion between the two cell types, and generates the syncytial muscle cells.

B. Myoblast fusion

Starting from embryonic stage 12 (7.5-9.5 hours AEL) and following the specification of FCs and FCMs, fusion between FCs and FCMs occurs to form the multinucleated body wall muscles (Richardson et al., 2008a). Later in the pupae stage, another wave of myoblast fusion occurs in order to generate the adult musculature.

The fusion between two cells requires a series of events. First, cells need to recognize and adhere to one another. Recognition and adhesion between the FC and FCMs are mediated by cell-specific immunoglobulin super family (IgSF) members. The IgSF members expressed in the FC are Dumbfounded (Duf) and Roughest (Rst) (Ruiz Gomez et al., 2000). Duf and Rst are transmembrane proteins that function redundantly to mediate recognition and adhesion (Strünkelnberg et al., 2001). The counterparts of Duf and Rst in FCMs are Sns and Hibris (Hbs) (Artero et al., 2001; Bour et al., 2000). Hbs can partially compensate for Sns function, but its activity is less efficient than Sns (Shelton et al., 2009). The interaction between Duf-Sns and Rst-Hbs is required for recognition and adhesion. Ectopic expression of Duf induces myoblast aggregation, but is insufficient to trigger fusion (Ruiz Gomez et al., 2000).

Figure 1.4. Molecular mechanisms that mediate myoblast fusion. A. Cellular events before fusion. Prior to fusion, a FC/myotube and a FCM recognize and adhere to each other. On the FCM side, actin filaments organize into a dense focus structure used to invade the opposing FC/myotube. On the FC/myotube side, a thin layer of actin filaments and myosin-II accumulates underneath the membrane and provides resistance against FCM invasion. **B.** Fusion machinery that mediates myoblast fusion. Recognition and adhesion between a FC/myotube and a FCM are mediated by transmembrane proteins Duf, Sns, Rst and Hbs. Signals from the membrane are transduced by PI(4,5)P2, which then triggers the remodeling of the actin cytoskeleton. Arp2/3 is one actin regulator that is required for myoblast fusion. In the FCMs, Arp2/3 is regulated by both SCAR and WASp. While in the FC/myotubes, Arp2/3 is only regulated by SCAR. (Adapted with permission from (Kim et al., 2015; Schulman et al., 2015)).

Figure 1.4. Molecular mechanisms that mediate myoblast fusion

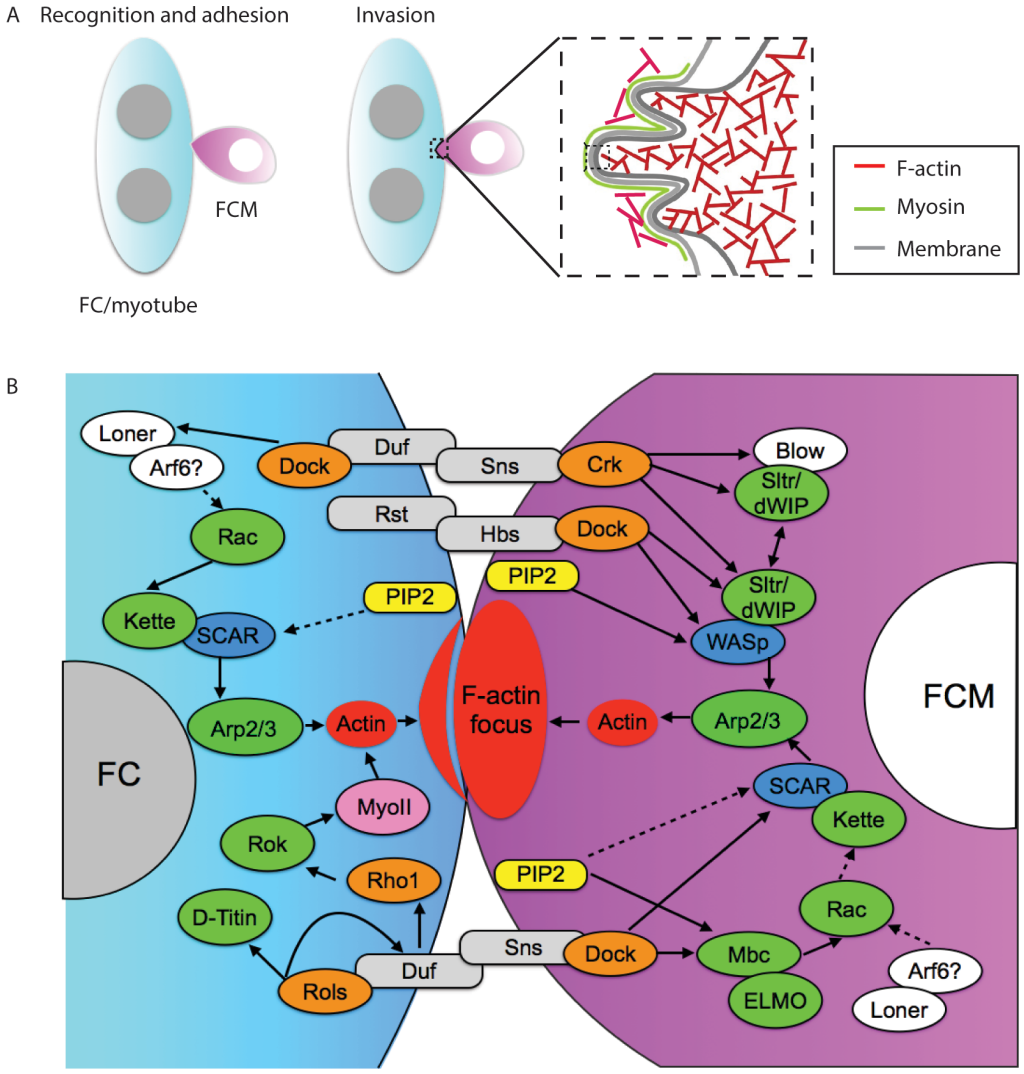

If the FC or myotube and FCMs are not in direct contact before adhesion, cell migration is required to bring two cells into close proximity (Richardson et al., 2007; Rochlin et al., 2010). After the cells adhere to one another, signals from these recognition and adhesion molecules cause the actin cytoskeleton in both the FC and FCM to undergo remodeling, resulting in a filamentous-actin (F-actin) based focus structure in the FCM, and a thin sheath of an F-actin network on the opposing inner membrane in the FC. The actin focus in the FCM mediates the formation of finger-like membrane protrusions (Sens et al., 2010). It is thought this actin structure at the fusion site provides the needed force to bring the lipid bilayers of the cells in close proximity, allowing for fusion pore formation. The fusion pore expands to allow cytoplasmic mixing and enables two cells to fuse into one. The binucleated myotube then reprograms the newly acquired nucleus to adopt the transcriptional profile of that particular FC and to repress the FCM program. The cell then prepares for another round of fusion (Baylies et al., 1998; Frasch, 1999) (Figure 1.4). Studies in *C. elegans* have revealed a role of fusogens such as EFF-1 and AFF-1 during epithelial cell fusion (Mohler et al., 2002; Sapir et al., 2007; Zeev-Ben-Mordehai et al., 2014). Fusogens are proteins that modify lipid bilayers to allow membrane fusion. Genetic screens performed thus far in *Drosophila*, however, have not identified a fusogen that is required for myoblast fusion, possibly due to maternally contributed fusogenic proteins, as well as redundant effects of more than one protein that contributes to the fusogenic activity or multiple fusogens (Chen, 2011).

Before I started my thesis, Arp2/3 was thought to be the only actin regulator that controlled actin rearrangement at the site of fusion. Arp2/3 can bind with an actin filament and polymerize new actin filaments at a 70-degree angle from a pre-existing actin filament. Arp2/3 is activated by the nucleation-promoting factors (NPFs): the Wiskott-Aldrich Syndrome protein (WASp) and SCAR (also known as

WAVE). The detailed molecular mechanism of Arp2/3 activation and function will be discussed in the "Actin cytoskeleton" section. In this section we will focus on the signaling pathways that trigger actin rearrangement during fusion. In my thesis work, we added another two factors that regulate myoblast fusion to the known fusion network: the phosphoinositide PI(4,5)P2 and the formin family protein Diaphanous (Dia). PI(4,5)P2 regulates both SCAR and WASp activity by localizing myoblast city (Mbc), Rac, and Blown fuse (Blow) at the fusion site (Bothe et al., 2014). Dia is another actin nucleation and polymerization factor that functions at the fusion site. Dia activity is also required for the proper localization of Arp2/3 regulators SCAR and WASp (Deng et al., 2015). The details of how PIP2 and Dia are involved in myoblast fusion will be discussed in Chapter Two, Chapter Three, and Chapter Four.

Signal transduction from the membrane to the actin cytoskeleton is partially mediated by the activity of Crk, as well as Dreadlock (Dock), the *Drosophila* homolog of Nck. Both Dock and Crk are adapter proteins with *src* homology 2 (SH2)/SH3 domains. Dock can interact with all four IgSF transmembrane proteins that have SH2 or SH3 domains, but it only genetically interacts with Duf, Sns and Hbs (Kaipa et al., 2013). In addition, rescue experiments using a series of *sns* deletions and site-directed mutations suggested that Sns functions through interacting with a complex array of proteins (Kocherlakota et al., 2008). In the FCMs, the Dock SH3 domain biochemically and genetically interacts with WASp, as well as the WASp regulator, Solitary (Sltr, also known as Vrp1 and DWip) (Kaipa et al., 2013). In both the FC and FCMs, Dock biochemically and genetically interacts with Arp2/3 NPF SCAR. Through a similar mechanism as Dock, Crk biochemically interacts with Sns. In an FCM, Crk physically interacts with the WASp regulatory proteins Sltr and Blow (Kim et al., 2007). Thus, the adaptor proteins Dock and Crk function as potential links

that transfer signals from the membrane to the actin cytoskeleton. In the FC, another adaptor protein that links the membrane and the actin cytoskeleton is Rolling pebbles (Rols, also known as Ants/Rols). Rols is recruited to the fusion site by Duf. In a positive feedback loop, Rols replenishes Duf at the membrane, and thus enables the additional rounds of fusion (Menon et al., 2005). Rols interacts with two proteins that regulate the actin cytoskeleton organization: Myoblast city (Mbc) (Chen and Olson, 2001; Rau et al., 2001) and D-titin (Menon and Chia, 2001). Mbc is the *Drosophila* homolog of the human protein DOCK180, which mediates actin rearrangements by acting as a guanine nucleotide exchange factor (GEF) for the small GTPase Rac. However, recent data suggest that the downstream target of Rols is not Mbc: rescue experiments suggest that the activity of Mbc is not required in FC for fusion. Another actin cytoskeletal protein that can bind to Rols is D-titin (Menon and Chia, 2001). D-titin is recruited to the fusion site by Rols, and mediates myoblast fusion in a mechanism that remains unclear. It also is involved in maintaining myotube morphology (Menon and Chia, 2001; Zhang et al., 2000). Recently study also reported the requirement of the non-muscle myosin IIA (NM-MHC-IIA) during myoblast fusion. NM-MHC-IIA is involved in the formation of the cortical actin wall in FC/myotube, as well as the appearance of the membrane-bound vesicle-like structures required for fusion pore formation (Duan and Gallagher, 2009).

While Mbc appears not to be required by the FCs during fusion, Loner, another GEF that regulates actin rearrangements, is required in FCs to mediate fusion. Loner is recruited to the fusion site by Duf and Rst (Bulchand et al., 2010). Domain analysis suggests that the function of Loner is to recruit and activate the small GTPase dARF6 at the fusion site. Loner and dARF6 control the membrane localization of Rac (Chen et al., 2003). However, *arf6* maternal/zygotic null mutants

does not affect myoblast fusion (Dyer et al., 2007), and the fusion phenotype in a dominant negative *dARF6* background is not as severe as that in the *loner* mutant, suggesting the real downstream target of Loner is another GTPase, or a possible redundancy with other dARF family members such as dARF1 (Chen et al., 2003). Once activated, Rac regulates the function of SCAR, and is critically important for both FCs and FCMs to mediate fusion. The activity of SCAR is controlled by the pentameric complex WRC (the WAVE/SCAR regulatory complex). The WRC is composed of Kette/Nap1, Sra1, Abi, Hspc300 and SCAR itself (Eden et al., 2002). Rac activity is essential for the localization of the WRC to the fusion site, as well as activation of SCAR via the release of the SCAR VCA domain from an inhibited state (Chen et al., 2010; Gildor et al., 2009). The molecular mechanism of SCAR activation will be discussed in detail in the "Actin cytoskeleton" section. As part of the WRC, Kette is also essential for myoblast fusion as it controls the localization and stability of SCAR (Richardson et al., 2007). It has not been reported whether the other WRC components, Sra1, Abi and Hspc300, play a role in myoblast fusion. This may be due to a lack of null mutant alleles, as well as a maternal supply of protein/mRNA in the embryo that masks the role of these proteins during the time period in which fusion takes place. In the FC, SCAR activates its downstream target, Arp2/3, and rearranges the actin cytoskeleton into a thin sheath along the fusion site (Sens et al., 2010).

In an FCM, SCAR activity is also regulated by Rac. However, Rac localization and activation is not regulated through Loner/Arf6/Arf1, but, as discussed earlier, through Mbc (Haralalka et al., 2011). Mbc is recruited to the fusion site by the phospholipids PI(4,5)P2 (PIP2) (Bothe et al., 2014). Mbc can bind with ELMO with its SH3 domain and form the Mbc/ELMO complex. The GEF activity of Mbc/ELMO is tightly regulated during myoblast fusion, and it controls the level of active Rac. Both

overexpression and loss of function of Mbc/ELMO cause defects in myoblast fusion, which are reminiscent of constitutively active Rac and Rac mutants, respectively (Geisbrecht et al., 2008). When activated by Mbc/ELMO, Rac, in turn, binds to the WRC and regulates Arp2/3 activity at the fusion site.

In addition to SCAR, the other NPF, WASp, also regulates Arp2/3 at the fusion site. Unlike SCAR, which functions both in FCs and FCMs, WASp activity is only required in the FCM. The activity of WASp is regulated by Blow and Sltr. The WASp-homology-1 (WH1) domain in WASp can bind to the WASp-binding domain (WBD) in Sltr (Ramesh and Geha, 2009). The interaction between WASp and Sltr is required to stabilize and localize WASp at the fusion site (Jin et al., 2011). The interaction is disrupted when Blow competes with WASp for Sltr WBD binding (Jin et al., 2011). Thus, after cell recognition and adhesion, a signal is transduced from the membrane via the adaptor protein Crk, which recruits Blow and Sltr to the site of fusion. At the fusion site, the WASp-Sltr complex promotes actin polymerization by regulating Arp2/3 activity. Blow suppresses WASp activity by competing with WASp for Sltr binding and by dissociating the WASp-Sltr complex. Since the binding affinity between Blow-Sltr is lower than WASp-Sltr, dissociated WASp can bind back to Sltr again and promote another round of branched actin polymerization (Jin et al., 2011).

C. Muscle maturation

After myoblast fusion is completed, multiple events take place to ensure final muscle differentiation, including myotube elongation, myotendinous junction formation, myonuclear positioning, and sarcomere assembly.

Myotendinous junction

The myotendinous junction is the site where a muscle forms contact with tendon cells. The force generated from muscle sarcomere contraction is transmitted to the tendon cell from the muscle via extracellular connective tissues, which altogether make up the myotendinous junction. The components that link the extracellular matrix to the cells, which form the myotendinous junction, include Laminin (Lam), Integrin, and Thrombospondin (Tsp). These, in turn, link to actin filaments both in the muscles and in the tendon cells (Figure 1.5).

The specification of tendon cells occurs around stage 12 (AEL 7.5h). Both Wg and Hh signaling is required in the ectoderm for tendon precursor specification. Both Wg and Hh promote the expression of the Egr-like transcription factor StripeB (SrB) in the epidermal cells at the segment borders. SrB is an isoform of the *stripe* gene that regulates the specification of tendon progenitor cells through its transcriptome (reviewed in (Schweitzer et al., 2010)). One downstream target of SrB is Held out wings (How), which suppresses SrB expression through a negative feedback loop. How maintains the low SrB level in the tendon progenitor cells and inhibits further tendon cell differentiation (Nabel-Rosen et al., 2002). Several downstream targets of SrB are required to mediate muscle targeting to tendon cells, such as *slit, Leucine-rich tendon-specific protein (Lrt), Thrombospondin (Tsp),* and *slowdown (slow)*. Tsp is an ECM protein and a component of the myotendinous junction; Slow can temporarily sequester Tsp to prevent myotendinous junction prematurity (Gilsohn and Volk, 2010). Both Slit and Lrt can bind with the transmembrane protein Robo (present at the muscle surface) and guide the elongation and targeting of muscles to tendon cells (Kramer et al., 2001). Muscle elongation is controlled by the transmembrane protein Kon-tiki and the adaptor protein Echinoid. Both proteins are located at the muscle elongation tips, promote muscle cell elongation and stabilize the connection between the muscle and tendon

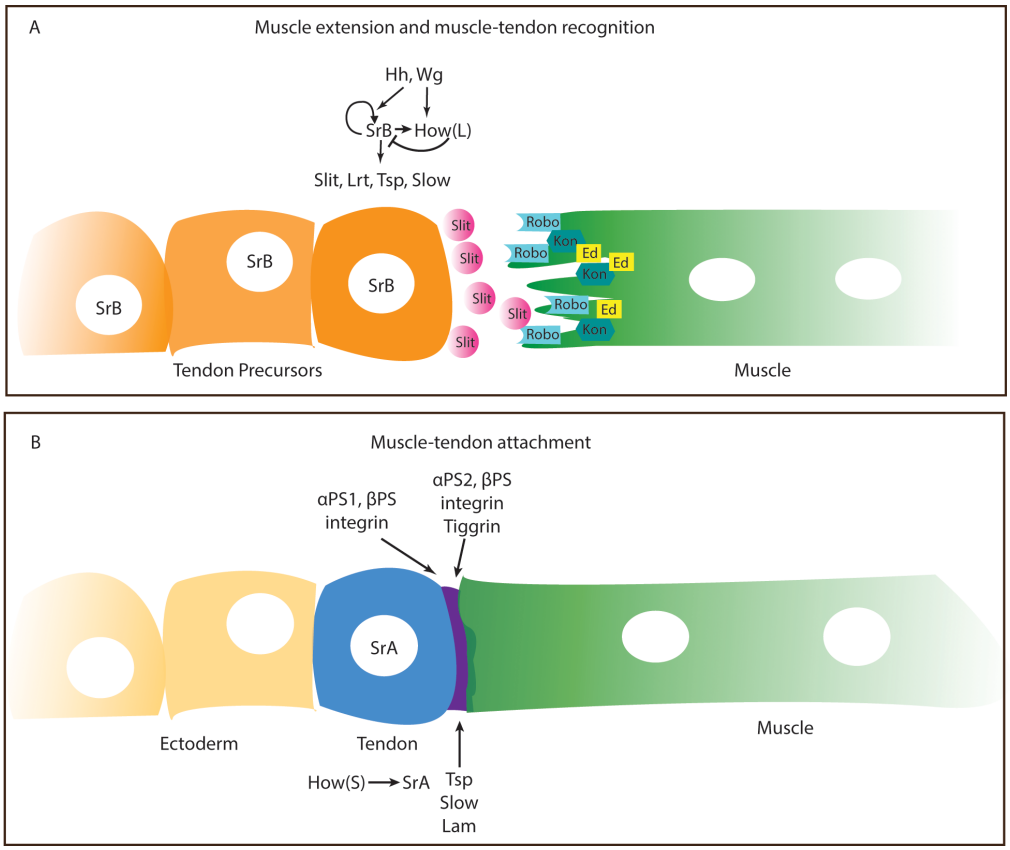

Figure 1.5 Overview of myotendinous junction formation. A. Diagram showing signaling pathways that guide muscle elongation and muscle-tendon recognition. At stage 12, tendon precursor cells express SrB, under the control of Hh and Wg. The level of SrB is controlled by its downstream target How through an inhibitory feedback mechanism. SrB also mediates the expression of ECM proteins such as Slit, Tsp and Slow. On the muscle side, transmembrane proteins Robo, Kon-tiki and the adaptor protein Echinoid (Ed) are required for targeting the muscle to tendon cells. **B.** Diagram showing proteins at the site of muscle-tendon attachment. αPS1- βPS expressed in the tendon cell binds with Lam in the ECM, while αPS2- βPS expressed in the muscle cell binds to Tiggrin and the tendon cell secreted ECM components, Tsp and Slow, to mediate attachment to the ECM. (Adapted with permission from (Schweitzer et al., 2010))

cell ECM (Schnorrer et al., 2007). After muscles attach to tendon cells, the EGFR ligand, Vein, is secreted by muscles into the muscle-tendon junction site. Vein activates the EGFR signaling pathway, which promotes terminal differentiation of the tendon cells that connect with muscles, while suppressing differentiation of the neighboring tendon precursors (Yarnitzky et al., 1997).

Mature tendon cells express the tendon specific proteins Tsp, Laminin (Lam), αPS1 integrin and βPS integrin. Muscle cells express Tiggrin, αPS2 integrin and βPS integrin. αPS1- βPS heterodimers can bind with Lam in tendon cells, while αPS2-βPS can bind with both Tiggrin and the tendon cell secreted ECM component Tsp, and mediate attachment to the ECM (reviewed in (Schweitzer et al., 2010)).

Myonuclear positioning

After fusion is complete, each myotube contains 3-25 nuclei, depending on the specific muscle. These myonuclei need to be positioned at specific locations in order to ensure proper muscle function. Using the four lateral transverse (LT) muscles as an example, the positioning of myonuclei is a multi-step process. Before myonuclear movement, all the nuclei in the LT muscles are located at the ventral side of the myotube (stage 14, 10h AEL). At stage 15 (11.5h AEL), the myonuclei separate into two clusters, one dorsal and one ventral; these migrate towards the opposite ends of the myotube, completing this step at the end of stage 16 (13h AEL). At stage 17 (18h AEL), nuclei in the two clusters move away from the poles and distribute evenly throughout the myotube (Metzger et al., 2012).

The proper positioning of myonuclei involves the microtubule cytoskeleton and motor proteins that move on microtubules. Still using LT muscles as an example, the microtubules originate from the nuclear envelope of each nucleus and

extend towards the poles of the LT muscle fiber. The microtubule-associated protein Ensconsin (Ens) links the motor protein Kinesin to the microtubule cytoskeleton. Kinesin crosslinks microtubules and slides microtubules to opposite directions, pushing nuclei away from each other (Metzger et al., 2012). Kinesin can also translocate a nucleus directly by pulling the nucleus at the front edge (Folker et al., 2014), a process that also requires the motor protein Dynein to function at the rear edge. After being transported to the cell cortex by Kinesin, Dynein can also function at the cell cortex and relocate the myonucleus by pulling microtubules to the cortex (Folker et al., 2012).

Another protein that plays a role in *Drosophila* myonuclear positioning is MSP-300. MSP-300 contains the Klaricht-Anc-1-Syne Homology (KASH) domain, and spans the outer nuclear membrane. The function of MSP-300 is thought to anchor the nucleus in place, since MSP-300 loss of function does not affect nuclear relocation in embryos, but it does impair nuclear position in later larval stages (reviewed in (Schulman et al., 2015)).

Sarcomerogenesis

A sarcomere is the basic contractile unit in striated muscles. The assembly of sarcomeres in a *Drosophila* embryo occurs at stage 17 (18h AEL). Sarcomeres arrange one after another to form a myofibril, and many myofibrils form within the muscle fiber. The proper formation of sarcomeres is critical for larval behaviors such as crawling and feeding.

Sarcomeres are muscle structures that are well conserved across several species. Sarcomeres are composed of actin thin filaments and myosin thick filaments, as well as other sarcomeric proteins including α-actinin, Zasp, Tropomodulin (Tmod). Since sarcomere structure is similar in larval musculature

and adult musculature, sarcomerogenesis will be discussed in detail in the "Sarcomerogenesis in *Drosophila* indirect flight muscles" section.

D. Adult muscle formation

The *Drosophila* adult muscles form during metamorphosis. Metamorphosis is the process in which the majority of larval tissues are eliminated, and the adult body plan is established. The adult tissues are generated either from differentiation of stem cells, or from remodeling of larval cells. At the beginning of metamorphosis, most of the muscles are destroyed through histolysis, but a few muscles, such as the dorsal oblique (DO1-3) muscles, escape degradation and serve as templates for the adult muscles (Fernandes et al., 1991).

Based on their morphology and gene expression, the adult somatic muscles can be divided into two types: tubular muscles and fibrillar muscles. The abdominal, jump, leg and direct flight muscles are tubular muscles, while the indirect flight muscles (IFMs) are fibrillar muscles (Peckham et al., 1990). Tubular muscles have aligned myofibrils. In some tubular muscles, such as the leg muscle, the myonuclei are located in the tube center. The fibrillar muscles have distinct, unaligned myofibrils. The myonuclei in the fibrillar muscles are usually located between myofibrils. The fibrillar muscles in *Drosophila* IFMs and vertebrate skeletal muscles have similar structures (Fernandes et al., 1991).

The transcription factor Spalt major (Salm) determines fibrillar cell fate in IFMs. Salm functions downstream of the transcription factor *vestigial (vg)*. In turn, Salm maintains Vg levels through a feedback loop. Salm drives the expression of IFM-specific proteins, such as Fln, TpnC4, and determines the fibrillar muscle cell type in IFMs (Schönbauer et al., 2011). In addition to regulating IFM-specific protein expression, Salm activates the expression of the ribonucleic acid-binding

protein Arrest (Aret). Through regulating alternative splicing, Arrest determines the isoforms of sarcomeric proteins, such as Sallimus (Sls) and Zasp52 (Oas et al., 2014).

IFMs control the contraction of the thorax and enable flight. In each hemi-thorax, there are 7 dorsal ventral muscles (DVMs) that regulate the upstroke of wings, and another 6 dorsal longitudinal muscles (DLMs) that regulate the downstroke of wings (AC, 1978). The DVMs form *de novo* from adult muscle progenitors (AMPs), fusing during the early pupal stage (8-36 hours APF), while DLMs form through fusion between AMPs and muscle templates that are preserved during histolysis (Fernandes et al., 1991).

The AMPs derive from muscle progenitor cells. In the embryonic stage, a muscle progenitor cell divides once into two sibling cells. The two sibling cells give rise to either two founder cells, or one FC and one AMP based on asymmetric expression of Numb (Carmena et al., 1998b; Ruiz Gomez and Bate, 1997). Under control of the Notch signaling pathway, *twi* is expressed in AMPs. The transcription factor Twi then triggers the expression of genes that repress differentiation, such as the *Holes in muscle (Him)*, thus maintaining the undifferentiated state of the AMPs (Anant et al., 1998; Liotta et al., 2007). AMPs proliferate at the larval wing imaginal discs (Fernandes et al., 1991). The differentiation of adult muscles requires the inhibition of the Notch pathway, which subsequently leads to decreased levels of Twi and Him (Anant et al., 1998). The elimination of Him allows the activation of Dmef2, which functions as the major differentiation factor for adult muscle development (Caine et al., 2014; Soler and Taylor, 2009) (Figure 1.6).

The signaling pathways that regulate myoblast fusion in *Drosophila* adult muscles are not fully understood. According to our current knowledge, the

Figure 1.6 Formation of *Drosophila* adult muscles. A. Diagram showing the development of indirect flight muscles (IMFs) in adult *Drosophila.* Starting from 0 hours after pupae formation (APF), larvae muscles are degraded through histolysis. Only the larval muscles that serve as templates for the dorsal ventral muscles (DVMs) are preserved during histolysis. At 12 hours APF, histolysis is completed. Adult precursor cells (AMPs) from the wing discs migrate to the muscle-forming region. Around 16 hours APF, DVM templates split and fuse with the myoblasts. At the same time, dorsal longitudinal muscles (DLMs) are formed *de novo* through myoblast fusion. Indirect flight muscles are formed by 24 hours APF. **B.** Signaling pathways involved in AMP differentiation. In the wing discs, the AMPs proliferate and migrate to muscle-forming regions. In the wing discs and during migration, AMP differentiation is repressed by the Notch signaling pathway, which triggers expression of *twi* and inhibits the expression of fusion genes such as *sns.* When migration is completed, the Notch pathway is inhibited, which subsequently leads to the expression of genes that mediate fusion. **C.** Diagram showing muscles of adult *Drosophila.* **D.** Diagram showing the two types of IFMs: the dorsal ventral muscles (DVMs) that regulate the upstroke of wings, and the dorsal longitudinal muscles (DLMs) that regulate the downstroke of wings. (Adapted with permission from (Dickinson, 2005; Dutta et al., 2004; Gildor et al., 2012; Hartenstein, 1993))

Figure 1.6 Formation of *Drosophila* adult muscles

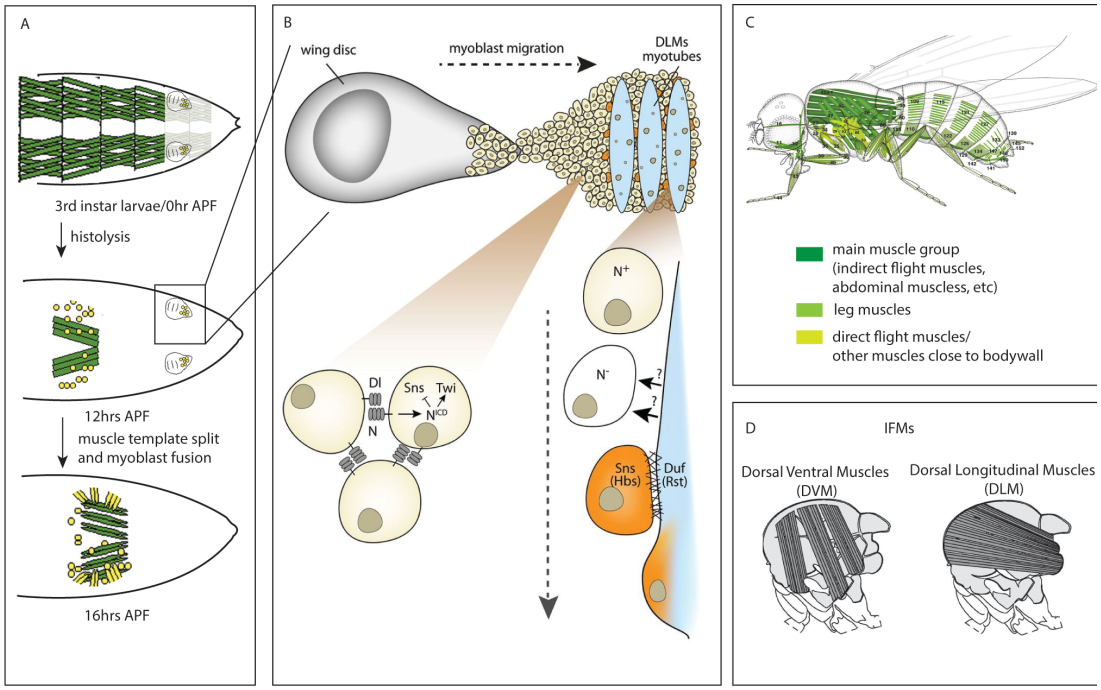

mechanisms that regulate myoblast fusion during adult myogenesis are similar to those that regulate embryo myogenesis. The same transmembrane proteins Duf, Rst, Sns and Hbs are required to mediate cell recognition and adhesion (Gildor et al., 2012). After adhesion, the myoblast flatten on the myotube, such that the cell membranes are in tight apposition (Dhanyasi et al., 2015). Receiving signals from the cell membrane, actin accumulates at the fusion site and forms a focus structure, which enables the formation and expansion of fusion pores. As with embryonic myogenesis, actin rearrangement during adult myogenesis requires both WASp and SCAR (Mukherjee et al., 2011). Despite all the similarities, however, there are differences between embryonic and adult myogenesis. In the embryos, FCMs and FCs are positioned relatively close to one another before fusion. FCMs in contact with FCs/myotubes are responsible for the early fusion events. FCMs that are located more internally need to migrate before making contact and fusing with the FCs/myotubes (Richardson et al., 2008b). During adult myogenesis, myoblasts need to migrate long distances from the imaginal discs to the muscle template/myotubes. More importantly, during migration, myoblasts maintain a semi-differentiated state through the Notch signaling pathway. Each myoblast expresses the Notch ligand, Delta, and represses the differentiation of its neighboring cells. Notch signaling decays when myoblasts reach the vicinity of the myotubes, and this allows for the terminal differentiation of myoblasts and the expression of FCM markers such as Sns (Gildor et al., 2012).

E. Sarcomerogenesis in *Drosophila* indirect flight muscles

Sarcomere structure

Drosophila indirect flight muscles (IFMs) are fibrillar muscles formed by parallel, but unaligned, myofibrils. Myofibrils are composed of a highly ordered array of sarcomeres (reviewed in (Schulman et al., 2015)). The most important components

of a sarcomere are the actin thin filaments and myosin thick filaments. In each sarcomere, actin thin filaments are arranged along the long axis of the muscle and attach to the Z-discs, which are located at the ends of each sarcomere. Myosin is a protein with a fibrous tail and globular head. Myosin is arranged into a bipolar structure with tails facing the middle and attached to the M-line, while heads are positioned at the ends. Both the Z-disc and M-line can be visualized as electron-dense lines under electron microscopy. Muscle contraction is achieved when thin filaments and thick filaments slide across each other. In addition to the Z-disc and M-line, there are also other distinct regions such as the A-band (A for Anisotropic) and the I-band (I for isotropic). The A-band covers the length of the thick filaments, while the I-band is the area where thin filaments do not overlap with thick filaments (Figure 1.7).

The relative movement of thin and thick filaments is mediated by the ATP/ADP-dependent conformational change of the myosin head. Signals from motor neuron synapses are relayed to the muscle, changing the membrane potential of muscles and triggering the release of calcium from the sarcoplasmic reticulum (SR). Calcium binds to Troponin C and changes its conformation, revealing myosin-binding sites on the actin thin filaments. The myosin-ADP then binds to the actin filament, followed by the dissociation of myosin and ADP. The release of ADP triggers distortion of the myosin head, which bends and therefore pulls the actin filament. The simultaneous pulling of actin filaments by all the myosin in the same sarcomere generates the contractile force. The releasing of actin from the myosin head is triggered when ATP binds to the myosin head and changes the myosin conformation. When calcium is transported back into the SR, the muscle relaxes as Troponin C masks the myosin-binding sites on the thin filaments (reviewed in (Geeves and Holmes, 1999)). In *Drosophila* IFMs, muscle contraction is initiated

Figure 1.7. Dissecting the mechanism of muscle contraction. A. Diagram showing the organization of *Drosophila* flight muscles at different scales. **B.** Images taken by a Transmission Electron Microscope showing a section of three myofibrils. Each myofibril is subdivided by a Z-disc (black line, arrows) into sarcomeres. Scale bar: 5 μm. **C.** Basic structure of a sarcomere. Sarcomeres are composed of thin (actin) filaments and thick (myosin) filaments. The region where thin filaments attach is called a Z-disc, and the site where thick filaments attach is the M-line. The region spanned by thick filaments is the A-band. The I-band is the region where there are no thick filaments. **D.** Model of molecular mechanisms of muscle contraction. The relative movement between thick and thin filaments requires energy released from ATP hydrolysis, as well as a conformational change of the myosin head. (Adaped with permission from (Hwang and Sykes, 2015; Vigoreaux, 2005))

Figure 1.7. Dissecting the mechanism of muscle contraction

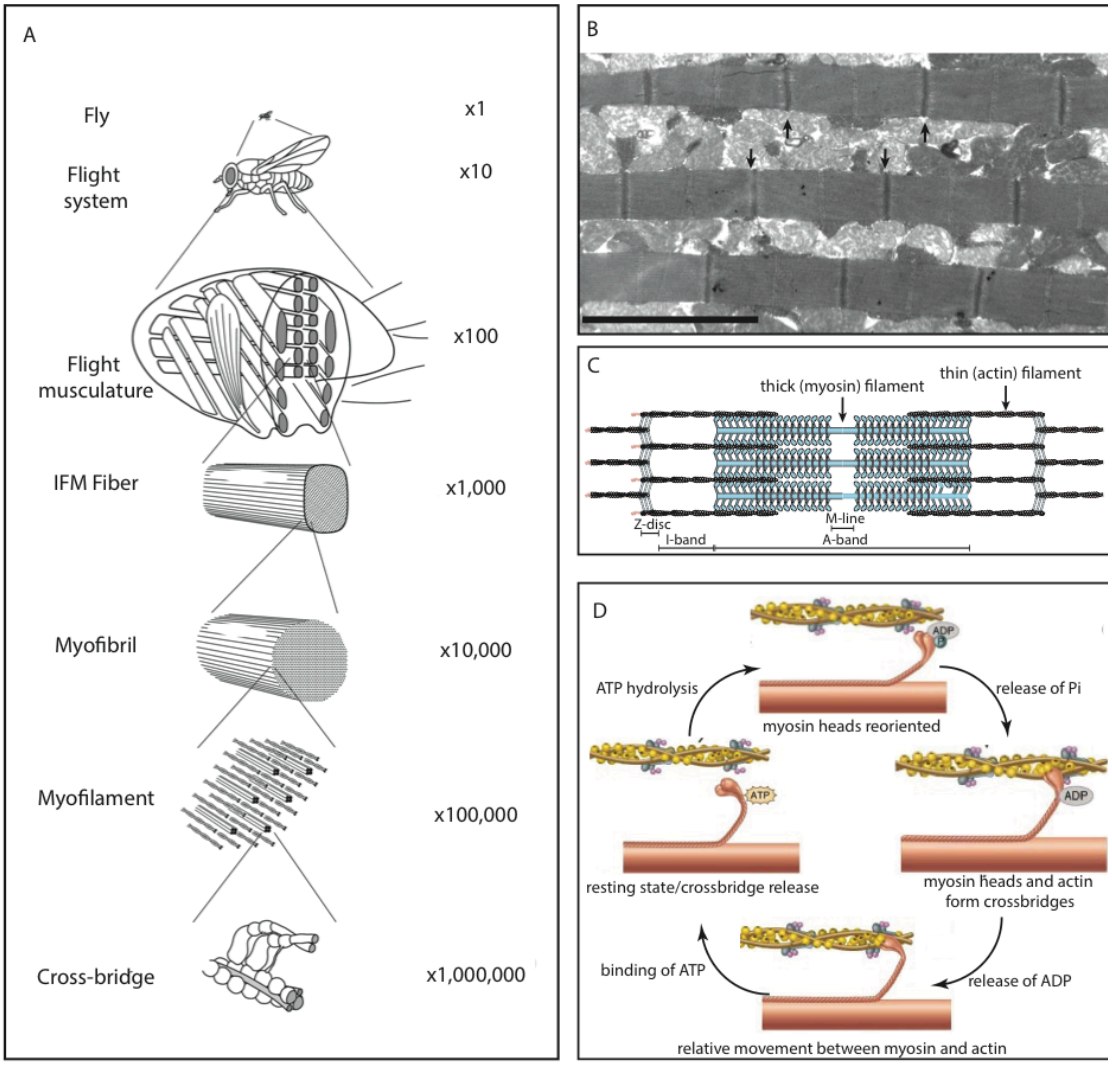

through a similar mechanism. However, the oscillation frequency required for flight is too rapid for the influx and outflux of calcium; therefore, the asynchromous IFMs adapted other ways to maintain muscle contraction. IFMs can be activated mechanically by periodic stretching, and low calcium concentration is enough to maintain constant contraction and relaxation of the IFMs (reviewed in (Bullard and Pastore, 2011)). Since IFMs are very sensitive to stretching, special structures are required to ensure IFMs' stiffness. *Drosophila* IFMs maintain stiffness by expressing IFM-specific isoforms of sarcomeric proteins such as Tropomyosin (isoform 127) and Troponin (TnT) (Bullard and Pastore, 2011). Another mechanism that sustains sarcomere stiffness is through a connecting filament that links a thick filament and actin. The vertebrate connecting filament contains the elastic protein Titin (also known as connectin), which extends from a Z-disc to the M-line. In *Drosophila* IFMs, elastic proteins do not extend from a Z-disc to the M-line, instead, the function of Titin is delegated to smaller proteins such as Projectin and Sls protein isoforms. Elastic proteins in *Drosophila* usually contain the immunoglobulin (Ig) domain, elastic PEVK domains, and fibronectin (Fn) domains (reviewed in (Bullard et al., 2005)). In the IFMs, *sls* encodes three different isoforms through alternative splicing: D-Titin (Sls), Zormin, and Kettin. D-Titin and Kettin extend from a Z-disc to the end of the A-band (Machado and Andrew, 2000). Zormin is the N-terminal part of Sls; it exists at both the Z-disc and the M-line. In the non-flight muscles such as leg muscles, *sls* encodes longer isoforms with different elastic PEVK regions, therefore contributing to the different length that sarcomeres are able to extend to in different type of muscles (Burkart et al., 2007).

The elastic protein D-Titin is anchored to a Z-disc through α-actinin. α-actinin is a member of the F-actin crosslinking superfamily proteins o(Oikonomou et

al., 2011). It is involved in linking the actin cytoskeleton to different transmembrane proteins. In *Drosophila* muscles, α-actinin localizes at Z-discs in all types of larval and adult muscles (Saide et al., 1989; Vigoreaux et al., 1991). It contains an actin-binding domain, a calcium-binding domain, and an internal domain composed of four spectrin repeats (Blanchard et al., 1989). α-actinin is required for Z-disc stabilization.

The size of a sarcomere is thought to be set by the ruler protein Lasp. Lasp belongs to the nebulin family of proteins. Nebulin is an actin-binding protein, which contains 185 copies of nebulin repeats (Pappas et al., 2011). As the only member of the nebulin family in *Drosophila*, Lasp is detectable in *Drosophila* larva body wall muscles (BWMs), jump muscles and IFMs. In BWMs and jump muscles, Lasp localizes at the Z-disc, as well as the A-band. In IFMs, however, Lasp is only found at the edge of the Z-disc (Fernandes and Schöck, 2014). Lasp contains a LIM domain, nebulin repeats, and SH3 domain. Both LIM and nebulin domains are important for Lasp localization in BWMs, but deletion or mutation of both domains does not change Z-disc localization in both BWMs and IFMs (Fernandes and Schöck, 2014). Lasp determines the length of a sarcomere by setting the thin filament length, either by binding with capping proteins CapZ (Pappas et al., 2008), or by binding and stabilizing the thin filament with nebulin domains (Pappas et al., 2010). It also determines the diameter of a sarcomere by interacting with myosin and setting filament spacing at the A-band. Lasp also sets the width of the I-band by interacting with α-actinin (Fernandes and Schöck, 2014).

III. Muscle development in vertebrates

Muscle cells make up about half of human body mass. Muscle function is crucial to many basic physiological activities, such as breathing, heartbeat and locomotion.

Based on differences in structure, localization, ways of stimulation, and function, muscles can be categorized into smooth muscles, cardiac muscles and skeletal muscles. Among them, skeletal muscle is the most abundant. Skeletal muscle is striated muscle that attaches to tendon cells and primarily exhibits voluntary contraction. In this section I summarize the process of vertebrate skeletal muscle development, aging and repair, and compare vertebrate muscles with *Drosophila* muscles.

Vertebrate muscle develops from the mesoderm. Similar to *Drosophila* development, the allocation of the mesoderm into different types also occurs during early development. The anterior-most portion of the paraxial mesoderm gives rise, in the trunk, to somites, which differentiate along the dorsal-ventral axis. The dorsal epithelial region of the somites then differentiates into the dermomyotome, which gives rise to muscle and the dermis. The ventral region differentiates into the sclerotome, which gives rise to cartilage and the skeleton (reviewed in (Tajbakhsh and Cossu, 1997)). Similar to *Drosophila*, the specification of muscle progenitor cells also requires a combination of signals from adjacent tissues. The BMP signal from the lateral plate mesoderm (Pourquié et al., 1996), Wnt signaling from the ectoderm (Fan et al., 1997) and the neural tube, as well as Sonic hedgehog signaling (Shh) from the floor plate and notocord (Münsterberg et al., 1995) are all required for the subdivision of somites and the development of muscles (Figure 1.8). Extracellular signals induce the expression of Paired Box 3 (Pax3) and Pax7 in the somites (Duprez et al., 1998). Pax genes have dual roles: they enhance the proliferation of muscle precursor cells (Relaix et al., 2005), and they activate the expression of the myogenic regulatory factors (MRFs) (Sato et al., 2010). MRFs are a family of four transcription factors: MyoD, Myf5, myogenin and MRF4. MRFs are transcription factors that activate the expression of genes required for muscle differentiation.

MyoD and Myf5 are the first MRFs expressed in muscles and function redundantly to trigger myoblast specification. Mice doubly mutant for *Myf5 and MyoD* have no muscle progenitor cells and therefore no muscle formation (Rudnicki et al., 1993). Myogenin is thought to function after muscle progenitor formation and regulate the terminal differentiation of committed myoblasts (Hasty et al., 1993). Similar to Myogenin, MRF4 also regulates terminal differentiation of myoblasts, but there is also a report that suggests MRF4 can function upstream of MyoD to direct the specification of myogenic cells (Kassar-Duchossoy et al., 2004). In addition to MRFs, other transcription factors, such as the Myocyte enhancer factor 2 (Mef2), are also required for muscle differentiation. Mef2 is a downstream target of MyoD. The combined activity of MyoD and Mef2 induces transcription of downstream target genes that contain E-box and MEF2-binding sites (Dodou et al., 2003; Molkentin et al., 1995).

The final pattern of vertebrate muscle is determined by two waves of myogenesis. The first wave generates primary myofibers. The primary fibers function similarly to founder cells in *Drosophila* and determine the shape and identity of muscles (slow or fast). The second wave generates secondary myofibers that align alongside the primary myofibers and add mass to the muscles (Harris et al., 1989). The formation of both myofibers requires fusion of myoblasts. *In vitro* experiments suggest that the fusion process occurs in two phases: the first involves the fusion of individual myoblasts to form the nascent myotubes; the second phase involves fusion between the myotube and additional single-nucleated myoblasts (reviewed in (Rochlin et al., 2010)).

Similar to the process of *Drosophila* myoblast fusion, the myotube-myoblast fusion in mammals is also asymmetric and requires recognition molecules located on the cell membrane. Examples of the recognition molecules are the integrin vLA-4

on the myotubes, and its receptor VCAM-1 on the myoblast. Interaction between vLA-4 and VCAM-1 is required for the alignment of the secondary myofiber with the primary myofiber, as well as the second phase of muscle cell fusion (Rosen et al., 1992). In addition to vLA-4 and VCAM-1, the transcription factor NFAT2C also mediates cell recognition by regulating the expression of IL-4. IL-4 is a cytokine that functions as a secreted myoblast recruitment factor (Horsley et al., 2003). A recent study has shown that Nephrin, an ortholog of the *Drosophila* transmembrane protein Sns, localizes at the myoblast side and mediates cell recognition (Sohn et al., 2009). After recognition, adhesion molecules such as M-cadherin (Hollnagel et al., 2002), N-cadherin (Radice et al., 1997) and integrin family members (Schwander et al., 2003)(Schwander 2003) mediate the adhesion and alignment of the myoblast. Unlike in *Drosophila,* an actin focus structure has not been observed during vertebrate myoblast fusion. Nevertheless, the actin cytoskeleton still plays a critical role in vertebrate muscle formation. Similar to *Drosophila mbc* mutants*, Dock180*-null mice embryos exhibit severely impaired myoblast fusion and skeletal muscle is reduced (Laurin et al., 2008). Dock180 is the mammalian ortholog of Mbc, and it functions as a GEF protein to activate Rac GTPase. In a conditional Rac1 knockout mouse model, Arp2/3 and F-actin accumulation is reduced, resulting in impaired myoblast migration and fusion (Vasyutina et al., 2009). Experiments using a C2C12 mouse myoblast cell culture suggest that Nap1, the mammlian ortholog of Kette and the downstream target of Rac1, is required for regulating WAVE dependent actin remodeling during myoblast fusion (Nowak et al., 2009). These data suggest a conserved role of actin during muscle development.

Cell fusion is required not only in early embryonic myogenesis, but also in muscle regeneration at the later stages of life. As with *Drosophila* adult muscle progenitors (AMPs), a pool of myoblasts remains undifferentiated during vertebrate

Figure 1.8. Development of vertebrate muscles. A. Myogenesis from a somite (S) requires signals from adjacent tissues. Bone Morphogenetic Protein (BMP) signals from the lateral mesoderm (LM), Wnt signaling from the dorsal ectoderm (DE) and the neural tube (NT), and Sonic hedgehog signaling (Shh) from the notocord (NC) are all required for somite partitioning. **B.** Signaling pathways that regulate muscle cell specification. Pax3 and Pax7 enhance the proliferation of muscle precursor cells and activate the expression of the myogenic regulatory factors. MyoD and Myf5 function redundantly to trigger myoblasts specification. Myogenin and MRF4 regulate the terminal differentiation of committed myoblasts. **C.** Stages of muscle development in mice. The diagram shows the formation of the myotome (Ci). Embryonic myoblasts from the myotome differentiate and fuse to form primary muscle fibers (Cii). Fetal myoblasts differentiate and fuse to form secondary fibers that surround the primary fibers (Ciii). Muscles then mature to form muscle fibers at the postnatal stage (Civ). **D.** Diagram showing vertebrate sarcomere structure and examples of conserved sarcomeric proteins. (Adapted with permission from (Chargé and Rudnicki, 2004; Kollias and McDermott, 2008; Sparrow and Schöck, 2009; Tajbakhsh and Cossu, 1997)).

Figure 1.8. Development of vertebrate muscles

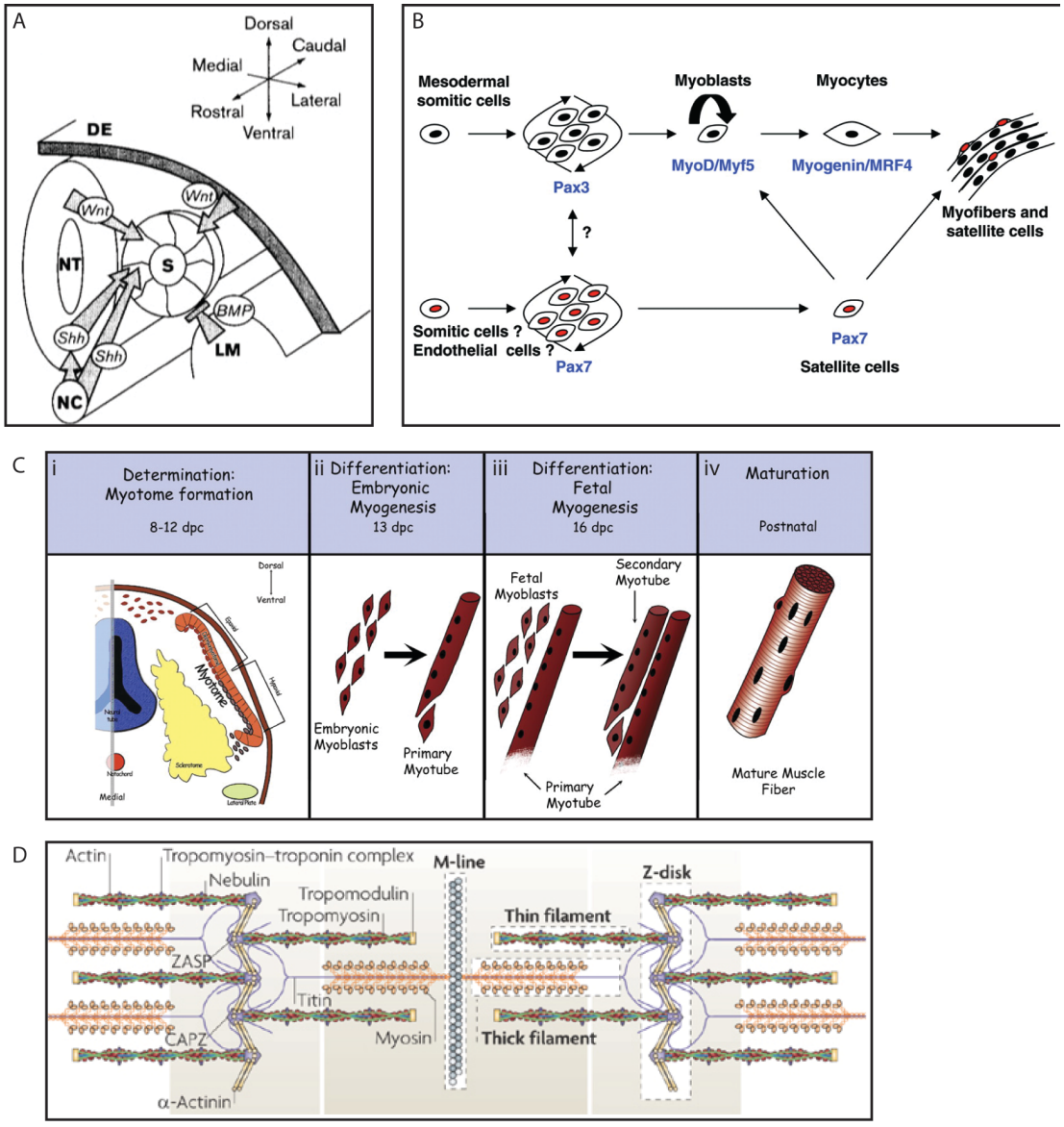

myogenesis. These myoblasts are satellite cells that locate around myofibers. Satellite cells are responsible for post-natal muscle growth, as well as muscle repair. The specification of satellite cells is critically dependent on Pax7, as no satellite cells are found in *Pax7* mutant mice (Seale et al., 2000). With intact muscles, satellite cells are mitotically quiescent and express Pax7 and Myf5, but not Myogenin or MyoD (reviewed in (Yin et al., 2013)). Upon muscle injury, myofiber necrosis triggers inflammatory responses, which induce satellite cells to proliferate (Tidball, 1995). After proliferation, the majority of satellite cells differentiate and start to express MyoD and myogenin (Rantanen et al., 1995). These cells later fuse with damaged myofibers or fuse with each other to generate new muscle fibers (Grounds and Yablonka-Reuveni, 1993). The process of satellite cell fusion is mechanistically similar to myoblast fusion during primary and secondary myofiber formation.

In both *Drosophila* and vertebrates, muscle fibers form and mature through similar mechanisms. In the mature muscle, the basic contractile unit, a sarcomere, is structurally conserved from flies to humans. As with the *Drosophila* sarcomere, the human sarcomere contains actin-based thin filaments and myosin-based thick filaments, and has a similar structure under an electron microscope. Many sarcomeric proteins that regulate sarcomere assembly and function are also conserved between flies and humans.

IV. Actin cytoskeleton

A. Overview of actin networks in cells

The actin monomer (G-actin) is one of the most conserved proteins. G-actin exists in different isoforms and can undergo different post-translational modifications. The most common isoform is the α-actin, which exists in skeletal, cardiac and smooth muscles. G-actin is able to assemble into filamentous actin (F-

actin) even without actin nucleation and polymerization factors. However, the nucleation process is not favored thermodynamically. It is after the actin trimer forms that the elongation rate accelerates rapidly (Wegner and Engel, 1975). G-actin under physiological conditions is associated with ATP. After actin polymerization, ATP is hydrolyzed into ADP. The ADP-bound actin then dissociates from the minus end of the actin filament. There are many actin-binding proteins that regulate the hydrolysis and dissociation process, and therefore regulate the dynamics between the G-actin and F-actin state.

The tertiary structure of globular actin is composed of two domains, which are separated by a cleft. Because all the G-actins in the same F-actin are orientated towards the same direction, the F-actin polymer has structural polarity. The end where the cleft is exposed is called the barbed end, or the plus (+) end, while the opposite end where the ATP binding site is exposed is called the pointed end, or the minus (-) end (reviewed in (Allingham et al., 2006)) (Figure 1.9).

The actin cytoskeleton undergoes remodeling in response to intracellular and extracellular signals. The result of actin cytoskeletal remodeling is the formation of specific cellular structures, such as filopodia, lamellipodia, and stress fibers, which mediate cell behaviors including migration, cell morphology change, and cytokinesis. Actin remodeling involves several processes including actin polymerization, the organization of actin filaments, and the depolymerization of actin filaments.

Filopodia are thin, actin-based protrusions. Cells use filopodia to probe their surrounding environment and sense mechanical forces in the extracellular matrix. For cells that undergo migration and elongation, filopodia are usually found at the leading edge of these cells. The actin filaments in filopodia are organized into

parallel bundles. Several actin-regulating proteins are responsible for filopodia formation, including Ena/VASP, formins, Fascin, I-BAR domain proteins and myosin-X. Among these proteins, Ena/VASP and formins promote actin polymerization and elongate the actin filaments (Bear et al., 2002; Goode and Eck, 2007). Ena/VASP enhances actin filament formation through two mechanisms: 1) it protects the actin filament from capping proteins, and 2) it can increase local G-actin levels through profilin-binding regions (Bear et al., 2002). Fascin can bundle actin filaments and maintain the integrity of the actin bundles in the filopodia (DeRosier and Edds, 1980). The I-BAR domain proteins promote filopodia formation through membrane deformation activity (Mattila et al., 2007). Myosin-X is a motor protein that transports filopodial components to the tip of the filopodia (Tokuo and Ikebe, 2004).

Lamellipodia are sheet-like, actin-based protrusions. The actin filaments in lamellipodia are organized into a branched network. Lamellipodia push the leading edge forward and enable cell migration. The actin network in lamellipodia is mainly regulated by Arp2/3, which generates actin filaments that branch off from the pre-existing filament. The end of the newly generated actin filament is either capped by capping proteins or elongated under control of ENA/VASP or formins (reviewed in (Krause and Gautreau, 2014)).

Stress fibers are actin- and myosin- based structures. The actin structures in stress fibers are composed of both actin bundles and a branched actin network. Stress fibers are organized parallel to the cell membrane and provide support to resist shear force. The interaction between actin and myosin in the stress fibers also provide contractile forces for cell morphological changes (reviewed in (Mattila and Lappalainen, 2008)).

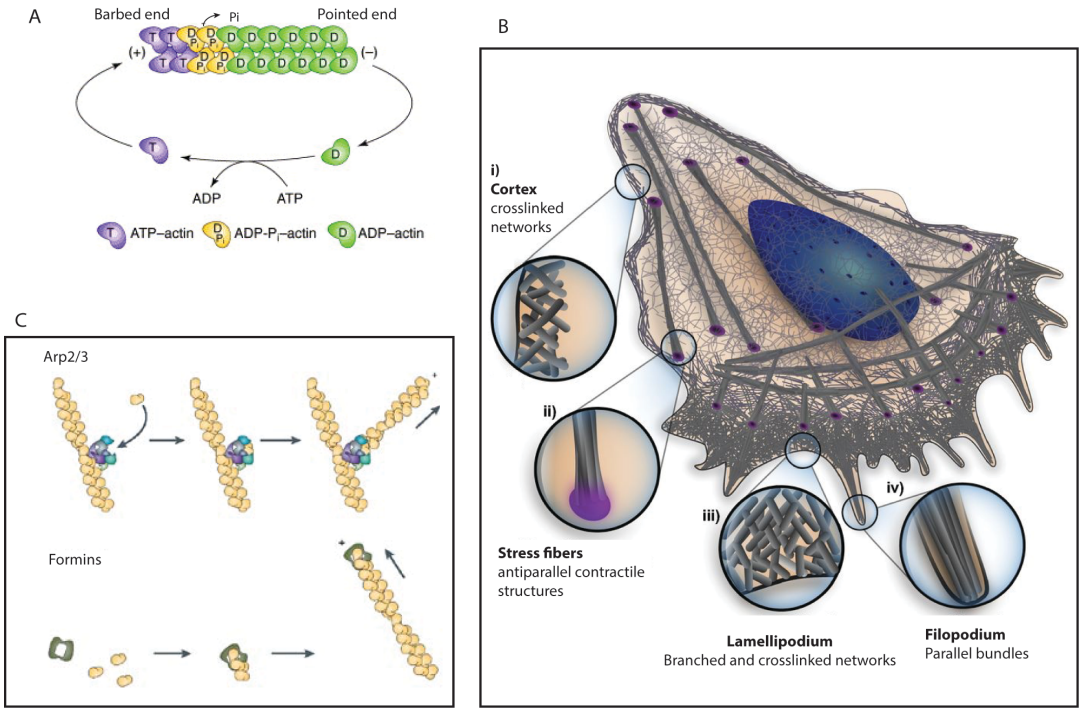

Figure 1.9. Overview of actin dynamics and actin-based structures. A. The polymerization and depolymerization of actin filaments (F-actin). The turnover of an actin filament involves ATP-bound G-actin assembly at the plus end or barbed end, ATP hydrolysis, the release of Pi and ADP-bound G-actin disassembly from the minus or pointed end. **B.** Examples of actin-based structures in a cell. The cell cortex is a network of crosslinked actin filaments beneath the plasma membrane. The stress fibers contain antiparallel actin bundles. The lamellipodium is a network of branched actin filaments at the leading edge of a migrating cell. The filopodium contains thin, parallel actin bundles that cell uses to probe its surrounding environment. **C.** Arp2/3 nucleates an actin filament at a 70° angle from a pre-existing filament. Formins nucleate and elongate actin filaments *de novo.* (Adapted with permission from (Blanchoin et al., 2014; Chen et al., 2000; Pak et al., 2008))

B. Actin regulators that control the dynamics of actin

Actin-related protein-2/3 (Arp2/3)

As mentioned previously, the polymerization of actin is not thermodynamically favored until the actin trimer forms. The Arp2/3 complex promotes actin polymerization by mimicking the structure of an actin dimer and serves as a template to initiate F-actin formation (reviewed in (Goley and Welch, 2006)). Arp2/3 is composed of seven subunits. The subunit Arp2 and Arp3 belong to the same superfamily as actin, and structurally resemble G-actin (Robinson et al., 2001). The other 5 subunits of the Arp2/3 complex are ARPC1-5. The Arp2/3 complex can bind to the side of a pre-existing actin filament through subunit ARPC2 and ARPC4, and generate a new filament at a 70-degree angle. The pointed end of the new filament is attached with Arp2 and Arp3 (Beltzner and Pollard, 2004; Egile et al., 2005). Similar to actin, Arp2 and Arp3 can bind to ATP. The binding of ATP promotes a conformational change in Arp2/3 and is crucial for its actin polymerization activity (Goley et al., 2004). The influence of ATP hydrolysis on Arp2/3 activity is controversial. It has been shown that ATP hydrolysis is crucial for actin nucleation and branching (Dayel and Mullins, 2004), while other studies have reported that ATP hydrolysis is essential for actin branch disassembly and Arp2/3 complex recycling (Le Clainche et al., 2003).

The nucleation-promoting factors (NPFs) activate Arp2/3, partly by increasing Arp2/3's affinity for nucleotide binding. There are numerous NPFs, but the most well studied NPFs are the Wiskott-Altrich syndrome protein (WASp), and the suppressor of cAMP receptor (SCAR), also known as the WASp family verprolin homolog (WAVE). Both WASp and SCAR share a C-terminal WCA domain, which is the functional domain that can activate Arp2/3. The WCA domain contains a WASp-

homology-2 (W) domain that binds with G-actin, a cofilin-homology and acidic (CA) domain that can bind to Arp2/3 and promote its conformation change (Goley et al., 2004).

Although both WASp and SCAR/WAVE activate Arp2/3 through the WCA domain, the activities of the two NPFs are regulated through different mechanisms. WASp is auto-inhibited by the interaction between the WCA domain and the Cdc42/Rac interactive binding (CRIB) domain (also known as the GTPase binding domain (GBD)), which sequesters WCA domain activity (Kim et al., 2000). The binding of a small GTPase and PI(4,5)P2 can compete with the WCA for GBD binding, and therefore release WCA from an inhibited state. In addition to a small GTPase and PI(4,5)P2, WASp activity is also regulated by tyrosine kinase phosphorylation. Phosphorylation of the WCA domain can increase its affinity for Arp2/3 and promote actin nucleation (Cory et al., 2003). In addition to activating WASp, PI(4,5)P2 and tyrosine kinase, Nck, could also regulate the membrane localization of WASp (Miki et al., 1996).

Unlike WASp, which is auto-inhibited, the WAVE protein by itself is activated and sufficient to promote Arp2/3-based actin nucleation. Under *in vivo* conditions, however, WAVE forms a complex with Nap1/Hem-2, Sra1/Cyfip1, Abi and Hspc300. This hetero-pentameric WAVE regulatory complex (WRC) inhibits WAVE activity towards Arp2/3. Analysis of the crystal structure of the WRC reveals the mechanism for WRC inhibition. In the WRC, Sra1 and Nap1 have similar structures and interact to form a pseudo-symmetric dimer. HSP300, Abi2 and WAVE form a trimer that contacts the Sra1-Nap1 dimer in a tripartite manner. Sra1 can bind with the functional WCA region of WAVE, making the WCA inaccessible to actin and Arp2/3. Mutations in the WCA-binding region of Sra1 constitutively activate WAVE, and trigger Arp2/3-based actin nucleation (Chen et al., 2010).

WAVE can be activated by various stimuli, such as Rac GTPase, phospholipids, and kinases. Rac activates WAVE by competing with the WCA domain for Sra1 binding, and releasing the WCA from an inhibitory state (Ismail et al., 2009). WAVE could also be activated by phosphorylation of a conserved sequence, such as Tyr 125 and Tyr 150 (Ardern et al., 2006; Stuart et al., 2006). The phosphorylation destabilizes the interaction between the WCA region and Sra1, leading to the release of the WCA from Sra1, and increases the WRC activity for Arp2/3.

When WAVE is activated, the WCA domain dissociates from Sra1. However, the WAVE regulatory complex (containing Nap1/Hem-2, Sra1/Cyfip1, Abi and Hspc300) itself does not dissociate and remains intact. It is reported that the WRC maintains the stability of WAVE, as ablation of Nap1/Hem-2, Sra1/Cyfip1 and Abi leads to the degradation of WAVE (Kunda et al., 2003). In addition to stabilizing WAVE, the WRC also regulates the localization of WAVE (Richardson et al., 2007). Phosphorylation can also promote the cell-edge localization of WAVE. Therefore, tyrosine kinases, such as Abl and Src, not only activate WAVE, but also regulate WRC localization. The negatively-charged phospholipids such as PI(3,4,5)P3 and PI(4,5)P2 could also bind with the WRC and contribute to the membrane localization of WAVE (Mendoza, 2013).

Formins

Formins are a family of proteins that regulate actin assembly and microtubule stability. The first formin was identified when characterizing the limb deformity (ld) locus (Mass et al., 1990; Woychik et al., 1990). The *ld* gene was assigned the name *formin* (*fmn*), because it was thought to be involved with anterior-posterior limb pattern formation. Although later studies have shown that the limb defects

were actually caused by a mutation of the neighboring gene *gremlin* (Michos et al., 2004; Zuniga et al., 2004), the name formin was retained. After the discovery of Fmn, more formin homologs were discovered, such as Diaphanous and Cappuccino in *Drosophila* (Castrillon and Wasserman, 1994; Emmons et al., 1995), Bni1p in *Saccharomyces cerevisiae* (Evangelista et al., 1997; Kohno et al., 1996) and Fus1 in *Schizosaccharomyces pombe* (Petersen et al., 1998). Formins were characterized by the formin homology 2 (FH2) domains, which have strong actin nucleation activity. Based on bioinformatics analysis, there are 15 formins in humans with the FH2 domain, and in *Drosophila* there are 6 formins (Higgs and Peterson, 2005). The best-studied formins are the Diaphanous (Dia)-related formins (DRFs), which are regulated through similar mechanisms. In *Drosophila,* DRFs include Dia and DAAM. Here we use Dia as an example to explain the domains of DRFs (Figure 10).

The FH2 domain is the functional actin-binding domain that exists in all formins. *In vivo* experiments demonstrate that FH2 is sufficient to trigger actin polymerization (Evangelista et al., 2002; Pruyne et al., 2002). FH2 binds to the barbed ends of actin filaments and nucleates linear F-actin (Pruyne et al., 2002; Sagot et al., 2002). FH2 domains in different formins bind to actin with different affinities, which is likely the reason why different formins catalyze actin polymerization with different efficiencies (Moseley et al., 2006). At the barbed end of F-actin, the FH2 domain dimerizes and processively moves with the growing filament (Xu et al., 2004). The FH1 domain is located adjacent to the FH2 domain and is present in almost all formins. FH1 can bind to Profilin, which recruits ATP-bound actin monomers (Witke, 2004). Therefore, the FH1 domain increases local actin monomer concentration by interacting with Profilin. Increased local G-actin levels drive the equilibrium to actin polymerization, and therefore increase the rate of actin filament elongation. The Dia auto-regulatory domain (DAD) is located at the

C-terminal ends. DAD can bind to the Dia inhibitory domain (DID), located at the N-terminal of the FH1 domain. The binding between DAD and DID results in a conformation change that masks the activity of the FH1 and FH2 domains. At the N-terminal end of DRFs is the GTPase-binding domain (GBD). When GTP-bound Rho interacts with the GBD, it triggers the disassociation of DAD from DID, and thus activates the DRF from an auto-inhibitory state. In addition to the functional and regulatory domains, there are also a dimerization domain (DD) and a coiled coil (CC) domain, which mediate the activation of DRFs. The regulatory domains including DAD, DID, GBD, DD and CC are not always present in formins, suggesting alternative ways of regulation (reviewed in (Higgs, 2005)).

The functions of formins have been documented in various species. In humans, DRF loss of function is associated with a variety of diseases, such as premature ovarian failure (Bione et al., 1998) and tumor metastasis (Hager et al., 2012). Over-expression of DIAPH2 is characterized as the cause for non-syndromic auditory neuropathy (AUNA1) (Schoen et al., 2010). Mouse models show that progressive hearing loss might be due to a reduction of synapses and abnormal cell fusion of inner hair cells caused by mDia3 over-expression (Schoen et al., 2013). In *Drosophila,* the most well studied formin, Dia, was identified in a P-element screen for male-sterile mutations: males homozygous for *dia* null alleles are sterile due to defects in cytokinesis during spermatogenesis (Castrillon et al., 1993). Formin loss or gain of function leads to misregulated actin polymerization and disrupts F-actin organization. Impaired actin structure in cells leads to defects in cell division, adhesion, migration and intracellular trafficking (reviewed in (Goode and Eck, 2007)). Interestingly, formins can also regulate cell behavior by controlling microtubule dynamics and arrangement (Bartolini and Gundersen, 2010; Chesarone et al., 2010). mDia was reported to regulate the stability and orientation of

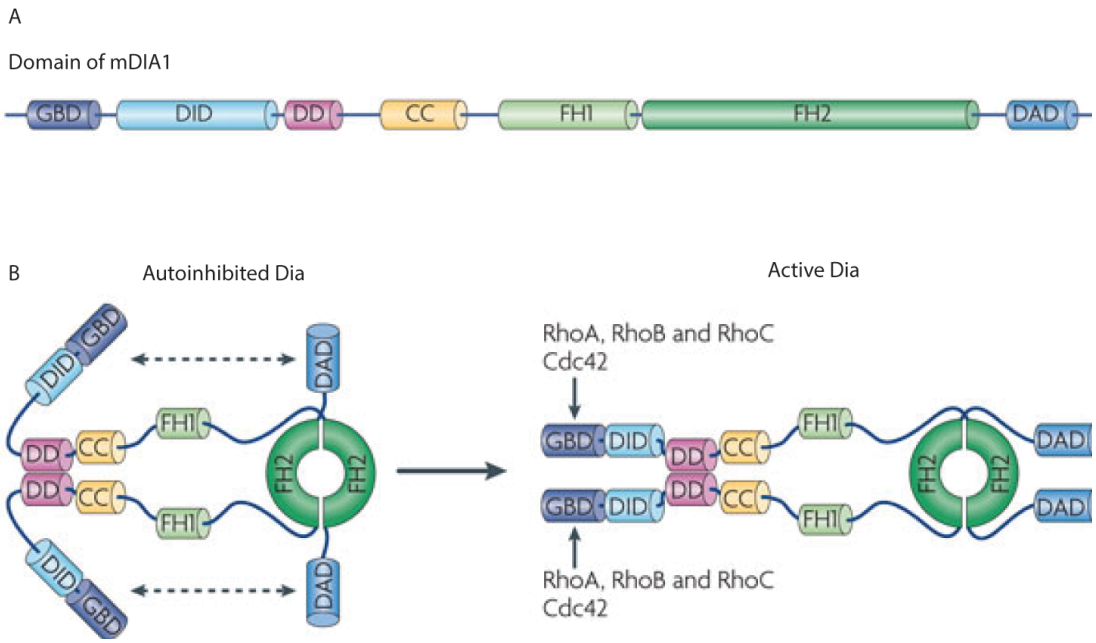

Figure 1.10. Domain organization of Dia. A. Diagram showing the protein domains of Dia. The conserved formin homology 1 (FH1) and formin homology 2 (FH2) domains are the modules that nucleate and polymerize actin filaments. GBD: GTPase-Binding Domain. DID: Diaphanous Inhibitory Domain. DD: Dimerization Domain. CC: coiled coil. DAD: Dia Auto-regulatory Domain. **B.** The dimeric structure of Dia and the mechanism of Dia regulation. The binding between DAD and DID autoinhibits the activity of the FH1 and FH2 domains. Dia is activated when Rho family GTPases binds with GBD and triggers the disassociation of DAD from DID. (Adapted with permission from (Campellone and Welch, 2010))

microtubules in NIH 3T3 cells (Palazzo et al., 2001), potentially by binding to the microtubule plus end protein EB1 and the Adenomatous Polyposis Coli protein (APC) to form a complex that stabilizes microtubules (Wen et al., 2004). FHOD1 and Cappuccino (Capu) were reported to crosslink microtubules with F-actin in HeLa cells (Gasteier et al., 2005) and *Drosophila* oocytes (Rosales-Nieves et al., 2006).

Actin depolymerization factors

The actin cytoskeleton in cells is a dynamic system that undergoes constant polymerization and depolymerization. *In vitro* experiments show that at steady state, G-actin is spontaneously added to the plus end. However, as the G-actin concentration needed for spontaneous polymerization at the minus end (~0.6μM) is six-fold higher than at the plus end (~0.1μM), F-actin depolymerizes from the minus end (Ono, 2007). This process is called treadmilling (Cleveland, 1982). The spontaneous depolymerization rate is low. However, under *in vivo* conditions, actin depolymerization factors can enhance actin turnover by accelerating G-actin dissociation from the minus ends, or severing F-actin to make more minus ends.

The Gelsolin family of proteins is widely present in various species. Gelsolin family proteins such as Gelsolin and Villin contain repeats of the Gelsolin homology domains. Gelsolin family proteins sever and cap actin filaments in a calcium-dependent manner. Here we use the most well-studied Gelsolin to explain the functions of the gelsolin-like domain, and how it regulates the severing and capping of an actin filament (reviewed in (McGough et al., 2003)).

Gelsolin contains six gelsolin-like domains (G1-G6). G1 can bind with actin in a calcium independent manner. The binding site for G1 on actin is located at the cleft between actin subdomains (McLaughlin et al., 1993), which is exposed at the surface of the F-actin plus (barbed) end, and overlaps with Profilin and the

ADF/cofilin binding site. Similar to Dia, the activity of Gelsolin is also controlled through auto-regulation. The N-terminal and C-terminal can bind together and mask the actin-binding domains. Upon calcium binding, Gesolin undergoes a conformational change that exposes actin-binding domains (Burtnick et al., 1997). After binding with the plus end, Gesolin severs actin filaments by triggering an F-actin conformational change and weakening longitudinal actin-actin interaction (Selden et al., 1998). In addition to calcium, Gesolin activity is also controlled by various factors such as pH, phospholipids, and ATP levels (Gremm and Wegner, 1999; Janmey and Stossel, 1987; Lamb et al., 1993).

Another family of proteins that depolymerizes actin filaments is the ADF/cofilin family. ADF/cofilin has a structure similar to the G1 domain in Gelsolin, while sharing no sequence similarity (reviewed in (Ono, 2007)). Due to different severing mechanisms, ADF/cofilin severs actin filaments less efficiently than Gelsolin (Ono et al., 2004). ADF/cofilin binds to F-actin and induces a conformational change in lateral contacts between G-actin and F-actin. The structural change results in an unstable conformation that triggers fragmentation of the F-actin (McGough and Chiu, 1999). In addition to actin severing activity, ADF/cofilin also enhances disassembly of actin monomer from the minus (pointed) ends (Carlier et al., 1997). Similar to Gelsolin, the activity of ADF/cofilin is also regulated by cellular pH (Hawkins et al., 1993; Maciver et al., 1998) and the presence of phospholipids (Ojala et al., 2001). Phosphorylation and dephosphorylation provide another level of ADF/cofilin regulation (Meberg et al., 1998).

V. Summary

Actin is one of the most conserved and abundant proteins present in muscles. Mutations in actin and actin-related proteins are linked to muscle disease (Sparrow et al., 2003). The molecular mechanisms and regulatory proteins that control actin dynamics are highly conserved in *Drosophila* muscle and human muscle. Therefore, we use the less complicated *Drosophila* muscle as a model system to study muscle formation. Investigating how actin structure is organized not only gives us insights to muscle development, but also promotes an understanding of how similar processes are regulated in humans. For example, studying the fusion of myoblasts in *Drosophila* reveals regulatory mechanisms of membrane fusion that can be found in a variety of pathological and developmental events, such as cancer cell fusion, fertilization, the formation of multinucleated syntrophoblasts and osteoclasts ((Horsley and Pavlath, 2004; Martens and McMahon, 2008)). Studying sarcomere assembly in *Drosophila* flight muscles reveals how cells contract and change shape in cardiac and smooth muscles, and in epithelial cells during apical constriction ((Clark et al., 2002; Martin et al., 2009)).

In different model systems, it has been demonstrated that actin structures are regulated by proteins that polymerize, depolymerize, and crosslink actin. In my thesis I report that the same actin polymerization factor, Diaphanous, in combination with different actin regulators, forms different actin structures during different developmental stages. I also propose another possible mechanism to regulate actin homeostasis: the maintenance of an actin monomer pool.

CHAPTER TWO

PI(4,5)P2 REGULATES MYOBLAST FUSION THROUGH ARP2/3 LOCALIZATION AT THE FUSION SITE*

I. Introduction

To convey extracellular signaling to the actin cytoskeleton, many molecules on the membrane function as messengers. One such example is the membrane lipid Phosphatidylinositol-(4,5)-bisphophate [PI(4,5)P2] and its metabolic derivatives (reviewed in (Zhang et al., 2012)). PI(4,5)P2 is a minor component of membranes in eukaryotic cells. In human erythrocytes, PI(4,5)P2 constitutes about 1% of the membrane lipids (Ferrell and Huestis, 1984). In cells, PI(4,5)P2 is synthesized either through phosphorylation of PI(4)P or PI(5)P by the respective PIP kinases, or through dephosphorylation of PI(3,4,5)P3 by a range of phosphatases. The level of PI(4,5)P2 is therefore controlled through metabolic synthesis and dissipation (reviewed in (Balakrishnan et al., 2015)). One enzyme that decreases PI(4,5)P2 levels is the phosphoinositide-specific phospholipase C (PLC), which hydrolyzes PI(4,5)P2 to generate the second messengers diacyl glycerol (DAG) and inositol-(1,4,5)-trisphosphate (IP3). The physical interaction between PLC and PI(4,5)P2 is mediated through the pleckstrin homology (PH) domain on PLC. The PH domain is a common feature in a variety of proteins that interact with phosphatidylinositol lipids and the actin cytoskeleton. Due to its high binding affinity to PI(4,5)P2, the GFP-tagged PH domain of PLC has been used to monitor the dynamics of PI(4,5)P2

---

*Bothe I, Deng S, Baylies M. PI(4,5)P2 regulates myoblast fusion through Arp2/3 regulator localization at the fusion site. Development 2014 141: 2289-2301; doi: 10.1242/dev.100743

in various cellular events, such as phagocytosis (Botelho et al., 2000), cytokinesis (Wong et al., 2005), endocytosis (Honda et al., 1999), reviewed in (Czech, 2000)), and myoblast fusion (Bach et al., 2010; Nowak et al., 2009). In these processes, PI(4,5)P2 is often observed to concentrate at actin-rich structures on the plasma membrane (Tall et al., 2000). PI(4,5)P2 influences actin remodeling possibly through two mechanisms: 1) PI(4,5)P2 interacts with actin capping proteins such as CapZ, and inhibits actin capping activity, thereby promoting actin poymerization (Heiss and Cooper, 1991). Or 2) PI(4,5)P2 localizes and activates actin polymerization factors such as WASp (Higgs and Pollard, 2000), triggering the polymerization and branching of the actin network.

In vitro experiments in C2C12 myoblasts showed that PI(4,5)P2 accumulates at the adhesion site between myoblast/myotube and myotube. Depletion of PI(4,5)P2 in C2C12 myoblasts results in decreased cell fusion (Bach et al., 2010; Leikina et al., 2013; Nowak et al., 2009). Due to the lack of markers that could reliably label the fusion site, where and how PI(4,5)P2 is involved in mammalian myoblast fusion has not been sufficiently investigated. In the *Drosophila* embryo, we used PH^{plc}::GFP to record the spatial and temporal dynamics of PI(4,5)P2. We dissected the role of PI(4,5)P2 in *Drosophila* myoblast fusion and investigated how PI(4,5)P2 regulates F-actin structures at the site of fusion.

Results:

PI(4,5)P2 is enriched at the site of fusion

To investigate the role of PI(4,5)P2 in *Drosophila* myogenesis, we first used time-lapse imaging to record the temporal and spatial dynamics of PI(4,5)P2 during myoblast fusion. Two constructs, $PH^{plc\delta}$::GFP (Verstreken et al., 2009) and $PH^{plc\gamma}$::GFP (Pinal et al., 2006), were used to label PI(4,5)P2 and both showed similar

Figure 2.1 PI(4,5)P2 is enriched at the site of fusion. A. Time-lapse imaging of a stage 14 *Drosophila* embryo. Boxed areas are magnified to show the attachment site between a VA1 muscle (turquoise) and a FCM (magenta). The localization of PI(4,5)P2 is detected using *UAS-PH$^{plc\gamma}$::GFP* (arrow). The PI(4,5)P2 signals at the fusion site are quantified by measuring fluorescence intensity (line scan at the yellow bar, a.u., arbitrary units). A single peak of fluorescence signal is found before fusion, and then it resolves as fusion proceeds. **B.** Time-lapse imaging of myoblasts expressing *UAS-PH$^{plc\gamma}$::GFP* and *UAS-mCherry:moesin*. F-actin and PI(4,5)P2 reporters overlap spatially and temporally (arrow) at the fusion site, and this is quantified by plotting fluorescence intensity curves. Scale bars: 5 μm. **C.** Fusion index of stage 17 lateral transverse (LT) muscles. The nuclei in the LT muscles are labeled with apME-NLS::dsRed. The number of nuclei in each hemisegment is counted for each genotype (n=15 embryos). **D.** Average time to F-actin or PI(4,5)P2 enrichment in different genotypes. Expressing F-actin or PI(4,5)P2 reporter constructs had no detectable effect on fusion. (Ingo Bothe and Su Deng performed the experiments. Ingo Bothe analyzed the data)

Figure 2.1 PI(4,5)P2 is enriched at the site of fusion.

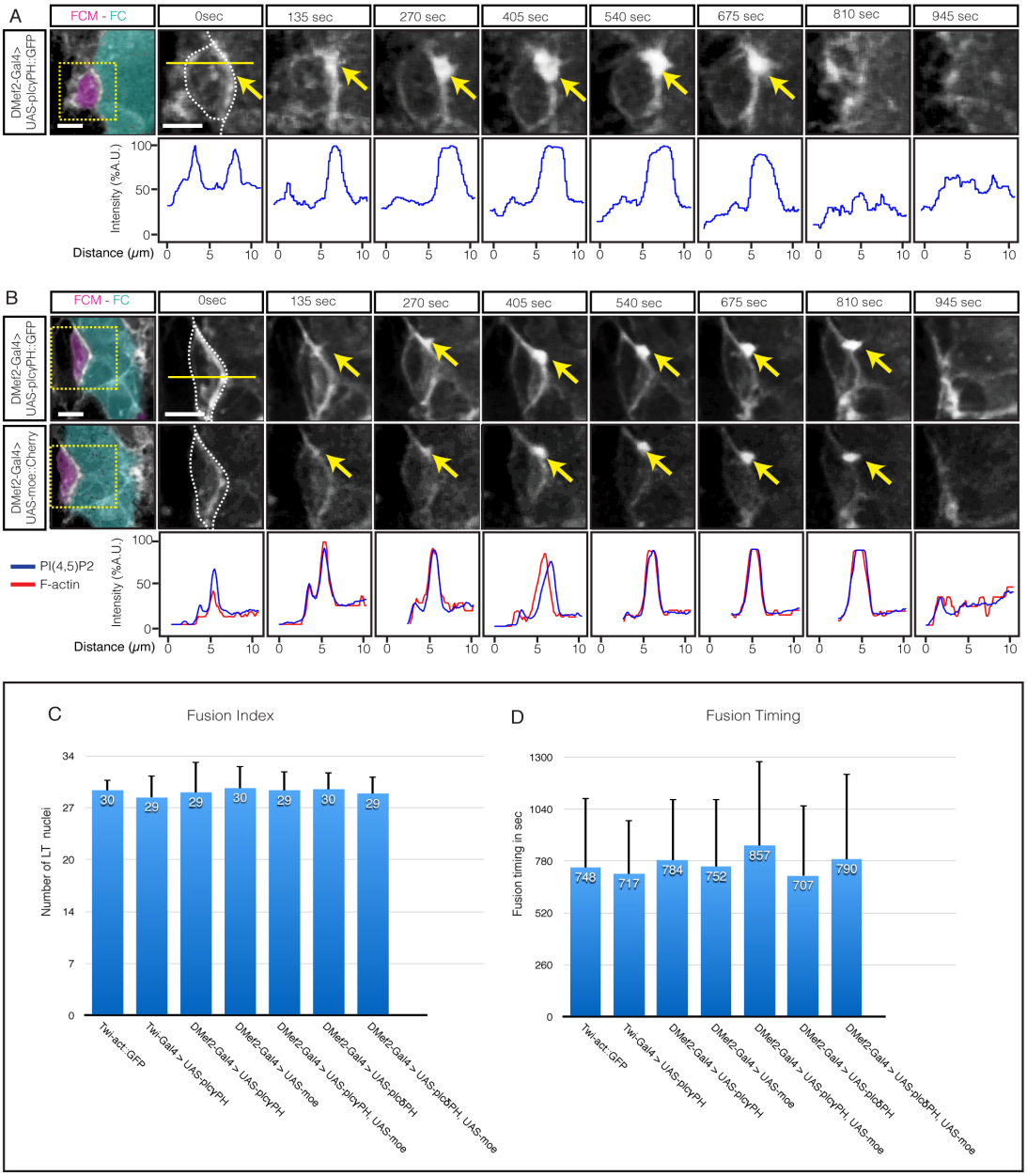

distribution and dynamics. Taking advantage of the well-characterized UAS-Gal4 system, we expressed the PI(4,5)P2 reporter specifically in the developing muscles. The signal of the PI(4,5)P2 reporters are present throughout the plasma membranes, with an accumulation at the attachment sites between the fusion competent myoblasts (FCMs) and founder cell (FC)/myotubes, suggesting a potential role of PI(4,5)P2 during fusion (Figure 2.1A).

Prior to fusion, F-actin accumulates at the fusion site to form a focus structure. We therefore used mCherry::Moe^{act} to label the fusion site. mCherry::Moe^{act} is a fusion protein that contains the actin binding domain of *Drosophila* moesin (C-terminal 137 residues) and the fluorophore mCherry (Millard and Martin, 2008). Expression of mCherry::Moe^{act} did not alter myoblast fusion dynamics nor the fusion index. When the reporters of PI(4,5)P2 and F-actin are co-expressed in the muscles, time-lapse imaging revealed that the accumulation of PI(4,5)P2 spatially and temporally coincides with the F-actin focus at the fusion site (Figure 2.1B).

PI(4,5)P2 accumulates at the fusion site after cell recognition and adhesion

We next attempted to place PI(4,5)P2 in the known fusion pathway by examining PI(4,5)P2 localization in the known fusion mutants. The transmembrane molecule Sns is a component of the machinery that regulates FC-FCM recognition and adhesion. In *sns* mutants, myoblast fusion is blocked due to impaired cell-cell recognition and adhesion. We did not find PI(4,5)P2 accumulation in *sns* mutants, placing PI(4,5)P2 downstream of cell recognition and adhesion (Figure 2.2B). We also checked PI(4,5)P2 localization in mutations that reduce Arp2/3 activity and found that PI(4,5)P2 is enriched at the fusion site, as identified by the presence of an

Figure 2.2 PI(4,5)P2 localization at the fusion site is dependent on FC/FCM recognition and adhesion, but independent of actin regulators. A-K. Time-lapse imaging of a stage 14 *Drosophila* embryo. The PI(4,5)P2 reporter, *UAS-PH^{plcγ}::GFP,* is expressed in the developing muscle and shows accumulation of PI(4,5)P2 in a wild-type control or in different fusion mutants. **A.** PI(4,5)P2 accumulates at the fusion site in wild-type control embryos (arrow). **B.** No PI(4,5)P2 enrichment is detected in a *sns^{XB3}* homozygous mutant embryo. **C-K.** Arrows showing PI(4,5)P2 accumulations are detected in *rols^{T687}*, *loner^{T1032}*, *DWip^{D30}*, *DWip^{sltr}*, *Rac1^{Tj11}, Rac2^{Δ}, Mtl^{Δ}* triple mutant, *mbc^{c1}*, *kette^{J4-48}*, *blow^{1}*, and *SCAR^{Δ37}* mutant backgrounds. Scale bar: 10 μm. (Ingo Bothe and Su Deng performed the experiments. Ingo Bothe analyzed the data)

Figure 2.2 PI(4,5)P2 localization at the fusion site is dependent on FC/FCM recognition and adhesion, but independent of actin regulators

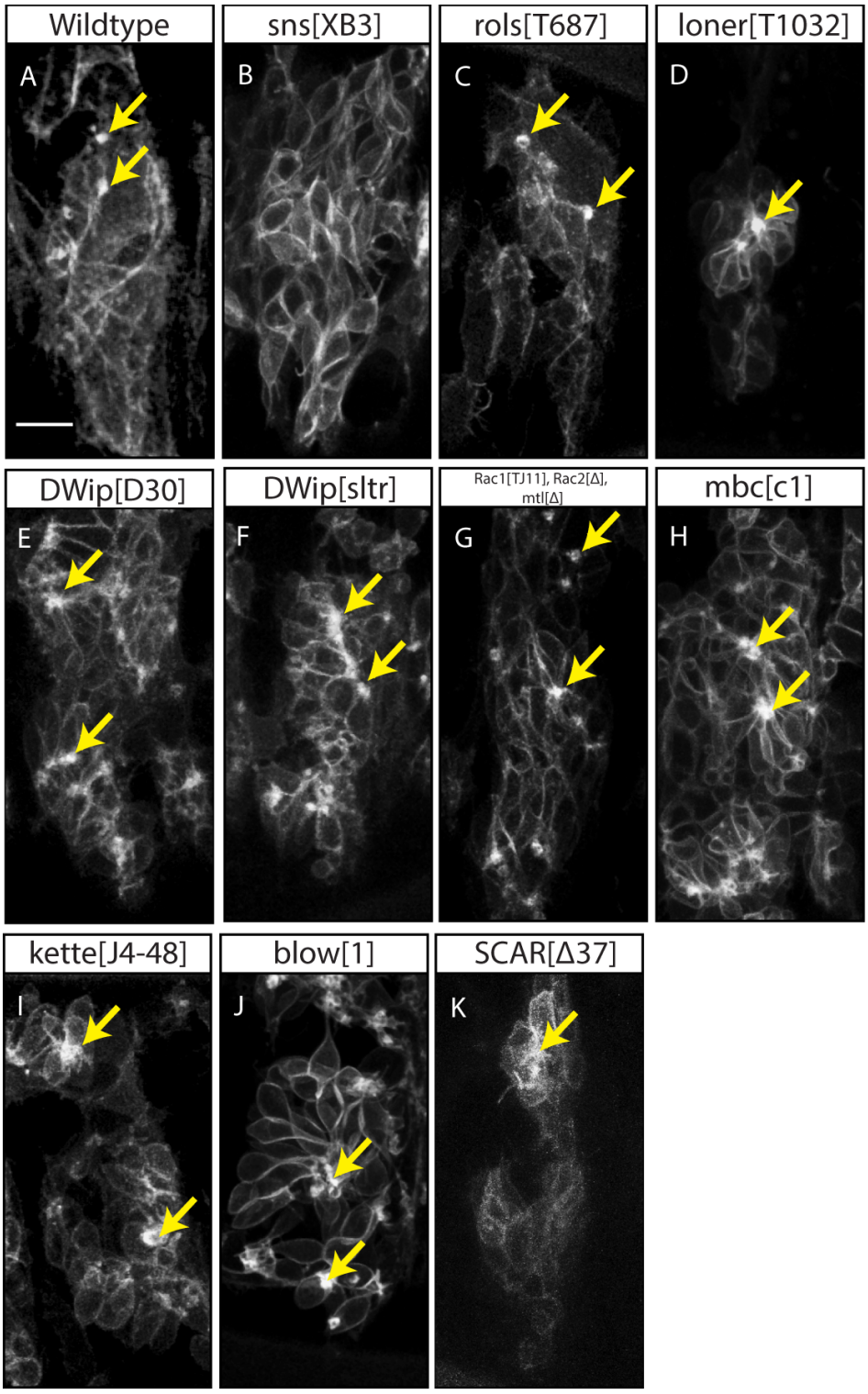

actin focus. The mutants we examined include *loner, sltr, blow, WASp, Rac1, mbc, kette* and *scar.* *Loner* encodes an ARF-GEF family member that regulates actin rearrangement in the FCs. *Sltr, blow* and *WASp* are involved with the WASp-mediated Arp2/3 activation. *Rac*, *mbc*, *kette* and *scar* are involved with the SCAR-mediated Arp2/3 activation. The enrichment of PI(4,5)P2 in these genetic backgrounds suggests PI(4,5)P2 localization is independent of Arp2/3 activity (Figure 2.2).

PI(4,5)P2 is required for myoblast fusion

The enrichment of PI(4,5)P2 at the fusion site suggested that it might play an essential role during myoblast fusion. To address the function of PI(4,5)P2 during fusion, we examined the muscle phenotype in embryos with reduced PI(4,5)P2 levels. One way to decrease PI(4,5)P2 levels is through manipulating the metabolic pathways that synthesize or deplete PI(4,5)P2. Mutants that impair PI(4,5)P2 generation, including the PI5-kinase *sktl* and PI4-kinase *fwd,* were analyzed for their muscle phenotype. Myoblast fusion proceeds normally when Sktl or Fwd levels are reduced in muscles.

Another way to reduce PI(4,5)P2 is to sequester PI(4,5)P2 from binding with its endogenous interaction partner. One molecule that can sequester PI(4,5)P2 is the $PH^{plc\gamma}$::GFP reporter protein. When we examined the localization of the PI(4,5)P2 reporter, $PH^{plc\gamma}$::GFP is expressed at low levels (one genetic copy). In this context, fusion was unaffected, quantified by counting the number of nuclei in the lateral transverse (LT) muscles in each hemisegment (29±4 nuclei/hemisegment vs 30±2 nuclei/hemisegment in control, n=14, p>0.1) (Figure 2.1C-D). When the $PH^{plc\gamma}$::GFP reporter level is increased through manipulating temperature and copy number of the transgenes, fusion defects were observed in a dosage dependent

manner (Figure 2.3A). Expressing two copies of $PH^{plc\gamma}$::GFP in the muscles at both 25°C and 29°C resulted in decreased myoblast fusion. The block of fusion was quantified via the fusion index (Figure 2.3B). The differentiation of myoblasts was unaffected by PH^{plc}::GFP overexpression, as confirmed by the expression of the muscle specific gene myosin heavy chain (MHC) and the muscle identify gene *apterous*.

PI(4,5)P2 is required for the formation of actin focus

PI(4,5)P2 has been shown to regulate actin remodeling in various cellular events (Botelho et al., 2000; Czech, 2000; Honda et al., 1999; Wong et al., 2005). To investigate whether PI(4,5)P2 mediates myoblast fusion through organizing the actin cytoskeleton during fusion, we examined actin structures in PI(4,5)P2 sequestering background. Under sequestering conditions, in embryos fixed with 4% PFA, accumulation of PI(4,5)P2 and F-actin were observed in the majority of FCMs (Figure 2.4A). Over 75% of these PI(4,5)P2 accumulation sites were also sites of F-actin accumulations, reminiscent of the F-actin focus (Figure 2.4B). These actin foci were smaller in size than in wildtype embryos ($1.12\pm0.34\mu m^2$ vs $2.01\pm0.52\mu m^2$, $p<0.001$, n=25). In addition, these actin foci were flat in morphology, which did not resemble the protrusive, podosome-like structure reported in wildtype embryos (Sens et al., 2010). We also noticed that in PI(4,5)P2 sequestered embryos, most FCMs with an actin focus were not attached to a FC/myotube. As the actin focus forms after FC-FCM recognition and adhesion, our data suggests, that most FCM detach from the FC/myotube after adhesion and formation of the actin focus. Loss of PI(4,5)P2 accumulation in the *sns* mutant background suggests that PI(4,5)P2 is involved in the process after cell recognition and adhesion. This hypothesis was confirmed by examination of the adhesion receptors Duf and Sns in PI(4,5)P2 sequestering

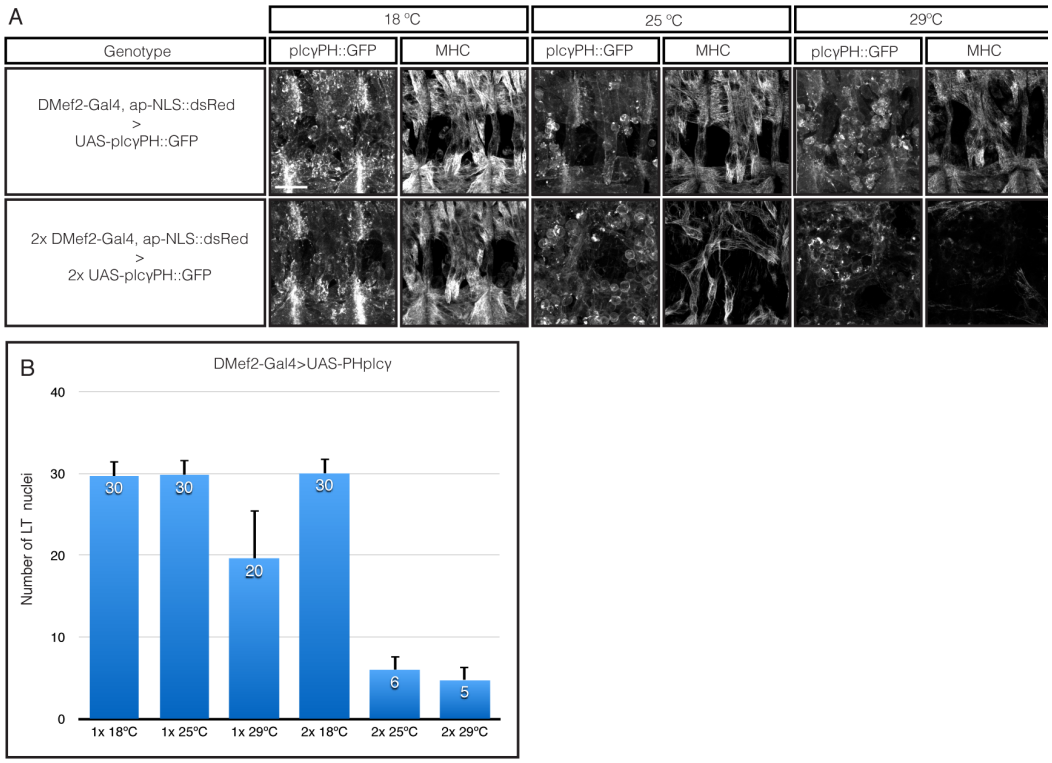

Figure 2.3 PI(4,5)P2 is required for myoblast fusion. A. Overexpressing of the PI(4,5)P2 reporter PH$^{plc\gamma}$::GFP blocks myoblast fusion in a dose-dependent manner. Increasing *UAS-PH$^{plc\gamma}$::GFP* concentration in myoblasts by raising the temperature and increasing the genetic copy number leads to an increased fusion block. Myoblasts were labeled for PH$^{plc\gamma}$::GFP and Myosin heavy chain (MHC). Scale bar: 10 μm. **B.** Fusion index based on nuclei number in LT muscles. Single-copy expression of *UAS-PH$^{plc\gamma}$::GFP* appears as wildtype at 18°C and 25°C. At 29°C, expression of a single copy of *UAS-PH$^{plc\gamma}$::GFP* leads to a mild fusion defect. Expression of two copies of *UAS-PH$^{plc\gamma}$::GFP* produces a complete fusion block at 25°C and 29°C. (Ingo Bothe and Su Deng performed the experiments. Ingo Bothe analyzed the data)

background embryos (Figure 2.4C-D). Sns is found to localize to the fusion sites in attached FCMs. In detached cells, Sns still localized close to the actin focus, but it does not form a ring structure as described in earlier reports (Kesper et al., 2007). Comparable to wildtype, Duf was also found to localize to the FCM attachment-site in the FC/myotubes. However, no enrichment of Duf was detected on the FC/myotube membrane without FCM attachment, or with detached FCMs. Together, our data indicate that PI(4,5)P2 is not involved in cell recognition nor the initiation of fusion, but rather in the expansion of the fusogenic interface at the fusion site.

PI(4,5)P2 regulates myoblast fusion through localizing Mbc

We next investigated how PI(4,5)P2 regulates actin cytoskeleton structures during myoblast fusion through both *in vitro* and *in vivo* assays. PI(4,5)P2 is known to interact with actin regulators through binding with pleckstrin homology (PH) domains and calcium-binding (C2) domains on these proteins. In *Drosophila*, the PH domain is present in several proteins that are involved in fusion, including blow (207-305), Loner (991-1089) and WASp (35-104). The C2 domain is present in Mbc. Based on an alignment algorithm, we identified a short (444-633), and a long version of the Mbc C2 domain. To examine if PI(4,5)P2 regulates fusion by directly interacting with actin regulators, we first tested lipid binding with these lipid-binding domains *in vitro* (Figure 2.5A). Among all the tested domains from actin regulators, the PH domain of Blow interacted with all tested phophoinositides except PI(3,4)P2. LonerPH interacted with all PIPs and PIP2s species, but only weakly with PIP3. The short Mbc C2 domain bound with PIPs, PI(4,5)P2 and PI(3,5)P2, while the long C2 domain had similar binding pattern, but more weakly with PI(3)P and PI(4)P. The WASpPH domain bound PIPs and PIP2s, but only

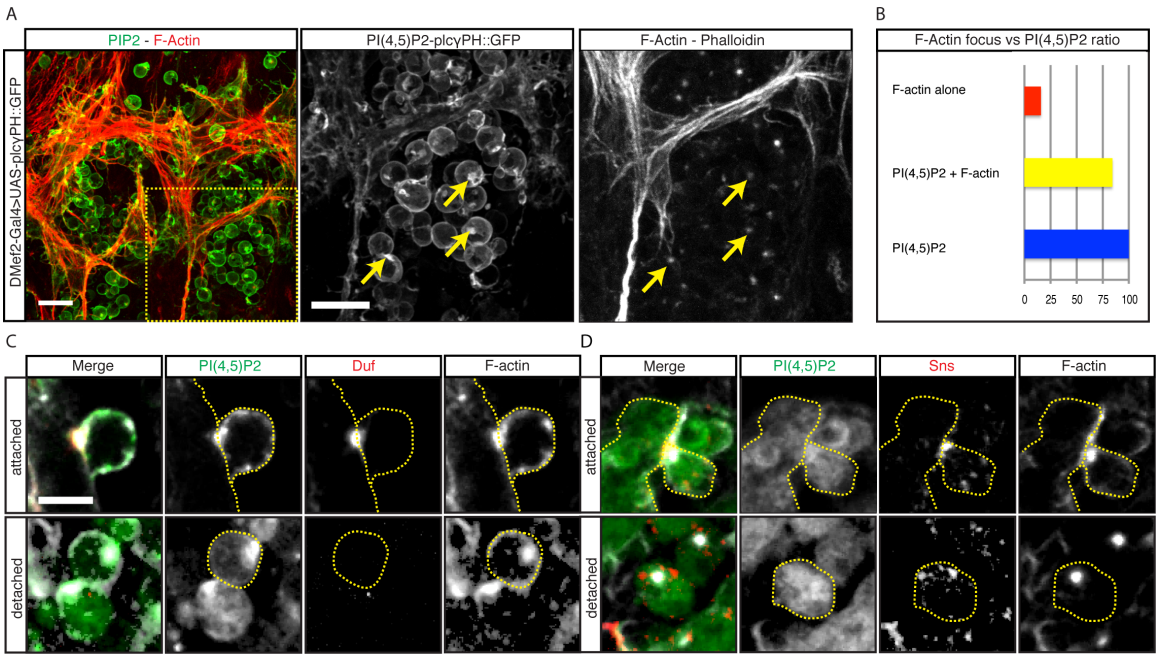

Figure 2.4 Effects of PI(4,5)P2 sequestration on the F-actin focus and FCM-FC/myotube attachment. A. Stage 15 embryo expressing 2x *UAS-PH$^{plc\gamma}$::GFP* in the developing muscles. The embryo was stained with phalloidin (red) and an antibody against GFP (green). PI(4,5)P2 aggregations were found in the FCMs. 75% of the aggregations colocalize with the F-actin foci (arrow). Scale bars: 10 μm **B.** Bar chart showing percentages of FCMs with an F-actin focus, F-actin and PI(4,5)P2 aggregations, or just PI(4,5)P2 aggregations. **C-D.** Recognition and adhesion between FCMs and FC/myotubes are unaffected in PI(4,5)P2 sequestered embryos. Similar to wildtype, embryos with PI(4,5)P2 sequestration showed Duf (C) accumulation at the fusion site in the FC/myotube. Sns (D) was also present at the fusion site in the attached FCMs. Scale bar: 5 μm. (Ingo Bothe and Su Deng performed the experiments. Ingo Bothe analyzed the data)

weakly to PI(3,4,5)P3. Our data indicate that all the tested proteins can bind with PI(4,5)P2 *in vitro* and could serve as potential downstream targets of PI(4,5)P2.

If PI(4,5)P2 regulates myoblast fusion through localizing actin regulators to the fusion site, sequestering of PI(4,5)P2 would result in the mislocalization of these actin regulators. We therefore tested this hypothesis *in vivo* (Figure 2.5B-E). As a control, we examined the localization of the target actin regulators in embryos expressing one genetic copy of $PH^{plc\delta}$::GFP (*1x Dmef2->UAS-$PH^{plc\delta}$::GFP*), where fusion is unaffected. In the control embryos, Blow was localized on the plasma membrane in the FCM, with slight accumulation at the actin focus. In accordance with previous report (Jin et al., 2011), no Blow was detected in the FC. In PI(4,5)P2 sequestering embryos (*2x Dmef2->UAS-$PH^{plc\delta}$::GFP*), Blow was no longer accumulated at the fusion site. Instead, Blow localized in puncta on the plasma membrane of FCMs that were attached to FC/myotubes. Compared with controls, the localization of Loner was not significantly altered in embryos with PI(4,5)P2 sequestering: Loner localized in puncta in the cytoplasma of both FCM and FC/myotubes. In control embryos, Mbc was localized at the base of the actin focus. The localization pattern of Mbc is disrupted in embryos with PI(4,5)P2 sequestering. Mbc was no longer accumulated at the fusion site, but relocated to the cytoplasm.

Mbc is a guanine nucleotide exchange factor (GEF) that activates Rac during myoblast fusion (Haralalka et al., 2011). The mislocalization of Mbc in PI(4,5)P2 sequestering embryos suggested that the localization of activated Rac, RacGTP, might also be altered. In control embryos, RacGTP is present at the fusion site in the FCMs. Similar to Mbc, RacGTP also marks the base of the actin focus. In PI(4,5)P2 sequestering embryos, however, RacGTP is absent from the fusion site. Instead, RacGTP is present at the distal side of the cell with respect to the fusion interface.

Figure 2.5 PI(4,5)P2 regulates RacGTP localization through Mbc. A. Relative phospholipid binding affinity of Blow, Loner, WASp PH domains and Mbc C2 domains. GST was used as a negative control. PlcδPH was used as a positive control for PI(4,5)P2 binding. **B-E.** Localization of Blow (B), Loner (C), Mbc (D) and RacGFP (E) in wild-type embryos and PI(4,5)P2 sequestered embryos. Fusion sites are double labeled with $PH^{plc\gamma}$::GFP (green) and F-actin (phalloidin, red). Compared with the control, Blow is less concentrated in FCMs in the PI(4,5)P2 sequestering background (B). Loner is present throughout the FCMs in puncta in both wild-type and in a PI(4,5)P2 sequestering background (C). Mbc is present at the FCM cortex and fusion site in wild-type, but is depleted from the cell cortex and fusion site in PI(4,5)P2 sequestering conditions (D). RacGTP localizes to the fusion site in wild-type, but in a PI(4,5)P2 sequestering background, RacGTP displays a reversed, distal localization (E). **F.** RacGTP localization in *mbc*^{c1} mutant embryos. Similar to PI(4,5)P2 sequestering condition, RacGTP displays distal localization from the fusion site in a *mbc*^{c1} mutant background (n=25 cells/genotype). Scale bar: 5 μm. (Su Deng and Ingo Bothe performed the experiments. Su Deng and Ingo Bothe analyzed the data)

Figure 2.5 PI(4,5)P2 regulates RacGTP localization through Mbc

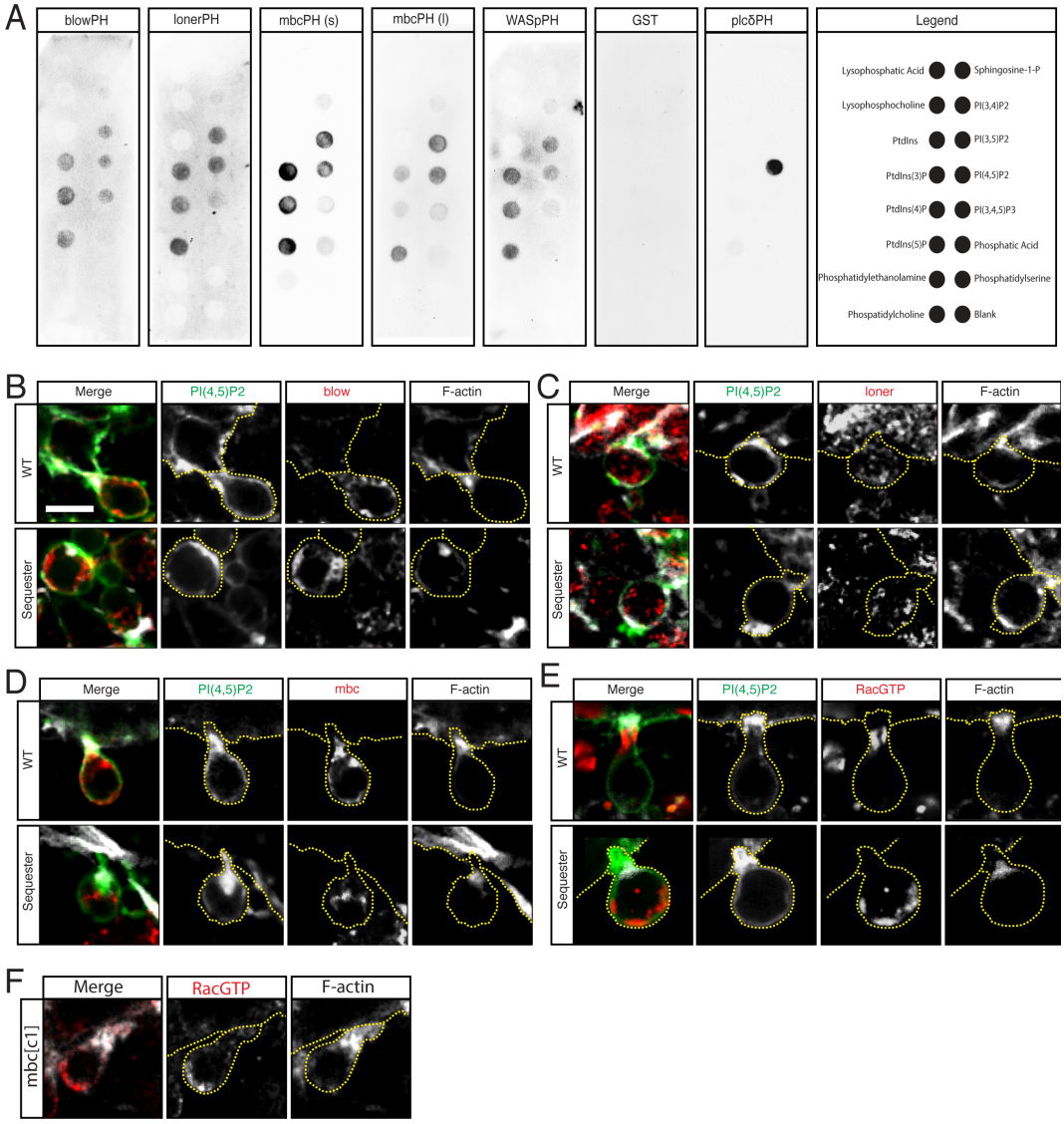

Similar RacGTP localization was observed in *mbc* mutant embryos (Figure 2.5F), confirming RacGTP mislocalization in PI(4,5)P2 sequestering embryo is due to the irregular Mbc distribution. Together, our data suggest a pathway in which PI(4,5)P2 signals to the actin cytoskeleton during fusion: PI(4,5)P2 regulates the localization of Mbc, which in turn determines the activation of Rac at the fusion site.

PI(4,5)P2 controls the localization of Arp2/3 regulators during fusion

In PI(4,5)P2 sequestered myoblasts, both Blow and Mbc/RacGTP are mislocalized. Blow regulates WASp activity by competing with WASp activator Sltr for WASp binding (Jin et al., 2011). Rac regulates SCAR activity by releasing SCAR's functional domain from its inhibited state (Chen et al., 2010). The mislocalized Blow and RacGTP suggests that the activity of WASp and SCAR is misregulated. The downstream target of both WASp and SCAR is Arp2/3, which nucleates branched actin structures. We therefore asked whether PI(4,5)P2 sequestering leads to mislocalization of WASp and SCAR, and furthermore, if the reduced actin focus size was caused by reduced Arp2/3 activity. In control embryos, SCAR accumulates on the membrane at the fusion site, while in $PH^{plc\gamma}$::GFP-overexpressing embryos, SCAR displays a diffuse localization (Figure 2.5A). Similarly, WASp concentrated at the fusion site in control embryos, while being distributed unevenly throughout the FCM in $PH^{plc\gamma}$::GFP-overexpressing embryos (Figure 2.5B). Our data confirmed our hypothesis that overexpressing of $PH^{plc\gamma}$::GFP embryos leads to the mislocalization of Arp2/3 regulators.

We next tested if the reduced actin focus size in $PH^{plc\gamma}$::GFP-overexpressing embryos was due to diminished WASp and SCAR activity, and therefore reduced Arp2/3 activity. The activity of WASP and SCAR can be abolished by reducing the level of the WASP-activator Sltr (DWip) and the SCAR-regulator Kette. In *$Dwip^{D30}$; $kette^{J4\text{-}48}$*

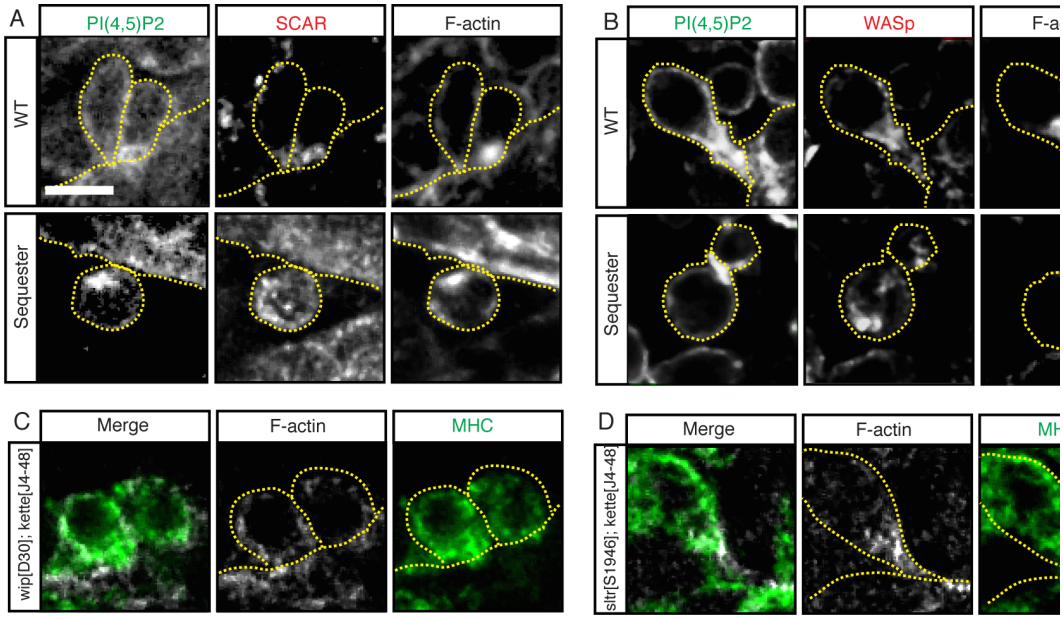

Figure 2.6 PI(4,5)P2 regulates the localization of Arp2/3 fusion machinery. A-B. Stage 15 embryos stained with phalloidin (F-actin) and antibodies against SCAR or WASp. In the wild-type control, SCAR (A) and WASp (B) accumulate at the fusion site. In PI(4,5)P2-sequestering embryos, both SCAR and WASp are mislocalized and display cytoplasmic localization. **C-D.** Analysis of actin structures in *Dwip* and *kette* double mutant embryos. Embryos were stained with phalloidin (F-actin) and antibodies against myosin heavy chain (MHC). Two different null alleles of *DWip* ($DWip^{D30}$ and $DWip^{sltr}$) and one *kette* allele ($kette^{J4\text{-}48}$) were used to abolish SCAR and WASp activity. No actin focus was observed at the fusion site in both genetic backgrounds (n=25 cells/genotypes). Scale bar: 5 μm. (Ingo Bothe and Su Deng performed the experiments. Ingo Bothe analyzed the data)

or *sltr*^{S1946}*; kette*$^{J4\text{-}48}$ double mutants, the activity of both WASp and SCAR is abolished, leading to Arp2/3 inactivation. Therefore, in the double mutant background, there was no actin focus detected at the fusion site (Figure 2.5C-D). Our data suggest that the reduced actin focus size in PI(4,5)P2-sequestered embryo is indeed due to misregulated Arp2/3 activity.

In conclusion, our research demonstrates the role of PI(4,5)P2 during myoblast fusion. PI(4,5)P2 accumulates at the fusion site after the recognition and adhesion between FC and FCM. The accumulation of PI(4,5)P2 provides localization cues for SCAR, WASp and their regulators, which in turn controls the activity of Arp2/3 at the fusion site. Loweing PI(4,5)P2 availability reduces Arp2/3 activity at the fusion site, resulting in reduced actin focus size and a block in myoblast fusion.

Discussion:

In this study, we found that PI(4,5)P2 is enriched at the interface between the FCM and FC/myotube during myoblast fusion. The accumulation of PI(4,5)P2 overlapped with the actin foci at the fusion site both spatial and temporally, suggesting a role of PI(4,5)P2 during cell-cell membrane fusion. In this study we focused on the function of PI(4,5)P2 and its interaction with actin at the fusion site. We found that PI(4,5)P2 functions downstream of cell recognition and regulates the localization of the Arp2/3 machinery at the fusion site. Our findings expand our understanding of myoblast fusion and places PI(4,5)P2 as part of the fusion machinery that regulate Arp2/3-mediated actin dynamics.

During myoblast fusion, F-actin accumulates at the fusion site and forms the actin focus (Richardson et al., 2007); this actin focus serves as the core of the invasive, podosome-like structure (Sens et al., 2010) on the FCM side of fusion. The formation of the actin focus depends on the function of Arp2/3, which can be

activated by both SCAR and WASp. Abolishing SCAR and WASp activities result in a lack of actin focus formation ((Mukherjee et al., 2011), this study). The activity of SCAR is regulated through the Mbc-Rac-Kette pathway, while WASp activity is regulated through the Blow-Dwip pathway. Our phospholipid binding assay suggests that Mbc, Blow and WASp have the potential to bind to PI(4,5)P2, suggesting further possible pathways of signaling transduction from the cell membrane to the actin cytoskeleton. Examination of Mbc, Blow, WASp and SCAR localization in PI(4,5)P2 sequestering condition supports the phospholipid binding assay and suggests that PI(4,5)P2 signaling is involved in myoblast fusion via the localization of Arp2/3 regulators. Notably, when Arp2/3 activity is completely abolished, no actin focus forms. In contrast, when PI(4,5)P2 is sequestered, small actin foci are observed in myoblast. We reason this may be due to incomplete masking of PI(4,5)P2, which allows for baseline activity of Arp2/3 at the fusion site. Our data show that SCAR and WASp are diffused, but still present at the fusion site under the sequestering conditions, which agrees with our hypothesis.

Mbc has been reported to bind strongly to PI(3,4,5)P3 in both *Drosophila* embryos and mammalian cell culture (Balagopalan et al., 2006; Côté et al., 2005). However, our phospholipid binding assay shows that the Mbc C2 domain only binds weakly with PI(3,4,5)P2. We also found that manipulation of PI(3,4,5)P3 levels does not generate fusion defects (data not shown). These data suggest the PI(3,4,5)P3-Mbc pathway is not utilized in the context of *Drosophila* myoblast fusion. Instead, we find that Mbc is mislocalized in PI(4,5)P2 sequestration background, which suggests that Mbc receives its localization cue through PI(4,5)P2. Moreover, we report that RacGTP displays a distal localization in the FCM cell under the PI(4,5)P2 sequestering condition compared to control conditions. A similar distal location was detected in *mbc* mutants. Together, these data suggest that PI(4,5)P2 regulates the

actin cytoskeleton through the PI(4,5)P2-Mbc-Rac-Kette-SCAR pathway. Lastly, our data show that Mbc loss of function results in RacGTP mislocalization, rather than Rac inactivation; this agrees with the finding that constitutively active Rac1 could not rescue *mbc* mutants (Haralalka et al., 2011), as overexpressed Rac can not be correctly localized.

Based on our data, we propose a model in which transmembrane molecules that mediate FCM-FC/myotube recognition and adhesion trigger a signaling cascade that leads to PI(4,5)P2 enrichment at the fusion site. PI(4,5)P2 then facilitates the localization of Mbc, which leads to proper localization of active Rac and Blow at the fusion site. PI(4,5)P2 and these upstream regulators control the localization and activation of SCAR and WASp, which ultimately leads to Arp2/3 activation. Signaling from PI(4,5)P2 to Arp2/3 triggers the rearrangement of the actin cytoskeleton and the formation of the invasive podosome-like structure at the site of fusion.

CHAPTER THREE

DIAPHANOUS REGULATES MYOBLAST FUSION THROUGH ACTIN POLYMERIZATION AND ARP2/3 REGULATION*

Abstract:

The formation of multinucleated muscle cells through cell-cell fusion is a conserved process from fruit flies to humans. Numerous studies have shown the importance of Arp2/3, its regulators, and branched actin for the formation of an actin structure, the F-actin focus, at the fusion site. This F-actin focus forms the core of an invasive podosome-like structure that is required for myoblast fusion. In this study, we find that the formin Diaphanous (Dia), which nucleates and facilitates the elongation of actin filaments, is essential for *Drosophila* myoblast fusion. Following cell recognition and adhesion, Dia is enriched at the myoblast fusion site, concomitant with, and having the same dynamics as, the F-actin focus. Through analysis of Dia loss-of-function conditions using mutant alleles, but particularly a dominant negative Dia transgene, we demonstrate that reduction in Dia activity in myoblasts leads to a fusion block. Significantly, no actin focus is detected, and neither branched actin regulators, SCAR or WASp, accumulate at the fusion site when Dia levels are reduced. Expression of constitutively active Dia also causes a fusion block that is associated with an increase in highly dynamic filopodia, altered actin turnover rates and F-actin distribution, and mislocalization of SCAR and WASp at the fusion site. Together our data indicate that Dia plays two roles during invasive

---

* Deng S, Bothe I, Baylies MK (2015) The Formin Diaphanous Regulates Myoblast Fusion through Actin Polymerization and Arp2/3 Regulation. PLoS Genet 11(8): e1005381. doi:10.1371/journal.pgen.1005381

podosome formation at the fusion site: it dictates the level of linear F-actin polymerization, and it is required for appropriate branched actin polymerization via localization of SCAR and WASp. These studies provide new insight to the mechanisms of cell-cell fusion, the relationship between different regulators of actin polymerization, and invasive podosome formation that occurs in normal development and in disease.

Author Summary:

Muscle formation and homeostasis critically depend on fusion between myoblasts to create and maintain multinucleated muscle fibers. Despite the importance of this process, the mechanisms regulating myoblast fusion are not fully understood. Previous studies have shown that actin polymerization factor Arp2/3 plays a critical role during myoblast fusion. However, whether other actin regulators also play a role during fusion, and how they coordinate with Arp2/3 in controlling actin dynamics remain unclear. Taking advantage of the model organism, *Drosophila melanogaster*, which shares the conserved muscle fiber with mammals, we identify the formin Diaphanous (Dia), which polymerizes linear actin filaments, as essential for myoblast fusion. We show that Dia is present at the fusion site, and with a new dominant negative Dia allele, we demonstrate that Dia functions after myoblast recognition and adhesion, but upstream of Arp2/3. Moreover, using *dia* loss and gain of function experiments, we show that Dia regulates myoblast fusion by regulating actin dynamics and by localizing the Arp2/3 regulators, SCAR and WASp, to the fusion site. Our study thus identifies new regulatory factors during muscle formation. It also suggests mechanisms by which Dia and Arp2/3 activities are

coordinated to regulate actin dynamics *in vivo* during development and homeostasis.

Introduction:

Actin filaments are major components of a cell's dynamic cytoskeleton. The remodeling of actin networks controls cell autonomous behaviors, such as cell shape changes and intracellular trafficking (Revenu et al., 2004). Highly regulated actin remodeling is also required in intercellular processes, such cell-cell adhesion and cell-cell fusion. Cell-cell fusion of myoblasts gives rise to the functional unit of muscle, the multinucleated myofiber (Aguilar et al., 2013; Shemer and Podbilewicz, 2000). A series of conserved steps, including cell-cell recognition, adhesion, membrane alignment, membrane pore formation and cytoplasmic mixing, have been identified during myogenic cell fusion across species. Given its powerful genetic approaches, its optical tractability, and its simplicity, the *Drosophila* embryonic body wall musculature is an ideal system to study the mechanisms underlying these steps in myoblast fusion *in vivo*. In *Drosophila*, a multinucleated muscle fiber arises through the fusion of two types of myoblasts: a single Founder Cell (FC), which determines muscle identity by expressing a unique combination of transcription factors (Bate, 1990; Beckett and Baylies, 2006; de Joussineau et al., 2012; Dohrmann et al., 1990), and multiple Fusion Competent Myoblasts (FCMs) (reviewed in (Abmayr and Pavlath, 2012; Rochlin et al., 2010; Simionescu and Pavlath, 2011)). Upon fusion, the nucleus of the FCM adopts the identity and transcriptional profile of the FC/Myotube (reviewed in (Baylies et al., 1998; Tixier et al., 2010)). As in vertebrates, fusion in *Drosophila* is an iterative process and in the fly embryo, the different individual muscles result from as few as 2 events to as many as 24 events (Bate, 1990).

Recognition and adhesion between the FCs/Myotubes and FCMs is mediated by four transmembrane molecules belonging to the immunoglobulin superfamily: the FC/Myotube-specific proteins, Dumbfounded (Duf; also known as Kirre) and Roughest, and their binding partners on the FCMs, Sticks and Stones (Sns) and Hibris (Artero et al., 2001; Bour et al., 2000; Ruiz Gomez et al., 2000; Strünkelnberg et al., 2001). After bidirectional signaling via these transmembrane receptors, a fusogenic synapse is established between the FC/Myotube and FCM, and accumulations of filamentous actin (F-actin) are observed on the opposing sides of the fusion site (Berger et al., 2008; Kesper et al., 2007; Kim et al., 2007; Richardson et al., 2007). On the FC/Myotube side, a thin sheath of F-actin is present. On the FCM side, the F-actin focus, which makes up the podosome-like, invasive structure (PLS), forms (Sens et al., 2010). These enrichments of F-actin are highly dynamic and resolve prior to cytoplasmic mixing between the two cells (Richardson et al., 2007). F-actin accumulation and resolution at the fusion site suggest a functional role for actin during fusion. Supporting this role, genetic screens have identified a number of fusion mutants that map to genes involved in Arp2/3-based actin remodeling (Abmayr and Pavlath, 2012; Haralalka et al., 2011; Rochlin et al., 2010; Simionescu and Pavlath, 2011). Arp2/3 is regulated by two nucleation-promoting factors (NPFs), SCAR/WAVE (WASp family verprolin-homologous protein) and WASp (Wiskott-Aldrich syndrome protein) (Higgs et al., 1999; Machesky et al., 1999). Both SCAR and WASp activate Arp2/3 through simultaneous binding of actin and Arp2/3 (Dayel and Mullins, 2004; Machesky et al., 1999). During myoblast fusion, the stability, localization, and activity of SCAR are regulated by the WAVE complex member, Kette (Nap1), and by the small GTPase Rac (Eden et al., 2002; Kunda et al., 2003; Richardson et al., 2007), which is activated by the bipartite GEF, Myoblast city (Mbc; Dock180) and Elmo (Geisbrecht et al., 2008; Haralalka et al., 2011). WASp is recruited to the fusion site via the WASp-interacting protein

Solitary (Sltr) (also known as DWIP and Verprolin) and Blown fuse (Blow) (Jin et al., 2011). The coordinated activities of SCAR and WASp lead to Arp2/3 activation and subsequently the formation of the F-actin focus, the invasive podosome, a fusion pore (Sens et al., 2010) and finally, cytoplasmic continuity (Berger et al., 2008; Gildor et al., 2009).

Arp2/3 has been shown to bind to an existing F-actin filament and nucleate a new branch. While Arp2/3 can nucleate F-actin filaments de novo, it does this slowly (Blanchoin et al., 2000). The presence of pre-existing filaments accelerates Arp2/3's ability to form branched F-actin(Pollard, 2007). Formins, another group of actin regulators, complement the activity of Arp2/3 by generating linear actin filaments. Studies have revealed both collaborative and antagonistic relationships between members of the WAVE regulatory complex, Arp2/3, and formins. As examples, Abi, a member of the WAVE complex, has been shown to interact with the formin mDia1 to positively regulate cell-cell adhesion in tissue culture cells (Ryu et al., 2009). In contrast, mDia2, WAVE, and Arp2/3 have been shown to form a multimeric complex, which inhibits mDia2-dependent filopodium formation in cultured cells (Beli et al., 2008). Arp2/3 and formins often act together in different in vivo contexts, including pseudocleavage furrow formation, cytokinesis, and filopodia formation in *Drosophila* primary neurons (Bogdan et al., 2013; Campellone and Welch, 2010). Particularly relevant for our studies in myoblast fusion are findings that, in cancer cells and macrophages, Arp2/3 and formins are required for the formation of podosomes, which resemble the invasive structure at the myoblast fusion site (Lizárraga et al., 2009; Mersich et al., 2010; Sens et al., 2010). How Arp2/3 and formins interact to regulate actin dynamics in different *in vivo* contexts, particularly myoblast fusion, remains to be investigated.

The best characterized formin in *Drosophila* is Diaphanous (Dia), where it is critical for cellularization (Afshar et al., 2000; Grosshans et al., 2005), wound healing (Abreu-Blanco et al., 2014; Antunes et al., 2013), segmental groove formation (Mulinari et al., 2008), dorsal closure (Homem and Peifer, 2009), and synapse growth (Pawson et al., 2008). Dia nucleates and elongates actin filaments through its FH1 and FH2 domains. The FH1 domain interacts with Profilin, which is an actin monomer-binding protein, to increase the local actin monomer concentration (Manseau et al., 1996; Watanabe et al., 1997). The FH2 domain binds to actin barbed ends, stabilizes newly formed actin dimers, and promotes the elongation of actin filaments (Bogdan et al., 2013; Campellone and Welch, 2010; Higgs, 2005; Paul and Pollard, 2009). The regulation of Dia activity involves autoinhibition and Rho GTPase-mediated activation. Dia autoinhibition relies on the interaction between its C-terminal DAD (Diaphanous Autoinhibitory Domain) region and the N-terminal DID (Diaphanous Inhibitory Domain) region (Alberts, 2001; Li and Higgs, 2005). The autoinhibited state of Dia is relieved when Rho-GTP binds to the N-terminal GBD (GTPase binding domain) region, thereby disrupting the DID-DAD interaction. Deletion of the Dia DAD domain inhibits the folding of Dia into the autoinhibitory conformation and results in constitutively active Dia (Homem and Peifer, 2009). Given the well-established role that Dia plays in actin regulation during development and the central position that actin plays in myoblast fusion, it is likely that Dia would play a role in myoblast fusion. However, no such role has been established.

Here we show that Dia-mediated F-actin polymerization is required for the formation of the podosome-like structure at the myoblast fusion site and is essential for the invasion of the FC/myotubes by the FCMs. We show that Dia is localized to the fusion site and there regulates F-actin polymerization: loss of Dia activity blocks

fusion, and no actin focus forms at the fusion site. Failure in focus formation arises from a block in F-actin polymerization as well as an inability to accumulate the Arp2/3 NPFs, SCAR and WASp, at the fusion site. Gain of Dia activity also blocks fusion and significantly changes the organization of the F-actin focus through increased actin turnover, leading to an excess of non-invasive filopodia at the fusion site. We further demonstrate that Dia-mediated SCAR and WASp localization is disrupted at the fusion site under these conditions. Based on our findings, we propose that Dia is necessary for two activities at the fusion site: Dia initiates invasive podosome formation through formation of linear actin filaments. Dia activity is also required for the accumulation of the Arp2/3 NPFs, SCAR and WASp, whose activity subsequently leads to Arp2/3 activation at the fusion site. The concerted F-actin elongation and branching processes likely provide the structural integrity and the necessary force generation for the invasive podosome, which ultimately leads to cell-cell fusion.

Results:

Diaphanous is Localized to the Fusion Site during Myoblast Fusion

To investigate the role of Dia during myoblast fusion, we first examined its subcellular localization in fusing myoblasts (S1 Fig). The fusion site is identified by the presence of the F-actin focus (Richardson et al., 2007; Sens et al., 2010). Immunostaining revealed that Dia is present in the cytoplasm and cell cortex of myoblasts (S1 Fig) and accumulates at the fusion site between adhered myoblasts (Fig 1A-1B). The specific accumulation of Dia at the fusion site was verified by quantification of Dia fluorescence intensity and comparison to phalloidin and Actin::GFP intensities (Fig 1B-1C, n=10; S2 Fig). Together, our analysis of fixed embryos indicates that Dia is enriched at the fusion site.

The F-actin focus is a dynamic structure that forms and subsequently resolves upon myoblast fusion. To determine whether Dia displays a similar profile, we used time-lapse analysis to compare the spatial and temporal dynamics of Dia and F-actin during fusion. Moesin::mCherry (Millard and Martin, 2008) and Dia::GFP (Homem and Peifer, 2009) were expressed in myoblasts to label F-actin and Dia, respectively. Dia::GFP is reported to retain all Dia activity (Homem and Peifer, 2009). In myoblasts co-expressing both constructs, the lifetime of the F-actin focus was, on average, 16.8±6.9 minutes (n=5), with a range from 9 to 25 min. This is comparable to expression of F-actin reporters alone (Bothe et al., 2014; Richardson et al., 2007). We also confirmed that expression of these constructs under these conditions had no observable effects on muscle differentiation. Subsequent analysis of Dia::GFP and Moesin::mCherry revealed that Dia is present at the fusion site during F-actin focus formation and resolution (Fig 1D-Di). While Dia localizes to the cell cortex before and after a fusion event, it clearly accumulates at the fusion site coincident with the F-actin focus. Together, these data indicate that Dia becomes enriched at the fusion site with the same spatial and temporal dynamics as the F-actin focus.

Myoblast fusion is an asymmetric process in which the FCM produces a podosome-like structure that invades and promotes fusion with the FC/myotube. On the subcellular level, this asymmetry manifests in an uneven distribution of F-actin (Sens et al., 2010). We therefore examined if Dia was also asymmetrically localized. To do this, we expressed Dia::GFP specifically in either FC/Myotubes or in FCMs and co-stained with the Dia antibody. By examining the overlap of exogenous and endogenous Dia signal, we can determine whether Dia is localized at the fusion site in one or both cell types.

We first expressed Dia::GFP specifically in FCs/Myotubes and examined Dia::GFP and Dia distribution. Before fusion pore formation and cytoplasm mixing, Dia::GFP could readily be detected only in the FC/Myotube. Dia antibody, in contrast, detected endogenous Dia in both the FC/Myotubes and FCMs. With this labeling approach, the Dia and Dia::GFP signals partially overlapped (Fig 1E). The partial colocalization between the FC/Myotube derived Dia::GFP and Dia antibody staining was confirmed by the separated peaks of the fluorescence intensity curves (Fig 1F). Thus, Dia is present in the FC/Myotube side during fusion, but this expression only constitutes a small portion of the total Dia enrichment at the fusion site.

Next, we examined the Dia accumulation on the FCM side. We expressed Dia::GFP specifically in FCMs, and assessed the localization of Dia::GFP and Dia. To prevent cytoplasmic mixing and the introduction of Dia::GFP into the FC/Myotube after fusion, Dia::GFP was expressed in FCMs of *mbc* mutant embryos, in which myoblast fusion is blocked prior to fusion pore formation (Doberstein et al., 1997; Rushton et al., 1995). Hence, no cytoplasmic exchange occurs between FCM and FC in *mbc* mutants. In FCMs, Dia::GFP accumulated at the fusion site (Fig 1G) and colocalized with endogenous Dia and the F-actin focus. The colocalization of Dia::GFP, Dia, and F-actin was confirmed by the overlapping fluorescence intensity curves (Fig 1H). These findings demonstrate that Dia enrichment at the fusion site, like F-actin, occurs primarily in the FCM, whereas in FC, only a thin layer of Dia is detected along the fusion interface.

Dia Localization is Dependent on FC/FCM Recognition and Adhesion, but is Independent of Arp2/3 dependent Actin Regulation

Dia enrichment at the fusion site suggested a role for Dia in myoblast fusion. To determine where in the fusion pathway Dia could function, we examined Dia localization in mutants in which myoblast fusion is blocked (Fig 2; S1 Table; S2 Fig). In *sns* mutants, where FCM-FC recognition is disrupted and no F-actin focus forms, Dia did not accumulate at the fusion site, but showed diffuse localization in the cytoplasm (Fig 2B, S1 Table), suggesting that Dia functions downstream of cell recognition and adhesion during fusion. Embryos carrying mutations in genes that regulate SCAR activity -- *rac*, *mbc* and *kette* -- display an enlarged actin focus that does not resolve. In these mutants, Dia accumulation is largely unaffected in the examined actin foci (Fig 2C-2E; S1 Table). We next examined embryos mutant for genes that regulate WASp activity: mutants in *blow* and *wsp* show enlarged F-actin foci, whereas mutants in *sltr/Dwip/vrp,* show normal sized foci. Dia localization appeared unchanged in all these mutants (Fig 2G-2I; S1 Table). Mutants in *loner*, which encodes an ARF-GEF family member (Chen et al., 2003) display normal-sized actin foci. In *loner* mutants, Dia accumulated at the F-actin focus at the stalled fusion site (Fig 2F; S1 Table). Dia's enrichment at the fusion site in all these mutant conditions was quantified by fluorescence intensity curves (Fig 2Aiv-Iiv, n= 5/genotype; S2 Fig). Together these data indicate that Dia localization at the fusion site is dependent on FC/FCM recognition and adhesion, but appears to be independent of Arp2/3 actin regulation.

Dia Loss of Function Leads to a Myoblast Fusion Block

The localization of Dia in fusion mutant embryos suggested a role for Dia downstream of FC/FCM recognition and adhesion. Hence, we examined muscle formation, and myoblast fusion in particular, in *dia* mutant embryos, using well-established *dia* alleles (Afshar et al., 2000; Castrillon and Wasserman, 1994). During *Drosophila* embryogenesis, Dia is required in numerous processes, including

metaphase furrow organization during division, cellularization, pole cell formation (Afshar et al., 2000), segmental groove formation (Mulinari et al., 2008) and dorsal closure (Homem and Peifer, 2008). In zygotic *dia*^{5}/*dia*^{5} and *dia*^{2}/*dia*^{2} mutants, abnormalities in the muscle pattern were found, including insufficient fusion (detected by free myoblasts), missing muscles, muscle morphology changes, and muscle detachment from its tendon cell (S2 Table; S3A Fig). We quantified the level of myoblast fusion by counting the total number of nuclei in the four Lateral Transverse (LT) muscles/hemisegments in both *dia*^{2} and *dia*^{5} homozygous mutants. Using this approach, we found a reduction in fusion (fusion index: *dia*^{2}: 14.1±1.3, n=21; *dia*^{5}: 21.5±1.3 n=20; control: 27.8±0.3 n=12; $p<0.001$; S3B Fig). These defects in the musculature could contribute to reduced viability of the *dia*^{2} and *dia*^{5} homozygous mutants, as less than 10% of *dia*^{2} homozygous mutants and only 20% of *dia*^{5} homozygous mutants hatched into larvae. While these data suggested a role for *dia* in myoblast fusion, we sought out genetic conditions that would enable us to study myoblast fusion in more detail. In particular, we wanted to: 1- eliminate the effects of loss of Dia's function in the ectoderm. The ectoderm is known to impact muscle development (Beckett and Baylies, 2006; Dobi et al., 2015); 2- increase the number of embryos which have Dia's function abrogated; and 3- increase, if possible, the level of fusion block when Dia's function is reduced. The Gal4/UAS system (Brand and Perrimon, 1993) allows generation of embryos in which 100% of the embryos express the transgene and can have a phenotype rather than 25% that results from traditional genetic alleles. Pairing the mesoderm/muscle specific *Dmef2-GAL4* with an appropriate UAS-line would allow manipulation of Dia in the cell type and during the time period in which fusion occurs. Available UAS-DiaRNAi lines, however, did not prove effective in knocking down Dia function during embryonic muscle development (S2 Table). We thus generated dominant negative

Dia (DiaDN::GFP) transgenic flies to reduce Dia activity specifically in the developing mesoderm/muscle during myoblast fusion.

The FH2 domain of mDia1, the mammalian homologue of *Drosophila* Dia, is required for its function in stress fiber generation in cultured cells (Copeland et al., 2004; Staus et al., 2007). A deletion of the first 21 amino acids of this domain was reported to act as a dominant negative protein, either by competing with endogenous mDia for F-actin binding or by binding to endogenous mDia to form non-functional dimmers (Copeland et al., 2004; Staus et al., 2007). Since the key amino acids in this domain are identical between mDia1 and *Drosophila* Dia, we designed a *Drosophila* dominant negative Dia (DiaDN) modeled after this mouse construct (Fig 3A).

To confirm that the DiaDN construct affects Dia-based actin regulation, we examined filopodia in cultured cells and in the *Drosophila* epidermis. Previous work indicated that reduction of Dia leads to reduction of actin-based structures, such as filopodia, in cell culture and *in vivo* (Homem and Peifer, 2009; Mellor, 2010). In S2R+ cells that express DiaDN the number of filopodia was greatly reduced compared to the neighboring control cells (5.7± 3.0 vs 17.5±5.8, n=20, $p<0.001$) (Fig 3B), consistent with a reduction of endogenous Dia activity. This reduction in filopodia was rescued by overexpression of a full length Dia with DiaDN, revealing the specificity of the DN construct (S3C-3D Fig). We also tested the efficiency of DiaDN *in vivo*, specifically by examining filopodia in leading edge (LE) cells during *Drosophila* dorsal closure. Similar to dia^{5} maternal and zygotic mutant embryos (Homem and Peifer, 2009), filopodium number was reduced in embryos expressing DiaDN (Fig 3C-Cii). Both these data sets are consistent with a reduction of Dia activity via our DiaDN construct. As additional test of our DiaDN construct, we examined another context in which Dia is known to play a role. dia^{1} homozygous

mutants are sterile due to defects in cytokinesis in the germline (Castrillon and Wasserman, 1994). Expression of DiaDN in the male germline leads to reduced fertility due to fewer sperm (S3F-3G Fig), consistent with a reduction in Dia activity in this context. Collectively, these data indicate the DiaDN construct reduces Dia activity.

We next examined the effects of DiaDN when expressed specifically in myoblasts. When one copy of DiaDN was expressed, we observed defects in muscle development, including myoblast fusion, in 50% of embryos (n=20; Fig 3D). Other muscle differentiation processes also were disrupted, including muscle attachment and morphology (S3E Fig). These phenotypes were similar to those observed in *dia* mutant embryos (S2 Table; S3A-3B Fig), reinforcing that the defects using DiaDN were due to Dia loss of function.

To increase the penetrance and expressivity of the fusion phenotype in embryos expressing DiaDN, we increased DiaDN expression levels in two ways: increasing genetic copy numbers of the mesoderm/muscle driver *DMef2-Gal4* driver and *UAS-DiaDN* and increasing the temperature at which we raised the embryos, since higher temperatures correlated with increased Gal4/UAS activity (Brand and Perrimon, 1993; Seroude et al., 2002). We generated a fusion index as described for *dia* mutants (Fig 3E-3F; S3 Fig). Expression of one copy of *DiaDN* with one copy of the Gal4 driver (1X) resulted in a significant decrease in myoblast fusion (22.5±2.2 vs 27.1±2.3 LT nuclei/ hemisegment in control, $p<0.001$). Free myoblasts also were detected, in addition to detached muscles. Expression of two copies of *Dia DN* with two copies of the Gal4 driver (2X) resulted in a more severe fusion block (15.5±2.7 $p<0.001$) and more free myoblasts were observed. Under these conditions, some myotubes also failed to properly attach to tendon cells, and, as a result, formed myospheres (Fig 3D, arrowheads; S3E Fig). Specification and differentiation of both

FCs and FCMs occurred normally under these conditions, as revealed by expression of MHC and apRed positive nuclei (Fig 3D-3E) (Bothe et al., 2014; Richardson et al., 2007). In combination with Dia's localization at the fusion site, these data indicate that Dia activity is necessary for myoblast fusion.

To determine which cellular step of fusion requires Dia activity, we next examined F-actin foci and myoblast morphology in embryos where *DiaDN::GFP* was expressed in myoblasts. We found that FCMs oriented towards the FC/Myotube, showing the characteristic teardrop shape (Doberstein et al., 1997; Richardson et al., 2007; Rochlin et al., 2010). FCMs also attached to FC/Myotubes. Localized expression of the recognition and adhesion receptors, Duf and Sns, at the fusion site confirmed that these FCMs were adhered to the FC/Myotube (Fig 4A). However, in 40% of the attached FCMs, an actin focus failed to form, consistent with the extent of fusion block found under these conditions (Fig 4B-4C). Further confirmation of these data was obtained using time-lapse imaging of myoblast fusion (Fig 4D, S3H Fig). Embryos expressing DiaDN::GFP in myoblasts showed movement of FCMs towards and attachment to FC/myotubes. A subset of these adhering FCMs showed no significant accumulation of actin that resembled the F-actin focus. The FCMs that failed to form a F-actin focus also failed to fuse to the FC/Myotube during the time-lapse sequence, consistent with reduction of Dia activity causing a fusion block. In agreement with Dia regulating actin at the fusion site, expression of DiaDN also significantly reduces actin focus size in the *blow*^{1} mutant, which normally has an enlarged actin focus (S3I Fig). Together these data support the critical role of Dia for the formation of the F-actin focus as well as the importance of the F-actin focus during the fusion process.

Previous data (Bothe et al., 2014; Sens et al., 2010) indicated that simultaneous loss of both Arp2/3 NPFs, SCAR and WASp, leads to a fusion block

with no F-actin foci, due to the loss of Arp2/3 activity. To address whether the lack of the actin focus in the DiaDN expressing myoblasts was due just to reduced F-actin polymerization by Dia or whether Dia loss could also influence Arp2/3 activity, we examined the localization of the Arp2/3 regulators, SCAR and WASp, in myoblasts expressing the DiaDN construct (Fig 4E-4F). We found that neither Arp2/3 regulator was present at the fusion site in those FCMs in which a focus failed to form (WASp: enrichment at 0% fusion site versus 100% in control. SCAR: enrichment at 20% fusion site vs 70% in control). These data suggest that Dia activity is required, through localization of SCAR and WASp, for Arp2/3 activity at the fusion site.

To further investigate whether Dia functions upstream of the Arp2/3 pathway, we examined Dia localization in *sltr*^{s1946}*; kette*$^{J4\text{-}48}$ double zygotic mutants. In this double mutant, Arp2/3 activity is reduced, due to the lack of activated SCAR and WASp, and no actin focus is observed at the fusion site (Bothe et al., 2014). Immunostaining of these mutants revealed that Dia accumulated at the fusion site (Fig 4G), suggesting that Dia accumulates at the fusion site prior to actin focus formation, and Dia's localization is independent to Arp2/3 activity. Moreover, these data imply that Dia expression, in the absence of Scar and Wasp activity (and by extension, absence of Arp2/3 activity), is not sufficient to build the F-actin focus.

As another test of our model, we examined Dia expression in embryos where PI(4,5)P2 signaling is reduced. In other contexts (Seroude et al., 2002), PI(4,5)P2 signaling provides a localization cue for Dia. However, under conditions in which reduction of PI(4,5)P2 signaling leads to a myoblast fusion block (Bothe et al., 2014), Dia was still localized to the fusion site (Fig 4H). Hence, PI(4,5)P2 signaling appears not to be required for Dia localization during fusion. In addition, reduction in PI(4,5)P2 signaling at the fusion site leads to a reduction in actin focus size. PI(4,5)P2 signaling functions upstream of Arp2/3 activity and the reduced

focus size correlated with reduced recruitment/maintenance/activity of Arp2/3 NPFs at the fusion site (Bothe et al., 2014). Localization of Dia at the fusion site in this background now provides, in part, a possible explanation for this smaller actin focus. Dia localization in this PI(4,5)P2 signaling mutant background would lead to low level recruitment/activity of Arp2/3 NPFs, subsequent Arp2/3 activity, and actin focus formation (albeit smaller). Nevertheless, Dia requires PI(4,5)P2 signaling to build an effective actin focus, capable of mediating myoblast fusion.

Taken together, we conclude that Dia is essential for myoblast fusion, and this function occurs after recognition and adhesion between FC and FCMs, but prior to Arp2/3-based actin polymerization. Importantly, Dia activity appears to be required for actin focus formation, both through its regulation of F-actin polymerization and the accumulation of Arp2/3 regulators at the fusion site.

Constitutively active Diaphanous blocks myoblast fusion

To gain further insight to Dia's role in actin polymerization and in the localization of the Arp2/3 NPFs at the fusion site, we examined the effects of constitutively active Dia on myoblast fusion (Fig 5, S4 Fig, S5 Fig). Several well-characterized constitutively active Dia constructs (DiaCA) were employed, including DiaΔDAD, which has a deletion of the DAD domain, and FH1FH2, which consists of only Dia's FH1 and FH2 domains (Fig 5A, S4A Fig) (Homem and Peifer, 2008). Expression of any of these DiaCA constructs in myoblasts blocked myoblast fusion in 100% of the embryos, as witnessed by the presence of unfused, free myoblasts (Fig 5B; S4B-4C

Fig). FCs were properly specified and myoblast recognition and adhesion, as measured by Sns and Duf localization, were unaffected (S5 Fig); however, fusion did not occur (LT muscle fusion index: 5.2±1.0 vs 26.6±1.5, $p<0.001$/ hemisegment; Fig 5C; S4C Fig).

Examination of the localization of constitutively active Dia during myoblast fusion revealed that, as with endogenous Dia, all DiaCA constructs showed enrichment at the fusion site (Fig 5D, S4D Fig). Time lapse imaging showed, however, that DiaCA was associated with highly dynamic filopodia; for example, DiaΔDAD::GFP was found concentrated at the tip of each of the multiple filopodia at the fusion site (Fig 5D, arrows). Under wild-type conditions or when Dia::GFP is overexpressed, such increased numbers of dynamic filopodia were not detected.

We next examined actin organization in myoblasts expressing DiaCA. GFP-tagged actin, which labels both G- and F-actin, was used to visualize actin (Fig 5E). We observed Actin::GFP accumulation at fusion sites, which were similar in size to that in control embryos (1.8±0.37μm vs 1.9±0.43μm, respectively; n=50, $p=0.25$). Multiple filopodia were also detected with Actin::GFP, extending from both the FCM and the FC/Myotube. The actin accumulation did not resolve during the 1h observation time, as fusion failed to occur. Together, these data indicate that DiaCA is recruited appropriately to the fusion site. There, DiaCA enhances actin polymerization, visualized as increased filopodia; however, this increase in actin polymerization appears not to be productive, as fusion progression is blocked.

Constitutively active Dia alters actin dynamics and organization at the fusion site

The highly dynamic filopodia at the fusion site suggested that actin undergoes rapid remodeling in myoblasts expressing DiaCA. We employed fluorescence recovery

after photobleaching (FRAP) to quantify the consequence of expressing DiaCA on actin dynamics at the fusion site. In control experiments, photobleaching of individual actin foci in wild-type embryos expressing Actin::GFP resulted in a rapid recovery of the fluorescent signal to pre-bleaching levels (Fig 6, S3 Table). Parallel experiments in myoblasts expressing both Actin::GFP and DiaCA revealed that DiaCA significantly enhanced the actin recovery rate relative to control (Fig 6A-6C): the half time of fluorescence recovery in embryos expressing DiaCA was significantly less than that in control (16.3±6.7s vs 53.3±17.7s, respectively, $p<0.001$). The percentage recovery for embryos expressing DiaCA, however, was similar to controls (Fig 6D). The rapid turnover rate of Actin::GFP upon DiaCA expression suggests that actin filaments undergo faster polymerization and depolymerization cycles than in control myoblasts. These data are consistent with the increase of rapidly extending filopodia observed in time lapse of myoblasts expressing constitutively active Dia.

The previous experiments with Actin::GFP measured both G- and F-actin at the fusion site. To examine the organization and distribution of F-actin alone at the fusion site, we used phalloidin staining in fixed preparations. In myoblasts expressing DiaCA, the F-actin focus displayed a diffuse distribution rather than a compact spherical organization seen in wild-type FCMs (Fig 7A-7B). This altered distribution was reflected in the fluorescence intensity curve: the peak of F-actin intensity curve in DiaCA myoblasts is broader in comparison to controls (Fig 7C). Together with the FRAP experiments, these data imply that DiaCA blocks myoblast fusion by altering actin dynamics and the actin focus organization at the fusion site.

Constitutively active Dia leads to mislocalization of Arp2/3 Regulators, SCAR and WASp

Our loss-of-function experiments indicate that Dia is required, not only for filamentous actin polymerization, but also for the localization of the Arp 2/3 NPFs, SCAR and WASp, at the fusion site. To better understand the link between Dia and the two Arp2/3 NPFs during fusion, we employed epistasis experiments, using the DiaCA and mutants in the NPF regulators (Fig 7). We first examined F-actin focus morphology in *kette*$^{J4\text{-}48}$ mutant embryos in which DiaCA is expressed in myoblasts. Kette regulates the stability and localization of SCAR during myoblast fusion. In *kette* mutants, myoblast fusion is blocked and F-actin foci are enlarged (Richardson et al., 2007). When expressing DiaCA in the *kette*$^{J4\text{-}48}$ background, F-actin did not form a dense focus, but rather, displayed diffuse localization, reminiscent of the F-actin distribution in DiaCA expressing myoblasts (Fig 7D). We also examined F-actin focus morphology in *sltr*^{S1946} mutant myoblasts; Sltr directly binds to and activates WASp. In *sltr*^{S1946} mutants, myoblast fusion is blocked but the size of the F-actin focus is not changed (Richardson et al., 2007). When expressing DiaCA in the *sltr*^{S1946} background, F-actin was diffuse at the fusion site and did not form a restricted focus, which again resembled F-actin distribution when DiaCA was expressed in myoblasts alone (Fig 7E). The distribution of F-actin in *kette*$^{-/-}$ and *sltr*$^{-/-}$ backgrounds when DiaCA was expressed suggested that Dia functions upstream of Arp2/3 in regulating F-actin assembly at the fusion site.

To confirm and build upon these data, we examined the localization of SCAR and WASp, the targets of Kette and Sltr activity in embryos expressing DiaCA. In control embryos, SCAR accumulated at the fusion site (Fig 7F). In embryos expressing DiaCA in myoblasts, SCAR was still present, but it was no longer enriched at, or restricted to, the fusion site: SCAR was found mislocalized throughout the FCM (Fig 7F). The mislocalization of SCAR was verified by fluorescence intensity curves: SCAR displayed several peaks in myoblasts expressing DiaCA, and only one

overlapped with the F-actin. WASp also localized at the fusion site in control embryos (Fig 7G). In myoblasts expressing DiaCA, WASp, like SCAR, displayed a diffuse localization in the cytosol. Interestingly, when we evaluated the localization of WASp using fluorescence intensity curves, we found that WASp colocalized with the diffuse F-actin foci at the fusion site (Fig 7G). The mislocalization of SCAR and WASp suggests that, in myoblasts expressing DiaCA, Arp2/3 was activated over a larger area compared to control, therefore, could contribute to the diffuse localization of F-actin at the fusion site. The mislocalization of SCAR and WASp in both DiaDN and DiaCA expressing myoblasts, as well as the lack of an F-actin focus in myoblasts expressing DiaDN, indicates that Dia functions upstream of Arp2/3 and its regulators and that a particular level of Dia actin polymerization activity at the fusion site is required for optimal Arp2/3 activity and focus formation at the fusion site.

Discussion:

In this study, we provide the first evidence that the formin family member, Dia, is essential for *Drosophila* myoblast fusion. We show that Dia is expressed in all myoblasts and is recruited to the myoblast fusion site. The spatial and temporal distribution of Dia at the fusion site parallels that of the F-actin focus, which forms the core of an invasive podosome. This actin rich podosome is critical for FCM invasion of the FC/Myotube during fusion. In keeping with its expression pattern, Dia is essential for myoblast fusion progression: both loss and gain of Dia function lead to a fusion block. Under both conditions, the integrity of the F-actin focus and hence the invasive podosome is compromised; myoblasts expressing DiaDN fail to form the focus, whereas myoblasts expressing DiaCA have many filopodia and have a diffuse organization of F-actin, both of which contribute to a failure in invasive podosome formation and fusion. Dia activity is required after FC/Myotube and FCM

recognition and adhesion but upstream of Arp2/3 activity. It is required, in parallel with PI(4,5)P2 signaling, to build a functional F-actin focus at the fusion site. Our experiments further indicate that Dia activity is critical for actin dynamics at the fusion site, which, in turn, regulate fusion progression. Moreover, the aberrant F-actin organization at the fusion site in both loss and gain of function is also due to altered localization of the Arp2/3 regulators, SCAR and WASp. Taken together, our data support a role for the formin Dia in a critical first step of actin polymerization at the fusion site, downstream of cell-cell recognition and adhesion, and link its activity to the formation of F-actin foci, required for myoblast fusion.

Dia is required for actin polymerization at the fusion site

Actin remodeling is critical for myoblast fusion, but Arp2/3 was the only known actin polymerization factor that was shown to be necessary for myoblast fusion (Berger et al., 2008; Richardson et al., 2007). We now show that the formin Dia is also required during myoblast fusion. Whereas Arp2/3 preferably binds to pre-existing actin filaments and generates uncapped F-actin, formins nucleate F-actin both *de novo* and from the barbed ends of pre-existing actin filaments. Thus, Dia can generate actin filaments *de novo*, which Arp2/3 can bind or elongate (Pollard and Borisy, 2003; Pruyne et al., 2002).

We also show that the level of Dia activity is critical for myoblast fusion. Too much actin polymerization leads to too many filopodia and absence of an invasive podosome with its characteristic F-actin core. Too little polymerization leads no actin focus and no podosome formation. Our FRAP data with DiaCA also hint at whether a limited pool of actin is available for the actin polymerization factors during myoblast fusion. Despite the high rates of actin turnover with expression of DiaCA, the final fluorescence levels of actin returns to the same value as in controls.

Additional actin monomers are not recruited to the site, even with high levels of polymerization activity. Interestingly, the rate of actin turnover has also been measured in mutants that affect Arp2/3 activity: specifically, mutations in *blow,* which regulates the Arp2/3 NPF WASp, show lower rates of actin exchange than in controls, due to a reduced exchange rate for WASp on the barbed ends of actin at the fusion site (Jin et al., 2011). Together these data suggest future experiments aimed at examination of whether rates of actin polymerization regulated by both Dia and Arp2/3 are optimized for the available actin pool and tightly controlled for myoblast fusion to properly occur.

Dia and Arp2/3 activities are linked during myoblast fusion

Both cooperative and antagonistic functions between Dia and Arp2/3 have been reported (Fukumi-Tominaga et al., 2009; Yan et al., 2013). Here we demonstrate that the coordinated and cooperative activities of these two actin polymerization factors leads to the formation of the F-actin focus. With the exception of *sltr*/*Dwip*/*vrp* mutants that form a focus of wild-type size, single mutants in the Arp2/3 NPF pathways, WASp and SCAR, lead to enlarged foci; however, double mutants in WASp and SCAR pathways do not form foci (Bothe et al., 2014). This is the same phenotype that we have seen in myoblasts expressing the DiaDN. Our data support Dia activity being upstream of WASp and SCAR activation of Arp2/3 at the fusion site. This suggests that, at the fusion site, Dia initially provides the necessary context upon which Arp2/3 can act and not vice versa, as has been suggested in other contexts in which linear actin filaments emerge from Arp2/3 based structures (Jin et al., 2011). Nevertheless, both sets of actin regulators are necessary for F-actin focus formation that provides the core of the invasive podosome. Neither Dia nor Arp2/3 alone are sufficient.

The interplay between Dia and Arp2/3 at the fusion site is also reflected by our localization studies. Too little or too much Dia activity resulted in improper localization and, by extension, improper activity of Arp2/3 NPFs. How could Dia regulate this localization? One possibility is that Dia indirectly regulates Arp2/3 localization. Dia could nucleate linear actin filaments, which then would provide the necessary substrate for recruitment, maintenance and /or activation of Arp2/3 and its regulators, such as the WASp-WIP complex (Jin et al., 2011). Another possibility is that Dia, through its interactions with members of the SCAR/WAVE complex such as Abi, may directly localize and/or maintain the localization of Arp2/3 regulators, which are then activated at the fusion site. Abi has been reported to bind directly with Dia *in vitro,* and this interaction is required for the formation and stabilization of cell-cell junctions (Ryu et al., 2009). Dia likely changes the localization and integrity of the SCAR/WAVE complex by competitively binding to the N-terminal part of Abi, dissociating Kette/Nap1 from the complex, and thus changing the stability and localization of SCAR/WAVE. It has also been established that the recognition and adhesion receptor, Sns, is capable of recruiting the Arp2/3 NPFs, such as WASp, to the fusion site (Jin et al., 2011). While Sns is still clustered at the fusion site in DiaDN and DiaCA, its recruitment activity appears not sufficient for focus formation capable of supporting an invasive podosome.

We have shown that localization of Arp2/3 NPFs is affected in Dia loss and gain of function. In addition to this spatial control, another important way of controlling Arp2/3 activity is through activation of the NPFs via small GTPases. SCAR is activated through Rac-dependent dissociation from SCAR inhibitory complex (Eden et al., 2002; Kunda et al., 2003; Richardson et al., 2007). WASp is activated by binding to Cdc42, which releases it from auto-inhibited state (Berger et al., 2008; Kesper et al., 2007; Kim et al., 2007; Richardson et al., 2007). In

this study, we did not examine the localization of these activated GTPases. However, previous work has shown that PI(4,5)P2 signaling is required for proper localization of activated Rac at the fusion site (Bothe et al., 2014). How the localization and activity of small GTPases at the fusion site contribute to the spatial and temporal interplay between Dia and Arp2/3 regulation of actin polymerization requires further investigation.

It remains unresolved how Dia itself is recruited to the fusion site. Our data suggest that the recognition and adhesion receptors Duf and Sns would be involved either directly or indirectly in recruiting Dia to the fusion site, as embryos that fail to express either of these adhesion receptors fail to recruit Dia to the fusion site. In addition, recent data from *Drosophila* epithelial tubes (Rousso et al., 2013) indicate that PI(4,5)P2 serves as a localization cue for Dia. Previous work in our lab has shown that PI(4,5)P2 accumulates at the fusion site after FC-FCM recognition and adhesion; sequestering of PI(4,5)P2 results in a significant fusion block (Bothe et al., 2014). We thus tested whether PI(4,5)P2 regulates Dia localization at the fusion site. We find that Dia is recruited to the fusion site in the PI(4,5)P2 sequestered myoblasts, suggesting that, in this context, PI(4,5)P2 signaling is not required for Dia localization. These data provide possible explanations for why in PI(4,5)P2 sequestering embryos, smaller actin foci are detected: the localized Dia may be sufficient to recruit low levels of Arp2/3 and its NPFs, which, upon activation, lead to the formation of small F-actin foci. Nevertheless, in the absence of PI(4,5)P2 signaling, Dia that is recruited to the fusion site is not sufficient to produce a functional actin focus, capable of directing a fusion event. Recent work (Ramalingam et al., 2010) also indicates that charged residues in the N- and C-termini of mDia1 are sufficient both for mDia's clustering of PI(4,5)P2 and its own membrane anchorage. This interaction between mDia1 and PI(4,5)P2, in turn,

regulates mDia1 activity. Whether such a mechanism is in play at the myoblast fusion site needs to be further investigated.

A model for interactions between actin polymerization factors during myoblast fusion

We propose a working model for the interplay between the actin regulators during myoblast fusion (Fig 8). Dia is recruited to the fusion site upon engagement of the recognition and adhesion receptors by a yet-to-be determined mechanism. We propose that PI(4,5)P2 signaling at the fusion site regulates the localization and activation of downstream targets such as Rho-family of small GTPases. These small GTPases lead to the activation of Dia. Activated Dia, in turn, polymerizes linear actin filaments and, in combination with the recognition and adhesion receptors and PI(4,5)P2, recruits the Arp2/3 NPFs, SCAR and WASp. Activation of these Arp2/3 NPFs at the fusion site would be accomplished by small GTPases such as Rac. These, in turn, would activate Arp2/3, leading to branched actin and formation of the F-actin focus and the invasive podosome. Whether the Arp2/3 NPFs such as SCAR/WAVE would negatively regulate Dia to downregulate linear actin polymerization, as suggested for mDia2 in cell culture (Beli et al., 2008), or whether Dia competes with WASp for barbed end binding remains to be investigated (Co et al., 2007). However, these mechanisms would underscore a switch from linear F-actin filopodium formation to the linear and branched F-actin invasive podosome–like structure that is necessary for fusion.

Invasive podosomes in development and disease

The actin focus formed at the fusion site is an F-actin rich, invasive podosome-like structure that has been suggested to provide a mechanical force for FCMs to invade the FC/Myotube (Jin et al., 2011). Similar invasive actin structures named invadosomes have been seen in different cell types, such as podosomes in macrophages and invadopodia in cancer cells (Linder, 2009). Arp2/3 is known to play a key role in invadosome formation, and recent studies have revealed the involvement of formins in developing invadosomes (Lizárraga et al., 2009; Mersich et al., 2010). Our data indicate that specific temporal and spatial interactions between the formin Dia and Arp2/3 are required for the actin focus and invasive podosome formation. Our data thus provide new mechanistic insights for the interplay of Arp2/3 and Formins during invadosome formation in these contexts.

Acknowledgements: We thank M. Peifer for constitutively active Dia alleles and the *dia*^{2} allele. We thank D Soffar, P Guo, D Jin, A Spencer for technical support. We also thank V Schulman, K Dobi and J Zallen for critical reading of the manuscript. This paper is also in memory of Alan Hall, a valued mentor and committee member.

Figures and Figure Legends:

Fig 1: Diaphanous is localized to the fusion site

A-D. Dia colocalizes with the actin focus at the site of fusion. **A.** Fusing myoblast (FCM, false colored magenta in all Figures) and FC/Myotube (false colored turquoise in all Figures, see Methods and S1 Fig) in a stage 15 *twist-actin::GFP* embryo stained for F-actin (phalloidin, white) and antibodies against Dia (red) and GFP (green). Dia accumulates at the fusion site, colocalizing with the F-actin focus. **B.** Signal intensity plot confirms Dia enrichment with actin at the fusion site. Average fluorescence intensity measured across the F-actin foci as shown in A. A line of predetermined length was dropped across the fusion site; fluorescence intensity along the line was measured in different channels, normalized, and plotted (n=10). See Methods and S2 Fig for details on intensity measurements and normalization. **C.** Fluorescent intensity curves with error bars for both control (n =10) and proteins of interest (n =10). **D.** Still images from a time-lapse series of a fusion event in a stage 14 embryo expressing Dia::GFP and Moesin::mCherry driven by *DMef2-Gal4* indicates that Dia::GFP has the same spatial and temporal pattern as actin at the fusion site. Moesin::mCherry (red) labels F-actin at the fusion site (arrows). **Di.** Signal intensity curve showing Dia::GFP (green) and Moesin::mCherry (red) colocalize during fusion at each time point. **E-H.** Dia is localized to the fusion site in both the FC/Myotube (turquoise) and FCM (magenta). Dia::GFP (green), phalloidin (white), endogenous Dia (red) **E.** *duf5.1-Gal4* driven Dia::GFP shows expression in myotubes/FCs in stage 14 embryos. Fusing FCM and myotube were captured before cytoplasmic mixing. Dia antibody staining (red) is present at the F-actin focus (phalloidin, white). FC driven Dia::GFP (green) expressed in FC/Myotubes partially overlaps with endogenous Dia at the fusion site. **F.** The signal intensity curve confirms that the peak of FC driven Dia::GFP partially overlaps with endogenous Dia. **G.** Stage 16 *sns-*

Gal4 driven Dia::GFP shows expression in *mbc*^{C1} mutant FCMs, where fusion is blocked. Staining as in F. Dia enrichment is seen on FCM side with both Dia (red) and FCM driven Dia::GFP (green). **H.** Signal intensity curve confirms Dia::GFP and Dia overlap and are within the F-actin peak. Scale bar: 2.5μM

Fig 1: Diaphanous is localized to the fusion site

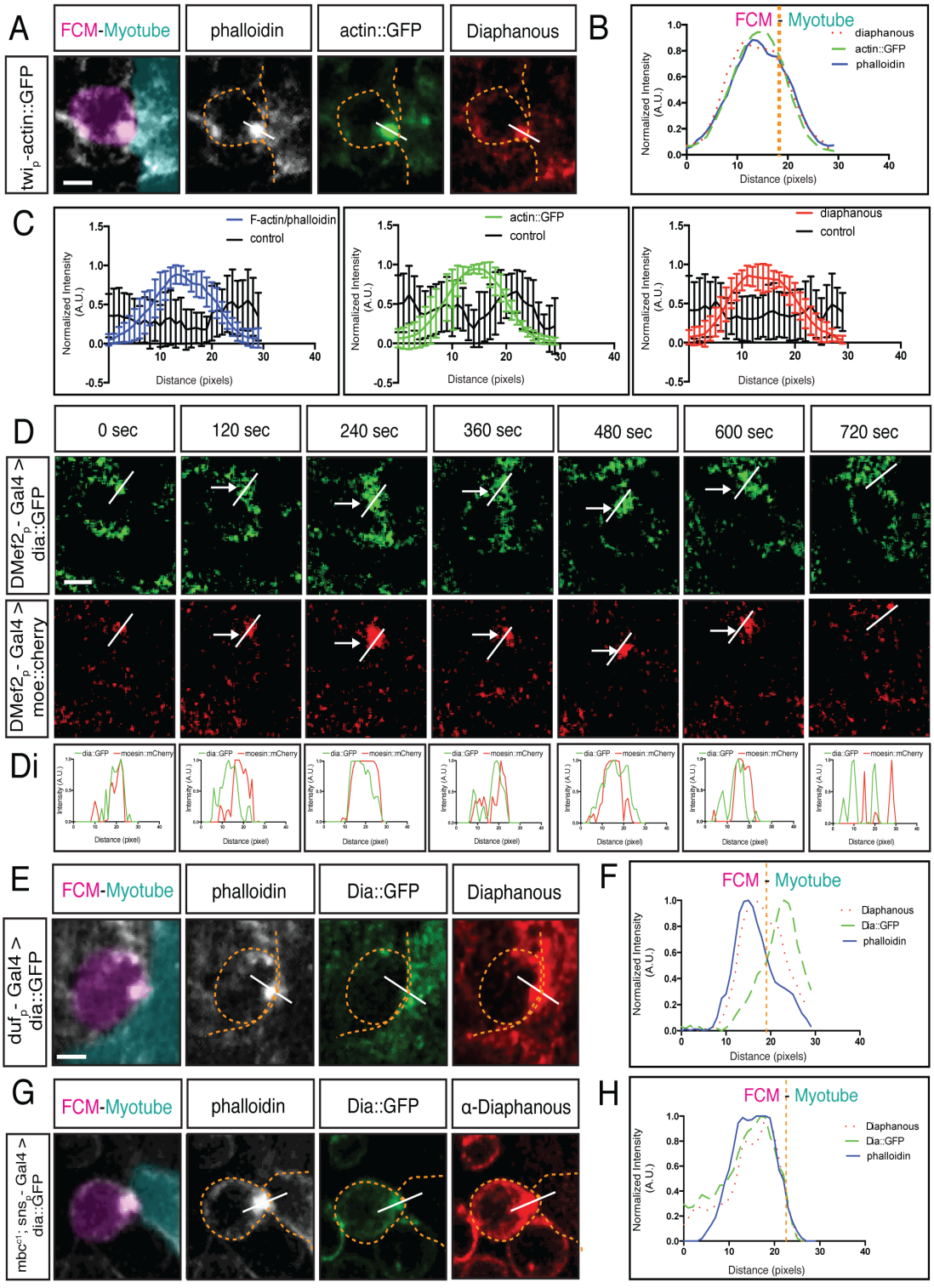

Fig 2: Dia localization at the fusion site is dependent on FC/FCM recognition and adhesion, but independent of regulators of Arp2/3.

Stage 15 embryos stained with phalloidin (**i.**), antibodies against Dia (**ii.**), and Myosin Heavy Chain (**iii.**, MHC). Phalloidin labels F-actin (focus and sheath) at the fusion site; MHC identifies myoblasts. FCM (magenta) and FC/Myotube (turquoise). **A-iv.** Dia localization in FCM and FC/myotube in a wild-type embryo during myoblast fusion. Dia accumulates at the fusion site. The averaged fluorescence intensity curve (Aiv, n=5) in wild-type embryos confirms Dia colocalization with actin. **B-iv.** In *sns* mutants, no F-actin focus is formed and no specific accumulation of actin or Dia are observed. Average fluorescence intensity curve of *sns* mutant embryos (Biv, n=5) supports that Dia does not accumulate at the fusion site and is cytoplasmic. **C-E-iv.** In *rac*, *mbc*, and *kette* mutants, SCAR activity is lost, an enlarged focus is observed at the fusion site, and Dia is enriched at the fusion site. Fluorescence intensity curves confirm Dia and actin colocalization in *rac* (Civ), *mbc* (Div), and *kette* (Eiv) mutants (n=5/genotype). **F-iv.** In *loner* mutant embryos, Dia accumulates at the F-actin focus, as confirmed by the fluorescence intensity curves (n=5). **G-I-iv.** In *blow*, *sltr(Dwip)* and *wsp* mutants, where WASp-mediated actin remodeling is lost, Dia accumulation at the fusion site is unaffected. Fluorescence intensity curves confirm the colocalization of Dia and F-actin in *blow* (Giv), *sltr(Dwip)* (Hiv)*, and wsp* (Iiv) mutants (n=5/genotype). Scale bar: 2.5μM

Fig 2: Dia localization at the fusion site is dependent on FC/FCM recognition and adhesion, but independent of regulators of Arp2/3.

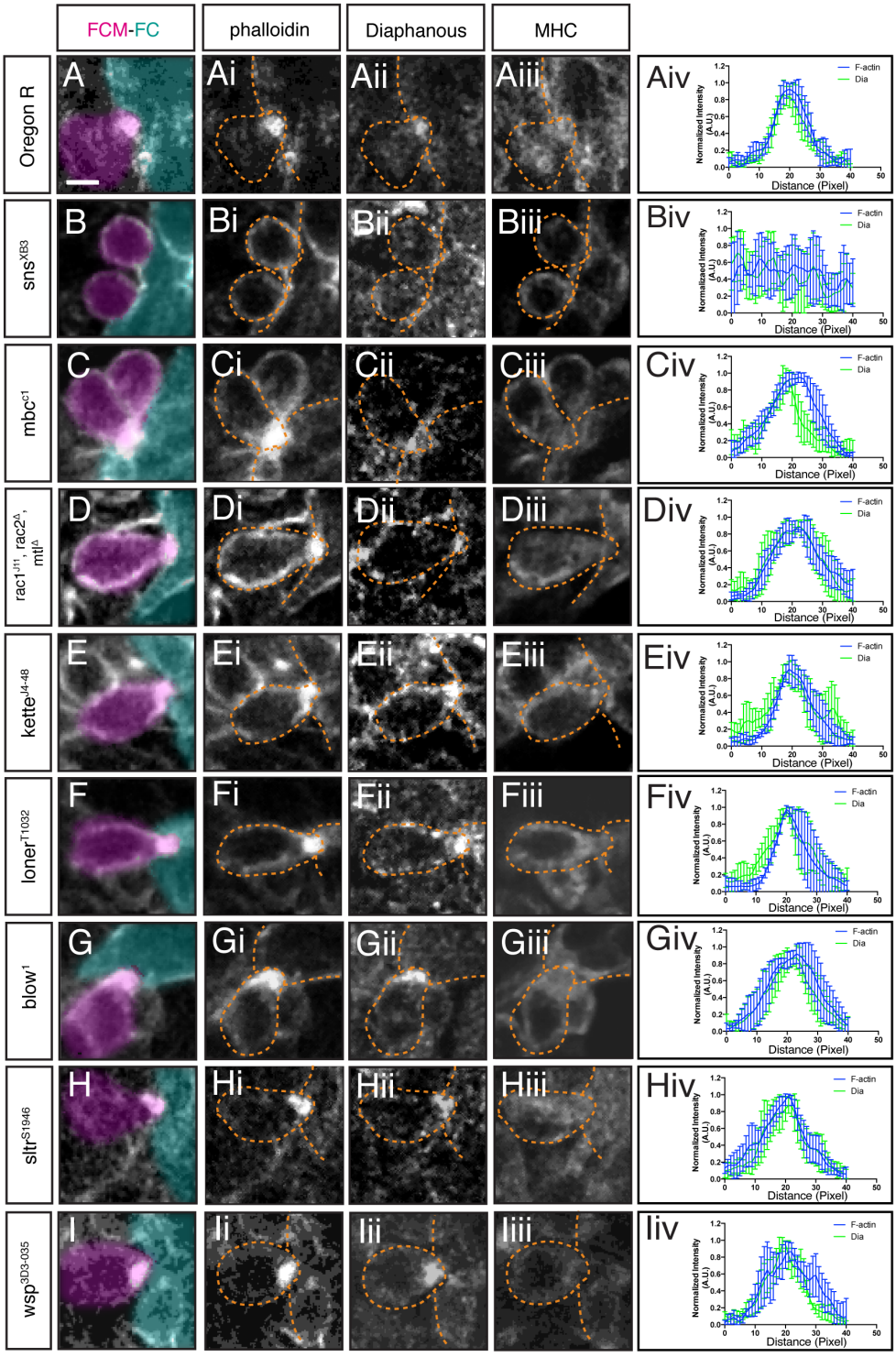

Fig 3: Diaphanous is required for myoblast fusion A. Schematic diagram of Dia domain structure and a deletion construct that renders Dia dominant negative (DiaDN). DiaDN consists of the FH1 domain and a partially deleted FH2 domain; the deleted aa 750-770 in the FH2 domain is indicated by the dashed area. **B**. Expression of DiaDN reduces filopodia number in S2R+ cells. S2R+ cells that were transfected with DiaDN::GFP (green in merge, grey in single channel) have less filopodia-like, protrusive structures (phalloidin, red in merge, grey in single channel) relative to untransfected cells ($n=20$, $p<0.001$). Scale bar: 10μM. This reduction was rescued by expression of Dia::GFP (S3C Fig). **C-Ci.** *UAS-diaDN::GFP* was expressed in leading edge cells using *wg-Gal4*. Moesin::mCherry was also expressed in leading edge cells to visualize actin. In stage 15, GFP-negative control cells, filopodia structures are seen (C, arrow). DiaDN::GFP significantly reduced filopodia formation (Ci). Scale bar: 2.5μM. **Cii.** Filopodium number was quantified in each wg-Gal4 expressing stripe. DiaDN significantly reduced filopodia formation in leading edge cells relative to control (2.1±1.29μM vs 3.95±1.15μM, $p<0.001$). **D.** Increasing DiaDN concentration in myoblasts through higher temperature and genetic copy number leads to an increased fusion block. Three hemisegments of a lateral view of a stage 16 embryos stained with GFP and MHC antibody are shown. Myoblast fusion is relatively normal in 1x*DMef2-Gal4>*1x*diaDN::GFP* embryos at 29°C (upper panel), with few free myoblasts (arrow). In 2x*DMef2-Gal4>*2x*diaDN::GFP* embryos (lower panel), a higher degree of fusion block (arrows) and muscle detachment (arrowheads) are observed. **E.** One hemisegment of stage 17 embryo showing apME-NLS::dsRed labeled nuclei in the four lateral transverse (LT) muscles: From left to right: apME-NLS::dsRed labeled nuclei in stage 17 LT muscles in control, in *1xDMef2-Gal4> 1xUAS-diaDN::GFP,* and in 2x*DMef2-Gal4> 2xUAS-diaDN::GFP* embryos **F.** Fusion index of Stage 17 lateral transverse (LT) muscles confirms the degree of fusion block in DiaDN embryos. In control embryos, 27.1±2.3 nuclei were

counted in each hemisegment (n=40 hemisegments). 1x*DMef2-Gal4>* 1x*UAS-diaDN::GFP* reduces the number of dsRed positive nuclei in each hemisegment to 22.5±2.2 ($p<0.001$), whereas 2x*DMef2-Gal4>* 2x*UAS-diaDN::GFP* further reduces the number to 15.5±2.7($p<0.001$). Scale bar: 24μM

Fig 3: Diaphanous is required for myoblast fusion

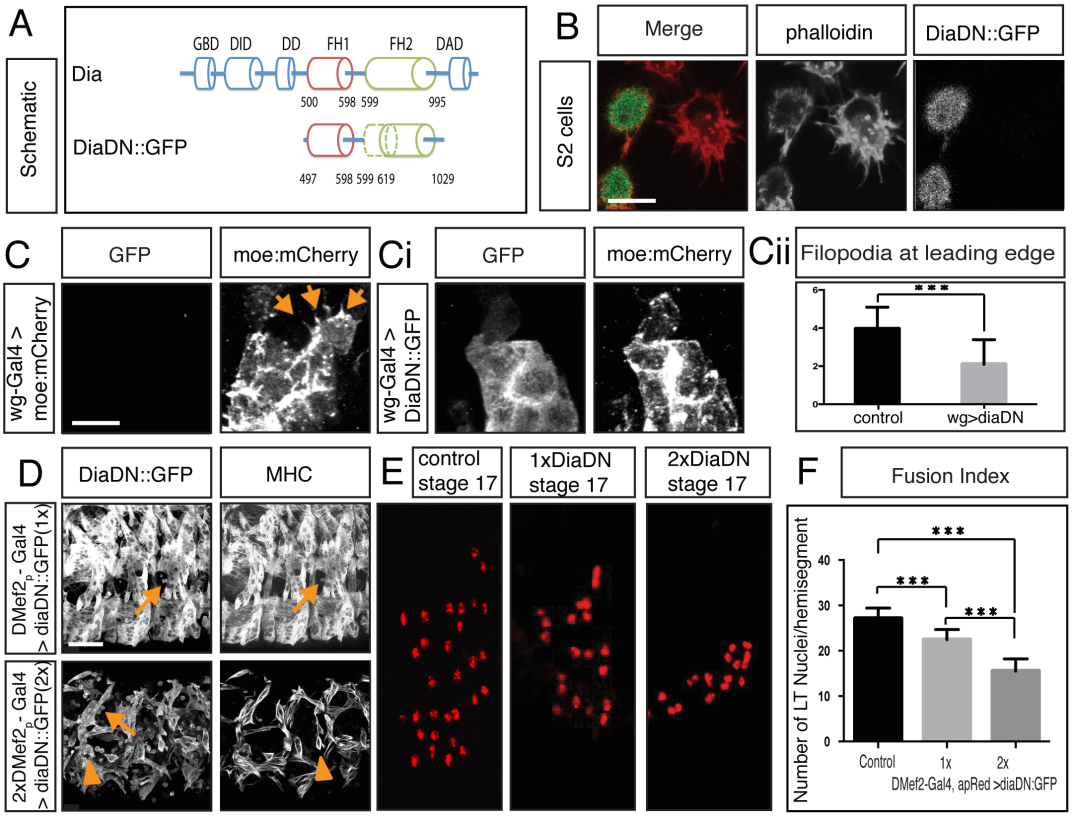

Fig 4. Dia regulates actin and Arp2/3 activity during myoblast fusion. A. In stage 15 embryos expressing 2x*UAS-diaDN::GFP*, myoblasts are stained with phalloidin and antibodies against DiaDN::GFP. Immunostaining for Sns and Duf was used to examine cell adhesion. Sns and Duf localize correctly at the fusion site, confirming adhesion between FCMs and FC/myotube. **B.** Stage 15 embryos expressing 2x*UAS-diaDN::GFP* with 2x*DMef2-Gal4.* Myoblasts are stained with phalloidin and antibodies against GFP. Arrowhead points to a myoblast adhering to the myotube but failing to generate a F-actin focus. **C.** Percentage of fusion sites with and without actin focus. Embryos expressing 2x *UAS-diaDN::GFP* were stained with phalloidin, and the formation of actin focus was quantified in these embryos. Actin focus forms in 60% of fusion sites and is absent in 40%. **D**. Time-lapse imaging of DiaDN fusion block. Three copies of *UAS-diaDN::GFP* and one copy of *UAS-moesin::mCherry* were driven by two copies of *Dmef2-Gal4*. F-actin dynamics were visualized by moesin::mCherry. Still images from the time-lapse sequence show 2-3 myoblasts adhered to a myotube (dashed lines), but unable to fuse. No F-actin focus was detected at the fusion site (arrow) (S3I Fig). **E-F.** Comparison of SCAR and WASp localization in DiaDN-expressing FCMs. In embryos expressing high levels of DiaDN, immunostaining was used to examine the localization of SCAR and WASp. At a fusion site in which an actin focus forms (upper panels), SCAR and WASp both correctly localize to the actin focus (arrow; phalloidin). When actin focus formation is disrupted by DiaDN (lower panels), SCAR and WASp no longer accumulate at the fusion site (asterisk). **G.** Dia localization in $sltr^{s1946}$; $kette^{J4\text{-}48}$ double mutant. In this double mutant, phalloidin was used to label F-actin, and Dia antibody to detect the localization of Dia. Fusion is blocked in double mutants, with no actin focus forming. Dia still accumulates at the fusion site. **H.** Dia localization in myoblasts expressing

UAS-PH^{plcγ}::GFP. Stage 15 embryos expressing 2x*PH^{plcγ}::GFP* with 2x*DMef2-Gal4.* Myoblasts are labeled with antibodies against GFP. *PH^{plcγ}* sequesters PI(4,5)P2, generating a small actin focus and blocking myoblast fusion (Bothe et al., 2014). In an FCM that adheres to a FC, immunostaining reveals that Dia accumulates at the fusion site. Scale bar: 2.5μM

Fig 4. Dia regulates actin and Arp2/3 activity during myoblast fusion.

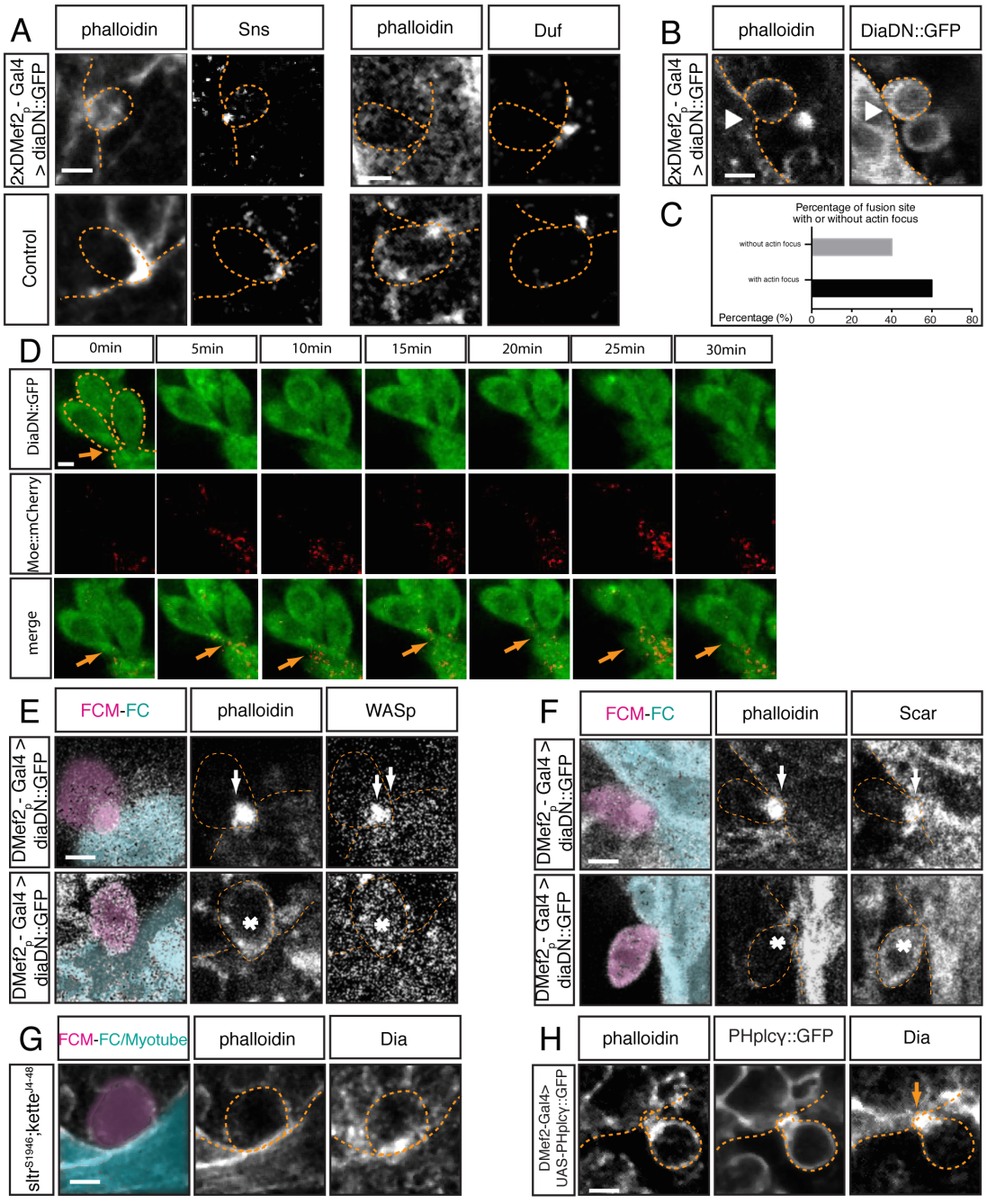

Fig 5: Constitutively active Dia blocks myoblast fusion.

A. Schematic diagram of Dia domain structure and different constitutively active Dia deletion constructs used in this study. **B.** Whole mount lateral view of three hemisegments from stage 16 embryos showing the (MHC) labeled muscles and nuclei (apME-NLS::dsRed) of the lateral transverse (LT) muscles. Scale bar: 24μM. Expression of DiaCA blocks myoblast fusion as visualized by many free myoblasts (arrows). This fusion defect is not due to a failure in FC specification as witnessed by expression of apME-NLS::dsRed in nuclei. **C.** Fusion index confirms a total block in myoblast fusion: dsRed positive nuclei in LT muscles/ hemisegment were counted in control (26.6±1.5) and *DMef2-Gal4>UAS-diaΔDAD::GFP* (5.2±1.0) (n=40 hemisegments/genotype) ($p<0.001$). **D.** Dynamics of DiaΔDAD::GFP expression in myoblasts. Still images from time-lapse of a stage 14 *DMef2-Gal4>UAS-diaΔDAD::GFP* embryo. Saturated image shows outline of cells and is used to localize myoblasts attempting to fuse. Filopodia-like protrusions undergo highly dynamic extension and retraction at areas of cell contact. DiaΔDAD::GFP localizes at the tip of those protrusions (arrows), and this signal moves as the filopodium extends and retracts. Scale bar: 5μM **E.** Still images from time-lapse of stage 14 *twist-actin::GFP; DMef2-Gal4>UAS-diaFH1FH2* embryo. Images at 0 and 3 min show filopodia-like protrusions (arrows) emanating from the FCM, which adheres to the FC but is unable to fuse. The Actin::GFP signal is enriched at the fusion site during the entire time lapse sequence (1 hr). Compare to control FCM (*twist-actin::GFP*, lower panel), which fuses with FC in 30 minutes. Scale bar: 4μM

Fig 5: Constitutively active Dia blocks myoblast fusion.

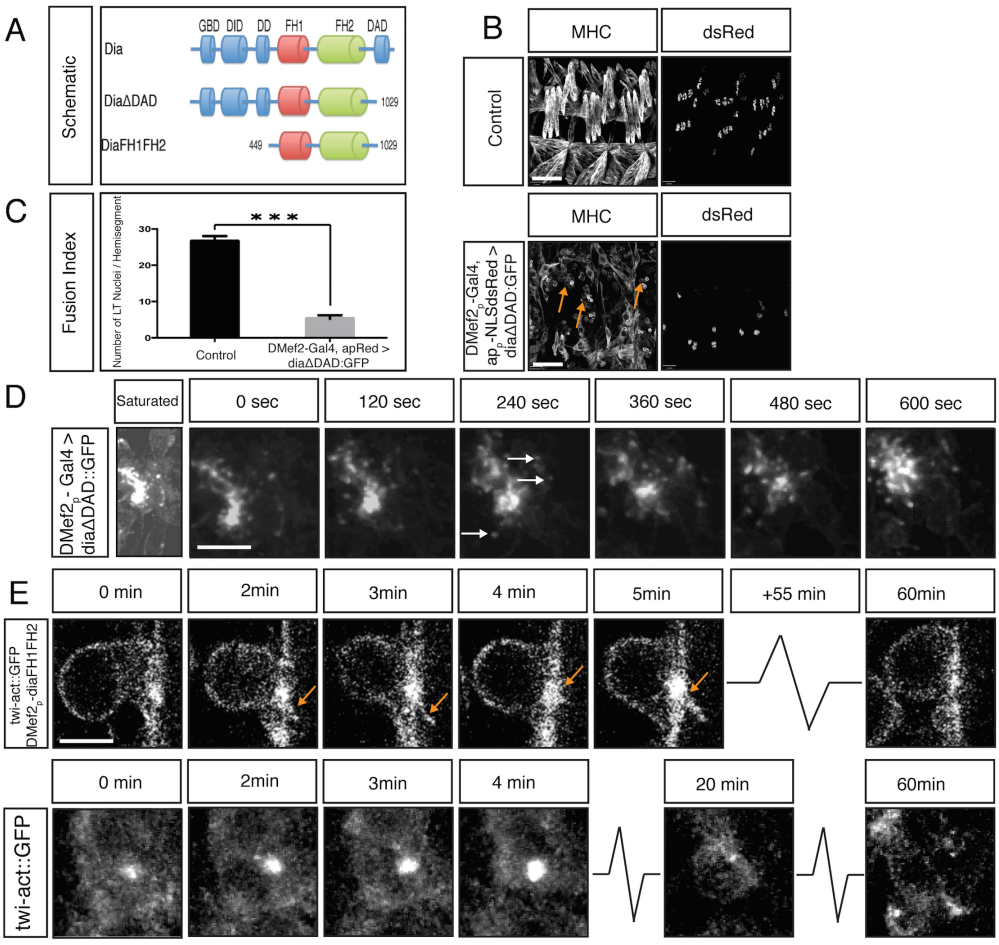

Fig 6: Constitutively active Diaphanous accelerates the actin exchange rate at the fusion site.

Fluorescence recovery of Actin::GFP after photobleaching. Newly formed Actin::GFP foci in stage 14 embryos were photobleached (arrows) to approximately 30% of the original intensity. The recovery rate was recorded every 3s after photobleaching for a total of 165 sec (endpoint). **A.** Stills from time-lapse showing Actin::GFP recovery at an actin focus after photobleaching in wild-type and *DMef2-Gal4> UAS-diaFH1FH2* embryos. Scale bar: 2.5μM **B.** Comparison of representative recovery kinetics of Actin::GFP foci in control (green) and *DMef2-Gal4> UAS-diaFH1FH2* (red) myoblasts. **C.** Half time of fluorescent recovery in control (n=8) and *DMef2-Gal4>UAS-diaFH1FH2* embryos (n=10). The half time of fluorescence recovery in *DMef2-Gal4> UAS-diaFH1FH2* embryos ($t_{1/2}$=17.7±6.7s) is significantly lower than control ($t_{1/2}$=53.3±6.7s). **D.** Percentage of final recovery in control and *DMef2-Gal4>UAS-diaFH1FH2* embryos. Final recovery in *DMef2-Gal4> UAS-diaFH1FH2* embryos (77.9±10.6%) is similar to wild-type embryos (78.6±10.5%) ($p>0.1$).

Fig 6: Constitutively active Diaphanous accelerates the actin exchange rate at the fusion site.

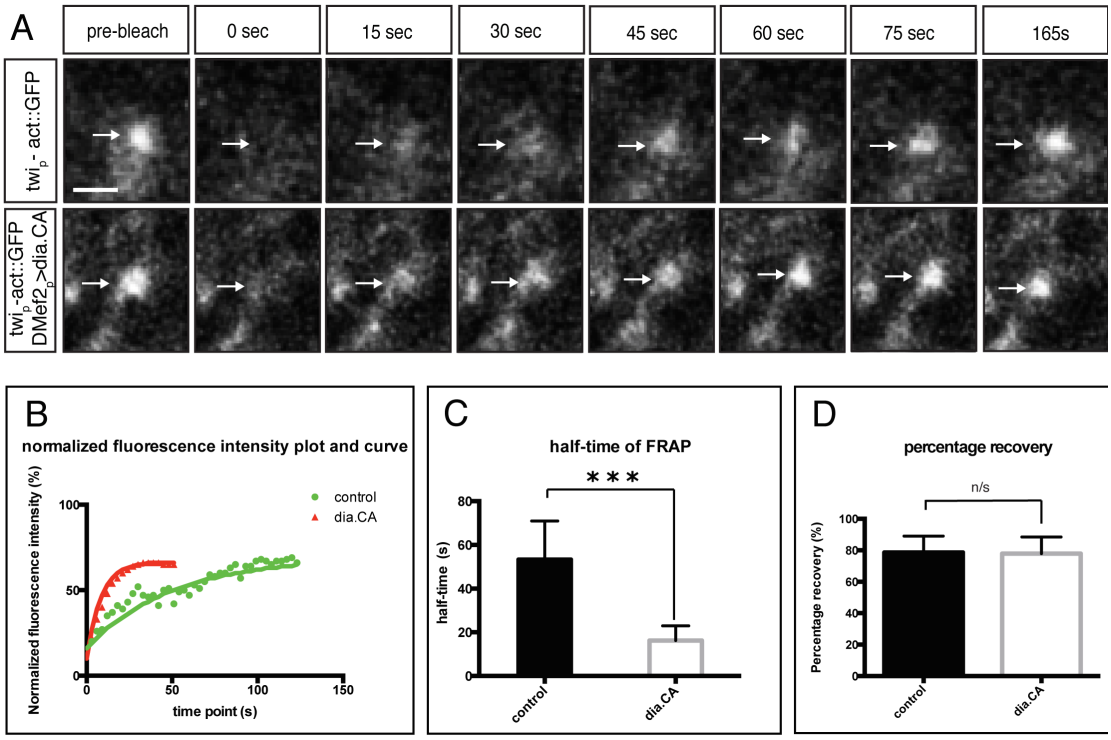

Fig 7. Constitutively active Dia alters the F-actin structure at the fusion site and regulates localization of Arp2/3 regulators.

A-B. Stage 14 embryos stained for F-actin (phalloidin, white) and for Dia::GFP or DiaΔDAD::GFP (GFP antibody, white); FCM (magenta), FC/Myotube (turquoise). Scale bar: 5μM. **A.** Control *DMef2-Gal4>UAS-dia::GFP* myoblasts show colocalization of Dia::GFP and the F-actin focus at the fusion site. **B.** *DMef2-Gal4>UAS-diaΔDAD::GFP* myoblasts show that F-actin does not form a well-defined focus at the fusion site but appears diffuse. DiaΔDAD::GFP localizes to the plasma membrane and is enriched at cell contact sites. **C.** Fluorescent intensity curves confirm the distribution of F-actin in embryos expressing Dia::GFP and DiaΔDAD::GFP. **D-E.** Stage 15 embryos stained for F-actin (phalloidin) and DiaΔDAD::HA (antibodies against HA) showing FCM (magenta) and FC/Myotube (turquoise). Scale bar: 5μM. **D.** *DMef2-Gal4* driven expression of DiaΔDAD::HA in *kette*$^{J4\text{-}48}$ mutant background. The morphology of the F-actin focus at the fusion site appears similar to *DMef2-Gal4>UAS-diaΔDAD::GFP* embryos. While F-actin localizes at the cell cortex, it spreads out at the fusion site and does not make a concentrated focus. **E.** *DMef2-Gal4* driven expression of DiaΔDAD::GFP in *sltr*^{s1946} mutant background. Similar to expression of DiaCA alone, the F-actin localizes at the cell cortex and spreads out at the fusion site. **F-G.** Stage 14 embryos stained for F-actin (phalloidin), Dia*ΔDAD*::GFP (GFP antibody) and SCAR or WASp. Scale bar: 5μM. **F.** SCAR localization in control and *DMef2-Gal4>UAS-diaΔDAD::GFP* embryos. In control embryos, SCAR accumulates at the fusion site, as confirmed by the fluorescent intensity curves. When expressing DiaΔDAD::GFP, SCAR loses its characteristic concentration at the fusion site and becomes found throughout the cytoplasm. The multiple peaks in the SCAR fluorescent intensity curve confirm SCAR's change in localization. **G.** Localization of WASp in control and *DMef2-Gal4>UAS-diaΔDAD::GFP* embryo. In

control embryos, WASp accumulates at the fusion site, as confirmed by the fluorescent intensity curves. When expressing DiaΔDAD::GFP, WASp displays a more diffused localization. Fluorescent intensity curves confirm the broader distribution of WASp signal in relation to the controls.

Fig 7. Constitutively active Dia alters the F-actin structure at the fusion site and regulates localization of Arp2/3 regulators.

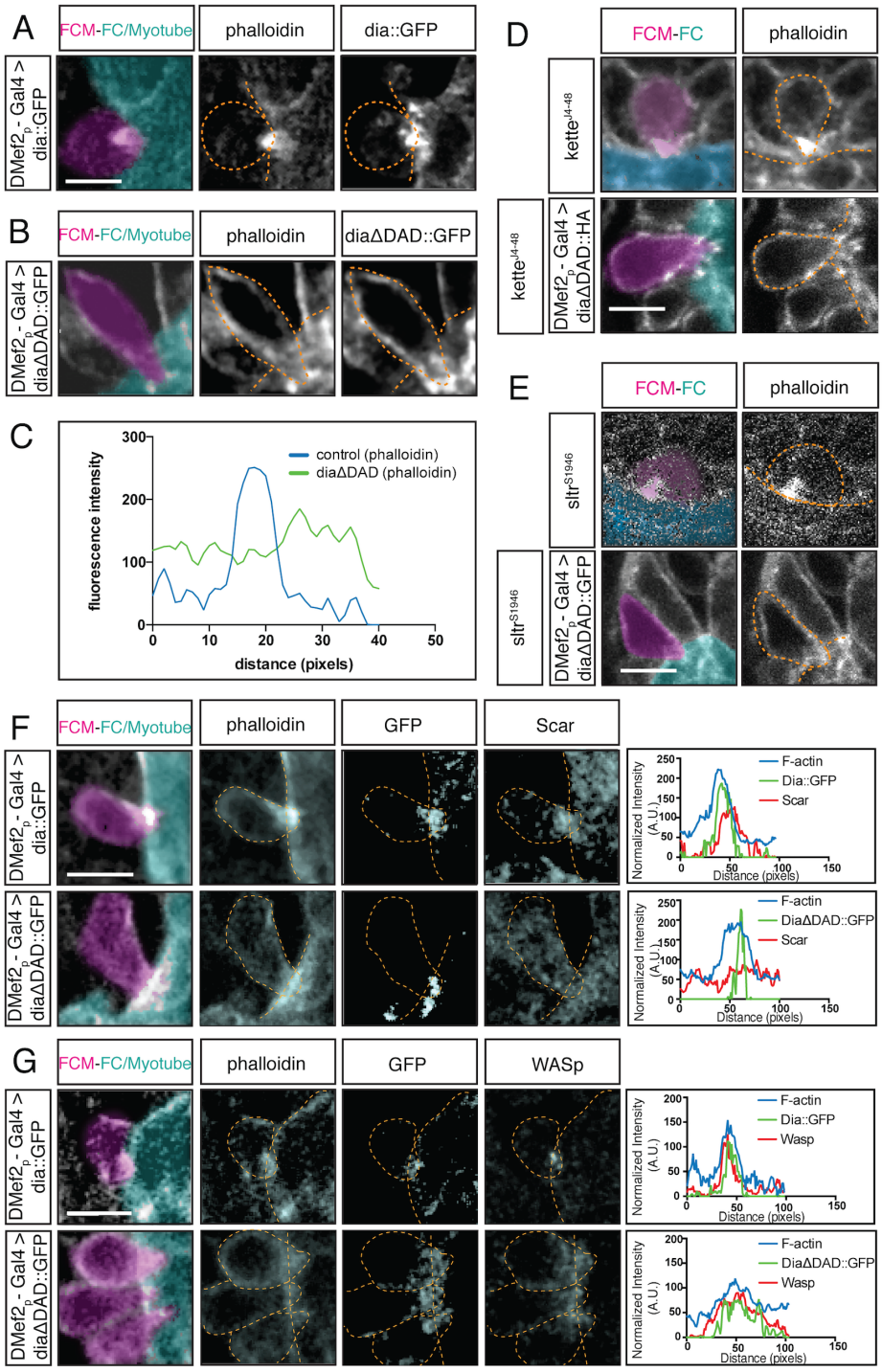

Fig 8. Model: Dia and Arp2/3 function together to regulate myoblast fusion

During myoblast fusion, the transmembrane molecules (e.g. Sns and Duf) mediate recognition and adhesion between the FCM and the FC/myotube. After cell adhesion, Dia is recruited to the fusion site, where it collaborates with PI(4,5)P2 signaling in making a functional F-actin focus, How PI(4,5)P2 signaling coordinates with Dia is unclear, but it may possibly be through the recruitment of small GTPases that activate Dia. Active Dia, in turn, nucleates F-actin particularly on the FCM side, which serves as a substrate for Arp2/3. Coordinated Dia and Arp2/3 activities allow the actin network to consolidate into invasive podosome-like structures. Loss of filamentous actin and reduction in Arp2/3 NPFs recruitment/maintenance due to Dia loss results in Arp2/3 being unable to nucleate enough actin filaments to build an invasive podosome-like structure. Hence no fusion can occur. In Dia gain of function embryos, Dia builds excessive actin filaments. Arp2/3 NPFs fail to localize properly, leading to an alteration in the distribution of activated Arp2/3. Since the actin network fails to consolidate into invasive podosome-like structures, no myoblast fusion can occur.

Fig 8. Model: Dia and Arp2/3 function together to regulate myoblast fusion

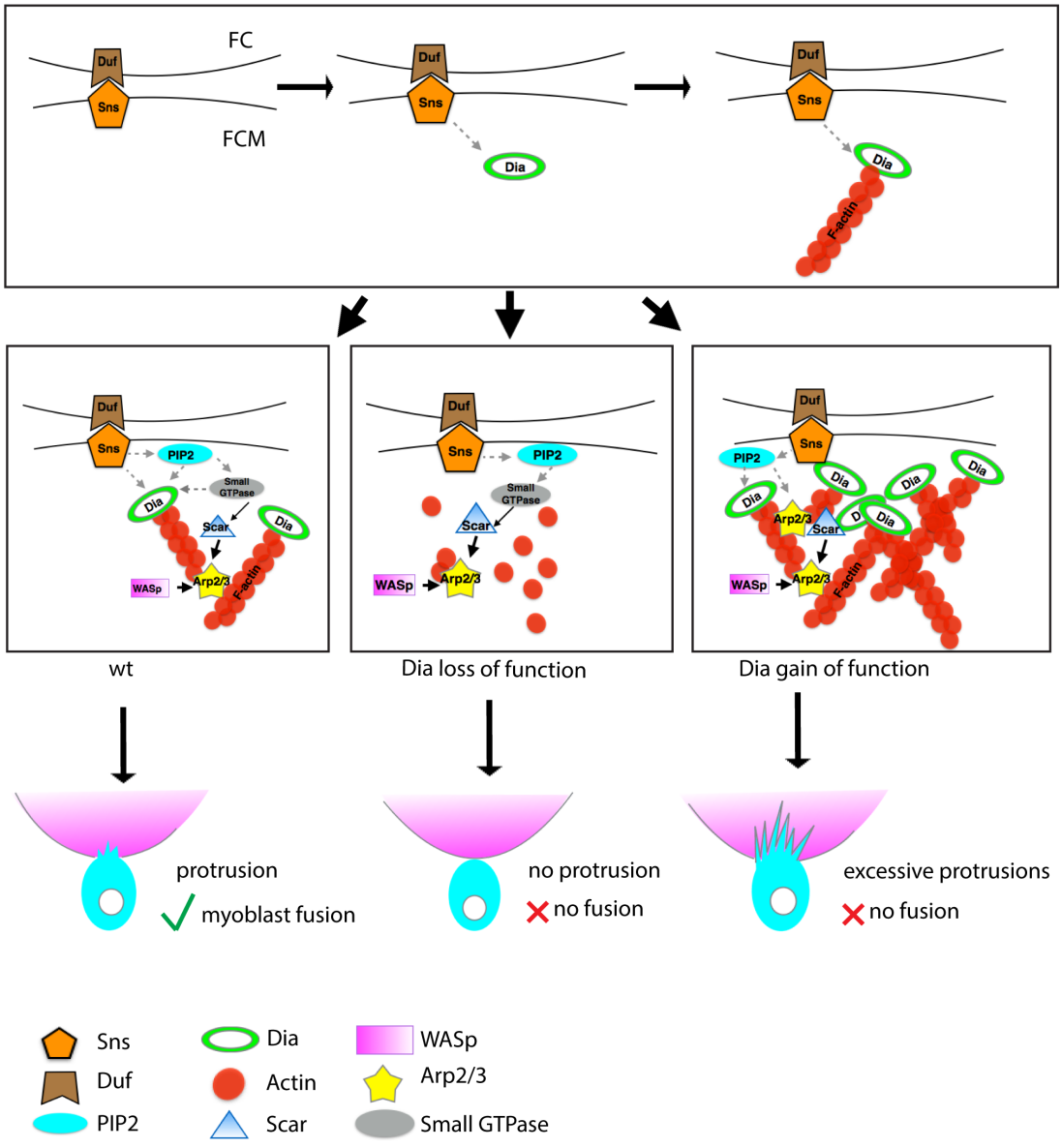

Supplemental Information

S1 Table: Quantification of Dia enrichment at the fusion site in control and fusion mutants.

	Number of embryos examined	Number of foci examined	Number of Dia Positive foci	Percentage of Dia positive foci
twi-actin::GFP	7	40	40	100%
sns^{XB3}/Cyo	1	5	5	100%
sns^{XB3}	4	0[1]	0	0
$rac1^{J11}$,$rac2^{\Delta}$,mtl^{Δ}/TM3	1	5	5	100%
$rac1^{J11}$,$rac2^{\Delta}$,mtl^{Δ}	5	25	24	96%
mbc^{c1}/TM3	1	5	5	100%
mbc^{c1}	5	25	22	88%
$loner^{T1032}$/TM3	1	5	5	100%
$loner^{T1032}$	5	20	20	100%
$kette^{J4-48}$/TM3	1	5	5	100%
$kette^{J4-48}$	5	25	23	92%
$blow^{1}$/Cyo	1	5	5	100%
$blow^{1}$	4	25	25	100%
$sltr^{S1946}$/Cyo	1	5	5	100%
$sltr^{S1946}$	5	25	25	100%
$WASp^{3D3-035}$/TM3	1	10	10	100%
$WASp^{3D3-035}$	3	25	25	100%
$sltr^{S1946}$; $kette^{J4-48}$	5	20	17	85%
PHplcγ (adhere myoblast)	5	20	20	100%

[1] No actin focus is formed in *sns* mutants, therefore, the number of actin focus examined is 0. We checked 25 potential FC-FCM contact sites, and did not see Dia enrichment.

S2 Table: Quantification of muscle phenotypes in *dia* mutant and *dia* knockdown.

genotype	Muscle phenotype at stage 16
dia^5/dia^5	Wild-type 57.7%, missing muscle 13.5%, detachment 21.2%, lack of fusion 3.8% muscle morphology 3.8%
dia^2/dia^2	Wild-type 0%, muscle defects including missing muscles, free myoblasts, detachment and muscle morphology changes (100%)
otu-Gal4; nos-Gal4; nos-Gal4 x UAS-dia-RNAi->F1x Dmef2-Gal4	No eggs
mat15-Gal4; mat67-Gal4 x UAS-dia-RNAi->F1 x Dmef2-Gal4	100% missing one LT muscle (off target effect of mat-Gal4)
UAS-dicer; Dmef2-Gal4 > UAS-dia-RNAi(Trip 33424)	100% wild-type
UAS-dicer; Dmef2-Gal4 > UAS-dia-RNAi(Trip 28541)	100% wild-type embryonic muscle 100% flightless adult fly

S3 Table: **FRAP summary:** Actin::GFP recovery rate and percentage of recovery in control embryos and constitutively active Diaphanous embryos

genotype	Half time of FRAP			Percentage recovery			N
	min	max	average	min	max	average	
twi-actin::GFP, DMef2-Gal4 > oregon R (control)	24.5	76.2	53.3±17.7	67.1	97.2	78.6±10.5	8
twi-actin::GFP; DMef2-Gal4 > UAS-dia.CA	5.7	28.9	16.2±6.7	66.0	101.6	77.9±10.6	10

S1 Fig: **Dia expression in fusing myoblasts**

A. Projection of three hemisegments of a stage 14 *twist-actin::GFP* embryo stained for GFP which reveals the myoblasts in each hemisegments as fusion occurs. **Ai.** Three hemisegments of a stage 16 control embryo stained for MHC. This image reveals the muscle pattern that results from myoblast fusion. Scale bar: 10μM **B.** Higher magnification image showing single scan of the boxed area: one hemisegment from a stage 14 *twist-actin::GFP* embryo stained for F-actin (phalloidin) and antibodies against Dia and GFP. The F-actin focus at the fusion site was visualized both by GFP antibody (green; *twist-actin::GFP*) and phalloidin staining (white). Dia (red) is present in muscles and is enriched at fusion sites (arrows). Scale bar: 10μM. **C.** Cell outline determination used in all Figures: we determine the FCM and myotube cell outlines manually by adjusting brightness and changing focal planes.

S1 Fig: Dia expression in fusing myoblasts

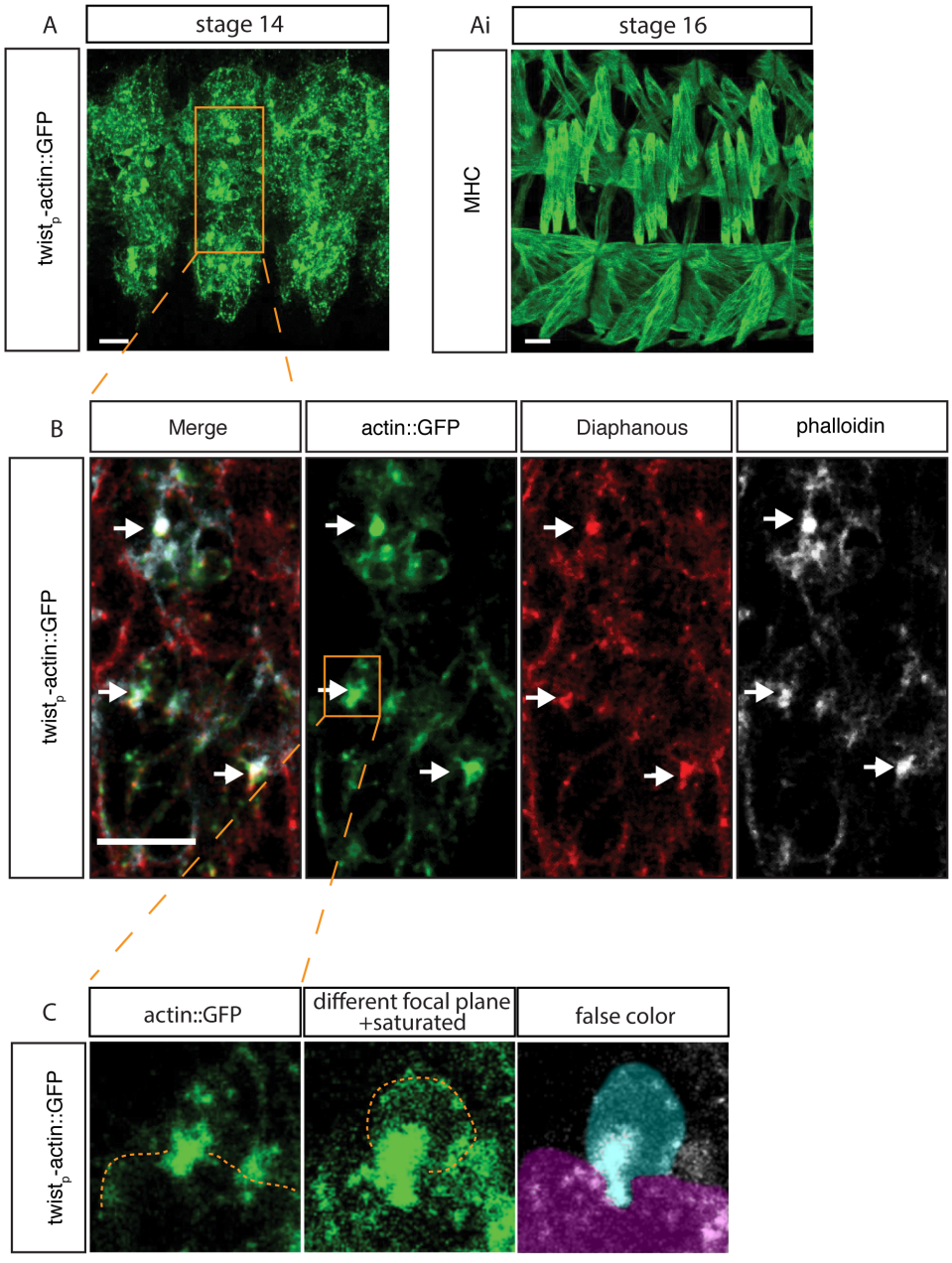

S2 Fig: Pipeline of measuring fluorescent intensity.

For all Figures except Fig 1: a line was drawn along cell cortex, with the center of the line localized at the actin focus or cell contact site. Fluorescent intensities were measured along the line and normalized using the equation shown in Figure. After the desired number of samples was measured, average relative intensities and standard deviations at each point were calculated and plotted.

S2 Fig: Pipeline of measuring fluorescent intensity.

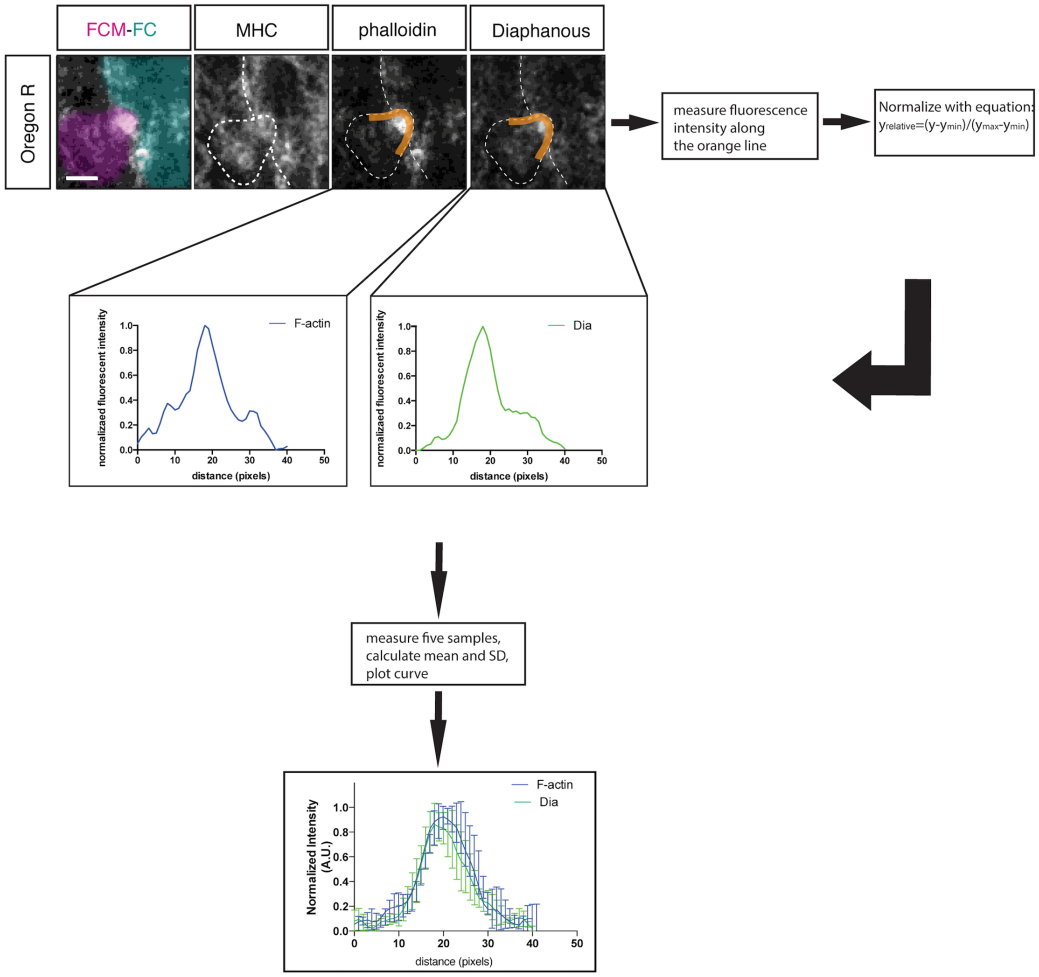

S3 Fig: Muscle phenotypes in *dia loss of function* embryos.

A. Stage 16 *dia*^{2} and *dia*^{5} homozygous embryos were stained with MHC to visualize muscle pattern. GFP antibody was used to identify balancer. *dia*^{2} is an amorphic allele and *dia*^{5} is a hypomorphic allele; both result in Dia loss of function. Homozygous *dia* mutants display a range of muscle defects, including muscle detachment (arrowhead), missing muscles (asterisk), free myoblasts (arrow), and muscle shape changes. Scale bar: 40μM. **B.** Fusion index of *dia*^{2} and *dia*^{5} homozygous mutants. *apMe-NLS::dsRed* was expressed in LT muscles to label nuclei, and fusion index was assessed in stage 17 embryos. Fusion was impaired in *dia*^{2} and *dia*^{5} homozygous mutant embryos (*dia*^{2}: 14.1±1.3, n=21, *dia*^{5}: 21.5±1.3 n=20 vs control: 27.8±0.3 n=12, $p<0.001$). **C.** Expression of Dia::GFP rescued filopodia reduction by DiaDN. S2R+ cells that were co-transfected with Dia::GFP (green), and/or DiaDN::mCherry (red) (n=7). Expression of DiaDN::mCherry results in a significant reduction of filopodia (phalloidin, grey in single channel). By contrast, expression of Dia::GFP resulted in increased cell spreading and increased numbers of filopodia (phalloidin, grey) compared to control. Expression of both contructs simultaneously results in more filopodia-like, protrusive structures relative to cells that are transfected with DiaDN::mCherry alone (n=5). Scale bar: 10μM. **D.** Filopodia numbers were quantified in cells expressing DiaDN::mCherry, DiaDN::mCherry+Dia::GFP, Dia::GFP and mock treated control. **E**. Two copies of *DMef2-Gal4* driving two copies of *UAS-diaDN::GFP* in myoblasts at 29°C. Antibodies to GFP were used to visualize the muscle cells. Embryonic muscle defects were found, including free myoblasts (arrow) and missing muscles (asterisk) at Stage 16 and severe muscle detachment (arrowhead) at Stage 17. Scale bar: 20μM and 40μM from left to right. **F-G.** In male flies which carry *net-Gal4;nos-Gal4>UAS-diaDN::GFP*, male fertility (**F**) and sperm number (**G**) were quantified and compared to control.

H. Time-lapse imaging showing a fusion site in embryos expressing DiaDN::GFP. Three copies of *UAS-diaDN::GFP* and one copy of *UAS-moesin::mCherry* were driven by two copies of *Dmef2-Gal4*. F-actin dynamics were visualized by moesin::mCherry. As DiaDN does not block myoblast fusion completely, fusion events can be observed. Still images from the time-lapse sequence show a myoblast fusing to a myotube, with a normal F-actin accumulation at the fusion site. Scale bar: 5μm **I.** Quantification of actin focus size of *blow*^{1} embryo and *blow*^{1}*;DMef2-Gal4,UAS-diaDN::GFP* embryos. The actin focus size is significantly reduced in *blow*^{1}*;DMef2-Gal4,UAS-diaDN::GFP* embryos (n=18) compared to that in the *blow*^{1} embryo (n=18, $P<0.01$).

S3 Fig: Muscle phenotypes in *dia loss of function* embryos.

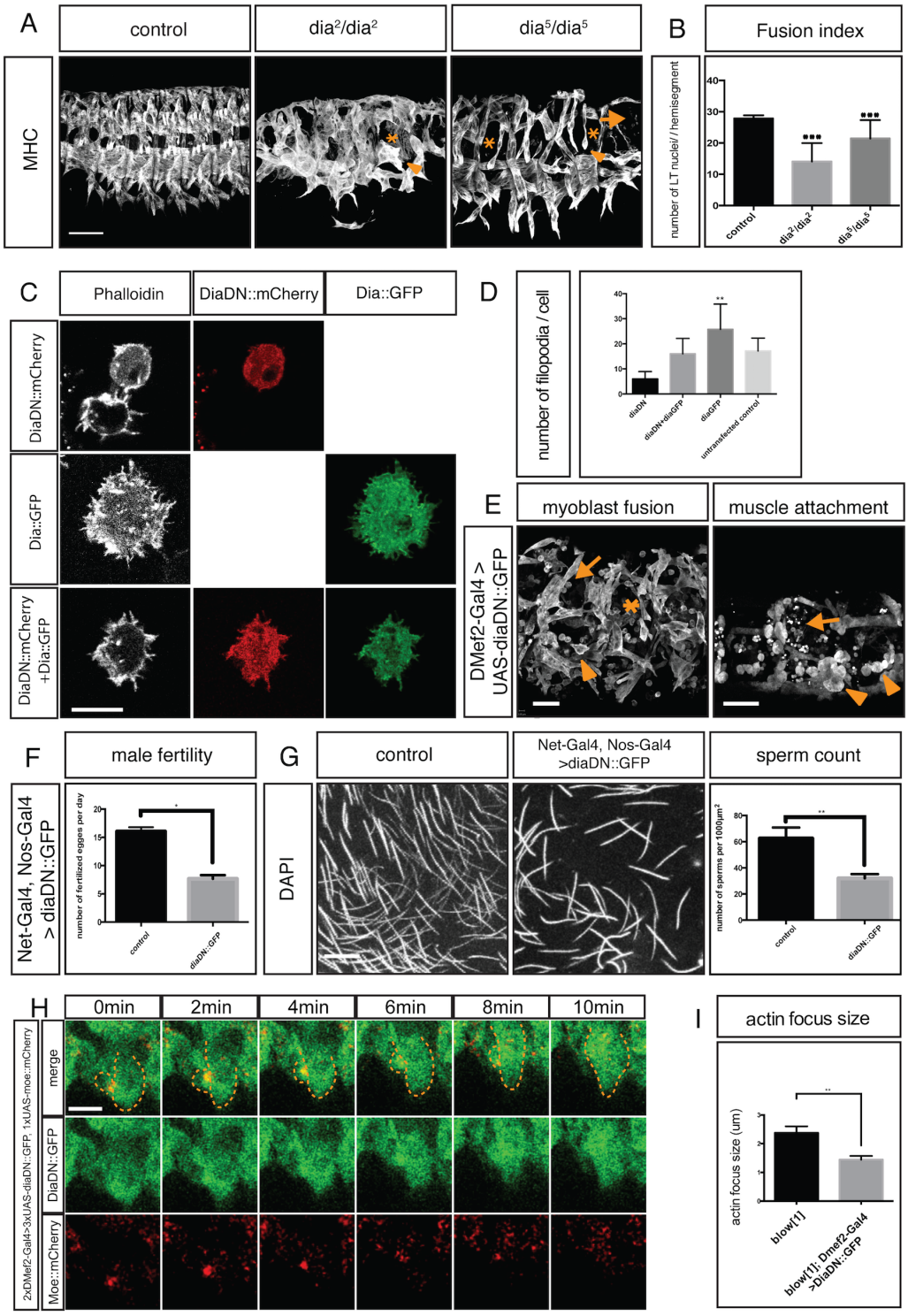

S4 Fig: Embryonic phenotypes found in embryos expressing different constitutively active Dia constructs.

A. Schematic diagram of Dia domain structure and the different constitutively active Dia (DiaCA) deletion constructs (DiaΔDAD, diaDDFH1FH2, DiaFH1FH2) used in this study. **B-C.** Muscle pattern in a single hemisegment and Fusion index in embryos expressing the different DiaCA constructs. *UAS-diaCA* was expressed in muscles using the *DMef2-Gal4* driver. MHC staining shows that myoblast fusion was blocked by DiaCA (high magnification of the LT Muscle area). To confirm this observation, apMe-NLS::dsRed was expressed in LT muscles to measure the fusion index. Compared with controls, all *diaCA* constructs significantly reduce myoblast fusion (graph in B. $p<0.001$). **D.** F-actin structure and DiaCA localization when expressing different *diaCA* constructs. F-actin was labeled with phalloidin. DiaCA localizations were visualized with GFP immunofluorescence staining. Instead of forming a defined actin focus at the fusion site, F-actin displayed a diffused localization in myoblasts expressing DiaCA. DiaDDFH1FH2 and DiaFH1FH2 both localize in the cytoplasm, while DiaΔDAD localizes primarily at the membrane. Intensity plot shows the colocalization of DiaCA (green) and actin structure (red) at the fusion site. Scale bars in **B-D**: 10μM

S4 Fig: Embryonic phenotypes found in embryos expressing different constitutively active Dia constructs.

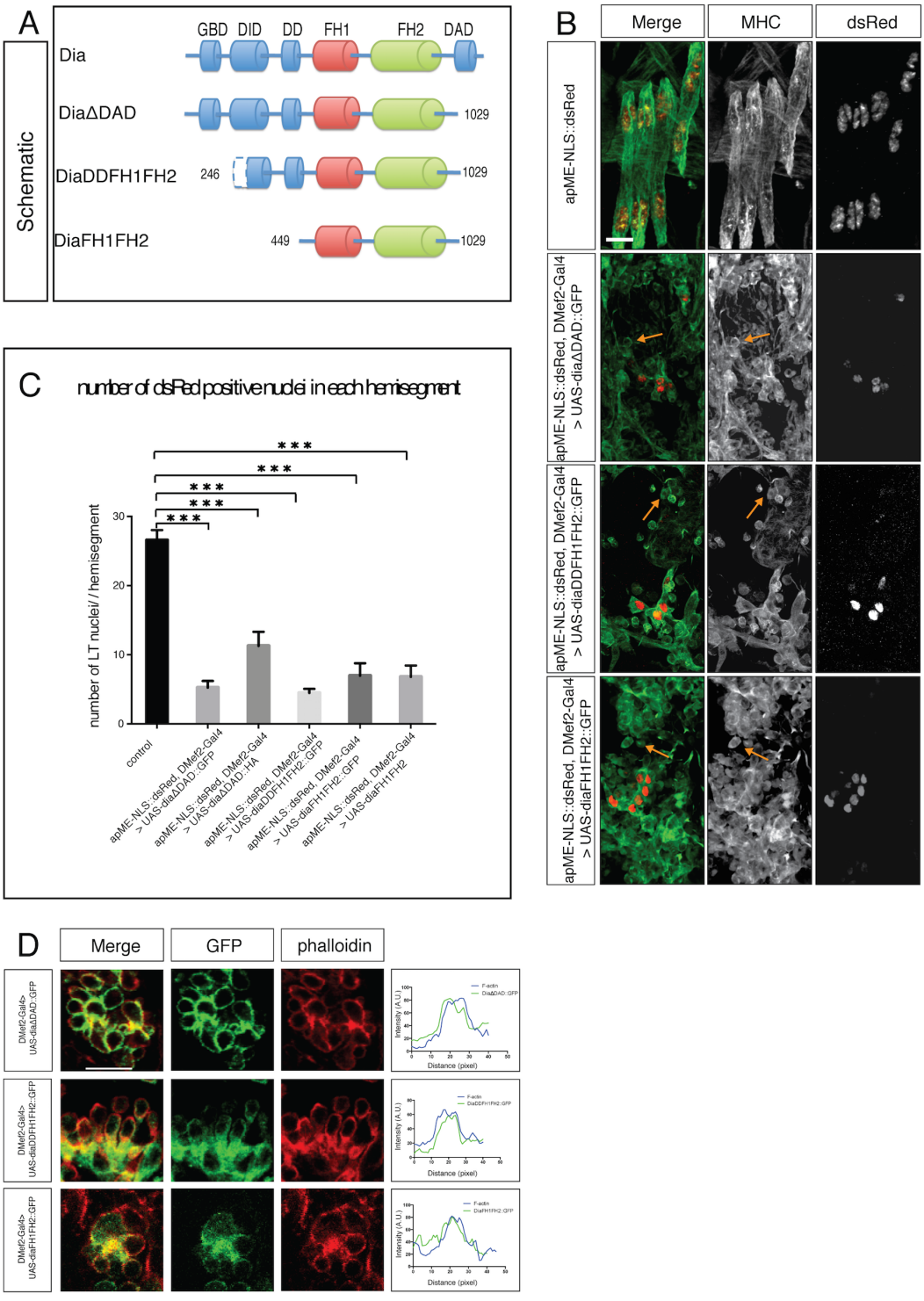

S5 Fig: Recognition and adhesion are not affected by constitutively active Dia.

A. Sns localization in control (DMef2-Gal4>UAS-dia::GFP) and DMef2-Gal4>UAS-diaΔDAD::GFP embryos. Stage 14 embryos stained with phalloidin and antibodies against GFP and Sns. In control embryos, Sns is localized at the fusion site on the FCM side. Constitutively active Dia does not change Sns localization at the fusion site. Fluorescent intensity curves confirm that the Sns peak colocalizes with F-actin peak in both control and DMef2-Gal4>UAS-diaΔDAD::GFP embryos. **B.** Duf localization in control and DMef2-Gal4>UAS-diaΔDAD::GFP embryos. Stage 14 embryos stained with phalloidin and antibodies against GFP and Duf. In control embryos, Duf is localized at the fusion site on the FC/myotube side. Similar to Sns, Duf localization is not changed by DiaΔDAD::GFP. Fluorescent intensity curves confirm that the Duf peak colocalizes with the F-actin peak for both control and DMef2-Gal4/UAS-diaΔDAD::GFP embryos. The peak of Duf is broader and less defined in DMef2-Gal4>UAS-diaΔDAD::GFP embryos. **C-D.** Projection image of myoblasts expressing the constitutively active Dia construct DiaΔDAD. Actin (phalloidin, white); Dia (GFP antibody, green), Sns or Duf (antibody, Red). Dashed lines indicate FCMS adhered to the FC. Compared to the control embryo, the accumulation of Sns and Duf appears stronger due to an increased number of unfused and adhered myoblasts. Scale bar: 2.5μM

S5 Fig: Recognition and adhesion are not affected by constitutively active Dia.

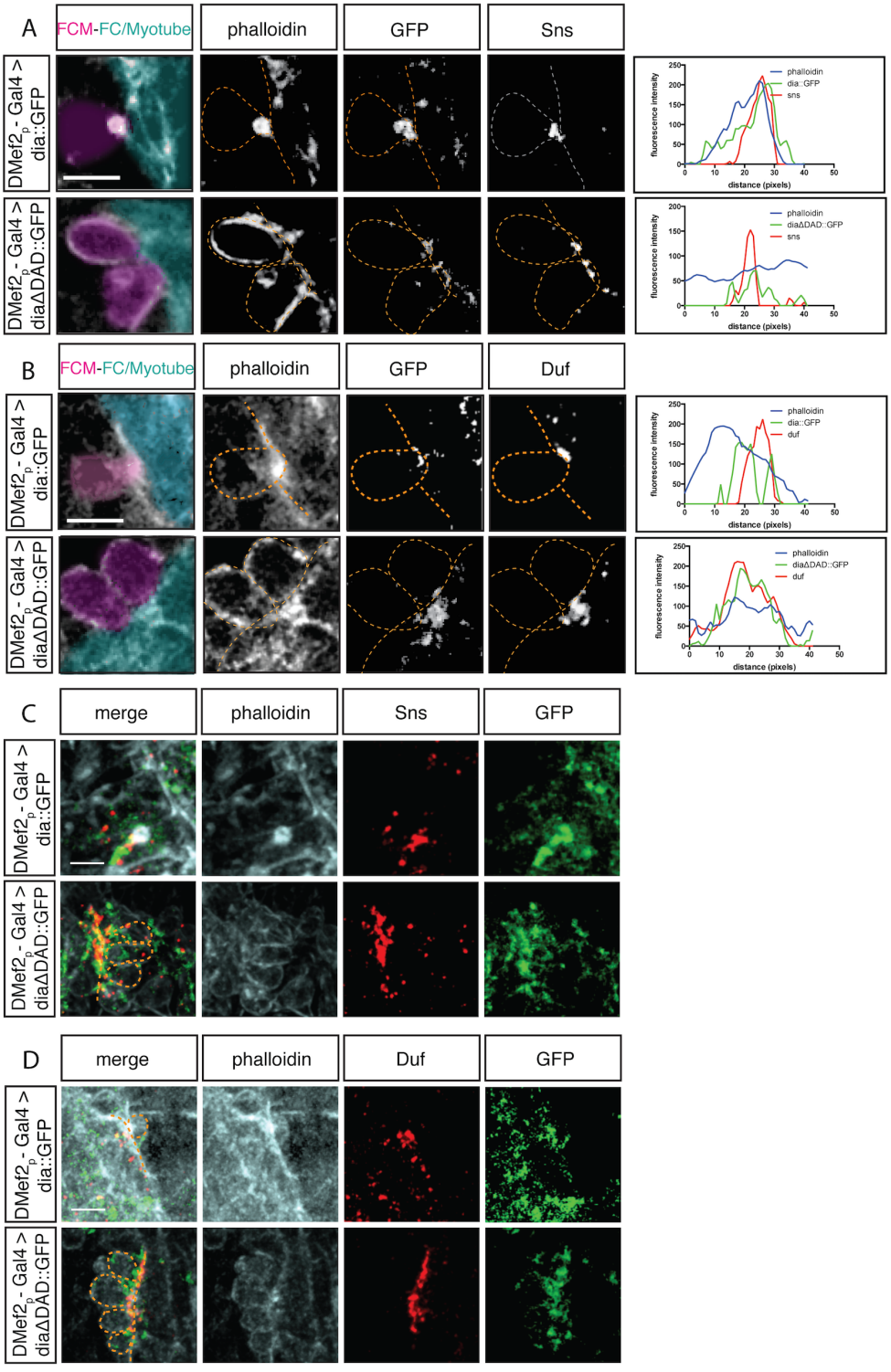

CHAPTER FOUR

DIAPHANOUS REGULATES SCAR COMPLEX LOCALIZATION DURING *DROSOPHILA* MYOBLAST FUSION*

Abstract:

From *Drosophila* to man, multinucleated muscle cells form through cell-cell fusion. Using *Drosophila* as a model system, researchers first identified, and then demonstrated, the importance of actin cytoskeletal rearrangements at the site of fusion. These actin rearrangements at the fusion site are regulated by SCAR and WASp mediated Arp2/3 activation, which nucleates branched actin networks. Loss of SCAR, WASp or both leads to defects in myoblast fusion. Recently, we have found that the actin regulator Diaphanous (Dia) also plays a role both in organizing actin and in regulating Arp2/3 activity at the fusion site. In this Extra View article, we provide additional data showing that the Abi-SCAR complex accumulates at the fusion site and that excessive SCAR activity impairs myoblast fusion. Using constitutively active Dia constructs, we provide further evidence that Dia functions upstream of SCAR activity to regulate actin dynamics at the fusion site and to localize the Abi-SCAR complex.

Introduction:

Cell-cell fusion is a crucial step in muscle development and repair (Abmayr and Pavlath, 2012; Kim et al., 2015; Simionescu and Pavlath, 2011). During *Drosophila*

---

* In revision. This chapter incorporated changes based on reviewer's comments.

muscle development, fusion occurs between the founder cells (FCs)/myotubes and the fusion competent myoblasts (FCMs). The FCs express transcription factors that determine the identity of individual muscles. When a naïve FCM fuses with a FC, the newly added myonucleus is reprogrammed to adopt the founder cell nucleus identity, and another round of fusion is initiated. During fusion, the formation of an actin-enriched focus occurs at the fusion site; this actin focus provides an invasive force from the FCM into the FC/myotube, promoting fusion (Sens et al., 2010). Actin polymerization at the fusion site is regulated by the actin nucleating complex Arp2/3 (Richardson et al., 2007; Rodal et al., 2015; Schulman et al., 2015). The activity of Arp2/3 is controlled by the nucleation promoting factors WASp and SCAR (also known as WAVE). WASp and SCAR share a C-terminal VCA domain that activates Arp2/3 by both promoting conformational changes in Arp2/3 and presenting G-actin to Arp2/3 (Eden et al., 2002; Ismail et al., 2009). The importance of WASp and SCAR during myoblast fusion has been demonstrated in previous studies from our lab and others in multiple systems (Berger et al., 2008; Gildor et al., 2009; Gruenbaum-Cohen et al., 2012; Haralalka et al., 2011; Kaipa et al., 2013; Kesper et al., 2007; Kim et al., 2007; Massarwa et al., 2007; Nowak et al., 2009; Richardson et al., 2007; Schäfer et al., 2007; Sens et al., 2010). Loss or reduction of WASp and/or SCAR activity results in a fusion block: FCMs make contact with FC/myotubes, but are unable to form or expand fusion pores, preventing myoblast fusion. As both WASp and SCAR are required for Arp2/3 activation, and therefore branched actin network formation at the fusion site, loss of both WASp and SCAR activity results in no actin focus formation (Bothe et al., 2014; Sens et al., 2010). Interestingly, loss of WASp function alone results in a fusion block with normal-sized actin foci, while loss of SCAR function alone results in a fusion block with enlarged actin foci (Richardson et al., 2007; Sens et al., 2010).

In our recent PLoS Genetics paper, "The formin Diaphanous regulates myoblast fusion through actin polymerization and Arp2/3 regulation", we reported that the formin Diaphanous (Dia), which nucleates and polymerizes linear actin filaments rather than branched microfilament arrays, plays a critical role in myoblast fusion (Deng et al., 2015). Dia controls actin rearrangements at the fusion site by a) nucleating and polymerizing actin filaments and b) localizing WASp and SCAR. Although we have demonstrated the importance of Dia in localizing Arp2/3 regulators, how Dia interacts with SCAR/WAVE and WASp and directs their localization to the fusion site remained unclear. In this Extra View article, we concentrate on the activity of the SCAR complex and investigate how Dia regulates SCAR at the fusion site.

The activity of SCAR/WAVE is controlled by the SCAR/WAVE regulatory complex (WRC). The WRC is a pentameric complex that contains SCAR/WAVE, Abi, Kette/Nap1, Hspc300, and Sra1/Cyfip1. *In vitro* experiments using purified protein suggest that when not associated with the complex, SCAR/WAVE exists in an active conformation and can stimulate Arp2/3 activity through its VCA domain (Machesky et al., 1999). However, in the WRC, the VCA domain of SCAR/WAVE is bound by Sra-1, and SCAR/WAVE's activity is inhibited (Ismail et al., 2009). Rac-GTP activates SCAR/WAVE by competitively binding to Sra1, triggering exposure of the VCA domain of SCAR/WAVE (Chen et al., 2010). *In vitro* experiments confirm that, when activated by Rac-GTP, SCAR/WAVE does not dissociate from WRC complex: only that its C-terminal VCA domain is no longer bound by Sra1 (Chen et al., 2010; Ismail et al., 2009). In addition to regulating SCAR/WAVE activity, the formation of the WRC is crucial for SCAR/WAVE localization and stability (Davidson et al., 2013; Echarri et al., 2004; Richardson et al., 2007). Removal of WRC components, such as Abi or Kette/Nap1, results in SCAR/WAVE degradation (Kunda et al., 2003).

Abi is a key component of the WRC that is important for the stability, localization, and activity of SCAR/WAVE (Davidson et al., 2013; Echarri et al., 2004; Leng et al., 2005). Recent experiments have shown that Abi also interacts physically with Dia to regulate actin dynamics and adhesion in A431 epidermoid carcinoma cells and 293T human embryonic kidney cells (Ryu et al., 2009). Moreover, these experiments indicate that Dia and SCAR/WAVE physically bind to partially overlapping regions of Abi (Ryu et al., 2009). Since the interaction between Abi and SCAR/WAVE is critical in localizing and stabilizing SCAR/WAVE (Echarri et al., 2004; Leng et al., 2005), the authors suggest that Dia regulates SCAR/WAVE activity through competition for Abi binding. In this Extra View article, we investigate whether Dia regulates SCAR/WAVE during *Drosophila* myoblast fusion through the mechanisms described in mammalian cell culture. We also report an unexpected fusion phenotype that is associated with excessive SCAR activity in embryos.

Results:

Excessive Scar activity blocks myoblast fusion

Mammalian tissue culture experiments using different cell types suggested that the binding of Abi to SCAR is required for several aspects of SCAR/WAVE activity, including stability (Echarri et al., 2004), localization, and activation (Leng et al., 2005). We hypothesized that this relationship between Abi and SCAR also exists during *Drosophila* myoblast fusion. To test our hypothesis and investigate how Abi regulates SCAR, we employed a bimolecular fluorescence complementation (BiFC) technique to visualize Abi-SCAR complex formation *in vivo* (Gohl et al., 2010). In the BiFC system, YFP is split into two non-fluorescent fragments: N-terminal YFP (NYFP) and C-terminal YFP (CYFP), and each fragment is fused to either SCAR or Abi. YFP is reconstituted when the two fragments are brought in close proximity

(Gohl et al., 2010). To visualize SCAR and Abi interaction during fusion, we expressed these split YFP-tagged SCAR and Abi constructs in the developing muscles using the muscle specific driver, *Dmef2-Gal4*. To control for background fluorescence, we used confocal microscopy to detect fluorescent levels when untagged NYFP and CYFP were similarly expressed. We did not observe fluorescent signal in the muscles expressing untagged split-YFP fragments simultaneously (Fig 1A, upper row); this indicated that the untagged split-YFP did not interact spontaneously to reconstitute YFP. We then visualized the interaction between SCAR and Abi by expressing both SCAR-NYFP and Abi-CYFP, or the converse, Abi-NYFP and SCAR-CYFP simultaneously in muscles. With either combination, we observed strong fluorescent YFP signal at the fusion site, which is marked by the F-actin focus (Fig 1A, middle and lower rows). Together, these data confirmed our hypothesis that SCAR and Abi physically interact at the fusion site during muscle formation.

In tissue culture, Abi binding is known to enhance SCAR stability and activity (Echarri et al., 2004; Kunda et al., 2003; Leng et al., 2005). As the actin polymerization activity of SCAR is required during fusion (Richardson et al., 2007; Sens et al., 2010), it is possible that the interaction between Abi and SCAR is critical for controlling SCAR levels and activity, and thus actin polymerization, at the fusion site. To test the function of the Abi-SCAR interaction at the fusion site, we next examined the impact of tagged Abi-SCAR expression on muscle development. Analysis of developing muscle cells which overexpress both the SCAR- and Abi-tagged split YFP constructs revealed that myoblast fusion at stage 16 was impaired (Figure 2A, middle and lower rows). To quantify the fusion block, we examined the fusion index in late stage 16 embryos. In contrast to control embryos in which 5-7 fusion events occur to form each Lateral Transverse (LT) muscle (Metzger et al.,

2012), we found that expression of Abi-NYFP and SCAR-CYFP resulted in severe fusion block with only 0-3 rounds of fusion per LT muscle ($p<0.001$). A fusion block was also observed in muscles expressing the reverse combination (SCAR-NYFP and Abi-CYFP), but it was less severe (0-4 rounds of fusion per LT, $p<0.001$), possibly due to lower expression levels of these specific transgenic constructs. This block in myoblast fusion was not seen when expressing untagged split-YFP constructs simultaneously (Fig 2A, upper row).

The block in fusion detected upon expression of both SCAR and Abi could be explained in two ways: First, co-expression of SCAR and Abi leads to excessive SCAR activity. This results in unregulated Arp2/3 activity at the fusion site, and a fusion block. Alternatively, expression of both SCAR and Abi produce a dominant negative effect by preventing interactions between endogenous SCAR, Rac-GTP, and Arp2/3. Due to this reduction in Arp2/3 activation at the fusion site, a fusion block occurs.

To test these two models, we first measured actin focus size in stage 15 embryos. If overexpressed Abi and SCAR produce a dominant negative effect, we would expect to see enlarged actin foci similar to SCAR loss of function mutant embryos. In muscles with Abi-NYFP and SCAR-CYFP overexpression, actin foci had an average diameter of 2.14±0.05μm, which is similar to and within the range of control foci (1.99±0.09μm, N=11). The wild-type size of the actin focus, therefore, suggested that over-expression of Abi and SCAR did not cause a dominant negative effect that suppresses SCAR activity. In addition, since it is Sra1, not SCAR or Abi, which binds to Rac-GTP, overexpression of SCAR and Abi should not sequester Rac-based WRC activation. When measuring the actin focus size, we observed that nearly every FCM in Abi-SCAR overexpressing embryos had an actin focus, not just those that were adhered to an FC/Myotube and were undergoing myoblast fusion. This suggested that actin polymerization is misregulated by Abi and SCAR

coexpression. Altogether, these observations indicated that fusion is blocked in these Abi and SCAR expressing embryos due to more SCAR activity, which in turn leads to more Arp2/3 activity.

To further test our model, we overexpressed SCAR or Abi alone in the muscle-forming mesoderm and examined the muscle pattern in stage 16 embryos. As described earlier, *in vitro* experiments suggested that SCAR itself can activate Arp2/3 (Machesky et al., 1999). Therefore, if our model is correct, namely that fusion is blocked due to upregulated Arp2/3 activity, just increasing the levels of SCAR itself should impair fusion. Indeed, when we overexpressed SCAR using two copies of the transgene, fusion was impaired. The size of the actin focus was similar to controls (2.02±0.09μm, N=11) and to simultaneous expression of both tagged SCAR and Abi. Expression of only one copy of SCAR was not sufficient to cause a fusion block, possibly due to the SCAR instability when not associated with the WRC. Nevertheless, the fusion phenotype in the low-level SCAR overexpression background can be enhanced by co-expression of Abi. This observation is consistent with the report that Abi can bind to SCAR and enhance its stability and activity (Echarri et al., 2004; Kunda et al., 2003; Leng et al., 2005). We also observed that expressing one or two copies of Abi did not result in a fusion block (Fig 2B), suggesting that increasing the availability of Abi alone is not sufficient to misregulate Arp2/3 activity and block fusion. Altogether we conclude that excessive SCAR activity impairs myoblast fusion.

Constitutively active Dia mislocalizes the Abi-SCAR complex during muscle formation

The split-YFP system also allowed us to interrogate Abi-SCAR interactions during myoblast fusion in other genetic backgrounds. Our previous work indicated that Dia

regulated SCAR localization during fusion, as in both Dia loss and gain of function, SCAR was no longer restricted to the fusion site (Deng et al., 2015). Data from mammalian tissue culture indicated that the Dia-binding SNARE domain in Abi partially overlaps with the SCAR/WAVE binding WAB domain, suggesting that Dia and SCAR compete for Abi binding (Ryu et al., 2009). Since binding to Abi is required for SCAR localization (Echarri et al., 2004), this competition might account for SCAR mislocalization in the Dia gain of function background during myoblast fusion. To test if competition between Dia and SCAR for Abi exists during myoblast fusion, we investigated whether Dia activity altered the Abi-SCAR interaction detected by the split-YFP constructs at the fusion site. To do this, we expressed constitutively active Dia (Dia.CA) specifically in the muscle-forming mesoderm together with SCAR-NYFP and Abi-CYFP and examined the distribution of the YFP signal. We used two Dia.CA constructs, one with and the second, without, the putative Abi-binding domain. In controls where there was no Dia.CA being expressed in the myoblasts, YFP reconstitution occurred through Abi-SCAR interaction, and the YFP signal accumulated at the fusion site (Figure 1A). When we expressed Dia.CA constructs together with split-YFP tagged SCAR and Abi, however, we found a diffuse cytoplasmic localization of the YFP signal (Figure 3A). No particular enrichment was found at between FC/Myotube and FCMS. We observed similar results with both constructs. The presence of the YFP signal suggested that the Abi-SCAR complex still formed in a constitutively active Dia-expressing background; however, the diffuse YFP signal indicated that the Abi-SCAR complex was no longer recruited to the fusion site. The mislocalization of the Abi-SCAR complex was consistent with our earlier report that constitutively active Dia changes the localization of SCAR (Deng et al., 2015). Since constitutively active Dia without the putative Abi binding domain also lead to a diffuse YFP signal, we suggest that Dia changes the localization of Abi-SCAR complex through its actin

polymerization activity. As we are unable to accurately quantify the diffuse YFP signal, it remains unclear, however, if Dia.CA only changes the localization of the Abi-SCAR complex or disrupts both Abi-SCAR interaction and localization.

Dia functions upstream of Arp2/3 to regulate actin at the fusion site

In our previous work, we have demonstrated that Dia functions upstream of Arp2/3 at the fusion site to polymerize linear actin filaments and to regulate the localization of SCAR and WASp (Deng et al., 2015). To further confirm these data, we performed epistasis experiments in embryos that overexpress Dia.CA, Abi, and SCAR. As discussed, the size of the actin focus provides insight to which step in fusion is disrupted in a particular fusion mutant (Richardson et al., 2007). Fusion mutants that impair SCAR-regulated Arp2/3 activation result in enlarged foci. Fusion mutants that impair WASp regulated Arp2/3 activation result in normal-sized foci. Fusion mutants that impair both SCAR and WASp-regulated Arp2/3 activation result in no actin focus (Bothe et al., 2014). Expression of constitutively active Dia (Dia.CA) changes actin dynamics during fusion and generates a diffuse distribution of F-actin at the fusion site (Deng et al., 2015). When expressed Dia.CA, together with SCAR-NYFP and Abi-CYFP in myoblasts, we found that myoblast fusion is still blocked in this context with F-actin organized into diffuse structures. These F-actin structures are similar to those seen in myoblasts expressing Dia.CA alone, rather than the round and normal-sized foci seen in a SCAR-NYFP/Abi-CYFP background (Fig 1A, 3A). These findings reinforce our conclusions that Dia functions upstream of Arp2/3 to regulate actin organization at the fusion site.

Discussion:

In this Extra View article, we show that Abi and SCAR interact at the fusion site to promote Arp2/3 activity. Excessive SCAR activity results in upregulated Arp2/3

activity and blocked fusion. Dia functions upstream of Arp2/3 to regulate actin polymerization. Excessive Dia leads to mislocalization of the Abi-SCAR complex, possibly through its actin polymerization activity.

The importance of Arp2/3 activity for myoblast fusion has been demonstrated in many studies (Kim et al., 2007; Massarwa et al., 2007; Richardson et al., 2007; Schäfer et al., 2007; Sens et al., 2010). Both SCAR and WASp can activate Arp2/3 and are known to regulate myoblast fusion in a cell type dependent manner: WASp is specifically required in the FCM (Jin et al., 2011), while SCAR is required for both FC/myotube and FCM (Gildor et al., 2009). It has also been speculated that SCAR and WASp are playing distinct roles in FCMs, with SCAR mediating the migration of myoblasts and initiating fusion (Gildor et al., 2009) and WASp promoting the formation of podosome-like structures and subsequent fusion pore expansion (Jin et al., 2011). The balance and switch between SCAR and WASp would allow for finely controlled regulation of Arp2/3 activation, which, in turn, controls the formation of the F-actin structures in the FC/myotube and FCM. In this study, we provided evidence that SCAR activity is highly regulated during myoblast fusion. Excessive SCAR activity results in mis- and upregulated Arp2/3 function and blocks myoblast fusion. It is still unclear how excessive SCAR mechanistically blocks fusion. However, the normal-sized actin focus suggests a possible model of SCAR-WASp interaction. In a WASp loss of function background, the size of the actin focus is similar to wildtype. A similar sized actin focus is also seen in SCAR overexpressing background. A possible explanation is that SCAR and WASp compete with each other for Arp2/3 binding. Therefore, SCAR overexpression leads to suppressed WASp activity, resulting in a normal-sized actin focus that phenocopies WASp loss of function. Similarly, in a SCAR loss of function background, where Arp2/3 activity is regulated by WASp only, the actin focus is

enlarged, as WASp is the major factor that promotes the formation of podosome-like structures at the FCM side (Jin et al., 2011). Together, these data suggest a possible mutual inhibition model /competition model for SCAR and WASP.

We also provide evidence for two distinct ways to control SCAR activity. The first is through direct regulation of SCAR stability, and the second is through the regulation of SCAR localization in a Dia-dependent manner. When we overexpress just one copy of SCAR, fusion is unaffected. We suggest that this may be a result of SCAR degradation when it is not associated with the WRC and reflects the cell's capacity to buffer SCAR activity. However, when one copy of Abi is added to this background, it stabilizes exogenous SCAR, leading to an increase in both the level and activity of SCAR. This, in turn, results in a fusion block. Similarly, as the majority of endogenous SCAR is either part of the WRC or degraded, overexpression of Abi alone does not lead to a significant increase in endogenous SCAR activity, and therefore fusion is unaffected. Thus, overall SCAR activity during myoblast fusion depends on the expression level of SCAR and whether it is associated with WRC components.

In our recent PLoS Genetics paper, "The formin Diaphanous regulates myoblast fusion through actin polymerization and Arp2/3 regulation", we reported that Dia functions upstream of SCAR, and that both Dia loss of and gain of function results in mislocalized SCAR. However, we did not show whether SCAR mislocalization is due to SCAR dissociation from the WRC or due to mislocalization of the entire complex. In this study, we report that in the DiaCA background, Scar remains bound to Abi and that this complex is mislocalized. Experiments in mammalian tissue culture suggested that Dia and SCAR may compete for Abi binding (Ryu et al., 2009). Since Abi is one of the components that regulate SCAR localization, these findings suggest that Dia.CA overexpression could result in

dissociation of SCAR from Abi. Our data, however, show that in a Dia.CA overexpression background, at least a portion of the mislocalized SCAR is still associated with Abi. We could not, however, exclude completely the competition model, as we are unable to measure whether the overall level of reconstituted GFP is altered.

It has also been reported that SCAR and Arp2/3 can function together to inhibit Dia activity in HeLa cells (Beli et al., 2008). As Dia activity is required during myoblast fusion, these data suggested to us that SCAR may impair fusion through inhibiting Dia. Our results, however, do not support this hypothesis: Dia loss of function resulted in actin focus absence (Deng et al., 2015), while SCAR overexpression led to normal sized actin foci.

In summary, we have demonstrated that Abi physically interacts with SCAR at the fusion site and enhances SCAR activity. We also showed that constitutively active Dia polymerizes actin upstream of SCAR function and changes the distribution of the Abi-SCAR complex. Lastly, we found that SCAR activity is highly regulated during fusion. Our data suggest that a balance between SCAR and WASp activities exist to spatially and temporally control Arp2/3 activity.

Disclosure of Potential Conflicts of Interest:

No potential conflicts of interest were disclosed.

Acknowledgements:

We thank S. Bogdan, M. Peifer and Bloomington Stock Center for fly stocks.

Funding:

This study was supported by the National Institute of Health (NIH) [GM078318, AR108981] to MKB and NCI [P30 CA 008748] core grant to MSKCC.

Figures and Figure Legends:

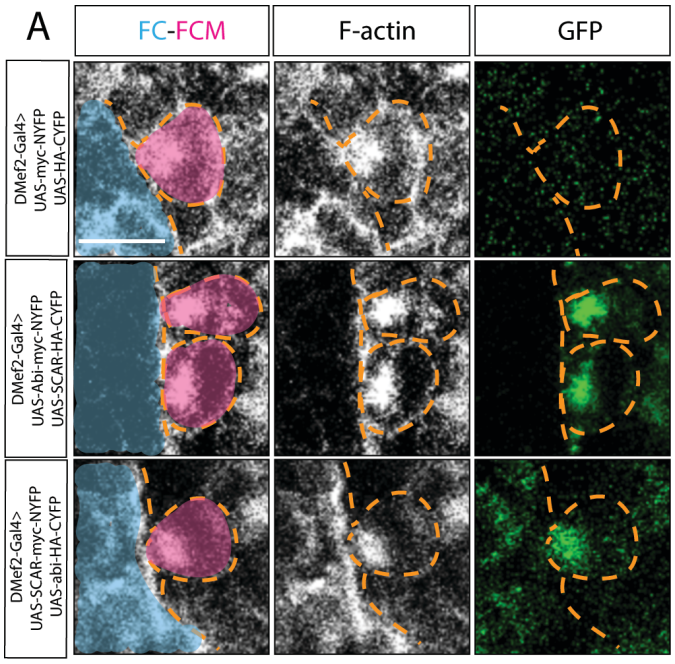

Figure 1: Visualization of Abi-SCAR complex formation using split YFP during myoblast fusion. A. Stage 15 embryo stained for F-actin (phalloidin, white) to label fusion site, and YFP (GFP antibody, green) to detect YFP reconstitution, FCM (magenta, false colored), and FC/myotube (turquoise, false colored). Top row: to visualize the background fluorescent level, *UAS-myc-NYFP* and *UAS-HA-CYFP* were expressed in the muscles under the control of muscles specific driver *DMef2-Gal4*. Middle and lower rows: *UAS-SCAR-myc-NYFP* and *UAS-Abi-HA-CYFP*, or *UAS-Abi-myc-NYFP* and *UAS-SCAR-HA-CYFP* were expressed in the muscles under the control of *DMef2-Gal4*. The reconstituted YFP signals indicate sites of Abi-SCAR interaction. Scale bar: 5μm

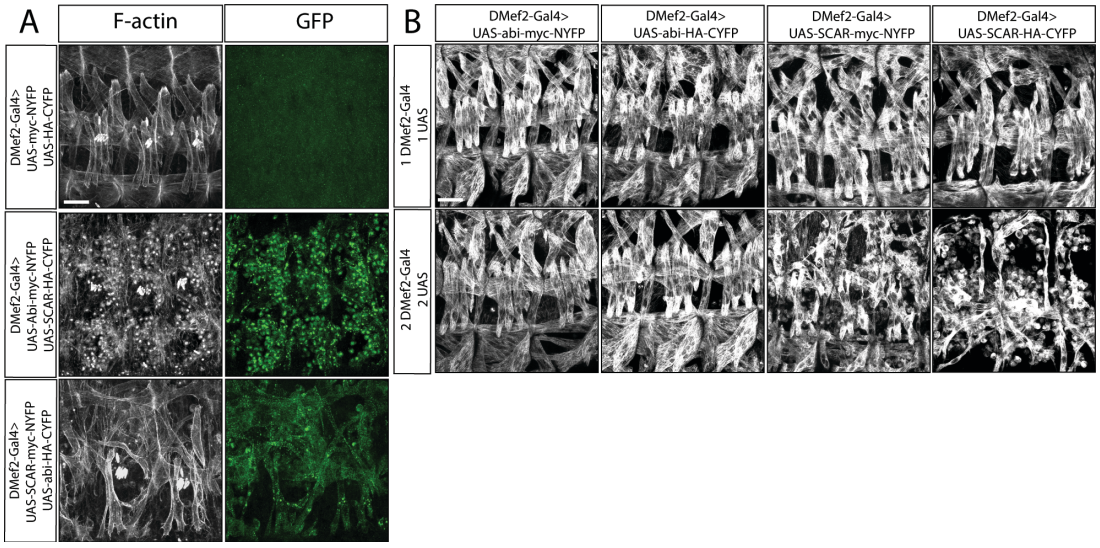

Figure 2: Increased SCAR activity results in fusion block. A. Three hemisegments from a stage 16 embryo. Embryos are stained for F-actin (phalloidin, white) to show the muscle pattern, and YFP (GFP antibody, green) to detect YFP reconstitution. Top row: in control embryos, *UAS-myc-NYFP* and *UAS-HA-CYFP* were expressed in muscles under the control of *DMef2-Gal4*. Phalloidin staining shows wild-type muscle pattern. Background fluorescent level was visualized with antibody against GFP. Middle and lower rows: *UAS-SCAR-myc-NYFP* and *UAS-Abi-HA-CYFP*, or *UAS-Abi-myc-NYFP* and *UAS-SCAR-HA-CYFP* were expressed in muscles under the control of *DMef2-Gal4*. Phalloidin staining shows impaired fusion and actin foci at the fusion site. GFP shows the localization of Abi-SCAR interaction. **B.** Muscle pattern from stage 16 embryos (antibody against Myosin Heavy Chain. white). Three hemisegments are shown from each embryo. One or two copies of split-YFP labeled Abi or SCAR were expressed in the muscles under the control of *DMef2-Gal4*. Abi overexpression does not change muscle pattern. Increased expression of SCAR results in myoblast fusion block in a dosage dependent manner. Scale bar: 20 μm

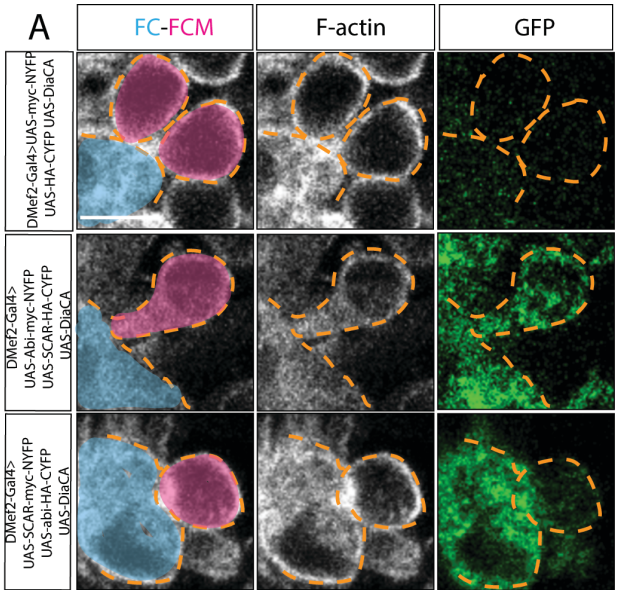

Figure 3. Constitutively active Dia changes Abi-SCAR localization and actin structure at the fusion site. A. Stage 16 embryo stained for F-actin (phalloidin, white) and YFP (GFP antibody, green), FCM (magenta, false colored), FC/myotube (turquoise/false colored). Upper row: as control, constitutively active Dia (*UAS-Dia.CA*) was expressed together with *UAS-myc-NYFP* and *UAS-HA-CYFP* in the muscles under the control of *DMef2-Gal4.* Fusion is blocked in this context. Background fluorescent level was visualized with antibody against GFP. Middle and lower rows: *UAS-Dia.CA* was expressed together with *UAS-SCAR-myc-NYFP* and *UAS-Abi-HA-CYFP*, or *UAS-Abi-myc-NYFP* and *UAS-SCAR-HA-CYFP* in the muscles. Actin structure at the fusion site was visualized by Phalloidin staining of F-actin. Abi-SCAR complex was visualized by YFP reconstitution and was labeled by antibody against GFP. Scale bar: 5μm

CHAPTER FIVE:

DIAPHANOUS AND FLIGHTLESS I CONTROL SARCOMERE SIZE IN *DROSOPHILA* INDIRECT FLIGHT MUCLES

I. Abstract:

The sarcomere is the basic contractile unit of skeletal and cardiac muscles, composed of repeated units of actin thin filaments and myosin thick filaments. The shortening of sarcomeres by the sliding of the myosin filaments on the actin filaments generates the force for muscle contraction. In muscle fibers, uniform-sized sarcomeres assemble into an aligned series, called the myofibril. A failure in the regulation of sarcomere size, uniformity, or alignment results in muscle dysfunction. Mutations in sarcomeric proteins have been linked to numerous muscle diseases, including actin myopathies, intranuclear rod myopathies and Nemaline Myopathies, further emphasizing the need to understand this structure. Since sarcomere structure is highly conserved from insects to humans, we used the *Drosophila* indirect flight muscles (IFMs) to study sarcomere assembly and homeostasis and its impact on muscle function. We now show that the formin family protein Diaphanous (Dia) is critical for sarcomere assembly, particularly in setting sarcomere length and width. Knockdown of Dia leads to sarcomeres that are shorter and thinner, due to changes in number and length of the actin thin filaments. Dia localizes primarily to the M-lines (actin pointed ends) during sarcomere growth, and then switches to the Z-discs (actin barbed ends) during muscle maturation. The localization of Dia in the sarcomere is mediated by PI(4,5)P2. In addition, Dia is involved in maintaining myosin levels in thick filaments through organization of the microtubule network required for myosin trafficking. Dia genetically interacts with Flightless I (FliI), the fly Gelsolin ortholog, to regulate thin filament length and

sarcomere size. Knockdown of FliI results in both smaller sarcomeres and long actin bundles. Double knockdown of *dia* and *fliI* further reduces sarcomere size. We propose that Dia and FliI regulate sarcomere growth through their actin polymerization and severing activity respectively, maintaining the G-actin pool and regulating actin dynamics of the thin filaments. Together these actin regulators generate uniformly sized sarcomeres tuned for the muscle contractions required for flight.

Introduction:

Sarcomeres, the basic units of striated muscles, are structurally conserved from *Drosophila* to humans. Sarcomeres are primarily composed of thin filaments and thick filaments. In each sarcomere, actin filaments of uniform length organize into a parallel pattern to form an array of thin filaments. The barbed ends of the actin filaments are anchored to the Z-disc through α-actinin, and their pointed ends are localized to the edge of the M-line. Thick filaments are composed of repeated myosin proteins. Upon stimulation, conformational changes in the myosin motor domain allow myosin to walk on the actin filaments. The relative movement between the myosin and actin filaments results in a shortening of the sarcomere, generating a contractile force. The uniform lengths of thin filaments and thick filaments are critical for the formation of uniform sized sarcomere. Sarcomeres are arranged, one after the other, to form multiple myofibrils within the muscle fiber. The uniform structure and simultaneous contraction of sarcomeres are the prerequisites for amplifying molecular-level force into visible muscle contraction.

How muscles set the size of sarcomeres, and how precisely uniform sarcomeres assemble are not well understood.

Sarcomeres are highly dynamic during both growth and maintenance stages. In different types of muscle, actin incorporates into thin filaments from both the barbed and the pointed ends of the actin filaments during sarcomere growth (Littlefield et al., 2001; Perkins and Tanentzapf, 2014). After muscle maturation, the dissociation and incorporation of actin into both ends of thin filaments still occur without disrupting the overall sarcomere organization and function (Ono, 2010; Perkins and Tanentzapf, 2014). The continuous turnover of actin suggests that the actin dynamics need to be precisely regulated to ensure uniform sarcomere length and thus optimal contraction. Previous studies have identified actin regulatory factors that regulate sarcomere size by controlling actin filament elongation, stabilization, and severing. These factors include the actin elongating protein Sals (Bai et al., 2007), capping proteins CapZ (Pappas et al., 2008; Schafer et al., 1995) and Tmod (Littlefield et al., 2001; Littlefield and Fowler, 2008; Mardahl-Dumesnil and Fowler, 2001; Sussman et al., 1998), the scaffolding proteins Sallimus (Titin) (Orfanos et al., 2015) and Lasp (Nebulin) (Fernandes and Schöck, 2014), and the severing protein Cofilin 2 (Kremneva et al., 2014). However, how these different types of proteins coordinate to ensure the uniform length of thin filaments remain largely unclear.

The assembly and stability of thick filaments also play a role in controlling sarcomere size (Contompasis et al., 2010; Reedy et al., 2000). Several studies have

focused on the incorporation of muscle Myosin into thick filaments. The M-line protein Obscurin has been reported to facilitate the assembly of myosin into thick filaments in both rats (reviewed by (Kontrogianni-Konstantopoulos and Bloch, 2005)) and *C. elegans* (Qadota et al., 2008). Thick filament assembly also depends on its interaction with actin, as well as with elastic filaments, such as the Sallimus (Titin)-based structure that anchors the thick filament to Z-disc (Myhre and Pilgrim, 2014; Orfanos et al., 2015). In mouse skeletal muscles, trafficking of myosin to the sarcomere depends on microtubules (Pizon et al., 2005; 2002). During *Drosophila* IFM sarcomerogenesis, microtubule networks form a "sleeve" within which myofibrils assemble. The microtubule "sleeve" later disassembles after myofibrillogenesis is completed (Reedy and Beall, 1993). Whether myosin is trafficked to the sarcomere via the microtubules in Drosophila IFMs is unknown

The similarity of proteins required to regulate sarcomere length in different types of muscles suggest that sarcomere assembly is controlled through a conserved mechanism. Moreover, mutations in these sarcomeric proteins are linked to muscle weakness in a number of human muscle diseases (Sevdali et al., 2013). Mutations on thin filament protein genes such as ACTA1, TNNI2, TNNT1, TNNT3, TPM2, TPM3, NEB are known to cause congenital myopathies such as actin myopathy, intranuclear rod myopathy and Nemaline Myopathy (reviewed by (Clarkson et al., 2004; Ochala, 2008)). Therefore, an investigation of sarcomere formation and homeostasis in one muscle system can provide valuable insights to the same process in different species as well as to human muscle disease.

The *Drosophila* indirect flight muscles (IFMs) provide an ideal system to study muscle formation. Due to the strong and continuous forces required for flight, IFMs are a sensitive system in which to record muscle function, as minor changes in muscle structure, myotendinous junctions, and neuromuscular junctions lead to changes in flight (Reedy et al., 2000). Moreover, in mammalian systems, severe defects in striated muscle usually result in lethality, especially in cardiac muscles. In contrast, defects in IFMs, which resemble human cardiac muscles both structurally (Spletter et al., 2015) and functionally (Tu and Daniel, 2004), affect only the ability of *Drosophila* to fly and do not affect survival rates.

Formins are family of proteins that control actin nucleation and polymerization. Due to their nature in elongating actin filaments, an increasing number of studies focused on the roles that the formin family in sarcomere development has emerged. *In C. elegans* body wall muscles, FHOD-1 and CYK-1 are involved in determining and maintaining sarcomere size and in anchoring thin filaments to Z-discs (Mi-Mi and Pruyne, 2015; Mi-Mi et al., 2012). In mammalian cardiac muscles, thirteen formins are expressed and play roles in myofibril development and maintenance (Arimura et al., 2013; Iskratsch et al., 2013; Kan-O et al., 2012; Rosado et al., 2014; Taniguchi et al., 2009; Wooten et al., 2013). In *Drosophila* IFMs, DAAM is required for thin filament assembly (Molnár et al., 2014). Moreover, in cancer-related skeletal muscle degeneration, mDia1 is reported to regulate sarcomere integrity by functioning downstream of the retinoblastoma protein (Rb) (Araki et al., 2013). Despite our understanding that formins are involved in thin filament assembly and maintenance, much remains unknown: it is

unclear how formins are recruited to their site of activity, how they regulate actin turnover, the types of proteins with which they interact at the sarcomere, and whether thin filaments are the only targets of formin function in sarcomeres.

Diaphanous (Dia), the first identified member of the *Drosophila* formin family of proteins (Afshar et al., 2000), has been shown to regulate actin polymerization in various developmental events, such as myoblast fusion (Deng et al., 2015), wing hair morphogenesis (Lu and Adler, 2015), dorsal closure (Bilancia et al., 2014; Nowotarski et al., 2014), wound healing (Matsubayashi et al., 2015), apical secretion of epithelial tubes (Rousso et al., 2013), synaptic growth (Pawson et al., 2008) and cytokinesis (Afshar et al., 2000). Dia is also known to stabilize microtubules (Daou et al., 2014) by interacting with the microtubule plus end tracking proteins, EB1 and adenomatous polyposis coli (APC) (Palazzo et al., 2001; Wen et al., 2004). The function of Dia has been extensively studied in migrating cells, dividing cells, and epithelial cells; these studies provided insights to the mechanisms by which Dia, and potentially other formins, regulate cell behaviors. However, the role of Dia during sarcomere assembly is still unknown.

In this study, we show that the Diaphanous (Dia) is required during sarcomere assembly in indirect flight muscles. Using a PI(4,5)P2 cue, Dia localizes to both pointed and barbed ends of thin filaments and determines the length and width of each sarcomere. Moreover, we find that Dia does not only regulate the actin dynamics of thin filaments, but also controls thick filament maintenance, by organizing microtubule networks around the myobrils. Altogether, we show how

Dia is localized to sarcomere and what sarcomeric structures require Dia activity. Taking advantage of the highly sensitive IFM system, we also identified Flightless I (FliI), the Gesolin ortholog and an actin severing protein, as a Dia interacting partner. Together these proteins regulate actin dynamics through regulation of available G-actin pools during sarcomere formation; this, in turn, generates sarcomeres with optimal thin filament number and length and sets the stage for the proper muscle contraction required for flight.

Results:

Diaphanous loss of function impairs flight ability and thin filament assembly in IFMs

We first tested the role of Dia in indirect flight muscles by reducing Dia levels specifically in muscles and examining the behavioral and muscular phenotypes. When we knocked down Dia with RNAi, we found that the ability to fly was significantly impaired (Figure 1A; Percentage of flightless flies: control: 1.3%±2.31%, *dia RNAi (IR)*: 100%±0%, *dia RNAi (TRiP)*: 98.7%±2.31%, n=25/day x3 days, $P<0.0001$). Similar phenotypes were found in flies that expressed a dominant negative Dia (Deng et al., 2015) in the muscles (Figure 1A; Percentage of flightless flies: control: 1.3%±2.31%, *diaDN* (intermediate): 97.3%±2.31%, *diaDN* (high): 97.3%±2.31%, n=25 flies/trial, 3 trial/genotype, $P<0.0001$). The flightless phenotype associated with Dia knockdown was specific for abrogation of Dia function. Expression of Dia::GFP in muscles rescued the flight phenotype associated with *dia RNAi* (Figure 1A; percentage of flightless flies: *dia-RNAi* (TRiP):

98.7%±2.31%, rescue: 49.7%±19.86%, n=25 flies/trial, 3 trials/genotype, P<0.0001).

As Dia is known to play a role in myoblast fusion and cell adhesion (Deng et al., 2015), we examined whether aberrations in these cellular functions could correlate with the loss in flight ability seen upon Dia knockdown using either *dia* RNAi or *diaDN*. The fusion index was derived by counting the number of myonuclei in the IFMs. We found no significant change in myonuclear number between wild-type and Dia-knockdown flies (Supplemental Figure 1B-C). As Dia is required for cell adhesion, we also tested whether the loss of flight ability was due to detachment of IFM from tendon cells. The integrity of the myotendinous junctions (MTJ) was tested by immunostaining with antibodies to β-PS integrin, a critical component of MTJ (Leptin et al., 1989). We found β-PS integrin was present at the myotendinous junctions similar to that seen in controls. No obvious change in distribution or levels was noted in *dia* RNAi conditions (Supplemental Figure 1D). Our data suggested Dia plays a role in flight muscle development beyond fusion and attachment.

As an additional control, we confirmed the *dia-RNAi* reduction of Dia levels by immunostaining for Dia. We found that *dia-RNAi* significantly reduced Dia levels in the knockdown muscles compared to the controls (Supplemental Figure 1E). However, when we adjusted the brightness and over saturated the image (increase signal to 3 fold using Volocity software), we found that residual Dia was detected in muscles expressing *dia-RNAi*. These data indicated that Dia knockdown was not 100% efficient (Supplemental Figure 1F) and may explain why muscles with *dia*

knockdown can surpass earlier events in myogenesis, such as fusion. Taken together, our results suggest that Dia loss of function impairs flight by disrupting adult muscle function after cell fusion and tendon attachment.

We next examined how *dia* loss of function impairs flight ability. Dia is known to regulate actin filament formation, and actin is the major component of thin filaments in sarcomeres. Therefore, we examined the morphology of sarcomeres in IFMs by immunostaining for F-actin. We found that the assembly of actin filaments was disrupted, which led to irregular myofibrils in *dia* loss of function IFMs (Figure 1B, Supplemental Figure 1A). Actin consistently organize into smaller-sized sarcomere. Disorganized actin filaments are also seen at the surface of muscle fiber and around nucleus (Supplemental Figure 1A). We determined through quantification that in *dia* loss of function muscles, the sarcomeres were shorter and thinner compared to controls (Figure 1C-D; Sarcomere length: control: 3.6±0.15μm, *diaDN* (intermediate): 2.9±0.32μm, *dia-RNAi* (IR): 2.3±0.39μm, *dia-RNAi* (TRiP): 2.6±0.28μm, n=100, P<0.0001, 20%-40% reduction in length. Sarcomere width: control: 1.6±0.13μm, *diaDN* (intermediate): 1.6±0.17μm, *dia-RNAi* (IR): 1.0±0.10μm, *dia-RNAi* (TRiP): 1.1±0.11μm. n=100, P<0.0001, 30%-40% reduction in width). In muscles expressing DiaDN (intermediate), individual myofibrils were difficult to distinguish, due to the frequent splitting and converging of the myofibrils. When examined flies in which the flight ability is restored by Dia::GFP, we found that the length and width of thin filaments were rescued by Dia::GFP (length: 3.5±0.14μm, width: 1.6±0.14μm, n=100, p<0.0001).

Using electron microscopy (EM), we further investigated the sarcomere morphological modifications in *dia* loss of function muscles. Similar to what we observed through immunostaining, the phenotype of range from reduced sarcomere size to highly irregular myofibrils. EM showed that reduced Dia levels could result in a reduced number of thin and thick filaments, which led to sarcomeres with reduced widths (Figure 1E-F). The distance between Z-discs was also significantly reduced in *dia* loss of function muscles, which led to sarcomeres with reduced lengths (Figure 1E-F).

Taken together, these results indicated that Dia controls IFM development and function by determining the length and width of sarcomeres.

The localization of Dia in sarcomeres changes during IFM development, and PI(4,5)P2 functions as a localization cue for Dia

To better understand how Dia functions to regulate sarcomere length and width, we investigated Dia localization and the cues required for Dia localization in the sarcomere. Using antibodies generated against Dia, we examined Dia localization in *Drosophila* IFMs 1-7 days after eclosion. We found that in flies which have just eclosed (day 1), Dia localizes mainly to the M-line (Figure 2A, arrows). As the flies aged (days 3 and 7), a higher level of Dia was found at the Z-discs (Figure 2A, arrowheads). This change in Dia's localization was confirmed by measuring fluorescence intensity across the sarcomere at the different time points (Figure 2A, Supplemental Figure 2C). Studies have shown that during sarcomere growth, thin filaments elongate at both the barbed and pointed ends; however, more

incorporation has been detected at the pointed end at the M-line (Littlefield et al., 2001; Perkins and Tanentzapf, 2014). We found that sarcomere growth continues in both length and width over the first few days following eclosion (Supplemental Figure 2A-B). The change in Dia localization suggested that Dia regulates the number and elongation thin filaments near the M-lines during sarcomere growth; it subsequently relocates to the Z-discs as muscles mature and sarcomere size stabilizes.

We next examined the cues for Dia localization in sarcomeres. Studies in *Drosophila* epithelial tracheal tubes suggested that PI(4,5)P2 and Rho GTPase controls the localization and targeting of Dia (Rousso et al., 2013). To test whether the same mechanism applied to Dia localization in sarcomeres, we expressed constructs containing GFP-tagged domains of Dia in the muscle. We reasoned that those that localized like endogenous Dia would provide important information as to how Dia is recruited to particular locales within the sarcomere. When we expressed a construct that contained the N-terminal basic domain (BD) of Dia (Dia-BD::GFP) in the muscles, we found that it reproduced the Dia pattern of expression (Supplemental Figure 2D-E). Since the Dia BD is responsible for binding PI(4,5)P2, these data suggested that PI(4,5)P2 could function as cue for Dia localization.

To further test this hypothesis, we used a PI(4,5)P2 reporter (Bothe 2014) to examine the pattern of PI(4,5)P2 localization; we found that PI(4,5)P2 showed the same spatial and temporal localization pattern as Dia. Similar to Dia, PI(4,5)P2 localized to the M-line at day 1 after eclosion and subsequently accumulated at the

Z-discs as muscles mature (day 3, Figure 2B). This observation was confirmed by plotting a fluorescent intensity curve of the PI(4,5)P2 reporter (Figure 2B).

The same pattern of localization of PI(4,5)P2 and Dia suggested that PI(4,5)P2 functions as a localization cue for Dia. If this hypothesis is true, then reducing PI(4,5)P2 levels should result in Dia mislocalization, changes in sarcomere morphology, and a loss of the fly's flight ability. Previous studies have indicated that overexpression of PI(4,5)P2 reporter results in PI(4,5)P2 sequestering and loss or reduction in PI(4,5)P2 signaling (Bothe et al., 2014). We found that increasing the level of PI(4,5)P2 reporter by placing flies to higher temperature (29°C) increased the percentage of flightless flies by 20%. In these flightless flies, Dia displayed a more diffused localization compared to controls (Supplemental Figure 2F-G). As Dia loss of function impaired flight in 100% of the flies, we sought to increase the expression of PI(4,5)P2 reporter to levels that would recapitulate the flightless phenotype seen in the Dia loss of function background. Unfortunately, increasing the PI(4,5)P2 reporter levels by increasing genetic copy numbers led to embryonic lethality due to blocked myoblast fusion (Bothe et al., 2014).

To investigate in detail the impact of PI(4,5)P2 on Dia localization, we turned to an alternative way to reduce PI(4,5)P2 levels through manipulation of Skittles (Sktl). Sktl is the kinase that catalyzes the phosphorylation of PI(4)P to produce PI(4,5)P2. A specific mutated form of Sktl (Sktl.KD) with an inactive kinase domain decrease the level and localization of PI(4,5)P2 (Rousso et al., 2013). When Sktl.KD was expressed in the muscles, 100% of flies were flightless. We next examined

sarcomere morphology and the Dia localization in the sktl.KD background. We found that the morphology of sarcomeres was altered in the sktl.KD background, like that seen in the Dia loss of function background (Supplemental Figure 2H-I). However, the expressivity of the phenotype varied: 100% of flies had thinner sarcomeres (control: 1.5±0.03 vs *sktl.KD*: 1.3±0.03, n=25, p<0.0001, 13% reduction in width), but only approximately 20% of those with thinner sarcomeres showed significantly shorter sarcomeres compared to control (control: 3.5±0.04 vs *sktl.KD*: 3.1±0.08, n=25, p<0.0001, 11% reduction in length).

We next examined Dia localization in the flies with thinner and shorter sarcomeres at 3 days after eclosion. At this time, Dia should distribute evenly at the M-line and Z-discs. By examining these day-3 adult flies, we would determine whether PI(4,5)P2 controls the Dia localization at the M-line, the redistribution of Dia to the Z-discs, or both. We found that in sktl.KD expressing muscles, Dia localized to both the M-line and Z-discs, but at a lower level (Figure 2C). This observation was confirmed by measuring Dia fluorescent intensity (Figure 2C). Together, these findings indicated that PI(4,5)P2 controls the localization of Dia during sarcomere growth, but that it acts redundantly with other cues.

Another factor that could function as cue for Dia localization is Rho GTPase. The Rho binding domain (RBD) of Dia is the interacting domain of Rho (Rousso et al., 2013). When we examined the localization of Dia-RBD::GFP 1 day after eclosion, we found that, similar as full-length Dia, Dia-RBD was also present in the M-lines (Supplemental Figure 2D-E). These data suggest that Rho GTPase functions as

another cue for Dia localization. Interestingly, another construct that contained the Dia N-terminus but without the basic (PI(4,5)P2) and Rho binding domains also showed M-line localization (Supplemental Figure 2D-E). These data indicated that additional factors could regulate Dia distribution.

Sarcomere localization of microtubules was disrupted in *dia* loss-of-function muscles

In addition to functioning in both actin nucleation and elongation, Dia is known to regulate microtubule formation and stabilization. Since these studies were conducted only in 3T3 fibroblasts in cell culture (Palazzo et al., 2001), we examined whether microtubule structures were affected in vivo in Dia-knockdown muscle. We first characterized microtubule organization in wild-type muscles using immunostaining. We found that microtubules are localized to M-lines as well as around the myonuclei in wild-type muscles after eclosion (Figure 3A, Supplemental Figure 3A). We confirmed this microtubule organization by expressing the microtubule binding protein Jupiter::GFP in the IFMs (Supplemental Figure 3B). We next examined microtubule organization in *dia* knockdown muscles. In flies 3 days after eclosion, we found that microtubules still localized around myonuclei, but they were absent from the M-lines (Figure 3A). We further investigated whether the aberrant localization of microtubules could be due to a disrupted M-line structure. We uncovered that the M-line marker, Obscurin, was present at the M-line in muscles with *dia* knockdown (Figure 3B). This result suggested that the absence of

microtubules at the M-line was not due to loss of M-line integrity, but rather a result of a disrupted microtubule network due to *dia* loss of function.

We next examined the consequence of the disrupted microtubule network. Microtubules have been reported to transport muscle myosin to the M line to form the thick filaments (Pizon et al., 2005). Therefore, we examined thick filaments by immunostaining for Myosin heavy chain (MHC). We found that in flies which have just eclosed (3 days after eclosion), Myosin is present in sarcomeres (Figure 3C). However, in older flies (10 days after eclosion), the levels of myosin in sarcomere thick filaments were decreased (Figure 3C). Together, these data suggested that M-line localization of microtubules is important for myosin maintenance of thick filaments and that Dia regulates thick filament maintenance through building and stabilizing microtubule networks.

Dia interacts with FliI to regulate sarcomere assembly

To further understand how Dia controls sarcomere growth, we performed a limited genetic screen to identify Dia-interacting proteins (Supplemental Table 1). We selected our candidate genes based on their known involvement in sarcomere structure, actin polymerization activity, or actin depolymerization activity (Supplemental Table 2). We examined whether knock down of these genes would enhance the Dia loss-of-function phenotypes, leading to a change in viability rates. Using this assay, we isolated two genes that genetically interacted with *dia* during adult myogenesis: *chickadee* (*chic*) and *flightless I* (*fliI*). Flies expressing *chic* RNAi alone in the muscles are viable and able to fly. Flies expressing *fliI* RNAi in the

muscles are viable but flightless. Double knockdowns of *dia* and *chic*, or *dia* and *fliI*, in the developing musculature resulted in pupae lethality (Supplemental Table 2).

Chickadee (Chic), the *Drosophila* Profilin, is a known Dia interacting protein that promotes actin filament elongation (Geisbrecht and Montell, 2004; Webb et al., 2009). Knockdown of *dia* does not change Chic localization in muscles (Supplemental Figure 4C). Examination of the developing IFMs at 100h APF revealed that reducing both Dia and Chic blocked myoblast fusion and impaired the formation of both the myotendinous junctions and the myofibrils (Supplemental Figure 4A-B). As the focus of this paper is sarcomere morphology, we no longer examined the interaction between Chic and Dia in this context.

Flightless I (FliI) is a member of the Gelsolin family of proteins that severs actin filaments. Studies in mammalian cell culture have shown that FliI physically interacts with Dia to promote Dia activity. To investigate if there is a direct interaction between Dia and FliI in *Drosophila*, we expressed FliI::HA and Dia::GFP in S2 cells and tested FliI-Dia biochemical interactions by co-IP. Despite the strong genetic interaction in developing adult musculature, we found no evidence of physical interactions between FliI and Dia in this context (Supplemental Figure 5A). To further study the genetic interaction between FliI and Dia during IFM growth, we examined localization of FliI in wild-type muscles. Using antibody staining, we found that FliI localizes to sarcomere Z-discs (Figure 4A). Unlike Dia, the localization of FliI does not change during muscle maturation. The different localization patterns supported our data that FliI does not physically interact with

Dia during IFM growth. Together, these data suggested an indirect, yet unidentified way of interaction between Dia and FliI to regulate sarcomere size and muscle

To better understand how FliI interact with Dia during sarcomere growth, we examined the muscle phenotype in *fliI* loss-of-function flies. Consistent with a previous screen (Schnorrer et al., 2010), *fliI* loss of function resulted in frayed myofibrils (Figure 4B). To confirm that the *fliI* phenotype was not due to an off target effect, we expressed FliI::HA in muscles to rescue *fliI* loss of function. We found that both the ability to fly and the sarcomere phenotype is 100% rescued by FliI::HA (Figure 4B).

We next examined in more detail myofibrils in *fliI* loss of function muscles. We categorized the myofibrils within an individual muscle into two classes. The first type was composed of bundles of actin and exhibited longer, thin filaments in comparison to the wild-type controls (Figure 4B). This phenotype could be explained by loss of the actin severing activity of FliI. The second class of myofibrils was composed of shorter and thinner sarcomeres (Figure 4B), possibly due to a limited actin pool resulting from insufficient actin severing and recycling from the first class of sarcomeres. Consistent with our interpretation, overexpression of FliI::HA in otherwise wild-type muscles resulted in shorter (control: 3.6±0.11 vs *fliI-HA*: 2.8±0.11, n=25, $p<0.0001$, 22% reduction in length on average) and slightly thinner (control: 1.7±0.15 vs *fliI-HA*: 1.5±0.20, n=25, $p<0.1$, 12% reduction in width on average) sarcomeres (Figure 4F-G), indicating that the actin severing activity of FliI controls sarcomere size.

We then investigated the mechanisms through which Dia and FliI genetically interact to regulate IFM development. By examining sarcomeres in 100h APF pupae, we found that a double knockdown of *dia* and *fliI* resulted in shorter (2.1±0.05μm, n=25, 30% reduction compare to control) and thinner (0.5±0.02μm, n=25, 50% reduction compare to control) sarcomeres compare to a knockdown of either *dia* (length: 2.3±0.03, $p<0.01$, width: 0.9±0.02μm, $p<0.0001$), or *fliI* (length: 2.3±0.04μm, $p<0.01$, width: 0.7±0.02μm, $p<0.0001$) alone. Based on the phenotype of sarcomeres in the knockdown muscles, we hypothesized that Dia interacts with FliI by controlling the G-actin pool: actin severed by FliI from a thin filament's barbed end re-enters the G-actin pool, while Dia incorporates G-actin from this pool into thin filaments to regulate sarcomere length and width.

We tested this model by expressing *dia* RNAi in a *fliI* overexpression background and examining the sarcomere phenotype (Figure 4F-G). Consistent with our hypothesis, excessive severing and insufficient polymerization of actin led to thin filaments that were both shorter (2.4±0.04μm, n=25, 33% reduction compare to control) and thinner (1.4±0.03μm, n=25, 18% reduction compare to control) compared to expression of *dia* RNAi alone (length: 3.6±0.04μm, $p<0.0001$, width: 1.5±0.04μm, $p<0.1$), or FliI::HA alone (length: 2.8±0.02μm, $p<0.0001$, width: 1.6±0.04μm, $p<0.1$).

Together, our data showed that Dia and FliI genetically interact to regulate sarcomere size. I provided evidence that Dia and FliI do not physically interact.

Instead, Dia and FliI localize at different ends of thin filament and control actin dynamics of the thin filament through balancing F-actin and G-actin levels.

Discussion:

In this study, we have identified Diaphanous as a novel regulator of sarcomere size. We found loss of Dia function in these muscles resulted in thinner and shorter sarcomeres, as well as disorganized myofibrils. As a functional readout of sarcomeric defects that we have uncovered, the flies are flightless. We found that Dia localizes primarily to the M-lines during sarcomere assembly, but relocates to Z-discs as muscles mature. Using domain analysis, our data indicate that that PI(4,5)P2 is involved in Dia localization (Supplemental Figure 2C-D). In addition to controlling actin dynamics, we found Dia is also involved in organizing microtubule networks. The role of microtubules during sarcomere assembly is still unclear, but we have shown that the maintenance of myosin thick filaments is impaired with Dia loss of function. Importantly, we also find that Dia genetically interacts with the actin severing protein Flightless I (FliI), and together these key actin regulators control sarcomere formation through their abilities to control the balance between F-actin and G-actin pools.

Dia determines sarcomere size by regulating thin filament formation

The actin-based thin filament is critical for muscle structure and function. Thus far, mutations on seven thin filament protein genes (ACTA1, TNNI2, TNNT1, TNNT3, TPM2, TPM3, NEB) are known to cause congenital myopathies such as actin myopathy, intranuclear rod myopathy and Nemaline Myopathy (reviewed by (Clarkson et al., 2004; Ochala, 2008)). How thin filaments are organized has been under extensive investigation, and studies have reported numerous proteins that regulate thin filament length, such as Sallimus (Titin), Lasp (nebulin) and DAAM.

We now report that the formin Dia is a novel thin filament regulator. With immunostaining and electron microscopy, we show that Dia controls the length and number of thin filaments in each sarcomere, thus determining sarcomere length and width. Changes in these sarcomere parameters impacts muscle function, as reduction of Dia activity in muscles result in a flightless phenotype.

Our observations about the role of Dia at the sarcomere are consistent with Dia's activity in both nucleating and elongating actin filaments. We found Dia loss of function does not affect the localization of CapZ, which caps actin barbed end at the Z-discs (Supplemental Figure 4C), but changes the localization of Tmod, which caps actin pointed end near the M-line (Supplemental Figure 4E-F). It is reported that the formin, DAAM, antagonizes the function of Tropomodulin (Tmod) during sarcomere assembly. The temporal localization of Dia is similar to DAAM (Molnár et al., 2014). Together, these data suggest a compensatory relationship between Dia and DAAM. The possible redundant effect between formin family members suggested the importance of actin polymerization in regulating sarcomere structures and hence, muscle function.

We identified FliI as a functional partner of Dia during sarcomere formation. *In vitro* experiments have reported that FliI enhances the activity of Dia by directly binding to the C-teminal of Dia. However, examination of the localization of Dia and FliI in sarcomeres, as well as Co-IP of FliI::HA and Dia::GFP from S2 cells, suggests an indirect interaction between Dia and FliI. We note that we could not rule out the possibility that Dia and FliI physically interact through different mechanisms in S2 cells and muscles. In addition, we did find that Dia localization switches to thin filaments' barbed ends as muscle mature. Therefore, it remains possible that Dia and FliI directly interact to maintain sarcomere structure in mature muscle.

Staining for F-actin in muscles with FliI knockdown revealed two classes of sarcomeres: class one has long and thick actin bundles and class two has shorter

and thinner sarcomeres with M-line and Z-disc proteins. Based on the two classes of myofibrils, as well as FliI's role in actin severing, we propose that FliI and Dia function together to regulate actin pools (Figure 5). Our model suggests that during sarcomere formation, FliI localizes to the barbed ends of thin filaments, severing the actin filaments. The severed and depolymerized G-actin then enters into the muscle G-actin pool and is then used by Diaphanous to integrate into the thin filaments' pointed ends. Our model (Figure 5) explains the sarcomere phenotypes that we observed in the FliI-Dia genetic experiments. In FliI and Dia double knockdown, both the G-actin pool and Dia activity are reduced, hence sarcomeres are both shorter and thinner than in the single knockdown. In muscles with FliI overexpression and Dia knockdown, sarcomeres are still shorter, despite an elevated G-actin pool, than those sarcomeres generated with either knockdown of Dia alone or an overexpression of FliI alone, due to excessive severing and insufficient polymerization.

The *Drosophila fliI* gene encodes a protein that shares a 56% identity with its human homologue. The human *FLII* gene locates at chromosome 17p11.2. This region of chromosome is deleted in patients with Smith-Magenis Syndrome. With the 29 genes located on chromosome 17p11.2, *RAI1* is believed to be the cause of Smith-Magenis Syndrome. However, there are clinical features that are seen in patients carrying the chromosome deletion more often than in patients with *RAI1* mutations alone, including cardiac abnormality (45% vs 20%), renal anomaly (19% vs 0%), and hearing loss (67% vs 20%) (Bi et al., 2004). Interestingly, these features are all related to mutations in Dia or Dia-related formins (Lynch et al., 1997; Rosado et al., 2014; Sun et al., 2014; Thelen et al., 2015). Hence, the interactions that we have uncovered between Dia and FliI provide a potential explanation for the expressivity and penetrance of Smith-Magenis Syndrome.

Dia localization in the sarcomere is control by PI(4,5)P2

Similar to epithelial cells, we found that Dia localization is controlled by PI(4,5)P2. Similar to the Dia RNAi experiments, we found that PI(4,5)P2 sequestering resulted in myofibril misalignment and loss of flight ability in ~20% flies. Due to the requirement of PI(4,5)P2 during embryonic myoblast fusion, we were unable to sequester PI(4,5)P2 to a level that enhanced this sarcomeric phenotype while allowing sufficient fusion for embryos to survive. Hence, we depleted PI(4,5)P2 by another means, by expressing a kinase-dead version of PIP5-kinase Sktl (Sktl.KD). We found loss of flight ability in 100% of flies that express Sktl.KD, and we also found that sarcomere size is altered due to insufficient targeting of Dia. Domain analysis also provides some evidence that Rho GTPase serves as cue for Dia localization (Supplemental Figure 2C-D). Future studies directed at examining the IFM phenotype and Dia localization in reduced Rho background would provide further support for Rho function of Rho in Dia localization. Interestingly, when PI(4,5)P2 and the Rho GTPase binding domain of Dia are removed or mutated, the N-terminal of Dia still shows weak accumulation at the M-line (Supplemental Figure 2C-D). Hence, while our data support PI(4,5)P2 and RhoGTPase in Dia localization in the sarcomere, these data also suggest additional localization cues for Dia during sarcomere formation.

Microtubule networks in sarcomeres

Microtubule networks play an important role in positioning myonuclei. In stage 16 embryos, microtubules emanate from myonuclei along the longitudinal axis (Folker et al., 2014). In larva muscles, microtubules radiate from the perinuclear region and to the Z-discs as well as along the long axis of the myofiber (reviewed by (Elhanany-Tamir et al., 2012; Folker and Baylies, 2013)). In pupae, microtubules organize into sleeves around myofibrils (Reedy and Beall, 1993). However, there are no reports

describing the microtubule network in adult flight muscles. We found in wild-type adult IFMs, microtubule networks are also present at the perinuclear region, as is seen in embryos and larvae. However, unlike in embryos and larvae, a strong accumulation of microtubules is detected along the M-lines in IFM sarcomeres. The pattern of *Drosophila* microtubule localization is similar to the pattern found in mammalian muscles, in which some microtubules run transversely at the I-band level (Boudriau et al., 1993; Kano et al., 1991). In IFMs expressing *dia* RNAi, microtubules still localize around the nuclei, but its localization to the M-line is lost. Microtubules are required for trafficking myosin in mouse skeletal muscle (Pizon et al., 2002; 2005). In muscles with *dia* loss of function, we did not see changes in myosin signals in newly formed myofibrils; instead, we detected a decrease of myosin signals over time, which suggests that a microtubule network is required for thick filament maintenance.

Using indirect flight muscles as a model system to study muscle formation, disease and aging

The *Drosophila* indirect flight muscles (IFMs) provide an ideal system for studying muscle development and muscle related defects for several reasons. First, the basic muscle structure is conserved from *Drosophila* to humans. Compared to single-cell muscle fiber in *Drosophila* embryonic and larva muscles, the muscle fibers in IFMs are composed of multiple myofibrils, which is similar to mammalian skeleton muscles (Schnorrer et al., 2010). Secondly, muscle defects that result in flightless flies are simple to identify using large-scale screening methodologies. Indeed, by screening for flightless flies, researchers have identified proteins that are crucial for muscle structure and function, such as myosin heavy chain (MHC), muscle actin (actin88F) and Tropomyosin (reviewed by (Vigoreaux, 2001)). More recent studies have used IFMs to screen for genes that are related to muscle differentiation,

myofibrillogenesis (Schnorrer et al., 2010) and muscular dystrophy (Kucherenko et al., 2011). Moreover, the activation and contraction patterns in IFMs resemble those patterns found in mammalian cardiac muscles, which provides a potential model system for studying heart disease (Vu Manh et al., 2005). In addition, the Gal4-UAS system and temperature sensitive Gal80 system allow genes to be switched on and off in specific tissues at a given time. In this study, we used the Gal4-UAS system to show that Dia is required in muscles during sarcomerogenesis.

In summary, we report that Diaphanous is a novel actin regulator that controls sarcomere assembly and maintenance. We identified PI(4,5)P2 as the upstream localization cue that controls the temporal localization of Dia. Dia regulates the formation of both actin and microtubule networks in myofibrils, and therefore controls thin filament formation and microtubule-dependent maintenance of myosin thick filaments. We also identified FliI as the interacting partner of Dia. We propose a model that describes FliI and Dia working together to maintain a G-actin pool that regulates the uniform size of sarcomeres.

Figure Legend:

Figure 1: Diaphanous loss of function impairs flight ability and thin filament assembly in IFMs

A. Flight assay. The ability to fly was tested 3 days after adult flies eclosed. DiaDN alleles were expressed in muscles with a *DMef2-Gal4* driver. *dia* RNAi alleles were expressed in muscles with *DMef2-Gal4; UAS-dicer2*. Reduced Dia activity resulted in impaired flight ability ($P<0.0001$). Rescue experiments were performed by expressing Dia::GFP in muscles that expressed dia RNAi (TRiP). The ability to fly was partially rescued by Dia::GFP ($P<0.0001$). **B.** Sarcomere phenotype of flight muscles. The Gal4 driver information is the same as described above. Sarcomere length is marked by the horizontal arrow, and sarcomere width is marked by the vertical arrow. Scale bar: 5μm **C-D.** Quantification of sarcomere length and width. In muscles with reduced Dia activity, sarcomere length is significantly reduced ($P<0.0001$). In muscles with reduced Dia activity, sarcomere width is significantly reduced ($P<0.0001$), except for diaDN (intermediate), where myofibrils split and converge as shown in panel **B** (arrowhead). In flies whose flight ability is restored by expressing Dia::GFP, sarcomere length and width is rescued ($P<0.0001$). **E-F.** IFM morphology under electron microscopy. Dia knockdown results in shorter and thinner sarcomeres. Scale bar: 2μm

Figure 1: Diaphanous loss of function impairs flight ability and thin filament assembly in IFMs

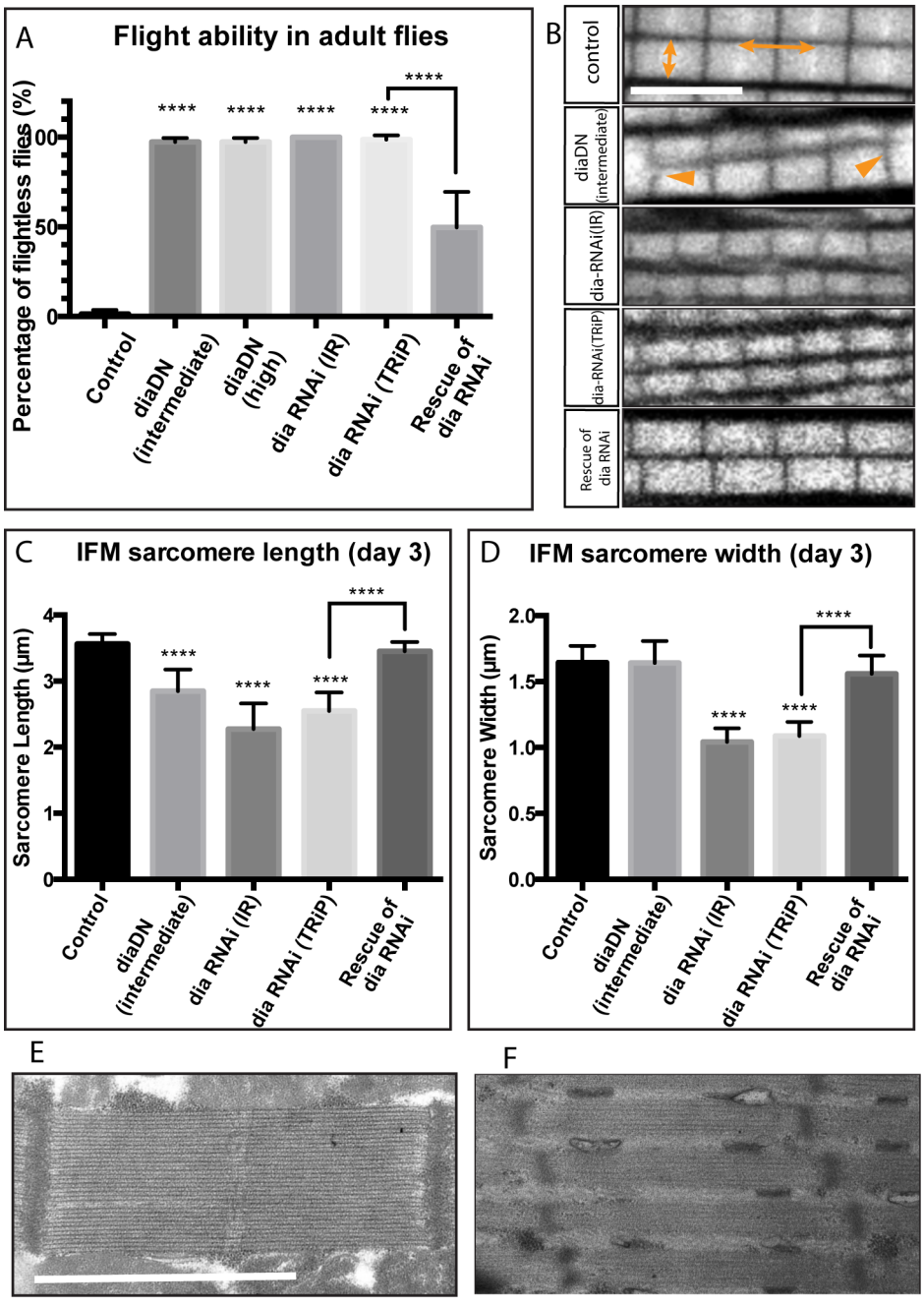

Figure 2: The localization of Dia to the sarcomere.

A. The localization of Dia is investigated in flies 1-7 days after eclosion. Sarcomere thin filaments are stained with phalloidin (white). Z-discs are labeled with antibodies against α-actinin (red). The localization of Dia is visualized by staining with antibodies against Dia (green). Dia localizes mainly to the M-lines (arrow) 1 day after eclosion, and shift to the Z-discs as muscles mature (arrow head). The shift in Dia localization is verified by plotting the fluorescent signals in the boxed area. **B.** Localization of PI(4,5)P2 in flies 1 or 3 days after eclosion. PlcγPH::GFP is expressed in muscles to label PIP2. IFMs are stained with phalloidin and antibodies against GFP. The shift of PIP2 signal is quantified by plotting the fluorescence signals in the boxed area. **C.** Dia localization in wild-type muscles and muscles expressing sktl.KD to reduce PI(4,5)P2. Flies are dissected 3 days after eclosion. Muscles are stained with phalloidin and antbodies against Dia. Images of different phenotypes are captured with the same setting to make the signal comparable. In muscles expressing sktl.KD, the level of Dia localized to the M-line and Z-discs are both reduced, as quantified by fluorescence intensity plotting. Scale bars: 5μm

Figure 2: The localization of Dia to the sarcomere.

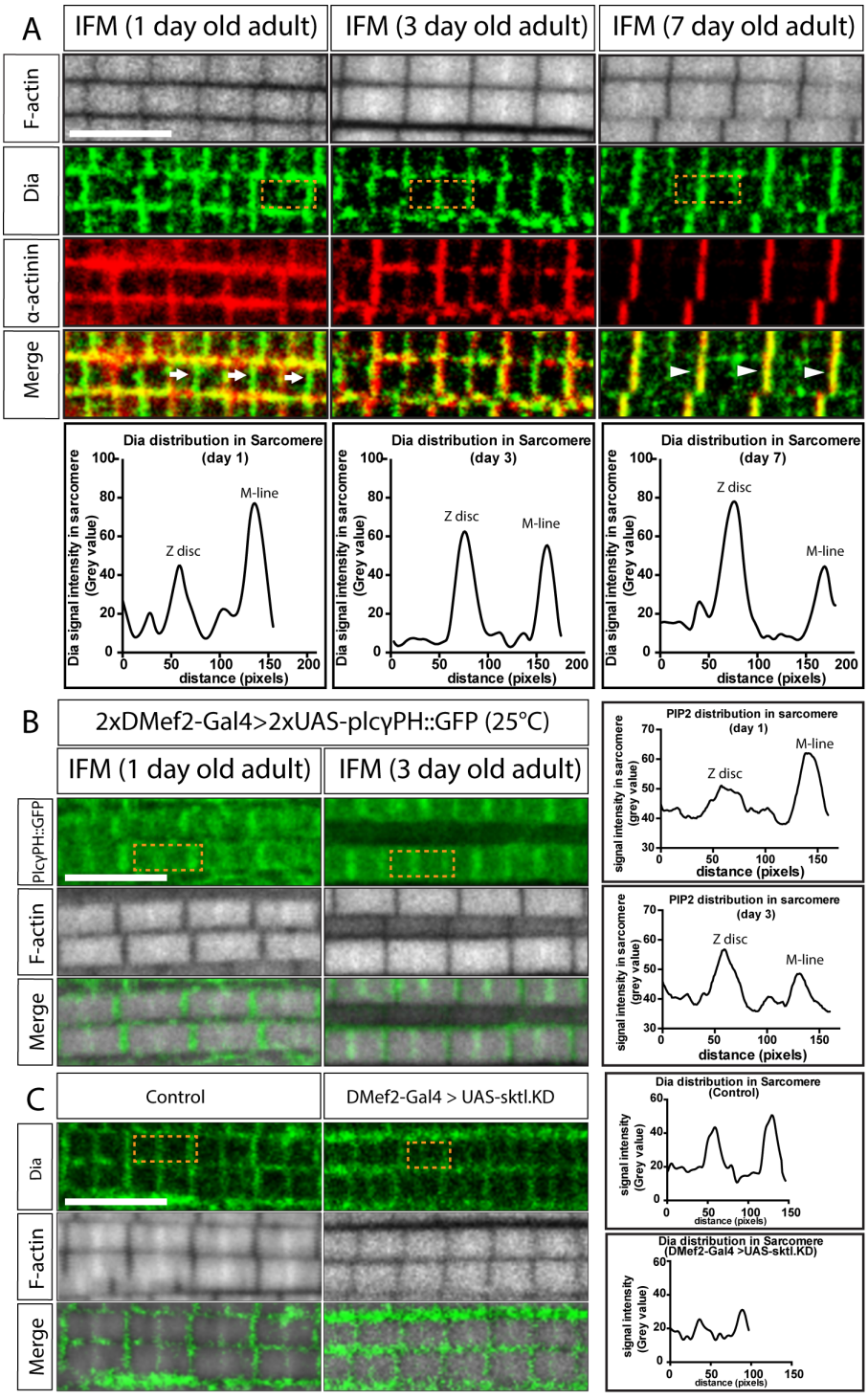

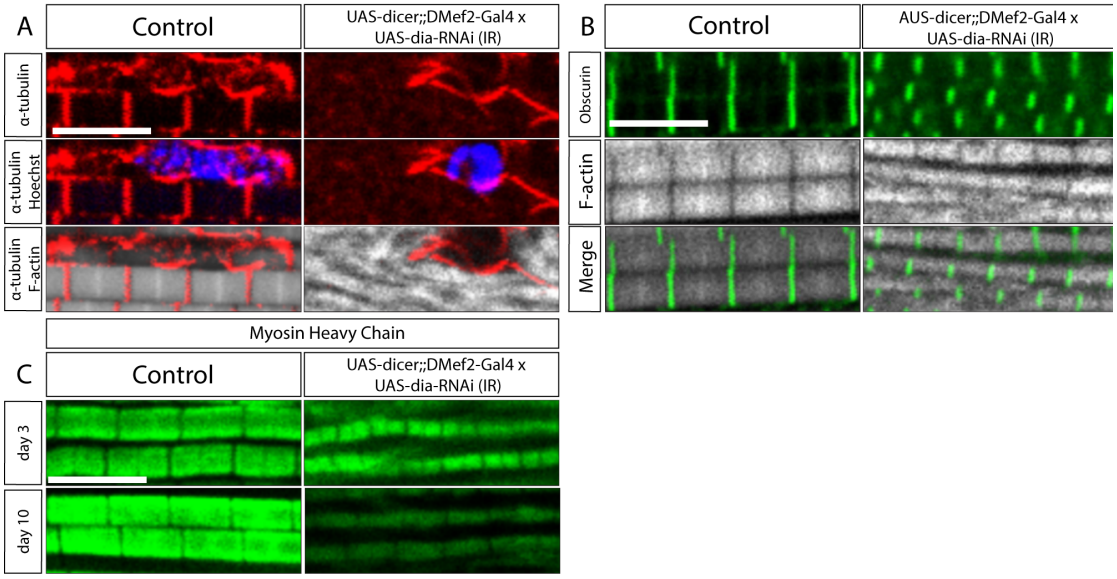

Figure 3. Dia loss of function impairs microtubule networks and myosin trafficking. A. Microtubule localization in IFMs. Flies are dissected 3 days after eclosion. Muscles are stained with phalloidin (white) and antibodies against α-tubulin (red). Nuclei are labeled with Hoechst (blue). **B.** The M-line protein is present in muscles with *dia* loss of function. Flies are dissected 3 days after eclosion. Muscles are stained with phalloidin (white) and antibodies against obscurin (green). Obscurin is present at the M-line in both wildtype and *dia* loss of function muscles. **C.** Thick filament maintenance is disrupted by *dia* knockdown. Flies are dissected at 3 days and 10 days after eclosion. Thick filaments are labeled with antibodies against myosin heavy chain (MHC). All images are taken with the same settings.

Figure 4: Dia and FliI genetically interact to regulate sarcomere size.

A. Localization of FliI in an IFM. Flies are dissected 1 to 7 days after eclosion. Muscles are stained with phalloidin (white) and antibodies against α-actinin. The localization of FliI is visualized with a FliI antibody, which co-localizes with α-actinin at the Z-discs. **B.** Sarcomere phenotype in muscles with FliI knockdown. Flies are dissected 3 days after eclosion. Myofibrils are stained with phalloidin (white), myofibrils without M-lines are marked with an arrow. Short sarcomeres are marked with an arrowhead, and shown in enlarged pictures. The bottom panel shows the sarcomere phenotype in flies that are rescued with FliI::HA. Scale bars: 5 μm. **C.** Survival assay. 25 embryos/genotype/day are selected for 3 days. Survival rates are calculated at larvae, pupae and adult stages. Knockdown of both Dia and FliI results in 100% lethality at pupae stage. **D.** Sarcomere phenotypes in pupae. 100 APF pupae are dissected. The morphology of myofibrils and sarcomeres are visualized by phalloidin staining. Scale bar: 5 μm **E.** Quantification of sarcomere size. Knockdown of both FliI and Dia significantly reduce sarcoemre length ($p<0.01$) and with ($p<0.0001$) compare to single knock down. **F.** Sarcomere phenotype in IFM with FliI overexpression and Dia knockdown. Morphology of myofibril and sarcomere are visualized by Phalloidin staining. Scale bar: 5μm. **G.** quantification of sarcomere size. Expressing both *dia* RNAi and FliI::HA in muscles with two copy of *DMef2-Gal4* significantly reduce sarcoemre length ($p<0.001$) and with ($p<0.1$) compare to just expressing *dia* RNAi or FliI::HA.

Figure 4: Dia and FliI genetically interact to regulate sarcomere size.

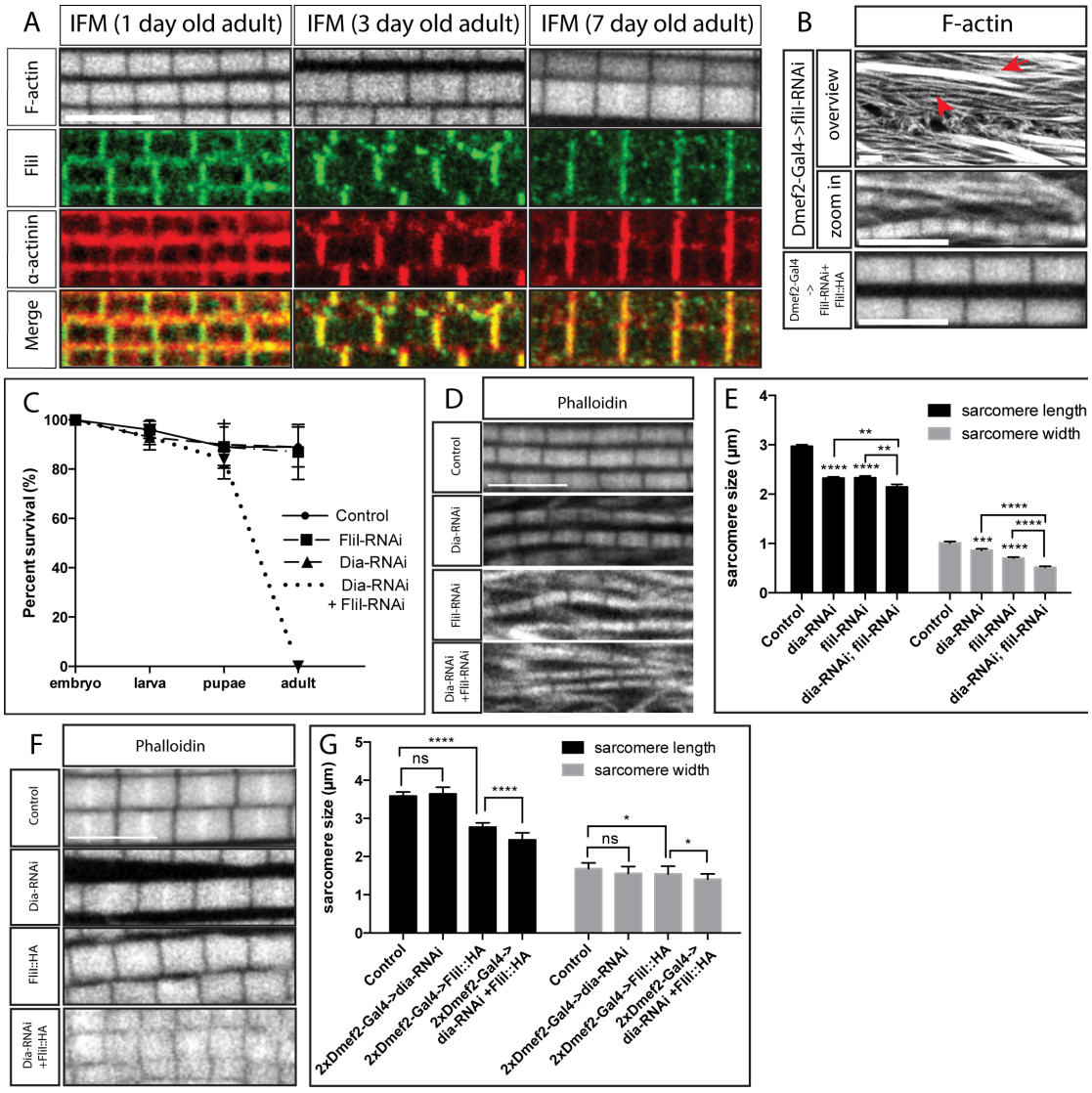

Figure 5: Model: Dia and FliI interact to maintain the G-actin pool in muscles and regulate the size and uniformity of sarcomeres.

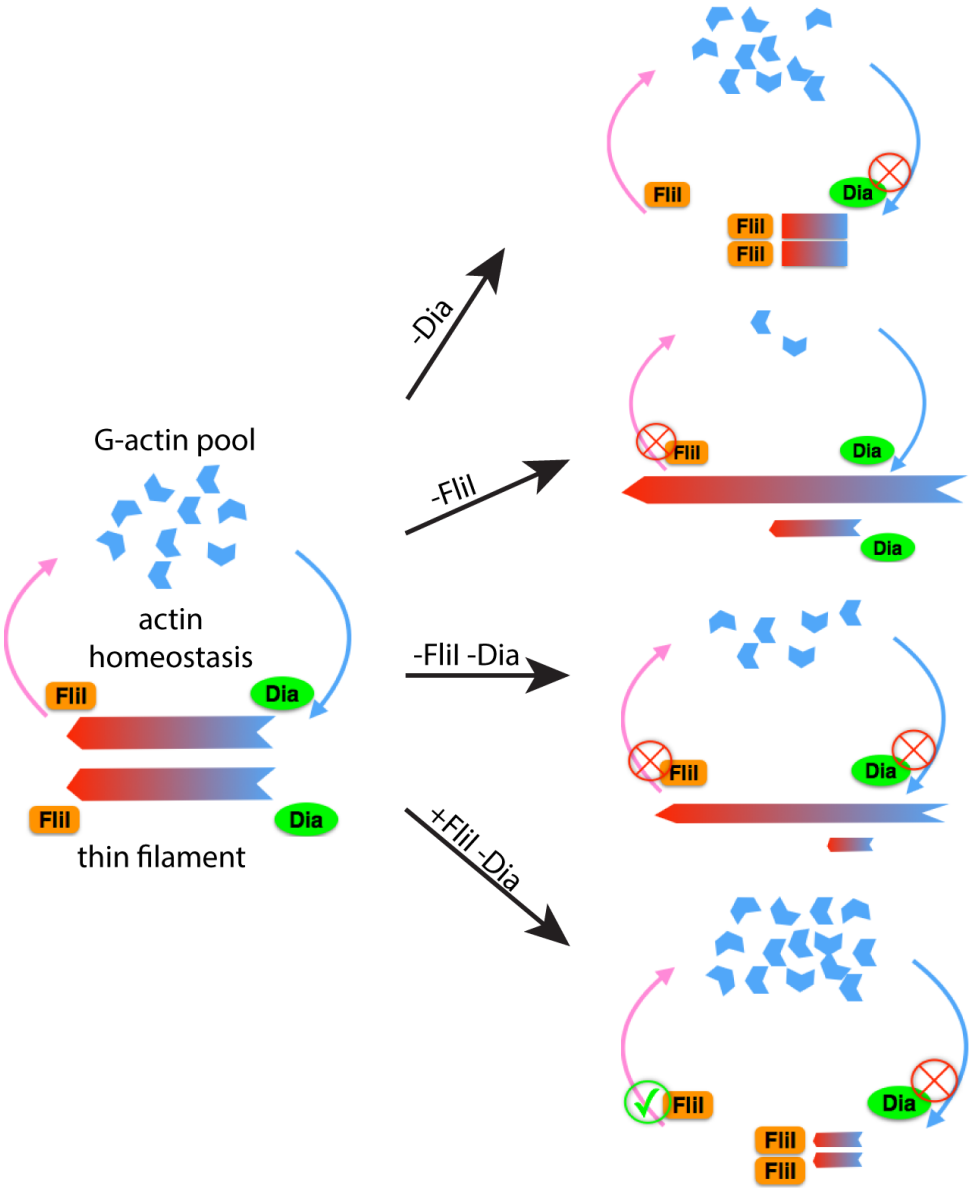

Supplementary Figure 1: A. The phenotype of muscles with reduced Dia function. Flies are dissected 3 days after eclosion and stained with phalloidin to label muscle structures. In muscles expressing DiaDN (intermediate), myofibrils undergo splitting and converge (arrow). No sarcomere structure could be detected in muscles expressing DiaDN (high). Both types of *dia* RNAi tested lead to shorter and thinner sarcomeres, as well as disorganized myofibrils. Scale bar: 5μm **B.** Myoblast fusion is sufficient in muscles with *dia* knockdown. Flies are dissected 3 days after eclosion. Muscles are labeled with phalloidin (white), and muscle nuclei are labeled with Hoechst (blue). Enlarged pictures showing the even distribution of nuclei in both control muscles and muscles with *dia* knockdown. Scale bar: upper panel: 100μm; lower panel: 5μm **C.** Fusion index in muscles with *dia* knockdown. A fusion index of IFMs is quantified by counting the number of nuclei in a 100μm x 5μm area. No significant difference is found in control muscles and muscles with *dia* knockdown. **D.** The myotendinous junction is not affected in muscles with *dia* knockdown. Flies are dissected 3 days after eclosion. Muscles are labeled with phalloidin (white), the myotendinous junction is labeled with β-PS-integrin (red). No significant difference of β-PS-integrin signal is seen between control and *dia* knockdown muscles. **E.** Knockdown efficiency of *dia* RNAi (IR). An IFM is dissected and stained with phalloidin (red) and Dia (green). Images are captured with the same settings and show a decreased level of Dia due to *dia* knockdown. In muscles with *dia* knockdown, we brought the signal up to 300% to show a residue of Dia in the sarcomere after *dia* knockdown. Scale bars: 5μm

Supplementary Figure 1

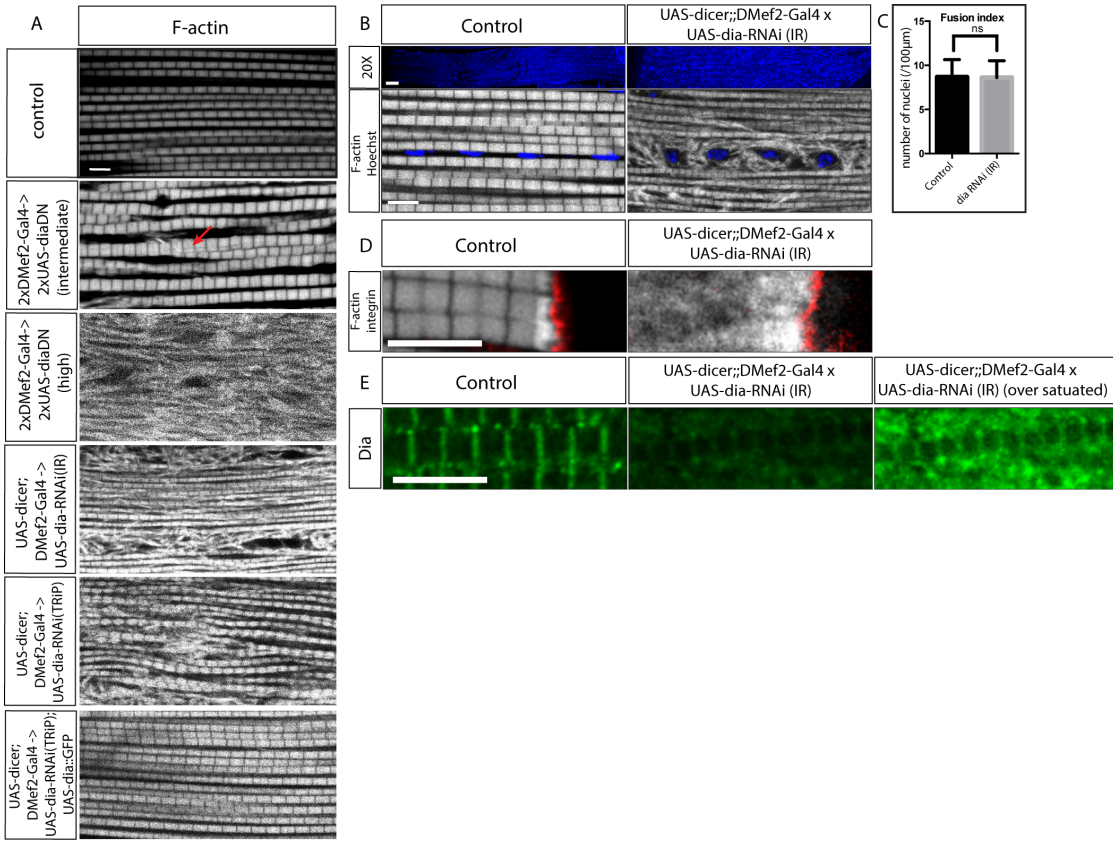

Supplemental Figure 2. A-B. The changes in IFM sarcomere size in adult flies. Wild-type flies are dissected from 1 to 7 days after eclosion. Sarcomeres are visualized with phalloidin staining. The size of each sarcomere is measured and compared. Sarcomeres in flies that have just eclosed are significantly shorter ($p<0.0001$) and thinner ($p<0.0001$) than the sarcomeres of flies measured 3 days after eclosion. There is no significant difference of sarcomere size between day 3 and day 7 adult flies. **C.** Diagram of Dia construct used in detecting Dia localization. The diagram is modified from (Tal Rousso, 2013). BD: basic domain. RBD: RhoGTPase binding domain. Dia-N'ΔBD-mut^{G}: Dia N-terminl domain without basic domain and Rho binding affinity. **D.** Localization of different Dia domains. Muscles are labeled with phalloidin (white). Antibodies against GFP label the localization of GFP fusion proteins. **E.** Dia localization in PI(4,5)P2 sequestered IFMs. Flies are dissected 3 days after eclosion. Localization of Dia is detected with antibodies stained against Dia. **F.** Fluorescent intensity in the boxed area. In PIP2 sequestering IFMs, higher levels of Dia are detected that are not specifically localized to either the Z-discs or M-line. **G-H.** Sarcomere size changes in muscles with reduced levels of PI(4,5)P2. Flies are dissected 3 days after eclosion. In muscles that express kinase dead PIP5-kinase Sktl (Sktl.KD), sarcomere is significantly shorter ($p<0.0001$) and thinner ($p<0.0001$) than control.

Supplemental Figure 2.

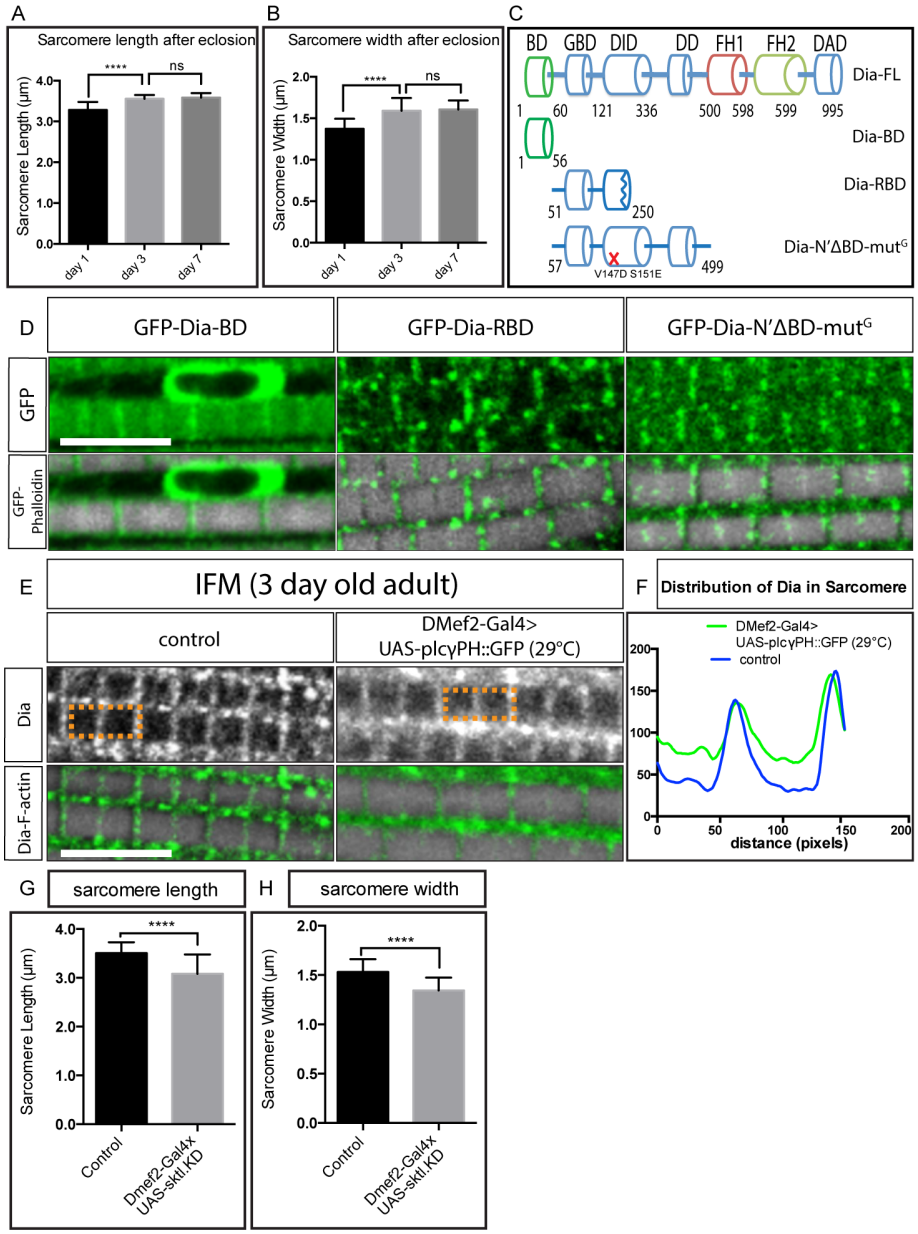

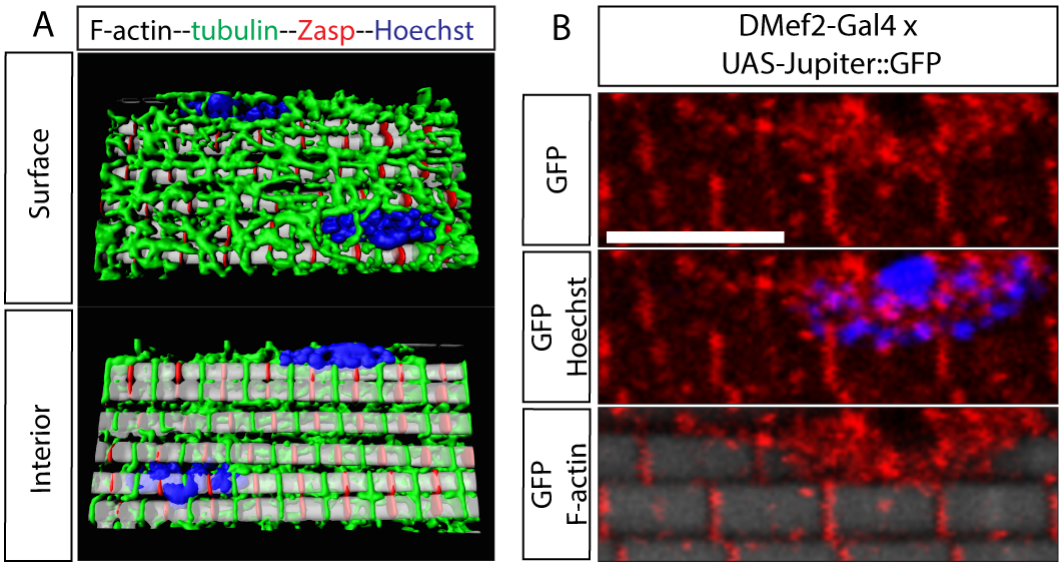

Supplemental Figure 3. A. 3-D reconstruction of six myofibrils showing microtubule network. Wild-type flies are dissected 3 days after eclosion. Muscles are labeled with phalloidin (white), antibody against α-tubulin (green) and Zasp (red). Nuclei are labeled with Hoechst (blue). The surface view shows microtubule networks at the periphery of the muscles. The interior view shows the localization of microtubules at the M-line. **B.** Jupiter::GFP is expressed in muscles with a *DMef2-Gal4* driver. Flies are dissected at day 3 after eclosion. Muscles are stained with phalloidin (white), and antibodies against GFP (red). Nuclei are labeled with Hoechst (blue). Microtubule networks in muscles are visualized by Jupiter::GFP. Scale bar: 5 μm.

Supplemental Figure 4. A-B. Muscle phenotypes in IFMs with *chic* and *dia* double knockdown. 100 APF pupae are dissected. Muscles are stained with phalloidin (white), and nuclei are labeled with Hoechst (green). Double knockdown of *chic* and *dia* result in few nuclei in the IFMs, and IFMs are not attached to the myotendinous junction. Enlarged picture are shown in **B**, with details of myofibrils. Scale bars: A: 40 μm, B: 5 μm. **C-D.** Chic and CapZ localization in dia loss of function IFMs. Flies are dissected 3 days after eclosion. Muscles are labeled with phalloidin (white) and antibodies against Chic (C) and Cpa (D), respectively. **E-F.** Tmod localization in *dia* loss of function IFMs. Flies are dissected 1 and 3 days after eclosion. Muscles are labeled with phalloidin (white) and antibodies against Tmod. Note the Z-disc localization of Tmod, which is seen in muscles expressing *dia* RNAi, but not in wild-type muscles. Scale bars: 5 μm.

Supplemental Figure 4.

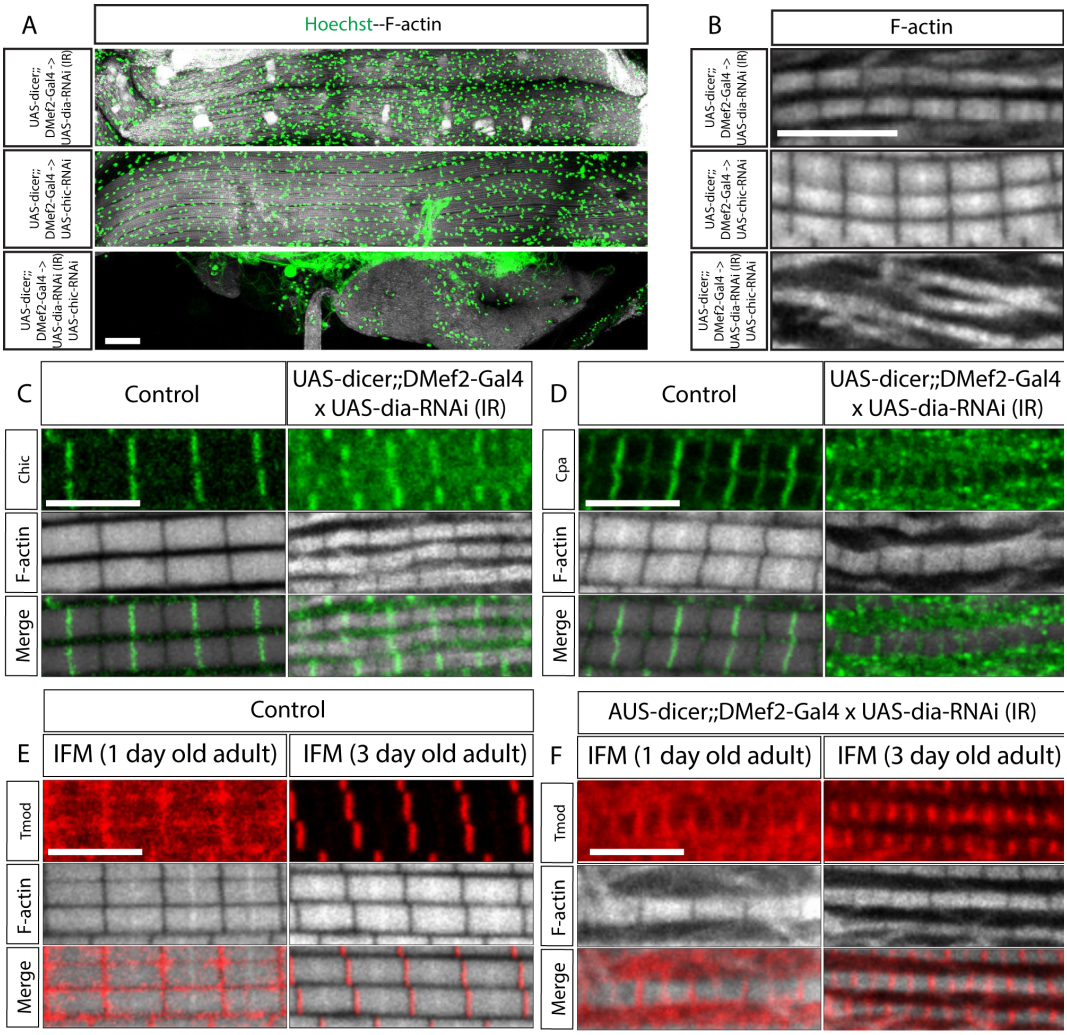

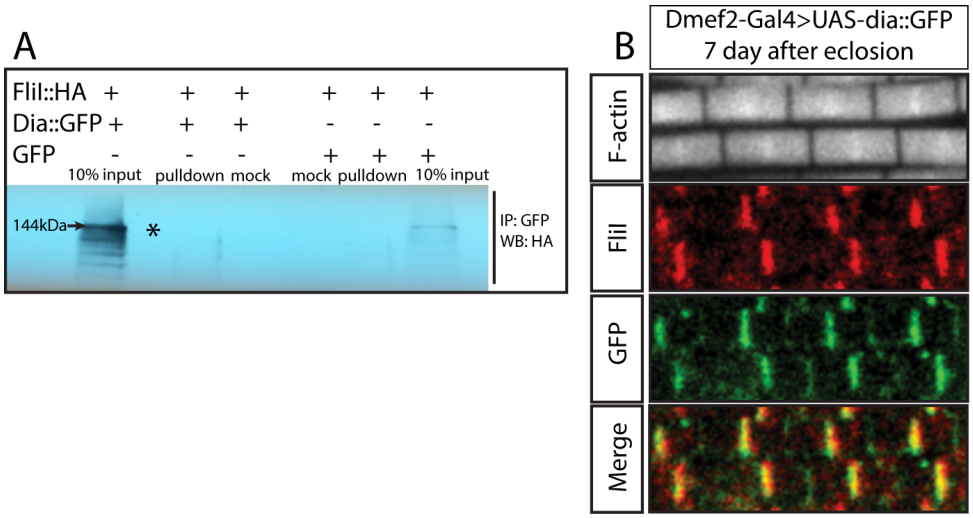

Supplemental Figure 5. A. Co-immunoprecipitation of Dia::GFP and FliI::HA. Dia::GFP and GFP (negative control) are immunoprecipitated from S2 cells with antibodies against GFP. Immunoprecipitation with nospecific lgGs are used as control (mock). Samples are analyzed by western blotting using antibodies against HA. No FliI::HA pulldown was detected (asterisk). **B.** Co-localization of Dia and FliI in mature IFMs. Flies expressing Dia::GFP in muscles are dissected 7 days after eclosion. Muscles are labeled with phalloidin, antibodies against GFP and FliI. Dia::GFP and FliI co-localize to the Z-discs.

Supplemental Table 1: Flow chart of Dia-interacting protein screen

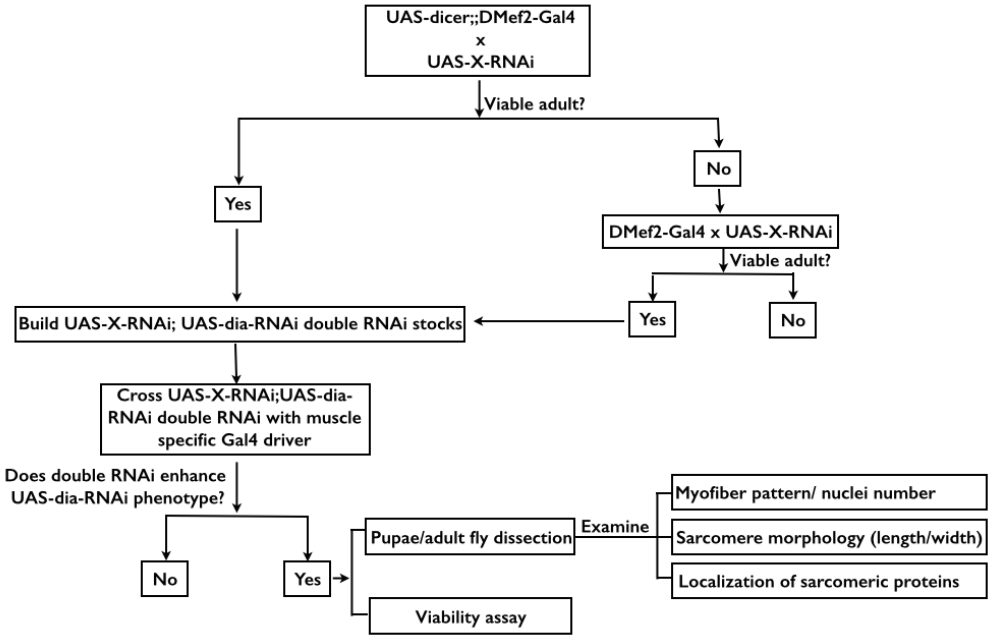

Supplemental Table 2: Candidate genes and RNAi lines used in Dia-interacting protein screen.

Supplemental Table 2: Dia-interacting Protein Screen

Gene/stock number	Gal4	Phenotype	Enhanced dia-RNAi phenotype?
cpb/Trip26298 (III)	UAS-dicer;;Dmef2-Gal4	wt	-
Cpa/Trip31124 (III)	UAS-dicer;;Dmef2-Gal4	wt	-
abi/Trip36707 (III)	UAS-dicer;;Dmef2-Gal4	wt	-
chic/Trip34523 (III)	UAS-dicer;;Dmef2-Gal4	wt	Pupae lethal
plcPH::GFP	2x Dmef2-Gal4	wt	-
rho/VDRC 107502	UAS-dicer;;Dmef2-Gal4	pupae lethal	N/A
	Dmef2-Gal4	wt	-
mwh/Trip34862 (III)	UAS-dicer;;Dmef2-Gal4	wt	-
Ena/TRiP31582 (III)	UAS-dicer;;Dmef2-Gal4	flightless	
cib/Trip 36630 (III)	UAS-dicer;;Dmef2-Gal4	Pupae lethal	-
cip4/Trip31646 (III)	UAS-dicer;;Dmef2-Gal4	wt	-
gel/Trip 31205 (III)	UAS-dicer;;Dmef2-Gal4	wt	-
fliI/VDRC 39528 (III)	UAS-dicer;;Dmef2-Gal4	flightless	Pupae lethal
tsr/VDRC (II)	MHC-Gal4	wt	-
CG5869/Trip 51452 (II)	UAS-dicer;;Dmef2-Gal4	wt	-
CG6873/TRiP 38226 (II)	UAS-dicer;;Dmef2-Gal4	wt	-
qua/TRiP 41856 (III)	UAS-dicer;;Dmef2-Gal4	wt	-
abp1/TRiP 38282 (II)	UAS-dicer;;Dmef2-Gal4	wt	-
twf/TRiP 35365 (III)	UAS-dicer;;Dmef2-Gal4	wt	-
CG45186 /TRiP 31579 (III)	UAS-dicer;;Dmef2-Gal4	flightless	-
CG45186 /TRiP 28914 (III)	UAS-dicer;;Dmef2-Gal4	Pupae lethal/ flightless	-
CG45186 /TRiP 34016 (III)	UAS-dicer;;Dmef2-Gal4	wt	-
obscurin /Trip34000 (III)	UAS-dicer;;Dmef2-Gal4	wt	-
zormin/VDRC 34513 (II)	UAS-dicer;;Dmef2-Gal4	Pupae semi-lethal/ flightless	-
msp300/VDRC 109023 (II)	UAS-dicer;;Dmef2-Gal4	Embryo /Larva lethal	N/A
msp300/VDRC 107183 (II)	UAS-dicer;;Dmef2-Gal4	Pupae lethal	N/A
	Dmef2-Gal4	wt	-
lasp/VDRC 109416 (II)	UAS-dicer;;Dmef2-Gal4	Pupae lethal	N/A
	Dmef2-Gal4	wt	-
myo/VDRC 110195 (II)	UAS-dicer;;Dmef2-Gal4	wt	-
a-Actn/VDRC 110719 (II)	UAS-dicer;;Dmef2-Gal4	Larva/ Pupae lethal	N/A
	DMef2-Gal4	wt	-
actn3/VDRC 106162 (II)	UAS-dicer;;Dmef2-Gal4	Wt/ flightless	N/A
	DMef2-Gal4	wt	-
sls/VDRC 20755 (X)	UAS-dicer;;Dmef2-Gal4	Larva lethal	N/A
sls/VDRC 47298(II)	UAS-dicer;;Dmef2-Gal4	Embryo/larva lethal	N/A
	DMef2-Gal4	wt	-
sls/VDRC 47301(II)	UAS-dicer;;Dmef2-Gal4	Embryo/larva lethal	N/A
zasp/VDRC 36563 (II)	UAS-dicer;;Dmef2-Gal4	Pupae semi-lethal/wt	-
Sals/TRiP 31547 (III)	UAS-dicer;;Dmef2-Gal4	pupae lethal	-
Sals/TRiP 31547 (III)	UAS-dicer;;Dmef2-Gal4	pupae lethal	-

CHAPTER SIX:

CONCLUSION

I. Elucidating the mechanisms of myoblast fusion

Cell-cell fusion is a highly regulated process that is critical for events including fertilization, bone remodeling, and the generation and homeostasis of skeletal muscle. Organisms in different species use this strategy to exchange genetic information, increase cell volume, and maintain cell function. Despite the differences in biological context, the steps required for cell-cell fusion are conserved: two cells make contact and their cell membranes align, then fusion pores form on the membranes that allow the separate lipid bilayers to merge and achieve cytoplasmic continuity. Studying cell fusion in one cell type may provide insights to how fusion is regulated in different cell types across species. In my thesis, I have demonstrated how the phospholipid PI(4,5)P2, as well as the formin Diaphanous are involved in regulating myoblast fusion during *Drosophila* embryonic muscle formation.

The process of *Drosophila* embryonic myoblast fusion has been well documented through fixed and live imaging, both *in vivo* and *in vitro* (Dobi et al., 2011; Richardson et al., 2008a; Shilagardi et al., 2013). Researchers have identified numerous factors that are prerequisites for fusion. These include transcription factors needed for myoblast specification (Dohrmann et al., 1990; Duan et al., 2001), membrane proteins required for cell recognition (Bour et al., 2000; Ruiz Gomez et al., 2000), cytoskeleton regulators that play roles in cell migration and adhesion (Geisbrecht et al., 2008; Gildor et al., 2009), and proteins that mediate the membrane fusion events (reviewed in (Kim et al., 2015)). These studies have laid the foundation for my thesis research.

In my thesis studies, I addressed two critical questions related to myoblast fusion: 1) In addition to transmembrane proteins, are there any other membrane components that transduce signals from the membrane and trigger cytoskeleton remodeling during fusion (Chapter 2)? And 2) Most of the actin regulators are known to play a role in fusion function through activating Arp2/3. Arp2/3 nucleates branched actin networks, but does not elongate actin filaments. Some studies propose that the actin regulators, WIP and WASp, can recruit G-actin to the fusion site, and therefore increase local G-actin concentration, allowing spontaneous elongation of actin filaments locally (Jin et al., 2011). This hypothesis however, has not been validated. And it is unknown whether there is any actin regulator that elongates the filaments that Arp2/3 binds to or nucleates (Chapter 3, Chapter 4).

Experiments in mammalian systems provided potential targets to address the first question: in mammalian muscles, phosphoinositide signaling is required for myogenesis (Bach et al., 2010; Leikina et al., 2013; Nowak et al., 2009). PI(4,5)P2 is one of the phosphoinositides that regulate actin polymerization by controlling the localization and activity of Arp2/3 activators. We therefore used PI(4,5)P2 reporters to record the spatial and temporal distribution of PI(4,5)P2 during myoblast fusion (Chapter 2). The accumulation of PI(4,5)P2 at the fusion site suggested a role of PI(4,5)P2 in myoblast fusion. Decreasing the availability of PI(4,5)P2 blocks myoblast fusion and confirms that PI(4,5)P2 is required during fusion. How PI(4,5)P2 regulates actin remodeling during *Drosophila* myoblast fusion has been examined through both *in vitro* and *in vivo* assays. We have shown that PI(4,5)P2 regulates the localization of Mbc, thereby controlling the localization of active Arp2/3.

To address the second question about additional actin regulators, we examined the muscle phenotypes of mutations in different formin family members.

Formins are a family of proteins that nucleate and elongate actin filaments. Because of their activity, formins can work upstream of Arp2/3, building the actin filaments to which Arp2/3 can then bind. Alternatively formins can act downstream of Arp2/3, capping or elongating the actin filaments that Arp2/3 seeded. We examined muscle phenotypes in all the available formin mutants. Some of the mutants tested were generated through random transposable element insertions, and the nature of these mutations has not been characterized. Nevertheless, we found that at least 4 formins in *Drosophila* are involved with muscle formation: a mild muscle detachment phenotype was observed in *daam* (*daam*^{G1567}) mutants; a severe muscle morphological change was observed in *fhos* (*fhos*^{A055}) mutants; and Cappuccino (Capu) mutants either failed to reach the stages of muscle formation (due to Capu's role in early embryogenesis events), or the mutant embryos formed muscle with normal patterns. However, when examining double heterozygous embryos for a putative *capu* null allele (*capu*^{12344}) and *blow*^{1}, some embryos showed a mild reduction of fusion and a minor muscle detachment phenotype. When examining doubly heterozygous embryos for c*apu*^{12344} and *mbc*^{c1}, the numbers of LT muscles in some embryos was significantly increased. Similar to Capu, Diaphanous (Dia) is also required in early embryogenesis events, therefore only a small proportion of *dia* mutant embryos proceeded to stages in which muscle formation could be assessed. Among these embryos, we observed a variety of muscle defects, including insufficient fusion, missing muscles, muscle morphological changes, and muscle detachment. We also noticed that overexpression of constitutively active Dia significantly blocks myoblast fusion. The muscle phenotypes in *dia* loss of function and overexpression backgrounds gave us the rationale to investigate the role of Dia during fusion.

In Chapter 3 we elucidated the function of Dia during fusion. I provided evidence that Dia and Arp2/3 cooperate in a highly regulated manner to build actin networks at the fusion site. We showed that Dia functions upstream of Arp2/3 to build linear actin filaments upon which Arp2/3 can bind. We also showed that Dia is required for the proper localization of Arp2/3 NPFs, SCAR and WASp. Our work suggested a balance exists between Arp2/3-mediated actin branching and Dia-mediated actin elongation. In Chapter 4, we took our research a step further to demonstrate that, like Dia, the activity of SCAR is also highly regulated to facilitate fusion, as either loss of function or overexpression of SCAR results in blocked fusion. Our work emphasized the importance of balanced activity between Dia and the ARP2/3 NFPs, SCAR and WASp. The expression levels and activity of these actin regulators determined the structure and dynamics of actin networks at the fusion site, and they are therefore essential if fusion is to proceed.

Collectively, this work has expanded our understanding of how myoblast fusion progresses and has identified two more factors that are required in *Drosophila* myoblast fusion. However, our data also raise more questions about how fusion is initiated and how it proceeds: what triggers the aggregation of transmembrane proteins Sns and Duf and recruits PI(4,5)P2 to the fusion site? Expression of Duf or Rst in S2 cells suggests these proteins localize at cell-cell contacts and mediate homotypic cell aggregation. Expression of Sns does not trigger homotypic aggregation (Galletta et al., 2004). In *Drosophila* embryos, ectopic expression of Duf or Rst induces migration and aggregation of FCMs at ectopic sites (Ruiz Gomez et al., 2000; Strünkelnberg et al., 2001). These FCM behaviors are mediated by Sns and its interacting proteins that transduce Sns signaling to actin cytoskeleton (Kim et al., 2007; Kocherlakota et al., 2008). However, it is unclear whether there is a feedback mechanism that triggers the aggregation of Sns. Our

data indicate that the PI(4,5)P2 enrichment at the fusion is dependent on Sns. However, the mechanism by which Sns recruits PI(4,5)P2 has not been investigated: it remains to be tested whether Sns recruits PI(4,5)P2 via a direct interaction or through interaction with PI(4,5)P2 binding proteins. To address this question, one can examine the enrichment of PI(4,5)P2 in Sns deletion backgrounds and determine the minimal Sns regions required for PI(4,5)P2 localization. By examining the required sequences and identifying potential binding partners of these regions, one can determine how Sns recruit PI(4,5)P2 to the fusion site. A series of deletion and site directed mutations are available for this purpose (Kocherlakota et al., 2008).

Another question that needs to be addressed is how Dia accumulates at the fusion site and how is it regulated there. Experiments in *Drosophila* epithelial tubes showed that PI(4,5)P2 regulates the apical localization of Dia. During myoblast fusion, both PI(4,5)P2 and Dia are enriched at the fusion site, suggesting Dia might be recruited to the fusion site through similar mechanisms. However, when we examined Dia localization in muscles under PI(4,5)P2 sequestering conditions, we found that Dia still accumulates at the fusion site. One explanation for this observation is that PI(4,5)P2 is not completely sequestered. The presence of a small actin focus in PI(4,5)P2 sequestering conditions, rather than no actin focus as that seen in *wip* and *kette* double mutant, supports this explanation. Another possibility is that there are redundant factors, in addition to PI(4,5)P2, that regulate Dia localization.

Our study showed that in *wip* and *kette* double mutant, Dia is present at the fusion site even when Arp2/3 activity is compromised. We use these data to support our model that Dia function upstream of Arp2/3 and its regulators. One aspect to note is that in *wip* and *kette* double mutant embryos, no actin focus is

formed, despite the fact that Dia is present at the fusion site. One explanation for this observation is that Dia, while present at the fusion site, is not actively polymerizing actin. Another explanation is that Dia is present and active at the fusion site, but the actin filaments that it polymerizes do not organize into a focus structure. Our model favors the second explanation. In fact, residual actin filaments are found at the fusion site in *wip* and *kette* double mutant embryos; these organize into a cortical actin cap-like structure (Bothe et al., 2014) or filopodia-like protrusions (Deng et al., 2015).

Our data suggest that a balance between Dia and Arp2/3 activities is crucial for myoblast fusion to proceed. What are the mechanisms that maintain the balance between Dia and Arp2/3? We have found that the activity of Arp2/3 during fusion can be evaluated by examining the localization of Arp2/3 regulatory proteins, such as SCAR and WASp. However, we have not examined the localization of Dia regulatory proteins. Instead, the activity of Dia has been only evaluated by examining Dia localization and actin structure as a readout. In the future, examining the localization and activity of Dia regulators, such as RhoGTPase and Profilin, will provide important information about how Dia is regulated during fusion.

Another question that attracts our attention is what are the actin depolymerization factors that resolve the actin focus after fusion pore formation? Studies in our lab have suggested that actin depolymerization factors, such as Twinstar/Cofilin (Tsr), play a critical role in myoblast fusion. However, due to the requirement for depolymerization activities in earlier embryogenesis events, maternal loading, and redundant depolmerization factors such as Gelsolin, we have found it difficult to recover mutants that specifically block fusion without disrupting embryonic patterning in general. Therefore, investigating muscle-specific isoforms of these actin depolymerization factors, or knocking down a combination of actin

depolymerization factors in muscles may provide the needed insights to how the actin focus is resolved prior to fusion.

These questions proposed above merit further investigation; the knowledge gained would illuminate how the key steps of fusion are controlled.

II. The balance between actin polymerization and depolymerization both determines actin structures and maintains the G-actin pool in muscle cells

The *Drosophila* flight muscles provide a sensitive and simple system to study sarcomere structure (Reedy and Beall, 1993; Vigoreaux, 2001). In my thesis, I used the indirect flight muscles to identify factors that control sarcomere size and to test for genetic interactions between these factors. The formin family of proteins, which both nucleate and polymerize actin filaments, has been shown to regulate sarcomere thin filament size and integrity in different systems: in the *C. elegans* body wall muscles, FHOD-1 and CYK-1 are required to determine and maintain sarcomere size (Mi-Mi and Pruyne, 2015; Mi-Mi et al., 2012). In cardiac muscle cells in culture, 13 formins are expressed and play roles in myofibril development and maintenance (Arimura et al., 2013; Iskratsch et al., 2013; Kan-O et al., 2012; Rosado et al., 2014; Taniguchi et al., 2009; Wooten et al., 2013). In *Drosophila* flight muscles, DAAM plays an important role in thin filament assembly (Molnár et al., 2014). My thesis work expanded our knowledge and identified the formin Dia as another key regulator that controls sarcomere size. In addition, I identified the actin severing protein Flightless I (FliI), a Gelsolin family member, as a functional partner of Dia. Unlike Dia, which localizes at the M-line and elongates actin filaments, FliI localizes at the Z-discs and severs actin filaments. Because of the activity of these two proteins, one would expect to see a rescue of sarcomere size in a knockdown of FliI in a Dia loss of function background. Instead, what we found is even smaller-sized

sarcomeres in this background. A reasonable explanation of this result is that FliI and Dia work together to regulate the homeostasis of the G-actin pool and, hence, sarcomere size.

As described in Chapter 1, the structures that are composed of actin filaments are regulated at different levels: at the signaling level that determines when and where actin remodeling occurs, at the regulatory level that determines actin turnover and dynamics, and at the organizational level that controls the arrangement of actin filaments. My thesis work suggests that, although actin is one of the most abundant proteins in eukaryotic cells, the available pool of monomeric G-actin serves as an important regulatory factor in the building and maintenance of F-actin structures. Moreover, using sarcomere size as an output, we elucidated how the G-actin pool is maintained through Dia and FliI (Chapter 5).

In addition to our work here, a broader discussion of how a limited G-actin pool is maintained and partitioned has been trending in the literature. For example, in fission yeast, Profilin was identified as one of the key factors that control the partitioning of the G-actin pool between Arp2/3 and formins through a competition mechanism (Suarez et al., 2015). Nevertheless, additional questions are raised: how does the muscle cell partition and distribute G-actin into different regions of the cytoplasm? Our data (Chapter 3 and 4) suggest Dia and Arp2/3 might directly compete for actin during fusion. Whether Chickadee/Profilin plays a role in partitioning G-actin between Dia and Arp2/3 remains unknown. In addition, whether muscle cells employ other mechanisms that partition G-actin, such as local synthesis of G-actin or directional transport of G-actin, is still unclear and requires further study.

Another area that attracts our interest focuses on the mechanisms that maintain the G-actin pool in different cell types. We have demonstrated that actin polymerization and depolymerization factors contribute to actin homeostasis in *Drosophila* adult muscles. Interestingly, low levels of G-actin trigger the transcription of actin through transcription factor MAL/SRF and maintain G-actin levels in the border cells in *Drosophila* ovary as well as MDA-MB-231 human breast cancer cells (Salvany et al., 2014). It would be exciting to examine the gene expression profile that responds to G-actin level change through RNA-Seq in the flight muscles.

Resolving these questions will not only help us understand how sarcomere size is determined in muscle, but it will also expand our understanding of how actin structures are regulated and how they ultimately determine cell shape, function, and behavior.

CHAPTER SEVEN:

METHODS AND MATERIALS

Fly stocks:

The following stocks were used: *Oregon R* (control, wild-type), *UAS-diaFH1FH2* (Bloomington #27616), *twist-actin::GFP*, *apME-NLS::dsRed*, *UAS-dia::GFP*, *UAS-DiaΔDAD::GFP*; *UAS-diaFH1FH2::GFP*, *UAS- DiaΔDAD::HA*, *UAS-DiaDDFH1FH2::GFP* (M Peifer), *UAS-SCAR-HA-CYFP*, *UAS-Abi-HA-CYFP*, *UAS-SCAR-Myc-NYFP*, *UAS-Abi-Myc-NYFP*, *UAS-HA-CYFP*, *UAS-Myc-NYFP* (Gohl et al., 2010). *UAS-DiaCA-HA* (Bilancia et al., 2014; Nowotarski et al., 2014). *duf5.1-GAL4* (5.1kb enhancer region of *duf* fused with Gal4, sequence information based on (Guruharsha et al., 2009; Ruiz Gomez et al., 2000), *Dmef2-Gal4*, $blow^{[1]}$, $sns^{[XB3]}$, $mbc^{[c1]}$, $kette^{[J4-48]}$, $loner^{[T1032]}$, $sltr^{[S1946]}$, $Rac1^{[J11]}$,$Rac2^{[\Delta]}$, $Mtl^{[\Delta]}$, $wsp^{[3D3-35]}$. Stocks were balanced over *CyO, dfd-GMR-YFP* or *TM3, dfd-GMR-YFP*, and identified by GFP staining. *UAS-moesin::mCherry*, *DMef2-Gal4*, dia^{5}, dia^{2}. *UAS-DiaDN*::*GFP* (this study), $fhos^{A055}$, $fhos^{EY09842}$, $fhos^{KG05956}$, $daam^{G1567}$, $daam^{MB03627}$, $CG32138^{ET03931}$, $capu^{12344}$, *UAS-capu::GFP*; *UAS-capu-RNAi*, *UAS-dicer;;Dmef2-Gal4*, *MHC-Gal4*, $fliI^{3}$, *UAS-fliI-RNAi*, *UAS-D-fliI::HA, UAS-H-fliI::HA,* $UAS\text{-}PH^{plc\gamma}$*::GFP*. The Gal4-UAS system was used for expression studies (Brand and Perrimon, 1993). Embryos were staged according to (Campos-Ortega and Hartenstein, 1985).

Immunohistochemistry:

Embryos were collected, fixed in 4% PFA, and stained according to standard lab protocol (Richardson et al., 2007). Antibodies were used at the following concentrations: α-Dia (1:500) (S. Wasserman), α-Duf (1:200) (K.-F. Fischbach), α-Sns (1:250) (S. Abmayr), α-WASp (1:500) (E. Schejter), α-SCAR(1:100) (J Zallen) (Zallen et al., 2002), α-GFP (1:500)(Invitrogen A-11120), α-dsRed (1: 500) (Clontech

32392), α-Blow (1:100; E. Chen, Johns Hopkins, USA), α-Loner (1:100; E. Chen), α-Mbc (1:100; S. Abmayr, Stowers Institute, USA), α-Rac1GTP (1:250; Neweast Bioscience 26903), Alexa Fluor 647-phalloidin (1:100) (Invitrogen A22287). For secondary antibodies, Alexa Fluor 488-, Alexa Fluor 555-, and Alexa Fluor 647-conjugated fluorescent secondary antibodies at 1:200 dilution (Invitrogen) were used. Fluorescent images were acquired on a Leica SP5 laser scanning confocal microscope equipped with a 63X 1.4 NA HCX PL Apochromat oil objective and LAS AF 2.2 software. Maximum intensity projections of confocal Z-stacks were rendered using Volocity.

Fusion index quantification:

Nuclei in LT muscles were specifically labeled by expressing DsRed fused to a nuclear localization signal under the control of the *apterous* mesodermal enhancer (apRed) (Metzger et al., 2012; Richardson et al., 2007). The fusion index was quantified by counting the number of dsRed positive nuclei in each hemisegment in stage 17 embryos.

Line scan for measuring fluorescence enrichment at actin foci:

Line scans were done in ImageJ (Schneider et al., 2012). The focal plane was chosen where the cross section area of the F-actin focus was the largest (Richardson et al., 2007). A line was drawn across the F-actin focus, with the center of the line aligned with the F-actin focus center. Grey values were measured along the line. The relative intensity was calculated at each point following the equation: $y_{relative}=(y-y_{min})/(y_{max}-y_{min})$. Ten F-actin foci were measured in the same way. The average relative intensity and standard deviation of mean at each point were calculated from those samples. Signal enrichment in different channels was measured in the same way.

Spermatogenesis

Male adult flies carrying *net-Gal4;nos-Gal4>UAS-diaDN*::*GFP* or *net-Gal4;nos-Gal4>w* (ctrl) (Schulz et al., 2004; Shivdasani and Ingham, 2003) were crossed to w female in a 1:2 ratio. Mated females were allowed to lay eggs for four days in 29°C. The number of larvae were counted, and this number was used to determine the number of larvae produced per male per day. Testis and seminal vesicles were dissected (n = 5), fixed in 4% PFA, and stained with DAPI (Wen et al., 2015). Sperm numbers were quantified using images taken on confocal microscope.

Fluorescence recovery after photobleaching:

Actin::GFP was used to label F-actin foci at the fusion site. FRAP experiments were performed on a Zeiss LSM710, with 40x oil objective. 488nm laser was set at 14%. Pinhole was set at AU 1.0. Region of interest (ROI) were identified and selected manually, two scans were taken before bleaching. 100% 488nm and 458nm lasers were used to quickly bleach ROI to around 30% of the original intensity. After photobleaching, images were acquired every 3s. For data analysis, the size of ROI was fixed for each movie, but the location was adjusted manually for each frame as the F-actin focus shifts over time. Fluorescence intensity was measured in ImageJ and was normalized to background. Half time was determined by $y=y_{min}+(y_{max}-y_{min})(1-e^{-kt})$, and kinetic curves were plotted according to the calculation (Jin et al., 2011).

Molecular cloning:

Dominant negative Dia (DiaDN) was designed according to (Staus et al., 2007). In mDia, the 567-1182 minus 21 amino acid from the 750-770 region is considered a dominant negative mDia. Alignment of mDia1 with *Drosophila* Dia identified the

497-1029 minus 21 amino acid from 599-619 (DiaDN) as a potential dominant negative Dia in *Drosophila*. DiaDN contains the FH1 domain and part of the FH2 domain. We cloned DiaDN into pUAST vector using two pairs of primers: 5'CACCGAATTCATGGGTGTGGCGGCTCCGTC3' and 5'AAAAGATCTGCCATGAGGCAGAACGGG3', 5'CACCGGATCCGTCCCGGCCAAAATGTCC3' and 5'AAAGGATCCCATCACGCCTTCCTGCG 3'. The DiaDN constructs were validated by sequencing and tested in S2 cells and *in vivo* before being sent out for injection.

Drosophila fliI was amplified from cDNA (BDGP DGC clones: LD21753) with primer : forward: 5'CACCATGAGCGTGCTGCCGTT3', reverse:5' TAAATACACCTTGAAGGC3'

Human *FLII* was amplified from cDNA (GE healthcare, BC025300) with primer: forward: 5'CACCATGGAGGCCACCGGGGTG 3', reverse: 5'GGCCAGGGCCTTGCAGAAG3'. Both genes were cloned into pUAST vectors with a C-terminal HA tag and sequenced.

Time-lapse imaging:

Embryos were raised at 25°C, collected, dechorinated and mounted on a Teflon membrane in Halocarbon oil 700 (Halocarbon Products Corp., Series 700, 9002-83-9). Images were acquired every 30 or 60 seconds as indicated, single z=0.5µm 18-20mm total on an upright Leica SP5 laser scanning confocal microscope equipped with a 63X 1.4 NA HCX PL Apochromat oil objective and LAS AF 2.2 software. Maximum intensity projections of confocal Z-stacks were rendered using Volocity Visualization software (Improvision).

Western blot:

DMef2-Gal4>UAS-DiaDN::GFP embryos were incubated at 25°C to stage 16. Embryos were harvested and lysed in cytoplasmic protein lysis buffer (10mM Tris PH 7.5,

2mM EDTA PH 8, 2mM EGTA PH7.5, 150mM NaCl, 1% Triton, 1% NP40, 1mM PMSF, DTT 1mM, 1µg/ml Leupeptin, 1µg/ml Pepstatin). Embryo lysates were separated on a 12.5% SDS-PAGE gel and then transferred to nitrocellulose membrane for Western analysis. DiaDN::GFP was detected by an α-GFP antibody (Torrey Pines TP401).

Cell culture:

S2R+ cells were grown in Schneider's medium. Transfection was done in Grace's medium with Cellfectin II reagent (invitrogen 10362-100). 0.5µg of UAS-DiaDN::GFP and 0.5µg of actin-Gal4 were co-transfected in S2R+ cells. Cells were incubated in 25°C for 24h, and fixed in 4% PFA. Phalloidin was used to label F-actin in S2R+ cells.

Co-Immunoprecipitation:

Drosophila S2 cells were co-transfected with Ubiquitin-Gal4, UAS- Dia::GFP (or UAS-GFP alone) and UAS-3xHA::FliI constructs. Cells were lysed at day 3 in lysis buffer (150mM NaCl, 2mM MgOAc, 20mM Tris, pH 7.5, 5% Glycerol, 0.5% NP40) for 30 minutes. Protein levels in the lysates were quantified. Cell lysates were then incubated with Protein G-Agarose beads overnight at 4°C using rabbit anti-GFP (Torrey Pines #TP401) or anti-rabbit IgG (Santa Cruz # SC-7392) for mock immunoprecipitation controls. The beads were washed four times with lysis buffer and boiled in 4x Laemmli Buffer. GFP-purified samples were then run on SDS-PAGE and blotted with rat anti-HA (Roche # 1867423).

Cloning for lipid strip:

To make GST fusion protein, Mbc-PH(short), Loner-PH, Blow-PH, WASp-PH domains were cloned into pENTR/D-TOPO vector (Invitrogen) and recombined into

pDEST15 vector using LR ClonaseTM II Enzyme Mix Kit (Invitrogen). mbc-PH(long) domain was cloned into pGEX-6p-1 vector (GE Healthcare Life Science). All constructs were sequenced after amplification.

Protein Expression and Purification

GST::PH constructs were transformed into BL21-CodonPlus competent cells (Stratagene). Protein expression was induced by 0.5mM IPTG, and incubated at 37°C for 3h. Cell pellets were collected and treated with lysis B buffer (50mM Tris PH7.5, 1mM EDTA, 1mM EGTA, 5mM MgCl2 1mM DTT, 1mM PMSF, 1ug/ml Leupeptin (Sigma), 1ug/ml Pepstatin (Sigma)) followed by sonication, 10% triton x-100 treatment and centrifuge. Proteins were purified from supernatant with Glutathione Sepharose 4B (Amersham Pharmacia Biotech Inc), and concentrated though centrifugal filter units (Millipore). The concentration of GST::PH protein was determined by protein assay (Bio-Rad protein assay dye reagent) and Western blot.

Lipid Strip

0.5μg/mL purified protein was applied to each strip membrane (echelon biosciences Inc) and incubated for 1h at room temperature. Proteins that bind to lipids were detected by HRP conjugated GST antibody (1:1000 Santa Cruz), and visualized using HyGLO HRP detection kit (Denville Scientific Inc).

Flight assay:

Flies were dropped into a cylinder and each insect's ability to fly was recorded (Banerjee et al., 2004). For each genotype, 25 flies were tested each day for 3 days (n=75). Flies were separated by their ability to fly and dissected for IFM staining.

Flight muscle dissection:

For adult flies: Flies were collected immediately after eclosion and were kept in room temperature. Thoraces from 3-day old adult flies were dissected according to a revised protocol (Hunt and Demontis, 2013; Schnorrer et al., 2010). After anaesthetizing flies with CO_2, we removed the head, abdomen, legs and wings from each thorax with scissors. Thoraces were kept in relaxing buffer before fixation (20mM PBS, pH=7.0, 5mM $MgCl_2$, 5mM EGTA). Thoraces were then pre-fixed in fresh 4% paraformaldehyde (PFA) in relaxing buffer for 10 minutes. After pre-fixation, thoraces were dissected into hemi-thoraces by cutting longitudinally with scissors and transferred into 24 well plates. Samples were washed twice with PBT (PBS+0.3% Triton x-100), and incubated in relaxing buffer for 15 minutes, followed by fixation in 4% PFA for 10 minutes. After fixation, samples were washed in PBT 2 x 10 minutes, and incubated in a primary antibody overnight at 4°C. The second day, thoraces were removed from the primary antibody, and washed in PBT 3 x 20 minutes. After washing, samples were incubated in a secondary antibody for 2 hours at room temperature. After rinsing in PBT 3 x 20 minutes, hemi-thoraces were mounted in prolong gold, and analyzed using a Leica SP5 confocal microscope.

Electron Microscopy:

IFM muscles were each dissected into a half thorax as described above and were fixed in a solution composed of 2% glutaraldehyde, 4% paraformaldehyde, 2mM Cacl2, 0.5% tannic acid in 0.1M sodium cacodylate buffer, pH 7.4. The samples were then fixed for 3 minutes using the Pelco Biowave (Ted Pella), followed by overnight fixation at 4°C. Samples were post-fixed with 1% osmium tetroxide containing 1.5% potassium ferrocyanide in cacodylate buffer for 1 hour on ice. After fixation, samples were stained with 1% uranyl acetate aqueous solution at room temperature for 30 minutes. The samples were then dehydrated in a graded series of ethanol using the Pelco Biowave, followed by acetone dehydration at room

temperature for 10 minutes. After dehydration, each half thorax was infiltrated and embedded with Eponate 12™ (Ted Pella) and sectioned into 60-70nm ultrathin sections. For each genotype, 3 samples were sectioned using a Reichert Jung Ultracut E microtome. After sectioning, samples were stained with 2% Uranyl acetate and Sato's lead stain. Images were taken under a JEOL 100CX Transmission Electron Microscope at 80kV equipped with an XR41-C camera and AmtV600 software (Advanced Microscopy Technology Corp., Woburn, MA).

CHAPTER EIGHT:

BIBLIOGRAPHY

Abmayr, S.M., and Pavlath, G.K. (2012). Myoblast fusion: lessons from flies and mice. Development *139*, 641–656.

Abreu-Blanco, M.T., Verboon, J.M., and Parkhurst, S.M. (2014). Coordination of Rho family GTPase activities to orchestrate cytoskeleton responses during cell wound repair. Curr. Biol. *24*, 144–155.

AC, C. (1978). The Genetics and Biology of Drosophila (London).

Afshar, K., Stuart, B., and Wasserman, S.A. (2000). Functional analysis of the Drosophila diaphanous FH protein in early embryonic development. Development *127*, 1887–1897.

Aguilar, P.S., Baylies, M.K., Fleissner, A., Helming, L., Inoue, N., Podbilewicz, B., Wang, H., and Wong, M. (2013). Genetic basis of cell-cell fusion mechanisms. Trends Genet. *29*, 427–437.

Alberts, A.S. (2001). Identification of a carboxyl-terminal diaphanous-related formin homology protein autoregulatory domain. J. Biol. Chem. *276*, 2824–2830.

Allingham, J.S., Klenchin, V.A., and Rayment, I. (2006). Actin-targeting natural products: structures, properties and mechanisms of action. Cell. Mol. Life Sci. *63*, 2119–2134.

Anant, S., Roy, S., and Vijayraghavan, K. (1998). Twist and Notch negatively regulate adult muscle differentiation in Drosophila. Development *125*, 1361–1369.

Anderson, K.V., Bokla, L., and Nüsslein-Volhard, C. (1985). Establishment of dorsal-ventral polarity in the Drosophila embryo: the induction of polarity by the Toll gene product. Cell *42*, 791–798.

Antunes, M., Pereira, T., Cordeiro, J.V., Almeida, L., and Jacinto, A. (2013). Coordinated waves of actomyosin flow and apical cell constriction immediately after wounding. J. Cell Biol. *202*, 365–379.

Araki, K., Kawauchi, K., Hirata, H., Yamamoto, M., and Taya, Y. (2013). Cytoplasmic translocation of the retinoblastoma protein disrupts sarcomeric organization. Elife *2*, e01228.

Ardern, H., Sandilands, E., Machesky, L.M., Timpson, P., Frame, M.C., and Brunton, V.G. (2006). Src-dependent phosphorylation of Scar1 promotes its association with

the Arp2/3 complex. Cell Motil. Cytoskeleton *63*, 6–13.

Arimura, T., Takeya, R., Ishikawa, T., Yamano, T., Matsuo, A., Tatsumi, T., Nomura, T., Sumimoto, H., and Kimura, A. (2013). Dilated cardiomyopathy-associated FHOD3 variant impairs the ability to induce activation of transcription factor serum response factor. Circ. J. *77*, 2990–2996.

Artero, R.D., Castanon, I., and Baylies, M.K. (2001). The immunoglobulin-like protein Hibris functions as a dose-dependent regulator of myoblast fusion and is differentially controlled by Ras and Notch signaling. Development *128*, 4251–4264.

Artero, R., Furlong, E.E., Beckett, K., Scott, M.P., and Baylies, M. (2003). Notch and Ras signaling pathway effector genes expressed in fusion competent and founder cells during Drosophila myogenesis. Development *130*, 6257–6272.

Azpiazu, N., Lawrence, P.A., Vincent, J.P., and Frasch, M. (1996). Segmentation and specification of the Drosophila mesoderm. Genes Dev. *10*, 3183–3194.

Bach, A.-S., Enjalbert, S., Comunale, F., Bodin, S., Vitale, N., Charrasse, S., and Gauthier-Rouvière, C. (2010). ADP-ribosylation factor 6 regulates mammalian myoblast fusion through phospholipase D1 and phosphatidylinositol 4,5-bisphosphate signaling pathways. Mol. Biol. Cell *21*, 2412–2424.

Bai, J., Hartwig, J.H., and Perrimon, N. (2007). SALS, a WH2-domain-containing protein, promotes sarcomeric actin filament elongation from pointed ends during Drosophila muscle growth. Dev. Cell *13*, 828–842.

Balagopalan, L., Chen, M.-H., Geisbrecht, E.R., and Abmayr, S.M. (2006). The CDM superfamily protein MBC directs myoblast fusion through a mechanism that requires phosphatidylinositol 3,4,5-triphosphate binding but is independent of direct interaction with DCrk. Mol. Cell. Biol. *26*, 9442–9455.

Balakrishnan, S.S., Basu, U., and Raghu, P. (2015). Phosphoinositide signalling in Drosophila. Biochim. Biophys. Acta *1851*, 770–784.

Banerjee, S., Lee, J., Venkatesh, K., Wu, C.-F., and Hasan, G. (2004). Loss of flight and associated neuronal rhythmicity in inositol 1,4,5-trisphosphate receptor mutants of Drosophila. J. Neurosci. *24*, 7869–7878.

Barrett, K., Leptin, M., and Settleman, J. (1997). The Rho GTPase and a putative RhoGEF mediate a signaling pathway for the cell shape changes in Drosophila gastrulation. Cell *91*, 905–915.

Bartolini, F., and Gundersen, G.G. (2010). Formins and microtubules. Biochim. Biophys. Acta *1803*, 164–173.

Bate, M. (1990). The embryonic development of larval muscles in Drosophila.

Development *110*, 791–804.

Baylies, M.K., Bate, M., and Ruiz Gomez, M. (1998). Myogenesis: a view from Drosophila. Cell *93*, 921–927.

Bear, J.E., Svitkina, T.M., Krause, M., Schafer, D.A., Loureiro, J.J., Strasser, G.A., Maly, I.V., Chaga, O.Y., Cooper, J.A., Borisy, G.G., et al. (2002). Antagonism between Ena/VASP proteins and actin filament capping regulates fibroblast motility. Cell *109*, 509–521.

Beckett, K., and Baylies, M.K. (2006). The development of the Drosophila larval body wall muscles. Int. Rev. Neurobiol. *75*, 55–70.

Beli, P., Mascheroni, D., Xu, D., and Innocenti, M. (2008). WAVE and Arp2/3 jointly inhibit filopodium formation by entering into a complex with mDia2. Nat. Cell Biol. *10*, 849–857.

Beltzner, C.C., and Pollard, T.D. (2004). Identification of functionally important residues of Arp2/3 complex by analysis of homology models from diverse species. J. Mol. Biol. *336*, 551–565.

Belvin, M.P., Jin, Y., and Anderson, K.V. (1995). Cactus protein degradation mediates Drosophila dorsal-ventral signaling. Genes Dev. *9*, 783–793.

Berger, S., Schäfer, G., Kesper, D.A., Holz, A., Eriksson, T., Palmer, R.H., Beck, L., Klämbt, C., Renkawitz-Pohl, R., and Onel, S.-F. (2008). WASP and SCAR have distinct roles in activating the Arp2/3 complex during myoblast fusion. J. Cell. Sci. *121*, 1303–1313.

Bergmann, A., Stein, D., Geisler, R., Hagenmaier, S., Schmid, B., Fernandez, N., Schnell, B., and Nüsslein-Volhard, C. (1996). A gradient of cytoplasmic Cactus degradation establishes the nuclear localization gradient of the dorsal morphogen in Drosophila. Mech. Dev. *60*, 109–123.

Bi, W., Saifi, G.M., Shaw, C.J., Walz, K., Fonseca, P., Wilson, M., Potocki, L., and Lupski, J.R. (2004). Mutations of RAI1, a PHD-containing protein, in nondeletion patients with Smith-Magenis syndrome. Hum. Genet. *115*, 515–524.

Bilancia, C.G., Winkelman, J.D., Tsygankov, D., Nowotarski, S.H., Sees, J.A., Comber, K., Evans, I., Lakhani, V., Wood, W., Elston, T.C., et al. (2014). Enabled negatively regulates diaphanous-driven actin dynamics in vitro and in vivo. Dev. Cell *28*, 394–408.

Bione, S., Sala, C., Manzini, C., Arrigo, G., Zuffardi, O., Banfi, S., Borsani, G., Jonveaux, P., Philippe, C., Zuccotti, M., et al. (1998). A human homologue of the Drosophila melanogaster diaphanous gene is disrupted in a patient with premature ovarian failure: evidence for conserved function in oogenesis and implications for human

sterility. Am. J. Hum. Genet. *62*, 533–541.

Blanchard, A., Ohanian, V., and Critchley, D. (1989). The structure and function of alpha-actinin. J. Muscle Res. Cell. Motil. *10*, 280–289.

Blanchoin, L., Amann, K.J., Higgs, H.N., Marchand, J.B., Kaiser, D.A., and Pollard, T.D. (2000). Direct observation of dendritic actin filament networks nucleated by Arp2/3 complex and WASP/Scar proteins. Nature *404*, 1007–1011.

Blanchoin, L., Boujemaa-Paterski, R., Sykes, C., and Plastino, J. (2014). Actin dynamics, architecture, and mechanics in cell motility. Physiol. Rev. *94*, 235–263.

Bodmer, R. (1993). The gene tinman is required for specification of the heart and visceral muscles in Drosophila. Development *118*, 719–729.

Bogdan, S., Schultz, J., and Grosshans, J. (2013). Formin' cellular structures: Physiological roles of Diaphanous (Dia) in actin dynamics. Commun Integr Biol *6*, e27634.

Botelho, R.J., Teruel, M., Dierckman, R., Anderson, R., Wells, A., York, J.D., Meyer, T., and Grinstein, S. (2000). Localized biphasic changes in phosphatidylinositol-4,5-bisphosphate at sites of phagocytosis. J. Cell Biol. *151*, 1353–1368.

Bothe, I., Deng, S., and Baylies, M. (2014). PI(4,5)P2 regulates myoblast fusion through Arp2/3 regulator localization at the fusion site. Development *141*, 2289–2301.

Boudriau, S., Vincent, M., Côté, C.H., and Rogers, P.A. (1993). Cytoskeletal structure of skeletal muscle: identification of an intricate exosarcomeric microtubule lattice in slow- and fast-twitch muscle fibers. J. Histochem. Cytochem. *41*, 1013–1021.

Bour, B.A., Chakravarti, M., West, J.M., and Abmayr, S.M. (2000). Drosophila SNS, a member of the immunoglobulin superfamily that is essential for myoblast fusion. Genes Dev. *14*, 1498–1511.

Brand, A.H., and Perrimon, N. (1993). Targeted gene expression as a means of altering cell fates and generating dominant phenotypes. Development *118*, 401–415.

Bulchand, S., Menon, S.D., George, S.E., and Chia, W. (2010). The intracellular domain of Dumbfounded affects myoblast fusion efficiency and interacts with Rolling pebbles and Loner. PLoS ONE *5*, e9374.

Bullard, B., and Pastore, A. (2011). Regulating the contraction of insect flight muscle. J. Muscle Res. Cell. Motil. *32*, 303–313.

Bullard, B., Burkart, C., Labeit, S., and Leonard, K. (2005). The function of elastic proteins in the oscillatory contraction of insect flight muscle. J. Muscle Res. Cell.

Motil. *26*, 479–485.

Burkart, C., Qiu, F., Brendel, S., Benes, V., Hååg, P., Labeit, S., Leonard, K., and Bullard, B. (2007). Modular proteins from the Drosophila sallimus (sls) gene and their expression in muscles with different extensibility. J. Mol. Biol. *367*, 953–969.

Burtnick, L.D., Koepf, E.K., Grimes, J., Jones, E.Y., Stuart, D.I., McLaughlin, P.J., and Robinson, R.C. (1997). The crystal structure of plasma gelsolin: implications for actin severing, capping, and nucleation. Cell *90*, 661–670.

Cadigan, K.M., Grossniklaus, U., and Gehring, W.J. (1994). Localized expression of sloppy paired protein maintains the polarity of Drosophila parasegments. Genes Dev. *8*, 899–913.

Caine, C., Kasherov, P., Silber, J., and Lalouette, A. (2014). Mef2 interacts with the Notch pathway during adult muscle development in Drosophila melanogaster. PLoS ONE *9*, e108149.

Campellone, K.G., and Welch, M.D. (2010). A nucleator arms race: cellular control of actin assembly. Nat. Rev. Mol. Cell Biol. *11*, 237–251.

Campos-Ortega, J.A., and Hartenstein, V. (1985). The Embryonic development of Drosophila melanogaster (Berlin: Springer).

Carlier, M.F., Laurent, V., Santolini, J., Melki, R., Didry, D., Xia, G.X., Hong, Y., Chua, N.H., and Pantaloni, D. (1997). Actin depolymerizing factor (ADF/cofilin) enhances the rate of filament turnover: implication in actin-based motility. J. Cell Biol. *136*, 1307–1322.

Carmena, A., Bate, M., and Jiménez, F. (1995). Lethal of scute, a proneural gene, participates in the specification of muscle progenitors during Drosophila embryogenesis. Genes Dev. *9*, 2373–2383.

Carmena, A., Gisselbrecht, S., Harrison, J., Jiménez, F., and Michelson, A.M. (1998a). Combinatorial signaling codes for the progressive determination of cell fates in the Drosophila embryonic mesoderm. Genes Dev. *12*, 3910–3922.

Carmena, A., Murugasu-Oei, B., Menon, D., Jiménez, F., and Chia, W. (1998b). Inscuteable and numb mediate asymmetric muscle progenitor cell divisions during Drosophila myogenesis. Genes Dev. *12*, 304–315.

Castrillon, D.H., and Wasserman, S.A. (1994). Diaphanous is required for cytokinesis in Drosophila and shares domains of similarity with the products of the limb deformity gene. Development *120*, 3367–3377.

Castrillon, D.H., Gönczy, P., Alexander, S., Rawson, R., Eberhart, C.G., Viswanathan, S., DiNardo, S., and Wasserman, S.A. (1993). Toward a molecular genetic analysis of

spermatogenesis in Drosophila melanogaster: characterization of male-sterile mutants generated by single P element mutagenesis. Genetics *135*, 489–505.

Chargé, S.B.P., and Rudnicki, M.A. (2004). Cellular and molecular regulation of muscle regeneration. Physiol. Rev. *84*, 209–238.

Chasan, R., Jin, Y., and Anderson, K.V. (1992). Activation of the easter zymogen is regulated by five other genes to define dorsal-ventral polarity in the Drosophila embryo. Development *115*, 607–616.

Chen, E.H., and Olson, E.N. (2001). Antisocial, an intracellular adaptor protein, is required for myoblast fusion in Drosophila. Dev. Cell *1*, 705–715.

Chen, E.H. (2011). Invasive podosomes and myoblast fusion. Curr Top Membr *68*, 235–258.

Chen, E.H., Pryce, B.A., Tzeng, J.A., Gonzalez, G.A., and Olson, E.N. (2003). Control of myoblast fusion by a guanine nucleotide exchange factor, loner, and its effector ARF6. Cell *114*, 751–762.

Chen, H., Bernstein, B.W., and Bamburg, J.R. (2000). Regulating actin-filament dynamics in vivo. Trends Biochem. Sci. *25*, 19–23.

Chen, Z., Borek, D., Padrick, S.B., Gomez, T.S., Metlagel, Z., Ismail, A.M., Umetani, J., Billadeau, D.D., Otwinowski, Z., and Rosen, M.K. (2010). Structure and control of the actin regulatory WAVE complex. Nature *468*, 533–538.

Chesarone, M.A., DuPage, A.G., and Goode, B.L. (2010). Unleashing formins to remodel the actin and microtubule cytoskeletons. Nat. Rev. Mol. Cell Biol. *11*, 62–74.

Ciglar, L., Girardot, C., Wilczyński, B., Braun, M., and Furlong, E.E.M. (2014). Coordinated repression and activation of two transcriptional programs stabilizes cell fate during myogenesis. Development *141*, 2633–2643.

Clark, K.A., McElhinny, A.S., Beckerle, M.C., and Gregorio, C.C. (2002). Striated muscle cytoarchitecture: an intricate web of form and function. Annu. Rev. Cell Dev. Biol. *18*, 637–706.

Clarkson, E., Costa, C.F., and Machesky, L.M. (2004). Congenital myopathies: diseases of the actin cytoskeleton. J. Pathol. *204*, 407–417.

Cleveland, D.W. (1982). Treadmilling of tubulin and actin. Cell *28*, 689–691.

Co, C., Wong, D.T., Gierke, S., Chang, V., and Taunton, J. (2007). Mechanism of actin network attachment to moving membranes: barbed end capture by N-WASP WH2 domains. Cell *128*, 901–913.

Contompasis, J.L., Nyland, L.R., Maughan, D.W., and Vigoreaux, J.O. (2010). Flightin is

necessary for length determination, structural integrity, and large bending stiffness of insect flight muscle thick filaments. J. Mol. Biol. *395*, 340–348.

Copeland, J.W., Copeland, S.J., and Treisman, R. (2004). Homo-oligomerization is essential for F-actin assembly by the formin family FH2 domain. J. Biol. Chem. *279*, 50250–50256.

Cory, G.O.C., Cramer, R., Blanchoin, L., and Ridley, A.J. (2003). Phosphorylation of the WASP-VCA domain increases its affinity for the Arp2/3 complex and enhances actin polymerization by WASP. Mol. Cell *11*, 1229–1239.

Costa, M., Wilson, E.T., and Wieschaus, E. (1994). A putative cell signal encoded by the folded gastrulation gene coordinates cell shape changes during Drosophila gastrulation. Cell *76*, 1075–1089.

Côté, J.-F., Motoyama, A.B., Bush, J.A., and Vuori, K. (2005). A novel and evolutionarily conserved PtdIns(3,4,5)P3-binding domain is necessary for DOCK180 signalling. Nat. Cell Biol. *7*, 797–807.

Czech, M.P. (2000). PIP2 and PIP3: complex roles at the cell surface. Cell *100*, 603–606.

Daou, P., Hasan, S., Breitsprecher, D., Baudelet, E., Camoin, L., Audebert, S., Goode, B.L., and Badache, A. (2014). Essential and nonredundant roles for Diaphanous formins in cortical microtubule capture and directed cell migration. Mol. Biol. Cell *25*, 658–668.

Davidson, A.J., Ura, S., Thomason, P.A., Kalna, G., and Insall, R.H. (2013). Abi is required for modulation and stability but not localization or activation of the SCAR/WAVE complex. Eukaryotic Cell *12*, 1509–1516.

Dayel, M.J., and Mullins, R.D. (2004). Activation of Arp2/3 complex: addition of the first subunit of the new filament by a WASP protein triggers rapid ATP hydrolysis on Arp2. PLoS Biol. *2*, E91.

de Joussineau, C., Bataillé, L., Jagla, T., and Jagla, K. (2012). Diversification of muscle types in Drosophila: upstream and downstream of identity genes. Curr. Top. Dev. Biol. *98*, 277–301.

Deng, S., Bothe, I., and Baylies, M.K. (2015). The Formin Diaphanous Regulates Myoblast Fusion through Actin Polymerization and Arp2/3 Regulation. PLoS Genet. *11*, e1005381.

DeRosier, D.J., and Edds, K.T. (1980). Evidence for fascin cross-links between the actin filaments in coelomocyte filopodia. Exp. Cell Res. *126*, 490–494.

Dhanyasi, N., Segal, D., Shimoni, E., Shinder, V., Shilo, B.-Z., Vijayraghavan, K., and

Schejter, E.D. (2015). Surface apposition and multiple cell contacts promote myoblast fusion in Drosophila flight muscles. J. Cell Biol. *211*, 191–203.

Dickinson, M.H. (2005). The initiation and control of rapid flight maneuvers in fruit flies. Integr. Comp. Biol. *45*, 274–281.

Doberstein, S.K., Fetter, R.D., Mehta, A.Y., and Goodman, C.S. (1997). Genetic analysis of myoblast fusion: blown fuse is required for progression beyond the prefusion complex. J. Cell Biol. *136*, 1249–1261.

Dobi, K.C., Metzger, T., and Baylies, M.K. (2011). Characterization of early steps in muscle morphogenesis in a Drosophila primary culture system. Fly (Austin) *5*, 68–75.

Dobi, K.C., Schulman, V.K., and Baylies, M.K. (2015). Specification of the somatic musculature in Drosophila. Wiley Interdiscip Rev Dev Biol *4*, 357–375.

Dodou, E., Xu, S.-M., and Black, B.L. (2003). mef2c is activated directly by myogenic basic helix-loop-helix proteins during skeletal muscle development in vivo. Mech. Dev. *120*, 1021–1032.

Dohrmann, C., Azpiazu, N., and Frasch, M. (1990). A new Drosophila homeo box gene is expressed in mesodermal precursor cells of distinct muscles during embryogenesis. Genes Dev. *4*, 2098–2111.

Duan, H., Skeath, J.B., and Nguyen, H.T. (2001). Drosophila Lame duck, a novel member of the Gli superfamily, acts as a key regulator of myogenesis by controlling fusion-competent myoblast development. Development *128*, 4489–4500.

Duan, R., and Gallagher, P.J. (2009). Dependence of myoblast fusion on a cortical actin wall and nonmuscle myosin IIA. Dev. Biol. *325*, 374–385.

Duprez, D., Fournier-Thibault, C., and Le Douarin, N. (1998). Sonic Hedgehog induces proliferation of committed skeletal muscle cells in the chick limb. Development *125*, 495–505.

Dutta, D., Anant, S., Ruiz-Gomez, M., Bate, M., and Vijayraghavan, K. (2004). Founder myoblasts and fibre number during adult myogenesis in Drosophila. Development *131*, 3761–3772.

Dyer, N., Rebollo, E., Domínguez, P., Elkhatib, N., Chavrier, P., Daviet, L., González, C., and González-Gaitán, M. (2007). Spermatocyte cytokinesis requires rapid membrane addition mediated by ARF6 on central spindle recycling endosomes. Development *134*, 4437–4447.

Echarri, A., Lai, M.J., Robinson, M.R., and Pendergast, A.M. (2004). Abl interactor 1 (Abi-1) wave-binding and SNARE domains regulate its nucleocytoplasmic shuttling,

lamellipodium localization, and wave-1 levels. Mol. Cell. Biol. *24*, 4979–4993.

Eden, S., Rohatgi, R., Podtelejnikov, A.V., Mann, M., and Kirschner, M.W. (2002). Mechanism of regulation of WAVE1-induced actin nucleation by Rac1 and Nck. Nature *418*, 790–793.

Egile, C., Rouiller, I., Xu, X.-P., Volkmann, N., Li, R., and Hanein, D. (2005). Mechanism of filament nucleation and branch stability revealed by the structure of the Arp2/3 complex at actin branch junctions. PLoS Biol. *3*, e383.

Elhanany-Tamir, H., Yu, Y.V., Shnayder, M., Jain, A., Welte, M., and Volk, T. (2012). Organelle positioning in muscles requires cooperation between two KASH proteins and microtubules. J. Cell Biol. *198*, 833–846.

Emmons, S., Phan, H., Calley, J., Chen, W., James, B., and Manseau, L. (1995). Cappuccino, a Drosophila maternal effect gene required for polarity of the egg and embryo, is related to the vertebrate limb deformity locus. Genes Dev. *9*, 2482–2494.

Evangelista, M., Blundell, K., Longtine, M.S., Chow, C.J., Adames, N., Pringle, J.R., Peter, M., and Boone, C. (1997). Bni1p, a yeast formin linking cdc42p and the actin cytoskeleton during polarized morphogenesis. Science *276*, 118–122.

Evangelista, M., Pruyne, D., Amberg, D.C., Boone, C., and Bretscher, A. (2002). Formins direct Arp2/3-independent actin filament assembly to polarize cell growth in yeast. Nat. Cell Biol. *4*, 260–269.

Fan, C.M., Lee, C.S., and Tessier-Lavigne, M. (1997). A role for WNT proteins in induction of dermomyotome. Dev. Biol. *191*, 160–165.

Fernandes, I., and Schöck, F. (2014). The nebulin repeat protein Lasp regulates I-band architecture and filament spacing in myofibrils. J. Cell Biol. *206*, 559–572.

Fernandes, J., Bate, M., and Vijayraghavan, K. (1991). Development of the indirect flight muscles of Drosophila. Development *113*, 67–77.

Ferrell, J.E., and Huestis, W.H. (1984). Phosphoinositide metabolism and the morphology of human erythrocytes. J. Cell Biol. *98*, 1992–1998.

Folker, E.S., and Baylies, M.K. (2013). Nuclear positioning in muscle development and disease. Front Physiol *4*, 363.

Folker, E.S., Schulman, V.K., and Baylies, M.K. (2012). Muscle length and myonuclear position are independently regulated by distinct Dynein pathways. Development *139*, 3827–3837.

Folker, E.S., Schulman, V.K., and Baylies, M.K. (2014). Translocating myonuclei have distinct leading and lagging edges that require kinesin and dynein. Development

141, 355–366.

Frasch, M. (1995). Induction of visceral and cardiac mesoderm by ectodermal Dpp in the early Drosophila embryo. Nature *374*, 464–467.

Frasch, M. (1999). Controls in patterning and diversification of somatic muscles during Drosophila embryogenesis. Curr. Opin. Genet. Dev. *9*, 522–529.

Fuerstenberg, S., and Giniger, E. (1998). Multiple roles for notch in Drosophila myogenesis. Dev. Biol. *201*, 66–77.

Fukumi-Tominaga, T., Mori, Y., Matsuura, A., Kaneko, K., Matsui, M., Ogata, M., and Tominaga, M. (2009). DIP/WISH-deficient mice reveal Dia- and N-WASP-interacting protein as a regulator of cytoskeletal dynamics in embryonic fibroblasts. Genes Cells *14*, 1197–1207.

Galletta, B.J., Chakravarti, M., Banerjee, R., and Abmayr, S.M. (2004). SNS: Adhesive properties, localization requirements and ectodomain dependence in S2 cells and embryonic myoblasts. Mech. Dev. *121*, 1455–1468.

Gasteier, J.E., Schroeder, S., Muranyi, W., Madrid, R., Benichou, S., and Fackler, O.T. (2005). FHOD1 coordinates actin filament and microtubule alignment to mediate cell elongation. Exp. Cell Res. *306*, 192–202.

Geeves, M.A., and Holmes, K.C. (1999). Structural mechanism of muscle contraction. Annu. Rev. Biochem. *68*, 687–728.

Geisbrecht, E.R., and Montell, D.J. (2004). A role for Drosophila IAP1-mediated caspase inhibition in Rac-dependent cell migration. Cell *118*, 111–125.

Geisbrecht, E.R., Haralalka, S., Swanson, S.K., Florens, L., Washburn, M.P., and Abmayr, S.M. (2008). Drosophila ELMO/CED-12 interacts with Myoblast city to direct myoblast fusion and ommatidial organization. Dev. Biol. *314*, 137–149.

Gildor, B., Massarwa, R., Shilo, B.-Z., and Schejter, E.D. (2009). The SCAR and WASp nucleation-promoting factors act sequentially to mediate Drosophila myoblast fusion. EMBO Rep. *10*, 1043–1050.

Gildor, B., Schejter, E.D., and Shilo, B.-Z. (2012). Bidirectional Notch activation represses fusion competence in swarming adult Drosophila myoblasts. Development *139*, 4040–4050.

Gilsohn, E., and Volk, T. (2010). Slowdown promotes muscle integrity by modulating integrin-mediated adhesion at the myotendinous junction. Development *137*, 785–794.

Gohl, C., Banovic, D., Grevelhörster, A., and Bogdan, S. (2010). WAVE forms hetero-

and homo-oligomeric complexes at integrin junctions in Drosophila visualized by bimolecular fluorescence complementation. J. Biol. Chem. *285*, 40171–40179.

Goley, E.D., and Welch, M.D. (2006). The ARP2/3 complex: an actin nucleator comes of age. Nat. Rev. Mol. Cell Biol. *7*, 713–726.

Goley, E.D., Rodenbusch, S.E., Martin, A.C., and Welch, M.D. (2004). Critical conformational changes in the Arp2/3 complex are induced by nucleotide and nucleation promoting factor. Mol. Cell *16*, 269–279.

Goode, B.L., and Eck, M.J. (2007). Mechanism and function of formins in the control of actin assembly. Annu. Rev. Biochem. *76*, 593–627.

Gremm, D., and Wegner, A. (1999). Co-operative binding of Ca2+ ions to the regulatory binding sites of gelsolin. Eur. J. Biochem. *262*, 330–334.

Grosshans, J., Wenzl, C., Herz, H.-M., Bartoszewski, S., Schnorrer, F., Vogt, N., Schwarz, H., and Müller, H.-A. (2005). RhoGEF2 and the formin Dia control the formation of the furrow canal by directed actin assembly during Drosophila cellularisation. Development *132*, 1009–1020.

Grossniklaus, U., Pearson, R.K., and Gehring, W.J. (1992). The Drosophila sloppy paired locus encodes two proteins involved in segmentation that show homology to mammalian transcription factors. Genes Dev. *6*, 1030–1051.

Grounds, M.D., and Yablonka-Reuveni, Z. (1993). Molecular and cell biology of skeletal muscle regeneration. Mol. Cell Biol. Hum. Dis. Ser. *3*, 210–256.

Gruenbaum-Cohen, Y., Harel, I., Umansky, K.-B., Tzahor, E., Snapper, S.B., Shilo, B.-Z., and Schejter, E.D. (2012). The actin regulator N-WASp is required for muscle-cell fusion in mice. Proc. Natl. Acad. Sci. U.S.a. *109*, 11211–11216.

Guruharsha, K.G., Ruiz-Gomez, M., Ranganath, H.A., Siddharthan, R., and Vijayraghavan, K. (2009). The complex spatio-temporal regulation of the Drosophila myoblast attractant gene duf/kirre. PLoS ONE *4*, e6960.

Hager, M.H., Morley, S., Bielenberg, D.R., Gao, S., Morello, M., Holcomb, I.N., Liu, W., Mouneimne, G., Demichelis, F., Kim, J., et al. (2012). DIAPH3 governs the cellular transition to the amoeboid tumour phenotype. EMBO Mol Med *4*, 743–760.

Haralalka, S., Shelton, C., Cartwright, H.N., Katzfey, E., Janzen, E., and Abmayr, S.M. (2011). Asymmetric Mbc, active Rac1 and F-actin foci in the fusion-competent myoblasts during myoblast fusion in Drosophila. Development *138*, 1551–1562.

Harris, A.J., Duxson, M.J., Fitzsimons, R.B., and Rieger, F. (1989). Myonuclear birthdates distinguish the origins of primary and secondary myotubes in embryonic mammalian skeletal muscles. Development *107*, 771–784.

Hartenstein, V. (1993). Atlas of Drosophila Development.

Hashimoto, C., Gerttula, S., and Anderson, K.V. (1991). Plasma membrane localization of the Toll protein in the syncytial Drosophila embryo: importance of transmembrane signaling for dorsal-ventral pattern formation. Development *111*, 1021–1028.

Hasty, P., Bradley, A., Morris, J.H., Edmondson, D.G., Venuti, J.M., Olson, E.N., and Klein, W.H. (1993). Muscle deficiency and neonatal death in mice with a targeted mutation in the myogenin gene. Nature *364*, 501–506.

Hawkins, M., Pope, B., Maciver, S.K., and Weeds, A.G. (1993). Human actin depolymerizing factor mediates a pH-sensitive destruction of actin filaments. Biochemistry *32*, 9985–9993.

Heiss, S.G., and Cooper, J.A. (1991). Regulation of CapZ, an actin capping protein of chicken muscle, by anionic phospholipids. Biochemistry *30*, 8753–8758.

Higgs, H.N., and Pollard, T.D. (2000). Activation by Cdc42 and PIP(2) of Wiskott-Aldrich syndrome protein (WASp) stimulates actin nucleation by Arp2/3 complex. J. Cell Biol. *150*, 1311–1320.

Higgs, H.N., Blanchoin, L., and Pollard, T.D. (1999). Influence of the C terminus of Wiskott-Aldrich syndrome protein (WASp) and the Arp2/3 complex on actin polymerization. Biochemistry *38*, 15212–15222.

Higgs, H.N. (2005). Formin proteins: a domain-based approach. Trends Biochem. Sci. *30*, 342–353.

Higgs, H.N., and Peterson, K.J. (2005). Phylogenetic analysis of the formin homology 2 domain. Mol. Biol. Cell *16*, 1–13.

Hollnagel, A., Grund, C., Franke, W.W., and Arnold, H.-H. (2002). The cell adhesion molecule M-cadherin is not essential for muscle development and regeneration. Mol. Cell. Biol. *22*, 4760–4770.

Homem, C.C.F., and Peifer, M. (2008). Diaphanous regulates myosin and adherens junctions to control cell contractility and protrusive behavior during morphogenesis. Development *135*, 1005–1018.

Homem, C.C.F., and Peifer, M. (2009). Exploring the roles of diaphanous and enabled activity in shaping the balance between filopodia and lamellipodia. Mol. Biol. Cell *20*, 5138–5155.

Honda, A., Nogami, M., Yokozeki, T., Yamazaki, M., Nakamura, H., Watanabe, H., Kawamoto, K., Nakayama, K., Morris, A.J., Frohman, M.A., et al. (1999). Phosphatidylinositol 4-phosphate 5-kinase alpha is a downstream effector of the

small G protein ARF6 in membrane ruffle formation. Cell *99*, 521–532.

Horsley, V., and Pavlath, G.K. (2004). Forming a multinucleated cell: molecules that regulate myoblast fusion. Cells Tissues Organs (Print) *176*, 67–78.

Horsley, V., Jansen, K.M., Mills, S.T., and Pavlath, G.K. (2003). IL-4 acts as a myoblast recruitment factor during mammalian muscle growth. Cell *113*, 483–494.

Hunt, L.C., and Demontis, F. (2013). Whole-mount immunostaining of Drosophila skeletal muscle. Nat Protoc *8*, 2496–2501.

Hwang, P.M., and Sykes, B.D. (2015). Targeting the sarcomere to correct muscle function. Nat Rev Drug Discov *14*, 313–328.

Ip, Y.T., Park, R.E., Kosman, D., Bier, E., and Levine, M. (1992). The dorsal gradient morphogen regulates stripes of rhomboid expression in the presumptive neuroectoderm of the Drosophila embryo. Genes Dev. *6*, 1728–1739.

Iskratsch, T., Reijntjes, S., Dwyer, J., Toselli, P., Dégano, I.R., Dominguez, I., and Ehler, E. (2013). Two distinct phosphorylation events govern the function of muscle FHOD3. Cell. Mol. Life Sci. *70*, 893–908.

Ismail, A.M., Padrick, S.B., Chen, B., Umetani, J., and Rosen, M.K. (2009). The WAVE regulatory complex is inhibited. Nat. Struct. Mol. Biol. *16*, 561–563.

Janmey, P.A., and Stossel, T.P. (1987). Modulation of gelsolin function by phosphatidylinositol 4,5-bisphosphate. Nature *325*, 362–364.

Jaynes, J.B., and Fujioka, M. (2004). Drawing lines in the sand: even skipped et al. and parasegment boundaries. Dev. Biol. *269*, 609–622.

Jin, P., Duan, R., Luo, F., Zhang, G., Hong, S.N., and Chen, E.H. (2011). Competition between Blown fuse and WASP for WIP binding regulates the dynamics of WASP-dependent actin polymerization in vivo. Dev. Cell *20*, 623–638.

Kaipa, B.R., Shao, H., Schäfer, G., Trinkewitz, T., Groth, V., Liu, J., Beck, L., Bogdan, S., Abmayr, S.M., and Onel, S.-F. (2013). Dock mediates Scar- and WASp-dependent actin polymerization through interaction with cell adhesion molecules in founder cells and fusion-competent myoblasts. J. Cell. Sci. *126*, 360–372.

Kan-O, M., Takeya, R., Abe, T., Kitajima, N., Nishida, M., Tominaga, R., Kurose, H., and Sumimoto, H. (2012). Mammalian formin Fhod3 plays an essential role in cardiogenesis by organizing myofibrillogenesis. Biol Open *1*, 889–896.

Kano, Y., Fujimaki, N., and Ishikawa, H. (1991). The distribution and arrangement of microtubules in mammalian skeletal muscle fibers. Cell Struct. Funct. *16*, 251–261.

Kassar-Duchossoy, L., Gayraud-Morel, B., Gomès, D., Rocancourt, D., Buckingham, M.,

Shinin, V., and Tajbakhsh, S. (2004). Mrf4 determines skeletal muscle identity in Myf5:Myod double-mutant mice. Nature *431*, 466–471.

Kesper, D.A., Stute, C., Buttgereit, D., Kreisköther, N., Vishnu, S., Fischbach, K.-F., and Renkawitz-Pohl, R. (2007). Myoblast fusion in Drosophila melanogaster is mediated through a fusion-restricted myogenic-adhesive structure (FuRMAS). Dev. Dyn. *236*, 404–415.

Kim, A.S., Kakalis, L.T., Abdul-Manan, N., Liu, G.A., and Rosen, M.K. (2000). Autoinhibition and activation mechanisms of the Wiskott-Aldrich syndrome protein. Nature *404*, 151–158.

Kim, J.H., Jin, P., Duan, R., and Chen, E.H. (2015). Mechanisms of myoblast fusion during muscle development. Curr. Opin. Genet. Dev. *32*, 162–170.

Kim, S., Shilagardi, K., Zhang, S., Hong, S.N., Sens, K.L., Bo, J., Gonzalez, G.A., and Chen, E.H. (2007). A critical function for the actin cytoskeleton in targeted exocytosis of prefusion vesicles during myoblast fusion. Dev. Cell *12*, 571–586.

Kocherlakota, K.S., Wu, J.-M., McDermott, J., and Abmayr, S.M. (2008). Analysis of the cell adhesion molecule sticks-and-stones reveals multiple redundant functional domains, protein-interaction motifs and phosphorylated tyrosines that direct myoblast fusion in Drosophila melanogaster. Genetics *178*, 1371–1383.

Kohno, H., Tanaka, K., Mino, A., Umikawa, M., Imamura, H., Fujiwara, T., Fujita, Y., Hotta, K., Qadota, H., Watanabe, T., et al. (1996). Bni1p implicated in cytoskeletal control is a putative target of Rho1p small GTP binding protein in Saccharomyces cerevisiae. Embo J. *15*, 6060–6068.

Kollias, H.D., and McDermott, J.C. (2008). Transforming growth factor-beta and myostatin signaling in skeletal muscle. J. Appl. Physiol. *104*, 579–587.

Kontrogianni-Konstantopoulos, A., and Bloch, R.J. (2005). Obscurin: a multitasking muscle giant. J. Muscle Res. Cell. Motil. *26*, 419–426.

Kosman, D., Ip, Y.T., Levine, M., and Arora, K. (1991). Establishment of the mesoderm-neuroectoderm boundary in the Drosophila embryo. Science *254*, 118–122.

Kramer, S.G., Kidd, T., Simpson, J.H., and Goodman, C.S. (2001). Switching repulsion to attraction: changing responses to slit during transition in mesoderm migration. Science *292*, 737–740.

Krause, M., and Gautreau, A. (2014). Steering cell migration: lamellipodium dynamics and the regulation of directional persistence. Nat. Rev. Mol. Cell Biol. *15*, 577–590.

Kremneva, E., Makkonen, M.H., Skwarek-Maruszewska, A., Gateva, G., Michelot, A., Dominguez, R., and Lappalainen, P. (2014). Cofilin-2 controls actin filament length in muscle sarcomeres. Dev. Cell *31*, 215–226.

Kucherenko, M.M., Marrone, A.K., Rishko, V.M., Magliarelli, H. de F., and Shcherbata, H.R. (2011). Stress and muscular dystrophy: a genetic screen for dystroglycan and dystrophin interactors in Drosophila identifies cellular stress response components. Dev. Biol. *352*, 228–242.

Kunda, P., Craig, G., Dominguez, V., and Baum, B. (2003). Abi, Sra1, and Kette control the stability and localization of SCAR/WAVE to regulate the formation of actin-based protrusions. Curr. Biol. *13*, 1867–1875.

Lamb, J.A., Allen, P.G., Tuan, B.Y., and Janmey, P.A. (1993). Modulation of gelsolin function. Activation at low pH overrides Ca2+ requirement. J. Biol. Chem. *268*, 8999–9004.

Laurin, M., Fradet, N., Blangy, A., Hall, A., Vuori, K., and Côté, J.-F. (2008). The atypical Rac activator Dock180 (Dock1) regulates myoblast fusion in vivo. Proc. Natl. Acad. Sci. U.S.a. *105*, 15446–15451.

Le Clainche, C., Pantaloni, D., and Carlier, M.-F. (2003). ATP hydrolysis on actin-related protein 2/3 complex causes debranching of dendritic actin arrays. Proc. Natl. Acad. Sci. U.S.a. *100*, 6337–6342.

Leikina, E., Melikov, K., Sanyal, S., Verma, S.K., Eun, B., Gebert, C., Pfeifer, K., Lizunov, V.A., Kozlov, M.M., and Chernomordik, L.V. (2013). Extracellular annexins and dynamin are important for sequential steps in myoblast fusion. J. Cell Biol. *200*, 109–123.

Leng, Y., Zhang, J., Badour, K., Arpaia, E., Freeman, S., Cheung, P., Siu, M., and Siminovitch, K. (2005). Abelson-interactor-1 promotes WAVE2 membrane translocation and Abelson-mediated tyrosine phosphorylation required for WAVE2 activation. Proc. Natl. Acad. Sci. U.S.a. *102*, 1098–1103.

Leptin, M. (1991). twist and snail as positive and negative regulators during Drosophila mesoderm development. Genes Dev. *5*, 1568–1576.

Leptin, M., and Grunewald, B. (1990). Cell shape changes during gastrulation in Drosophila. Development *110*, 73–84.

Leptin, M., Bogaert, T., Lehmann, R., and Wilcox, M. (1989). The function of PS integrins during Drosophila embryogenesis. Cell *56*, 401–408.

Li, F., and Higgs, H.N. (2005). Dissecting requirements for auto-inhibition of actin nucleation by the formin, mDia1. J. Biol. Chem. *280*, 6986–6992.

Linder, S. (2009). Invadosomes at a glance. J. Cell. Sci. *122*, 3009–3013.

Liotta, D., Han, J., Elgar, S., Garvey, C., Han, Z., and Taylor, M.V. (2007). The Him gene reveals a balance of inputs controlling muscle differentiation in Drosophila. Curr. Biol. *17*, 1409–1413.

Littlefield, R., Almenar-Queralt, A., and Fowler, V.M. (2001). Actin dynamics at pointed ends regulates thin filament length in striated muscle. Nat. Cell Biol. *3*, 544–551.

Littlefield, R.S., and Fowler, V.M. (2008). Thin filament length regulation in striated muscle sarcomeres: pointed-end dynamics go beyond a nebulin ruler. Semin. Cell Dev. Biol. *19*, 511–519.

Lizárraga, F., Poincloux, R., Romao, M., Montagnac, G., Le Dez, G., Bonne, I., Rigaill, G., Raposo, G., and Chavrier, P. (2009). Diaphanous-related formins are required for invadopodia formation and invasion of breast tumor cells. Cancer Res. *69*, 2792–2800.

Lu, Q., and Adler, P.N. (2015). The diaphanous gene of Drosophila interacts antagonistically with multiple wing hairs and plays a key role in wing hair morphogenesis. PLoS ONE *10*, e0115623.

Lynch, E.D., Lee, M.K., Morrow, J.E., Welcsh, P.L., León, P.E., and King, M.C. (1997). Nonsyndromic deafness DFNA1 associated with mutation of a human homolog of the Drosophila gene diaphanous. Science *278*, 1315–1318.

Machado, C., and Andrew, D.J. (2000). D-Titin: a giant protein with dual roles in chromosomes and muscles. J. Cell Biol. *151*, 639–652.

Machesky, L.M., Mullins, R.D., Higgs, H.N., Kaiser, D.A., Blanchoin, L., May, R.C., Hall, M.E., and Pollard, T.D. (1999). Scar, a WASp-related protein, activates nucleation of actin filaments by the Arp2/3 complex. Proc. Natl. Acad. Sci. U.S.a. *96*, 3739–3744.

Maciver, S.K., Pope, B.J., Whytock, S., and Weeds, A.G. (1998). The effect of two actin depolymerizing factors (ADF/cofilins) on actin filament turnover: pH sensitivity of F-actin binding by human ADF, but not of Acanthamoeba actophorin. Eur. J. Biochem. *256*, 388–397.

Manseau, L., Calley, J., and Phan, H. (1996). Profilin is required for posterior patterning of the Drosophila oocyte. Development *122*, 2109–2116.

Mardahl-Dumesnil, M., and Fowler, V.M. (2001). Thin filaments elongate from their pointed ends during myofibril assembly in Drosophila indirect flight muscle. J. Cell Biol. *155*, 1043–1053.

Martens, S., and McMahon, H.T. (2008). Mechanisms of membrane fusion: disparate

players and common principles. Nat. Rev. Mol. Cell Biol. *9*, 543–556.

Martin, A.C., Kaschube, M., and Wieschaus, E.F. (2009). Pulsed contractions of an actin-myosin network drive apical constriction. Nature *457*, 495–499.

Mass, R.L., Zeller, R., Woychik, R.P., Vogt, T.F., and Leder, P. (1990). Disruption of formin-encoding transcripts in two mutant limb deformity alleles. Nature *346*, 853–855.

Massarwa, R., Carmon, S., Shilo, B.-Z., and Schejter, E.D. (2007). WIP/WASp-based actin-polymerization machinery is essential for myoblast fusion in Drosophila. Dev. Cell *12*, 557–569.

Matsubayashi, Y., Coulson-Gilmer, C., and Millard, T.H. (2015). Endocytosis-dependent coordination of multiple actin regulators is required for wound healing. J. Cell Biol. *210*, 419–433.

Mattila, P.K., and Lappalainen, P. (2008). Filopodia: molecular architecture and cellular functions. Nat. Rev. Mol. Cell Biol. *9*, 446–454.

Mattila, P.K., Pykäläinen, A., Saarikangas, J., Paavilainen, V.O., Vihinen, H., Jokitalo, E., and Lappalainen, P. (2007). Missing-in-metastasis and IRSp53 deform PI(4,5)P2-rich membranes by an inverse BAR domain-like mechanism. J. Cell Biol. *176*, 953–964.

McGough, A., and Chiu, W. (1999). ADF/cofilin weakens lateral contacts in the actin filament. J. Mol. Biol. *291*, 513–519.

McGough, A.M., Staiger, C.J., Min, J.K., and Simonetti, K.D. (2003). The gelsolin family of actin regulatory proteins: modular structures, versatile functions. FEBS Lett. *552*, 75–81.

McLaughlin, P.J., Gooch, J.T., Mannherz, H.G., and Weeds, A.G. (1993). Structure of gelsolin segment 1-actin complex and the mechanism of filament severing. Nature *364*, 685–692.

Meberg, P.J., Ono, S., Minamide, L.S., Takahashi, M., and Bamburg, J.R. (1998). Actin depolymerizing factor and cofilin phosphorylation dynamics: response to signals that regulate neurite extension. Cell Motil. Cytoskeleton *39*, 172–190.

Mellor, H. (2010). The role of formins in filopodia formation. Biochim. Biophys. Acta *1803*, 191–200.

Mendoza, M.C. (2013). Phosphoregulation of the WAVE regulatory complex and signal integration. Semin. Cell Dev. Biol. *24*, 272–279.

Menon, S.D., and Chia, W. (2001). Drosophila rolling pebbles: a multidomain protein

required for myoblast fusion that recruits D-Titin in response to the myoblast attractant Dumbfounded. Dev. Cell *1*, 691–703.

Menon, S.D., Osman, Z., Chenchill, K., and Chia, W. (2005). A positive feedback loop between Dumbfounded and Rolling pebbles leads to myotube enlargement in Drosophila. J. Cell Biol. *169*, 909–920.

Mersich, A.T., Miller, M.R., Chkourko, H., and Blystone, S.D. (2010). The formin FRL1 (FMNL1) is an essential component of macrophage podosomes. Cytoskeleton (Hoboken) *67*, 573–585.

Metzger, T., Gache, V., Xu, M., Cadot, B., Folker, E.S., Richardson, B.E., Gomes, E.R., and Baylies, M.K. (2012). MAP and kinesin-dependent nuclear positioning is required for skeletal muscle function. Nature *484*, 120–124.

Mi-Mi, L., and Pruyne, D. (2015). Loss of Sarcomere-associated Formins Disrupts Z-line Organization, but does not Prevent Thin Filament Assembly in Caenorhabditis elegans Muscle. J Cytol Histol *6*.

Mi-Mi, L., Votra, S., Kemphues, K., Bretscher, A., and Pruyne, D. (2012). Z-line formins promote contractile lattice growth and maintenance in striated muscles of C. elegans. J. Cell Biol. *198*, 87–102.

Michos, O., Panman, L., Vintersten, K., Beier, K., Zeller, R., and Zuniga, A. (2004). Gremlin-mediated BMP antagonism induces the epithelial-mesenchymal feedback signaling controlling metanephric kidney and limb organogenesis. Development *131*, 3401–3410.

Miki, H., Miura, K., and Takenawa, T. (1996). N-WASP, a novel actin-depolymerizing protein, regulates the cortical cytoskeletal rearrangement in a PIP2-dependent manner downstream of tyrosine kinases. Embo J. *15*, 5326–5335.

Millard, T.H., and Martin, P. (2008). Dynamic analysis of filopodial interactions during the zippering phase of Drosophila dorsal closure. Development *135*, 621–626.

Mohler, W.A., Shemer, G., del Campo, J.J., Valansi, C., Opoku-Serebuoh, E., Scranton, V., Assaf, N., White, J.G., and Podbilewicz, B. (2002). The type I membrane protein EFF-1 is essential for developmental cell fusion. Dev. Cell *2*, 355–362.

Molkentin, J.D., Black, B.L., Martin, J.F., and Olson, E.N. (1995). Cooperative activation of muscle gene expression by MEF2 and myogenic bHLH proteins. Cell *83*, 1125–1136.

Molnár, I., Migh, E., Szikora, S., Kalmár, T., Végh, A.G., Deák, F., Barkó, S., Bugyi, B., Orfanos, Z., Kovács, J., et al. (2014). DAAM is required for thin filament formation and Sarcomerogenesis during muscle development in Drosophila. PLoS Genet. *10*,

e1004166.

Moseley, J.B., Maiti, S., and Goode, B.L. (2006). Formin proteins: purification and measurement of effects on actin assembly. Meth. Enzymol. *406*, 215–234.

Mukherjee, P., Gildor, B., Shilo, B.-Z., Vijayraghavan, K., and Schejter, E.D. (2011). The actin nucleator WASp is required for myoblast fusion during adult Drosophila myogenesis. Development *138*, 2347–2357.

Mulinari, S., Barmchi, M.P., and Häcker, U. (2008). DRhoGEF2 and diaphanous regulate contractile force during segmental groove morphogenesis in the Drosophila embryo. Mol. Biol. Cell *19*, 1883–1892.

Münsterberg, A.E., Kitajewski, J., Bumcrot, D.A., McMahon, A.P., and Lassar, A.B. (1995). Combinatorial signaling by Sonic hedgehog and Wnt family members induces myogenic bHLH gene expression in the somite. Genes Dev. *9*, 2911–2922.

Myhre, J.L., and Pilgrim, D. (2014). A Titan but not necessarily a ruler: assessing the role of titin during thick filament patterning and assembly. Anat Rec (Hoboken) *297*, 1604–1614.

Nabel-Rosen, H., Volohonsky, G., Reuveny, A., Zaidel-Bar, R., and Volk, T. (2002). Two isoforms of the Drosophila RNA binding protein, how, act in opposing directions to regulate tendon cell differentiation. Dev. Cell *2*, 183–193.

Neuman-Silberberg, F.S., and Schüpbach, T. (1993). The Drosophila dorsoventral patterning gene gurken produces a dorsally localized RNA and encodes a TGF alpha-like protein. Cell *75*, 165–174.

Nilson, L.A., and Schüpbach, T. (1999). EGF receptor signaling in Drosophila oogenesis. Curr. Top. Dev. Biol. *44*, 203–243.

Nowak, S.J., Nahirney, P.C., Hadjantonakis, A.-K., and Baylies, M.K. (2009). Nap1-mediated actin remodeling is essential for mammalian myoblast fusion. J. Cell. Sci. *122*, 3282–3293.

Nowotarski, S.H., McKeon, N., Moser, R.J., and Peifer, M. (2014). The actin regulators Enabled and Diaphanous direct distinct protrusive behaviors in different tissues during Drosophila development. Mol. Biol. Cell *25*, 3147–3165.

Oas, S.T., Bryantsev, A.L., and Cripps, R.M. (2014). Arrest is a regulator of fiber-specific alternative splicing in the indirect flight muscles of Drosophila. J. Cell Biol. *206*, 895–908.

Ochala, J. (2008). Thin filament proteins mutations associated with skeletal myopathies: defective regulation of muscle contraction. J. Mol. Med. *86*, 1197–1204.

Oikonomou, K.G., Zachou, K., and Dalekos, G.N. (2011). Alpha-actinin: a multidisciplinary protein with important role in B-cell driven autoimmunity. Autoimmun Rev *10*, 389–396.

Ojala, P.J., Paavilainen, V., and Lappalainen, P. (2001). Identification of yeast cofilin residues specific for actin monomer and PIP2 binding. Biochemistry *40*, 15562–15569.

Ono, S. (2007). Mechanism of depolymerization and severing of actin filaments and its significance in cytoskeletal dynamics. Int. Rev. Cytol. *258*, 1–82.

Ono, S. (2010). Dynamic regulation of sarcomeric actin filaments in striated muscle. Cytoskeleton (Hoboken) *67*, 677–692.

Ono, S., Mohri, K., and Ono, K. (2004). Microscopic evidence that actin-interacting protein 1 actively disassembles actin-depolymerizing factor/Cofilin-bound actin filaments. J. Biol. Chem. *279*, 14207–14212.

Orfanos, Z., Leonard, K., Elliott, C., Katzemich, A., Bullard, B., and Sparrow, J. (2015). Sallimus and the dynamics of sarcomere assembly in Drosophila flight muscles. J. Mol. Biol. *427*, 2151–2158.

Pak, C.W., Flynn, K.C., and Bamburg, J.R. (2008). Actin-binding proteins take the reins in growth cones. Nat. Rev. Neurosci. *9*, 136–147.

Palazzo, A.F., Cook, T.A., Alberts, A.S., and Gundersen, G.G. (2001). mDia mediates Rho-regulated formation and orientation of stable microtubules. Nat. Cell Biol. *3*, 723–729.

Pappas, C.T., Bhattacharya, N., Cooper, J.A., and Gregorio, C.C. (2008). Nebulin interacts with CapZ and regulates thin filament architecture within the Z-disc. Mol. Biol. Cell *19*, 1837–1847.

Pappas, C.T., Bliss, K.T., Zieseniss, A., and Gregorio, C.C. (2011). The Nebulin family: an actin support group. Trends Cell Biol. *21*, 29–37.

Pappas, C.T., Krieg, P.A., and Gregorio, C.C. (2010). Nebulin regulates actin filament lengths by a stabilization mechanism. J. Cell Biol. *189*, 859–870.

Parks, S., and Wieschaus, E. (1991). The Drosophila gastrulation gene concertina encodes a G alpha-like protein. Cell *64*, 447–458.

Paul, A.S., and Pollard, T.D. (2009). Review of the mechanism of processive actin filament elongation by formins. Cell Motil. Cytoskeleton *66*, 606–617.

Pawson, C., Eaton, B.A., and Davis, G.W. (2008). Formin-dependent synaptic growth: evidence that Dlar signals via Diaphanous to modulate synaptic actin and dynamic

pioneer microtubules. J. Neurosci. *28*, 11111–11123.

Peckham, M., Molloy, J.E., Sparrow, J.C., and White, D.C. (1990). Physiological properties of the dorsal longitudinal flight muscle and the tergal depressor of the trochanter muscle of Drosophila melanogaster. J. Muscle Res. Cell. Motil. *11*, 203–215.

Perkins, A.D., and Tanentzapf, G. (2014). An ongoing role for structural sarcomeric components in maintaining Drosophila melanogaster muscle function and structure. PLoS ONE *9*, e99362.

Petersen, J., Nielsen, O., Egel, R., and Hagan, I.M. (1998). FH3, a domain found in formins, targets the fission yeast formin Fus1 to the projection tip during conjugation. J. Cell Biol. *141*, 1217–1228.

Pinal, N., Goberdhan, D.C.I., Collinson, L., Fujita, Y., Cox, I.M., Wilson, C., and Pichaud, F. (2006). Regulated and polarized PtdIns(3,4,5)P3 accumulation is essential for apical membrane morphogenesis in photoreceptor epithelial cells. Curr. Biol. *16*, 140–149.

Pizon, V., Gerbal, F., Diaz, C.C., and Karsenti, E. (2005). Microtubule-dependent transport and organization of sarcomeric myosin during skeletal muscle differentiation. Embo J. *24*, 3781–3792.

Pizon, V., Iakovenko, A., Van Der Ven, P.F.M., Kelly, R., Fatu, C., Fürst, D.O., Karsenti, E., and Gautel, M. (2002). Transient association of titin and myosin with microtubules in nascent myofibrils directed by the MURF2 RING-finger protein. J. Cell. Sci. *115*, 4469–4482.

Pollard, T.D. (2007). Regulation of actin filament assembly by Arp2/3 complex and formins. Annu Rev Biophys Biomol Struct *36*, 451–477.

Pollard, T.D., and Borisy, G.G. (2003). Cellular motility driven by assembly and disassembly of actin filaments. Cell *112*, 453–465.

Pourquié, O., Fan, C.M., Coltey, M., Hirsinger, E., Watanabe, Y., Bréant, C., Francis-West, P., Brickell, P., Tessier-Lavigne, M., and Le Douarin, N.M. (1996). Lateral and axial signals involved in avian somite patterning: a role for BMP4. Cell *84*, 461–471.

Pruyne, D., Evangelista, M., Yang, C., Bi, E., Zigmond, S., Bretscher, A., and Boone, C. (2002). Role of formins in actin assembly: nucleation and barbed-end association. Science *297*, 612–615.

Qadota, H., Blangy, A., Xiong, G., and Benian, G.M. (2008). The DH-PH region of the giant protein UNC-89 activates RHO-1 GTPase in Caenorhabditis elegans body wall muscle. J. Mol. Biol. *383*, 747–752.

Radice, G.L., Rayburn, H., Matsunami, H., Knudsen, K.A., Takeichi, M., and Hynes, R.O. (1997). Developmental defects in mouse embryos lacking N-cadherin. Dev. Biol. *181*, 64–78.

Ramalingam, N., Zhao, H., Breitsprecher, D., Lappalainen, P., Faix, J., and Schleicher, M. (2010). Phospholipids regulate localization and activity of mDia1 formin. Eur. J. Cell Biol. *89*, 723–732.

Ramesh, N., and Geha, R. (2009). Recent advances in the biology of WASP and WIP. Immunol. Res. *44*, 99–111.

Rantanen, J., Hurme, T., Lukka, R., Heino, J., and Kalimo, H. (1995). Satellite cell proliferation and the expression of myogenin and desmin in regenerating skeletal muscle: evidence for two different populations of satellite cells. Lab. Invest. *72*, 341–347.

Rau, A., Buttgereit, D., Holz, A., Fetter, R., Doberstein, S.K., Paululat, A., Staudt, N., Skeath, J., Michelson, A.M., and Renkawitz-Pohl, R. (2001). rolling pebbles (rols) is required in Drosophila muscle precursors for recruitment of myoblasts for fusion. Development *128*, 5061–5073.

Reedy, M.C., and Beall, C. (1993). Ultrastructure of developing flight muscle in Drosophila. I. Assembly of myofibrils. Dev. Biol. *160*, 443–465.

Reedy, M.C., Bullard, B., and Vigoreaux, J.O. (2000). Flightin is essential for thick filament assembly and sarcomere stability in Drosophila flight muscles. J. Cell Biol. *151*, 1483–1500.

Relaix, F., Rocancourt, D., Mansouri, A., and Buckingham, M. (2005). A Pax3/Pax7-dependent population of skeletal muscle progenitor cells. Nature *435*, 948–953.

Revenu, C., Athman, R., Robine, S., and Louvard, D. (2004). The co-workers of actin filaments: from cell structures to signals. Nat. Rev. Mol. Cell Biol. *5*, 635–646.

Richardson, B.E., Beckett, K., and Baylies, M.K. (2008a). Live imaging of Drosophila myoblast fusion. Methods Mol. Biol. *475*, 263–274.

Richardson, B.E., Beckett, K., Nowak, S.J., and Baylies, M.K. (2007). SCAR/WAVE and Arp2/3 are crucial for cytoskeletal remodeling at the site of myoblast fusion. Development *134*, 4357–4367.

Richardson, B., Beckett, K., and Baylies, M. (2008b). Visualizing new dimensions in Drosophila myoblast fusion. Bioessays *30*, 423–431.

Riechmann, V., Irion, U., Wilson, R., Grosskortenhaus, R., and Leptin, M. (1997). Control of cell fates and segmentation in the Drosophila mesoderm. Development *124*, 2915–2922.

Riechmann, V., Rehorn, K.P., Reuter, R., and Leptin, M. (1998). The genetic control of the distinction between fat body and gonadal mesoderm in Drosophila. Development *125*, 713–723.

Robinson, R.C., Turbedsky, K., Kaiser, D.A., Marchand, J.B., Higgs, H.N., Choe, S., and Pollard, T.D. (2001). Crystal structure of Arp2/3 complex. Science *294*, 1679–1684.

Rochlin, K., Yu, S., Roy, S., and Baylies, M.K. (2010). Myoblast fusion: when it takes more to make one. Dev. Biol. *341*, 66–83.

Rodal, A.A., Del Signore, S.J., and Martin, A.C. (2015). Drosophila comes of age as a model system for understanding the function of cytoskeletal proteins in cells, tissues, and organisms. Cytoskeleton (Hoboken) *72*, 207–224.

Rosado, M., Barber, C.F., Berciu, C., Feldman, S., Birren, S.J., Nicastro, D., and Goode, B.L. (2014). Critical roles for multiple formins during cardiac myofibril development and repair. Mol. Biol. Cell *25*, 811–827.

Rosales-Nieves, A.E., Johndrow, J.E., Keller, L.C., Magie, C.R., Pinto-Santini, D.M., and Parkhurst, S.M. (2006). Coordination of microtubule and microfilament dynamics by Drosophila Rho1, Spire and Cappuccino. Nat. Cell Biol. *8*, 367–376.

Rosen, G.D., Sanes, J.R., LaChance, R., Cunningham, J.M., Roman, J., and Dean, D.C. (1992). Roles for the integrin VLA-4 and its counter receptor VCAM-1 in myogenesis. Cell *69*, 1107–1119.

Roth, S., Neuman-Silberberg, F.S., Barcelo, G., and Schüpbach, T. (1995). cornichon and the EGF receptor signaling process are necessary for both anterior-posterior and dorsal-ventral pattern formation in Drosophila. Cell *81*, 967–978.

Rousso, T., Shewan, A.M., Mostov, K.E., Schejter, E.D., and Shilo, B.-Z. (2013). Apical targeting of the formin Diaphanous in Drosophila tubular epithelia. Elife *2*, e00666.

Rudnicki, M.A., Schnegelsberg, P.N., Stead, R.H., Braun, T., Arnold, H.H., and Jaenisch, R. (1993). MyoD or Myf-5 is required for the formation of skeletal muscle. Cell *75*, 1351–1359.

Ruiz Gomez, M., and Bate, M. (1997). Segregation of myogenic lineages in Drosophila requires numb. Development *124*, 4857–4866.

Ruiz Gomez, M., Coutts, N., Price, A., Taylor, M.V., and Bate, M. (2000). Drosophila dumbfounded: a myoblast attractant essential for fusion. Cell *102*, 189–198.

Rushton, E., Drysdale, R., Abmayr, S.M., Michelson, A.M., and Bate, M. (1995). Mutations in a novel gene, myoblast city, provide evidence in support of the founder cell hypothesis for Drosophila muscle development. Development *121*, 1979–1988.

Ryu, J.R., Echarri, A., Li, R., and Pendergast, A.M. (2009). Regulation of cell-cell adhesion by Abi/Diaphanous complexes. Mol. Cell. Biol. *29*, 1735–1748.

Sagot, I., Rodal, A.A., Moseley, J., Goode, B.L., and Pellman, D. (2002). An actin nucleation mechanism mediated by Bni1 and profilin. Nat. Cell Biol. *4*, 626–631.

Saide, J.D., Chin-Bow, S., Hogan-Sheldon, J., Busquets-Turner, L., Vigoreaux, J.O., Valgeirsdottir, K., and Pardue, M.L. (1989). Characterization of components of Z-bands in the fibrillar flight muscle of Drosophila melanogaster. J. Cell Biol. *109*, 2157–2167.

Salvany, L., Muller, J., Guccione, E., and Rørth, P. (2014). The core and conserved role of MAL is homeostatic regulation of actin levels. Genes Dev. *28*, 1048–1053.

Sapir, A., Choi, J., Leikina, E., Avinoam, O., Valansi, C., Chernomordik, L.V., Newman, A.P., and Podbilewicz, B. (2007). AFF-1, a FOS-1-regulated fusogen, mediates fusion of the anchor cell in C. elegans. Dev. Cell *12*, 683–698.

Sato, T., Rocancourt, D., Marques, L., Thorsteinsdóttir, S., and Buckingham, M. (2010). A Pax3/Dmrt2/Myf5 regulatory cascade functions at the onset of myogenesis. PLoS Genet. *6*, e1000897.

Schafer, D.A., Hug, C., and Cooper, J.A. (1995). Inhibition of CapZ during myofibrillogenesis alters assembly of actin filaments. J. Cell Biol. *128*, 61–70.

Schäfer, G., Weber, S., Holz, A., Bogdan, S., Schumacher, S., Müller, A., Renkawitz-Pohl, R., and Onel, S.-F. (2007). The Wiskott-Aldrich syndrome protein (WASP) is essential for myoblast fusion in Drosophila. Dev. Biol. *304*, 664–674.

Schneider, C.A., Rasband, W.S., and Eliceiri, K.W. (2012). NIH Image to ImageJ: 25 years of image analysis. Nat. Methods *9*, 671–675.

Schnorrer, F., Kalchhauser, I., and Dickson, B.J. (2007). The transmembrane protein Kon-tiki couples to Dgrip to mediate myotube targeting in Drosophila. Dev. Cell *12*, 751–766.

Schnorrer, F., Schönbauer, C., Langer, C.C.H., Dietzl, G., Novatchkova, M., Schernhuber, K., Fellner, M., Azaryan, A., Radolf, M., Stark, A., et al. (2010). Systematic genetic analysis of muscle morphogenesis and function in Drosophila. Nature *464*, 287–291.

Schoen, C.J., Burmeister, M., and Lesperance, M.M. (2013). Diaphanous homolog 3 (Diap3) overexpression causes progressive hearing loss and inner hair cell defects in a transgenic mouse model of human deafness. PLoS ONE *8*, e56520.

Schoen, C.J., Emery, S.B., Thorne, M.C., Ammana, H.R., Sliwerska, E., Arnett, J., Hortsch, M., Hannan, F., Burmeister, M., and Lesperance, M.M. (2010). Increased

activity of Diaphanous homolog 3 (DIAPH3)/diaphanous causes hearing defects in humans with auditory neuropathy and in Drosophila. Proc. Natl. Acad. Sci. U.S.a. *107*, 13396–13401.

Schönbauer, C., Distler, J., Jährling, N., Radolf, M., Dodt, H.-U., Frasch, M., and Schnorrer, F. (2011). Spalt mediates an evolutionarily conserved switch to fibrillar muscle fate in insects. Nature *479*, 406–409.

Schulman, V.K., Dobi, K.C., and Baylies, M.K. (2015). Morphogenesis of the somatic musculature in Drosophila melanogaster. Wiley Interdiscip Rev Dev Biol *4*, 313–334.

Schulz, C., Kiger, A.A., Tazuke, S.I., Yamashita, Y.M., Pantalena-Filho, L.C., Jones, D.L., Wood, C.G., and Fuller, M.T. (2004). A misexpression screen reveals effects of bag-of-marbles and TGF beta class signaling on the Drosophila male germ-line stem cell lineage. Genetics *167*, 707–723.

Schwander, M., Leu, M., Stumm, M., Dorchies, O.M., Ruegg, U.T., Schittny, J., and Müller, U. (2003). Beta1 integrins regulate myoblast fusion and sarcomere assembly. Dev. Cell *4*, 673–685.

Schweitzer, R., Zelzer, E., and Volk, T. (2010). Connecting muscles to tendons: tendons and musculoskeletal development in flies and vertebrates. Development *137*, 2807–2817.

Seale, P., Sabourin, L.A., Girgis-Gabardo, A., Mansouri, A., Gruss, P., and Rudnicki, M.A. (2000). Pax7 is required for the specification of myogenic satellite cells. Cell *102*, 777–786.

Selden, L.A., Kinosian, H.J., Newman, J., Lincoln, B., Hurwitz, C., Gershman, L.C., and Estes, J.E. (1998). Severing of F-actin by the amino-terminal half of gelsolin suggests internal cooperativity in gelsolin. Biophys. J. *75*, 3092–3100.

Sen, J., Goltz, J.S., Stevens, L., and Stein, D. (1998). Spatially restricted expression of pipe in the Drosophila egg chamber defines embryonic dorsal-ventral polarity. Cell *95*, 471–481.

Sens, K.L., Zhang, S., Jin, P., Duan, R., Zhang, G., Luo, F., Parachini, L., and Chen, E.H. (2010). An invasive podosome-like structure promotes fusion pore formation during myoblast fusion. J. Cell Biol. *191*, 1013–1027.

Seroude, L., Brummel, T., Kapahi, P., and Benzer, S. (2002). Spatio-temporal analysis of gene expression during aging in Drosophila melanogaster. Aging Cell *1*, 47–56.

Sevdali, M., Kumar, V., Peckham, M., and Sparrow, J. (2013). Human congenital myopathy actin mutants cause myopathy and alter Z-disc structure in Drosophila flight muscle. Neuromuscul. Disord. *23*, 243–255.

Shelton, C., Kocherlakota, K.S., Zhuang, S., and Abmayr, S.M. (2009). The immunoglobulin superfamily member Hbs functions redundantly with Sns in interactions between founder and fusion-competent myoblasts. Development *136*, 1159–1168.

Shemer, G., and Podbilewicz, B. (2000). Fusomorphogenesis: cell fusion in organ formation. Dev. Dyn. *218*, 30–51.

Shilagardi, K., Li, S., Luo, F., Marikar, F., Duan, R., Jin, P., Kim, J.H., Murnen, K., and Chen, E.H. (2013). Actin-propelled invasive membrane protrusions promote fusogenic protein engagement during cell-cell fusion. Science *340*, 359–363.

Shivdasani, A.A., and Ingham, P.W. (2003). Regulation of stem cell maintenance and transit amplifying cell proliferation by tgf-beta signaling in Drosophila spermatogenesis. Curr. Biol. *13*, 2065–2072.

Simionescu, A., and Pavlath, G.K. (2011). Molecular mechanisms of myoblast fusion across species. Adv. Exp. Med. Biol. *713*, 113–135.

Sohn, R.L., Huang, P., Kawahara, G., Mitchell, M., Guyon, J., Kalluri, R., Kunkel, L.M., and Gussoni, E. (2009). A role for nephrin, a renal protein, in vertebrate skeletal muscle cell fusion. Proc. Natl. Acad. Sci. U.S.a. *106*, 9274–9279.

Soler, C., and Taylor, M.V. (2009). The Him gene inhibits the development of Drosophila flight muscles during metamorphosis. Mech. Dev. *126*, 595–603.

Sparrow, J.C., and Schöck, F. (2009). The initial steps of myofibril assembly: integrins pave the way. Nat. Rev. Mol. Cell Biol. *10*, 293–298.

Sparrow, J.C., Nowak, K.J., Durling, H.J., Beggs, A.H., Wallgren-Pettersson, C., Romero, N., Nonaka, I., and Laing, N.G. (2003). Muscle disease caused by mutations in the skeletal muscle alpha-actin gene (ACTA1). Neuromuscul. Disord. *13*, 519–531.

Spletter, M.L., Barz, C., Yeroslaviz, A., Schönbauer, C., Ferreira, I.R.S., Sarov, M., Gerlach, D., Stark, A., Habermann, B.H., and Schnorrer, F. (2015). The RNA-binding protein Arrest (Bruno) regulates alternative splicing to enable myofibril maturation in Drosophila flight muscle. EMBO Rep. *16*, 178–191.

Staehling-Hampton, K., Hoffmann, F.M., Baylies, M.K., Rushton, E., and Bate, M. (1994). dpp induces mesodermal gene expression in Drosophila. Nature *372*, 783–786.

Staus, D.P., Blaker, A.L., Taylor, J.M., and Mack, C.P. (2007). Diaphanous 1 and 2 regulate smooth muscle cell differentiation by activating the myocardin-related transcription factors. Arterioscler. Thromb. Vasc. Biol. *27*, 478–486.

Strünkelnberg, M., Bonengel, B., Moda, L.M., Hertenstein, A., de Couet, H.G., Ramos,

R.G., and Fischbach, K.F. (2001). rst and its paralogue kirre act redundantly during embryonic muscle development in Drosophila. Development *128*, 4229–4239.

Stuart, J.R., Gonzalez, F.H., Kawai, H., and Yuan, Z.-M. (2006). c-Abl interacts with the WAVE2 signaling complex to induce membrane ruffling and cell spreading. J. Biol. Chem. *281*, 31290–31297.

Suarez, C., Carroll, R.T., Burke, T.A., Christensen, J.R., Bestul, A.J., Sees, J.A., James, M.L., Sirotkin, V., and Kovar, D.R. (2015). Profilin regulates F-actin network homeostasis by favoring formin over Arp2/3 complex. Dev. Cell *32*, 43–53.

Sun, H., Al-Romaih, K.I., MacRae, C.A., and Pollak, M.R. (2014). Human Kidney Disease-causing INF2 Mutations Perturb Rho/Dia Signaling in the Glomerulus. EBioMedicine *1*, 107–115.

Sussman, M.A., Baqué, S., Uhm, C.S., Daniels, M.P., Price, R.L., Simpson, D., Terracio, L., and Kedes, L. (1998). Altered expression of tropomodulin in cardiomyocytes disrupts the sarcomeric structure of myofibrils. Circ. Res. *82*, 94–105.

Tajbakhsh, S., and Cossu, G. (1997). Establishing myogenic identity during somitogenesis. Curr. Opin. Genet. Dev. *7*, 634–641.

Tall, E.G., Spector, I., Pentyala, S.N., Bitter, I., and Rebecchi, M.J. (2000). Dynamics of phosphatidylinositol 4,5-bisphosphate in actin-rich structures. Curr. Biol. *10*, 743–746.

Taniguchi, K., Takeya, R., Suetsugu, S., Kan-O, M., Narusawa, M., Shiose, A., Tominaga, R., and Sumimoto, H. (2009). Mammalian formin fhod3 regulates actin assembly and sarcomere organization in striated muscles. J. Biol. Chem. *284*, 29873–29881.

Tapanes-Castillo, A., and Baylies, M.K. (2004). Notch signaling patterns Drosophila mesodermal segments by regulating the bHLH transcription factor twist. Development *131*, 2359–2372.

Thelen, S., Abouhamed, M., Ciarimboli, G., Edemir, B., and Bähler, M. (2015). Rho GAP myosin IXa is a regulator of kidney tubule function. Am. J. Physiol. Renal Physiol. *309*, F501–F513.

Tidball, J.G. (1995). Inflammatory cell response to acute muscle injury. Med Sci Sports Exerc *27*, 1022–1032.

Tixier, V., Bataillé, L., and Jagla, K. (2010). Diversification of muscle types: recent insights from Drosophila. Exp. Cell Res. *316*, 3019–3027.

Tokuo, H., and Ikebe, M. (2004). Myosin X transports Mena/VASP to the tip of filopodia. Biochem. Biophys. Res. Commun. *319*, 214–220.

Tu, M.S., and Daniel, T.L. (2004). Cardiac-like behavior of an insect flight muscle. J. Exp. Biol. *207*, 2455–2464.

Vasyutina, E., Martarelli, B., Brakebusch, C., Wende, H., and Birchmeier, C. (2009). The small G-proteins Rac1 and Cdc42 are essential for myoblast fusion in the mouse. Proc. Natl. Acad. Sci. U.S.a. *106*, 8935–8940.

Verstreken, P., Ohyama, T., Haueter, C., Habets, R.L.P., Lin, Y.Q., Swan, L.E., Ly, C.V., Venken, K.J.T., De Camilli, P., and Bellen, H.J. (2009). Tweek, an evolutionarily conserved protein, is required for synaptic vesicle recycling. Neuron *63*, 203–215.

Vigoreaux, J.O. (2001). Genetics of the Drosophila flight muscle myofibril: a window into the biology of complex systems. Bioessays *23*, 1047–1063.

Vigoreaux, J.O., Saide, J.D., and Pardue, M.L. (1991). Structurally different Drosophila striated muscles utilize distinct variants of Z-band-associated proteins. J. Muscle Res. Cell. Motil. *12*, 340–354.

Vigoreaux, J.O. (2005). Molecualr Basis of Muscle Structrue. In Muscle Development in Drosophila, H. Sink, ed.

Vu Manh, T.P., Mokrane, M., Georgenthum, E., Flavigny, J., Carrier, L., Sémériva, M., Piovant, M., and Röder, L. (2005). Expression of cardiac myosin-binding protein-C (cMyBP-C) in Drosophila as a model for the study of human cardiomyopathies. Hum. Mol. Genet. *14*, 7–17.

Watanabe, N., Madaule, P., Reid, T., Ishizaki, T., Watanabe, G., Kakizuka, A., Saito, Y., Nakao, K., Jockusch, B.M., and Narumiya, S. (1997). p140mDia, a mammalian homolog of Drosophila diaphanous, is a target protein for Rho small GTPase and is a ligand for profilin. Embo J. *16*, 3044–3056.

Webb, R.L., Zhou, M.-N., and McCartney, B.M. (2009). A novel role for an APC2-Diaphanous complex in regulating actin organization in Drosophila. Development *136*, 1283–1293.

Wegner, A., and Engel, J. (1975). Kinetics of the cooperative association of actin to actin filaments. Biophys. Chem. *3*, 215–225.

Wen, J., Duan, H., Bejarano, F., Okamura, K., Fabian, L., Brill, J.A., Bortolamiol-Becet, D., Martin, R., Ruby, J.G., and Lai, E.C. (2015). Adaptive regulation of testis gene expression and control of male fertility by the Drosophila hairpin RNA pathway. [Corrected]. Mol. Cell *57*, 165–178.

Wen, Y., Eng, C.H., Schmoranzer, J., Cabrera-Poch, N., Morris, E.J.S., Chen, M., Wallar, B.J., Alberts, A.S., and Gundersen, G.G. (2004). EB1 and APC bind to mDia to stabilize microtubules downstream of Rho and promote cell migration. Nat. Cell Biol. *6*, 820–830.

Witke, W. (2004). The role of profilin complexes in cell motility and other cellular processes. Trends Cell Biol. *14*, 461–469.

Wong, R., Hadjiyanni, I., Wei, H.-C., Polevoy, G., McBride, R., Sem, K.-P., and Brill, J.A. (2005). PIP2 hydrolysis and calcium release are required for cytokinesis in Drosophila spermatocytes. Curr. Biol. *15*, 1401–1406.

Wooten, E.C., Hebl, V.B., Wolf, M.J., Greytak, S.R., Orr, N.M., Draper, I., Calvino, J.E., Kapur, N.K., Maron, M.S., Kullo, I.J., et al. (2013). Formin homology 2 domain containing 3 variants associated with hypertrophic cardiomyopathy. Circ Cardiovasc Genet *6*, 10–18.

Woychik, R.P., Maas, R.L., Zeller, R., Vogt, T.F., and Leder, P. (1990). "Formins": proteins deduced from the alternative transcripts of the limb deformity gene. Nature *346*, 850–853.

Xu, Y., Moseley, J.B., Sagot, I., Poy, F., Pellman, D., Goode, B.L., and Eck, M.J. (2004). Crystal structures of a Formin Homology-2 domain reveal a tethered dimer architecture. Cell *116*, 711–723.

Yan, S., Lv, Z., Winterhoff, M., Wenzl, C., Zobel, T., Faix, J., Bogdan, S., and Grosshans, J. (2013). The F-BAR protein Cip4/Toca-1 antagonizes the formin Diaphanous in membrane stabilization and compartmentalization. J. Cell. Sci. *126*, 1796–1805.

Yarnitzky, T., Min, L., and Volk, T. (1997). The Drosophila neuregulin homolog Vein mediates inductive interactions between myotubes and their epidermal attachment cells. Genes Dev. *11*, 2691–2700.

Yin, H., Price, F., and Rudnicki, M.A. (2013). Satellite cells and the muscle stem cell niche. Physiol. Rev. *93*, 23–67.

Zallen, J.A., Cohen, Y., Hudson, A.M., Cooley, L., Wieschaus, E., and Schejter, E.D. (2002). SCAR is a primary regulator of Arp2/3-dependent morphological events in Drosophila. J. Cell Biol. *156*, 689–701.

Zeev-Ben-Mordehai, T., Vasishtan, D., Siebert, C.A., and Grünewald, K. (2014). The full-length cell-cell fusogen EFF-1 is monomeric and upright on the membrane. Nat Commun *5*, 3912.

Zhang, L., Mao, Y.S., Janmey, P.A., and Yin, H.L. (2012). Phosphatidylinositol 4, 5 bisphosphate and the actin cytoskeleton. Subcell. Biochem. *59*, 177–215.

Zhang, Y., Featherstone, D., Davis, W., Rushton, E., and Broadie, K. (2000). Drosophila D-titin is required for myoblast fusion and skeletal muscle striation. J. Cell. Sci. *113 (Pt 17)*, 3103–3115.

Zuniga, A., Michos, O., Spitz, F., Haramis, A.-P.G., Panman, L., Galli, A., Vintersten, K.,

Klasen, C., Mansfield, W., Kuc, S., et al. (2004). Mouse limb deformity mutations disrupt a global control region within the large regulatory landscape required for Gremlin expression. Genes Dev. *18*, 1553–1564.